

# For Reference

NOT TO BE TAKEN FROM THIS ROOM

For Reference

---

NOT TO BE TAKEN FROM THIS ROOM

Ex LIBRIS  
UNIVERSITATIS  
ALBERTAENSIS





Digitized by the Internet Archive  
in 2019 with funding from  
University of Alberta Libraries

<https://archive.org/details/Bellow1963>





THE UNIVERSITY OF ALBERTA

ANTICLASTIC BEHAVIOUR OF FLAT PLATES

by

DONALD G. BELLOW, BSc (British Columbia), MSc (Alberta)

A THESIS

SUBMITTED TO THE FACULTY OF GRADUATE STUDIES

IN PARTIAL FULFILMENT OF THE REQUIREMENTS

FOR THE DEGREE OF DOCTOR OF PHILOSOPHY

DEPARTMENT OF MECHANICAL ENGINEERING

EDMONTON, ALBERTA  
SEPTEMBER, 1963



THE UNIVERSITY OF ALBERTA  
FACULTY OF GRADUATE STUDIES

The undersigned certify that they have read, and recommend to the Faculty of Graduate Studies for acceptance, a thesis entitled "Anticlastic Behaviour of Flat Plates" submitted by Donald G. Bellow in partial fulfilment of the requirements for the degree of Doctor of Philosophy.





## ABSTRACT

The problem of transverse deflections of beams and plates when bent into large longitudinal curvatures was discussed as early as the seventeenth century. In 1891 Lamb presented a solution to the problem embodying both beam and plate actions by considering the equilibrium of a transverse strip in the deformed state. This thesis presents an historical review for the problem and discusses in detail the significance of Lamb's solution. It is also shown how Lamb's solution was used by Timoshenko in 1925 to develop a relationship between the bending moment, curvature, and stiffness. Tabulated values from a digital computer are given for Lamb's solution and the Timoshenko bending moment relationship.

Previous experimental work carried out to verify the theory of Lamb is discussed and reasons are given for the need for further experimentation. A numerical procedure is developed for calculating deflections from strains measured by electrical resistance gauges.

It is shown that the deflected form of the transverse strip depends on the dimensionless parameter  $b^2/Rd$ . It was found that the experimental deflections, using the strain gauge technique, agreed reasonably well with theory for  $b^2/Rd$  ratios up to 55, and above this there is every reason to expect even better agreement. It is also shown, by experiment, that the



transverse deflections are unaffected by the support and loading conditions for an equivalent span to width ratio of  $1/3$ .

In order to record the readings from electrical resistance strain gauges, a multi-channel digital data processor was constructed. The development and construction of this apparatus is discussed, and it is shown how it is used in conjunction with a digital computer for the evaluation of the transverse deflections.

An example problem is cited which emphasizes the practical significance of the work of this thesis. Some problems for possible further study are mentioned.





## ACKNOWLEDGEMENTS

The author welcomes this opportunity to express appreciation and thanks to Professor G. Ford for suggesting the research topic, supervising the thesis, and putting at his disposal the necessary funds for building the experimental apparatus. He also expresses thanks to Professors J.S. Kennedy, J.B. Haddow, and J.J. McNamee for their patience in reading the first drafts and offering many constructive criticisms.

To Mr. R. Marak for helping with the construction of the apparatus and subsequent testing, to Miss E.A. Sprinkle for assisting in the task of reducing the data, and to Mrs. P.M. Falconer for her care and attention in typing the thesis, the author offers his thanks.

To the staff of the University of Alberta Computing Center the author acknowledges his appreciation. Without their assistance and cooperation the author's task would have been most arduous.

To the National Research Council, Ottawa, the author is very grateful for the financial assistance received during the summer of 1961 and for their aid in assisting with the purchase of the experimental apparatus under N.R.C. Grant A-1234.

To the Government of the Province of Alberta the author is indeed grateful and honored to have received the Province of Alberta Graduate Scholarship for the years 1961-62 and 1962-63.

In conclusion, the author wishes to thank his wife, Jean, for her constant encouragement, patience, and understanding.



## CONTENTS

	PAGE
INTRODUCTION . . . . .	1

## CHAPTER I

THEORETICAL CONSIDERATIONS OF ANTICLASTIC CURVATURE IN BEAMS AND PLATES . . . . .	6
--	---

1.1 HISTORICAL REVIEW . . . . .	6
1.1.2 Preliminary Remarks . . . . .	6
1.1.2 Saint-Venant . . . . .	7
1.1.3 Kelvin and Tait . . . . .	9
1.1.4 Lamb . . . . .	10
1.1.5 Searle . . . . .	22
1.1.6 Timoshenko . . . . .	37
1.1.7 Case . . . . .	41
1.1.8 Ashwell . . . . .	41
1.1.9 Fung and Wittrick . . . . .	45
1.1.10 Concluding Remarks . . . . .	46
1.2 COMPUTER RESULTS OF LAMB'S SOLUTION . . . . .	48
1.2.1 Governing Equations for Deflection . . . . .	48
1.2.2 Remarks on Case's "Discontinuity" . . . . .	51
1.2.3 Comparison of Results With Those of Earlier Investigators . . . . .	53
1.2.4 Edge Effect . . . . .	56





	PAGE
1.3 CURVATURE, BENDING MOMENT RELATION . . . . .	57
1.3.1 Computer Solution of Timoshenko Relation .	57
1.3.2 Comparison with Timoshenko and Ashwell . .	61
1.4 PROBLEM OF CYLINDRICAL SHELL . . . . .	63

## CHAPTER II

EXPERIMENTAL METHODS IN DETERMINING SMALL TRANSVERSE DEFLECTIONS . . . . .	67
2.1 PREVIOUS EXPERIMENTAL WORK . . . . .	67
2.1.1 General Remarks . . . . .	67
2.1.2 Ashwell and Greenwood . . . . .	68
2.1.3 Experiments at the University of Alberta .	70
2.1.4 Discussion and Summary . . . . .	71
2.2 MEASUREMENT OF TRANSVERSE DEFLECTIONS BY MEANS OF ELECTRICAL RESISTANCE STRAIN GAUGES . . . . .	73
2.2.1 Basic Assumptions . . . . .	73
2.2.2 Analysis of Strains to Obtain Deflections .	74
2.2.3 Numerical Methods of Integration . . . . .	76
2.2.4 Trapezoidal Rule . . . . .	76
2.2.5 Application of the Trapezoidal Rule to Obtain Deflections . . . . .	79
2.2.6 Calculation of Centroidal Axis . . . . .	80
2.3 COMPUTER ANALYSIS OF EXPERIMENTAL DATA . . . . .	83



	PAGE
2.4 EXPERIMENTAL APPARATUS . . . . .	83
2.4.1 Loading Frame . . . . .	83
2.4.2 Plate Size . . . . .	84
2.4.3 Strain Gauges . . . . .	86
2.4.4 Transverse Sensitivity . . . . .	88
2.4.5 Adhesive, Wire, Solder, Waterproofing . . .	91
2.4.6 Application of DIDAP to the Plate Problem . . . . .	93
2.5 SUMMARY . . . . .	94

### CHAPTER III

EXPERIMENTAL RESULTS OF A RECTANGULAR PLATE UNDER LARGE LONGITUDINAL CURVATURES . . . . .	95
3.1 GENERAL REMARKS . . . . .	95
3.2 SERIES I . . . . .	96
3.2.1 Testing Procedure . . . . .	96
3.2.2 Experimental Results . . . . .	97
3.2.3 Symmetry . . . . .	98
3.2.4 Comparison with Theory . . . . .	99
3.3 SERIES II . . . . .	101
3.3.1 Testing Procedure . . . . .	101
3.3.2 Experimental Results . . . . .	103
3.3.3 Symmetry . . . . .	104
3.3.4 Comparison with Theory . . . . .	105





3.4	EXPERIMENTAL ERROR . . . . .	107
3.4.1	Calibration Error . . . . .	107
3.4.2	Measurement Error . . . . .	107
3.4.3	Truncation Error . . . . .	108
3.4.4	Summary . . . . .	110
3.5	GENERAL DISCUSSION . . . . .	110
3.6	CONCLUSIONS . . . . .	114

## CHAPTER IV

DEVELOPMENT OF MULTI-CHANNEL DIGITAL DATA PROCESSOR . . .		137
4.1	DESIGN CONSIDERATIONS . . . . .	137
4.1.1	Preliminary Remarks . . . . .	137
4.1.2	National Aeronautical Establishment . . . .	138
4.2	CONSTRUCTION . . . . .	139
4.2.1	General Remarks . . . . .	139
4.2.2	Circuit Design . . . . .	143
4.3	DESCRIPTION OF SYSTEM . . . . .	148
4.3.1	Circuit Scanner . . . . .	148
4.3.2	Amplifier . . . . .	148
4.3.3	Analog Digital Voltmeter . . . . .	149
4.3.4	Program Unit . . . . .	152



	PAGE
4.3.5 Paper Tape Punch . . . . .	152
4.3.6 Typewriter . . . . .	153
4.3.7 Combined Operation . . . . .	153
4.4 SENSITIVITY . . . . .	155
4.5 NOISE . . . . .	155
4.5.1 General Remarks . . . . .	155
4.5.2 Inherent Noise . . . . .	156
4.5.3 Noise Filter . . . . .	157
4.5.4 Common Mode Rejection . . . . .	157
4.6 DRIFT . . . . .	159
4.6.1 General Remarks . . . . .	159
4.6.2 Sources of Drift . . . . .	160
4.6.3 Drift Measurements . . . . .	162
4.7 ACCURACY . . . . .	162
4.7.1 General Remarks . . . . .	162
4.7.2 Accuracy of DIDAP . . . . .	163
4.8 CALIBRATION . . . . .	164
4.8.1 General Remarks . . . . .	164
4.8.2 From Microvolts to Microinches per Inch . .	164



4.9	SPEED OF OPERATION . . . . .	166
4.9.1	General Remarks . . . . .	166
4.9.2	Output Speeds . . . . .	166
4.9.3	Speed of ADVN . . . . .	167
4.9.4	Amplifier Speed . . . . .	167
4.9.5	Modifications and Operating Speed of System . . . . .	167
4.10	DISCUSSION OF SYSTEM . . . . .	168
4.10.1	General Remarks . . . . .	168
4.10.2	Advantages . . . . .	169
4.10.3	Disadvantages . . . . .	171
4.10.4	Summary . . . . .	172
4.10.5	Recommendations . . . . .	172
CHAPTER V		
	CONCLUDING REMARKS . . . . .	174
5.1	SUMMARY . . . . .	174
5.2	IMPROVEMENTS AND RECOMMENDATIONS . . . . .	175
5.3	PRACTICAL APPLICATIONS . . . . .	176
5.4	PROBLEMS FOR FURTHER STUDY . . . . .	178
	REFERENCES . . . . .	179
APPENDIX I		
	FORTRAN PROGRAM FOR EVALUATION OF THEORETICAL TRANSVERSE DEFLECTIONS . . . . .	182





## APPENDIX II

FORTTRAN PROGRAM FOR EVALUATION OF RELATIONSHIP BETWEEN BENDING MOMENT, CURVATURE AND STIFFNESS . . . . .	203
--	-----

## APPENDIX III

COMPUTER PROGRAM FOR LGP-30 . . . . .	210
---------------------------------------	-----



## TABLES

TABLE		PAGE
1.1	COMPARISON OF BEAM THEORY WITH LAMB'S SOLUTION . .	54
1.2	EDGE EFFECT . . . . .	56
2.1	TRANSVERSE SENSITIVITY OF STRAIN GAUGES . . . . .	91
3.1	ADJUSTMENT OF $b^2/Rd$ RATIOS . . . . .	98



## FIGURES

FIGURE		PAGE
1.1	FLEXURE OF A BEAM . . . . .	8
1.2	PLATE ELEMENT . . . . .	12
1.3	PLATE TRANSVERSE SECTION . . . . .	12
1.4	LONGITUDINAL SECTION . . . . .	24
1.5	TRANSVERSE SECTION . . . . .	24
1.6	FORCES ON CROSS SECTION . . . . .	29
1.7	TWO MODES OF DEFORMED CROSS SECTION . . . . .	32
1.8	PLATE TRANSVERSE SECTION . . . . .	32
1.9	TRANSVERSE DEFLECTION (LAMB'S THEORY) . . . . .	49
1.10	TRANSVERSE DEFLECTION (ENLARGED SCALE) . . . . .	50
1.11	TRANSITION FROM ANTICLASTIC TO SYNCLASTIC BEHAVIOUR AT CENTERLINE . . . . .	52
1.12	COMPARISON OF BEAM THEORY WITH LAMB'S THEORY . . . . .	55
1.13	"K" AND PERCENTAGE INCREASE IN $\phi$ . . . . .	59
1.14	"K" AND PERCENTAGE INCREASE IN $\phi$ (ENLARGED SCALE) . . . . .	60
1.15	"K", BENDING MOMENT CURVATURE RELATIONSHIP . . . . .	62
1.16	SECTION OF A CYLINDRICAL SHELL . . . . .	65
2.1	STRAIGHT LINE INTERPOLATION . . . . .	77
2.2	COMPUTER CALCULATION OF DEFLECTIONS FROM STRAINS . . . . .	82
2.3	LOAD HANGER ASSEMBLIES . . . . .	85
2.4	PLATE UNDER LOAD . . . . .	85





3.1	TRANSVERSE DEFLECTION FOR $b^2/Rd$ RATIOS	115
to	FROM 0 to 18.48.	to
3.20	TEST SERIES I . . . . .	124
3.21	TRANSVERSE DEFLECTION FOR $b^2/Rd$ RATIOS	125
to	FROM 23.88 to 54.77.	to
3.42	TEST SERIES II . . . . .	135
3.43	LOCATION OF STRAIN GAUGES, SUPPORTS, AND LOADING HANGERS . . . . .	136
4.1	WHEATSTONE BRIDGE . . . . .	140
4.2	SIMPLIFIED CIRCUIT . . . . .	140
4.3	BLOCK DIAGRAM OF DIDAP . . . . .	144
4.4	PHOTOGRAPH OF JUNCTION BOX . . . . .	145
4.5	CIRCUIT FOR SINGLE COMPENSATING GAUGE . . . . .	146
4.6	PHOTOGRAPH OF BALANCING BRIDGE . . . . .	145
4.7	BLOCK DIAGRAM OF AMPLIFIER . . . . .	150
4.8	ADVM CIRCUIT DIAGRAM . . . . .	150
4.9	PROGRAM SEQUENCE SELECTOR BOARD . . . . .	154
4.10	NOISE FILTER . . . . .	158
4.11	MODIFICATION TO SCANNER . . . . .	158
4.12	DIDAP . . . . .	170



## NOTATION

### CHAPTERS I, II, III, AND V.

$b$	Width of beam or plate.
$D$	Flexural rigidity of plate $D = Ed^3/12(1-\nu^2)$ .
$d$	Thickness of beam or plate.
$E$	Modulus of elasticity.
$e_x, e_y, e_z$	Normal strains in $x$ , $y$ , and $z$ directions.
$I$	Second moment of area of cross section.
$k$	Relationship between bending moment, curvature, and stiffness.
$M_x, M_y$	Bending moments per unit distance.
$N_x, N_y$	Normal forces per unit distance.
$Q_x, Q_y$	Shearing forces per unit distance.
$R$	Radius of curvature of neutral surface in longitudinal direction.
$R_x, R_y$	Radii of curvatures of middle surface.
$x, y, z$	Rectangular coordinates, where the $x$ -axis is in the transverse direction and passes through the centroid of the deformed cross section, the $y$ -axis is in the longitudinal direction, and the $z$ -axis is perpendicular to the $x$ - $y$ plane.
$w$	Displacement of the middle surface in the $z$ direction measured from the $x$ -axis.
$\nu$	Poisson's ratio.
$\sigma_x, \sigma_y, \sigma_z$	Normal stresses in $x$ , $y$ , and $z$ directions.
$\phi$	Relationship between bending moment, curvature, and stiffness.



## NOTATION

### CHAPTER IV

$E_o$	Voltage output of Wheatstone bridge.
$E_v$	Excitation voltage of Wheatstone bridge.
$I$	Current.
$k$	Strain gauge factor.
$R_c$	Variable resistor of Wheatstone bridge.
$R_d$	Resistance of dummy gauge.
$R_g$	Resistance of active gauge.
$R_s$	Shunt resistance.





## INTRODUCTION

### HISTORY OF THE PROBLEM

The bending of beams and plates has engaged the attention of distinguished minds ever since the seventeenth century. In 1632 Galileo discussed the problem of a beam when bent by loads, but it was Saint-Venant, in 1864, who was the first to record the transverse distortion of a beam when bent by couples applied to the ends. However, the theory developed by Saint-Venant is not valid when the cross section is very wide compared to its depth. This was noticed by Kelvin and Tait in 1879 but they believed there were two solutions to the problem of flexure; one for beams and one for plates. Two years later, in 1891, Lamb presented a solution to the problem which considered both beam and plate behaviour. In 1923 Timoshenko used Lamb's solution to develop a theoretical relationship ( $k$  or  $\phi$ ) between the applied moment, the resulting curvature, and the stiffness ( $EI$ ).

Various experiments were proposed by Searle in 1908 to observe how a beam or plate deflected. It was not until 1950, using an optical technique to measure the transverse slopes, that some verification was given for Lamb's theory by Ashwell and Greenwood. Ashwell also showed, using Lamb's solution, that the mode of transverse deflection depended on the dimensionless parameter  $b^2/Rd$ . That is, when  $b^2/Rd$  is less than one, beam theory is valid, and when  $b^2/Rd$  is greater than 100, plate theory is valid.



## AIM OF THE THESIS

This problem was first brought to the attention of the author in 1959 by an internal report published by the National Research Council, Ottawa, in which the effective modulus of elasticity found in tests conducted on swept-back aircraft wings did not coincide with the "plate E" as expected. As a result, the author attempted to investigate in his M.Sc. thesis the transverse distortion of plates under very large longitudinal curvatures ( $b^2/Rd$  ratios up to 190 were recorded). Instead of agreeing with the results of Ashwell and Greenwood, and the theory of Lamb, these results disagreed markedly. In fact, synclastic bending of the transverse strip was observed instead of the anticlastic form which was expected.

Because of the disagreement between theory and experiment observed in the author's M.Sc. thesis, and the fact that the experimental results of Ashwell and Greenwood were not completely conclusive (they tested only up to a  $b^2/Rd$  ratio of 11.8), the question was reopened to establish whether Lamb's solution was valid, especially in the range of large  $b^2/Rd$  values.

In this thesis good agreement between experiment and theory was found for  $b^2/Rd$  ratios up to 55. Larger  $b^2/Rd$  ratios were impossible because of the geometric configurations of the test plate and loading frame. It was first believed that the abnormal results recorded in the author's M.Sc. thesis were due to the manner in which the loads were applied and the influence of the support conditions. However, this is not





supported by the present work and, in fact, the supports and loaded conditions did not affect the transverse deflections for  $b^2/Rd$  ratios up to 55. It is now believed that the discrepancies noted between experiment and theory in the M.Sc. thesis were due to initial imperfections in the plates and use of a poor technique in the loading of the plates.

Generally, the experimental method in the present work is the same as that used in the author's M.Sc. thesis. Instead of using a manual strain gauge recorder to measure the transverse strains, an automatic multi-channel digital data processor was used. It was found with this apparatus that the readings were more accurate and the speed of operation was increased by at least a factor of ten. A suitable program using a numerical integration procedure was written for a digital computer so that strain gauge readings recorded on perforated tape could be fed directly into the computer with no intermediate operations. The use of the computer reduced the computation time from days to a matter of minutes.

## CONTENTS OF THE THESIS

In Chapter I of this thesis an historical review and development of the theory is given for all known investigators who have concerned themselves with the problem of transverse deflections of beams and plates when bent into large longitudinal curvatures.

Three different experimental methods used in determining





the transverse distortions are discussed in Chapter II. The merits of previous experimental work are discussed. A numerical procedure, based on the trapezoidal rule, is developed for use with a digital computer in order to calculate deflections from the readings of electrical resistance strain gauges.

In Chapter III the experimental results are presented for a rectangular plate when bent into large longitudinal curvatures. The experimental values are compared to Lamb's solution for  $b^2/Rd$  ratios from 0 to 55. Also, the results of a series of tests are given which evaluated the influence of the supports and load conditions on the transverse deflections.

The apparatus used in gathering the experimental data from strain gauges was developed at the University of Alberta, Department of Mechanical Engineering. This equipment (a multi-channel digital data processor) is fully discussed in Chapter IV. It is shown how this equipment can be used in conjunction with the LGP-30 digital computer.

A summary of the thesis is given in Chapter V in which the practical application of the problem is discussed. The work of this thesis has suggested some additional problems and these are mentioned.

In Appendix I the Fortran program for the IBM-1620 digital computer is given for evaluating the transverse deflections using the theory developed by Lamb. Representative values of the transverse deflection ( $w/d$ ) versus the distance across the width of the plate are given for  $b^2/Rd$  ratios of 0.32 to 320.



A similar Fortran program is presented in Appendix II for the evaluation of the theoretical relationship ( $k$  or  $\phi$ ) between the bending moment, curvature, and stiffness. Values of  $k$ ,  $\phi$ , and the percentage increase in  $\phi$  are given for Poisson's ratios of 0.300, 0.310, 0.320 and 0.333 for  $b^2/Rd$  ratios from 0.1 to 1000.

The computer program for the evaluation of deflections from strains, using the trapezoidal rule, is given in Appendix III. This program, which includes all subroutines, was written in machine language for the LGP-30 computer. A list of operator instructions is also given.



## CHAPTER I

### THEORETICAL CONSIDERATIONS OF ANTICLASTIC CURVATURE IN BEAMS AND PLATES

An historical review is given for the problem of transverse distortions of a beam or plate when bent by uniform moments applied along two opposite edges, the other two edges being free. It is concluded that the theory developed by Lamb is the most plausible presented since it yields a solution to the problem for both beam action and plate action and the transition between these two extremes. The curvature bending moment relationship developed by Timoshenko is derived using the theory of Lamb. Finally, it is shown that Lamb's theory can be used to solve the problem of a closed cylindrical shell bent by uniform moments applied along the edges.

#### 1.1 HISTORICAL REVIEW

##### 1.1.1 Preliminary Remarks

When a beam, whose breadth is of the same order of magnitude as its depth, is bent by uniform couples applied to its ends producing a given curvature in the longitudinal direction, there is a corresponding curvature in the transverse or lateral direction. Although the problem of flexure of beams was discussed as early as 1632 by Galileo it was Saint-Venant in 1864 who was the first<sup>1,2</sup> to record the mathematical analysis of the contraction

---

1 Todhunter J., and Pearson K., A History of the Theory of Elasticity, Cambridge, 1893, Vol. II, Part 2, p. 414.

2 Timoshenko, S.P., History of Strength of Materials, McGraw-Hill 1953, p. 135.





and elongation of the transverse fibers of a beam bent by longitudinally applied couples. The problem was further discussed in 1879 by Kelvin and Tait who actually reposed the problem in terms of a plate. In 1891 Lamb presented a solution to the problem which considered the behaviours of both beams and plates.

The following sections present the work of all the known investigators who have discussed the problem of transverse distortions from the time of Saint-Venant to the present date. In the interests of completeness, considerable detail is given.

### 1.1.2 Saint-Venant

Saint-Venant showed in his notes to Navier's<sup>3</sup> work that the theory of a beam, when bent to a circular arc of radius  $R$  by equal and opposite couples applied to the ends, is founded on two hypotheses, namely:

1. Plane sections, normal to the length of the beam, before deformation remain the same during deformation;
2. That the longitudinal fibers can be considered as small isolated prisms such that adjacent prisms act independently one from the other. That is to say, there are no stresses acting on the sides of the prisms, so that in bending, the longitudinal fibers experience only pure tension or compression.

Saint-Venant went on to show that if a beam were bent, as in Figure 1.1, to a curvature  $1/R$  there would be an anti-clastic curvature  $-\nu/R$  in the transverse direction, where  $\nu$  is

---

3 Navier, L.M.H., Résumé des Leçons, Troisième édition avec des notes et des appendices par M. Barré de Saint-Venant, Paris 1864, pp. 32-36.





Poisson's ratio for the beam material. The minus sign indicates the curvature is opposite in sense to that in the longitudinal direction.

In the longitudinal direction it can be shown that

$$\frac{1}{R_y} = - \frac{e_y}{z} ,$$

where  $e_y$  is the strain in the y-direction and  $z$  is the distance measured radially from the neutral surface. Similarly, in the transverse direction

$$\frac{1}{R_x} = - \frac{e_x}{z} .$$

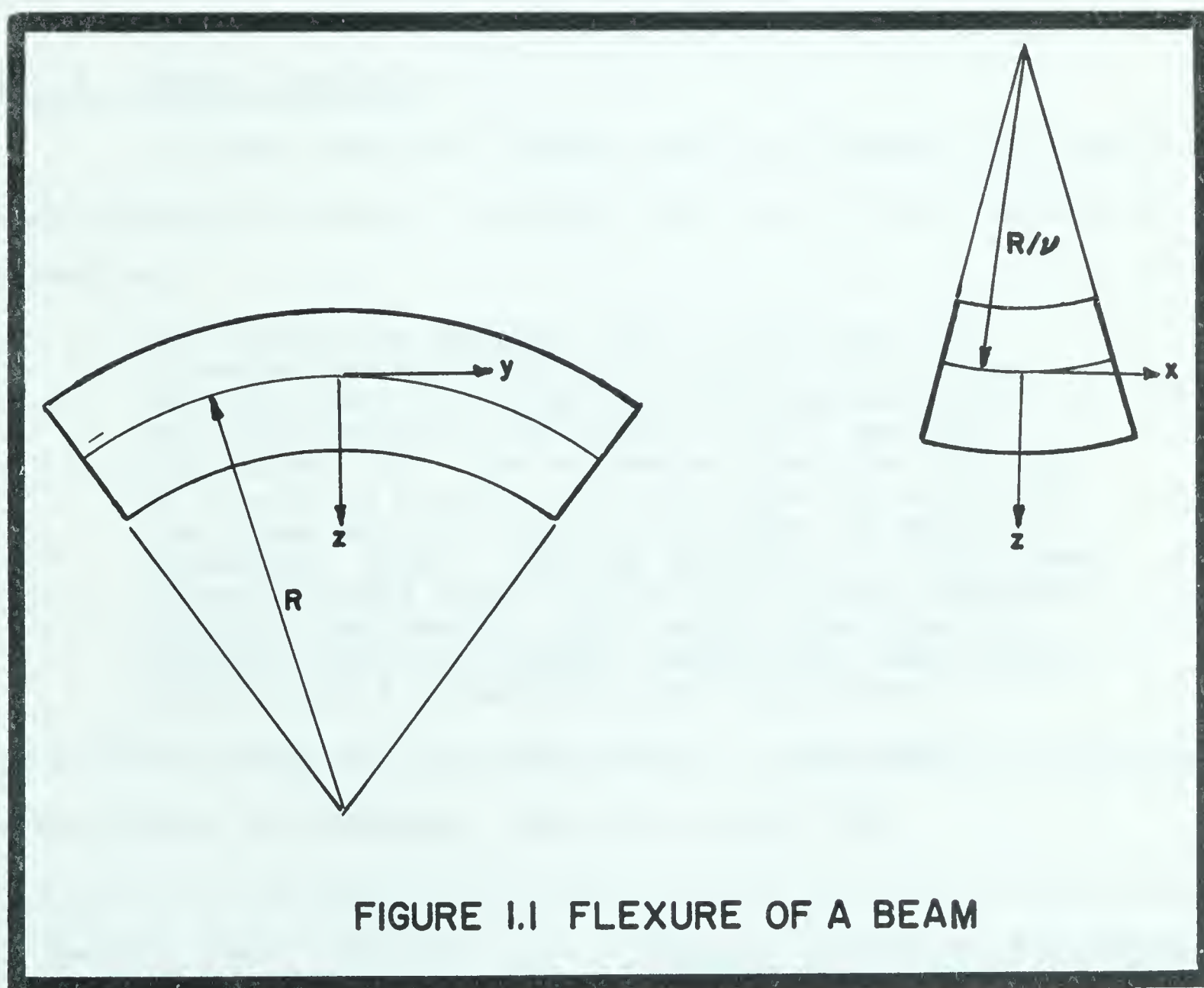


FIGURE 1.1 FLEXURE OF A BEAM



But, from the definition of Poisson's ratio it is known that

$$e_x = -\nu e_y,$$

thus,

$$\frac{1}{R_x} = \frac{\nu e_y}{z}$$

and,

$$\frac{1}{R_x} = -\frac{\nu}{R_y}.$$

Although Saint-Venant was well aware that to obtain a constant transverse curvature the two mentioned assumptions must be rigorously fulfilled, it is not clear whether he investigated the range of values of  $R_y$  within which these assumptions remain valid.

### 1.1.3 Kelvin and Tait

In their treatise<sup>4</sup> Kelvin and Tait discuss the limits under which anticlastic curvature can occur in the transverse direction.

For unless the breadth,  $[b]$ , of the bar (or diameter perpendicular to the plane of flexure) be very small in comparison with the mean proportional between the radius,  $[R/\nu]$ , and the thickness,  $[d]$ , the distances from [the midline of the cross section] to the [upper] corners [of the cross section] would fall short of half the thickness,  $[d/2]$ , and the distances to [the lower corners] would exceed it by differences comparable with its own amount. This would give rise to sensibly less and greater shortenings and stretchings in the filaments towards the corners....

If  $b$  is the width of the cross section,  $d$  the depth,  $R/\nu$  the transverse radius of curvature, then this means that

---

<sup>4</sup> Kelvin, Lord, and Tait, P.G., Treatise on Natural Philosophy, Cambridge, 1879, Part II, Sec. 716-717.





$$b < \left[ \frac{R}{v} d \right]^{1/2} ,$$

or

$$\frac{b^2}{Rd} < 3 ,$$

where Poisson's ratio has been taken as one-third.

On the margin of their book next to the quotation above, Kelvin and Tait make the remark that these are "Uncalculated effects of ordinary bendings of a thin flat spring." They go on to say

Unhappily mathematicians have not hitherto succeeded in solving, possibly not even tried to solve, the beautiful problem thus presented by the flexure of a broad very thin band (such as a watch spring) into a circle of radius comparable with a third proportional to its thickness and its breadth.

#### 1.1.4 Lamb

The challenge issued by Kelvin and Tait did not go unnoticed. In 1891 Horace Lamb gave a complete solution to the problem in a paper presented to the Philosophical Society<sup>5</sup>. He noted that

The extensions and contractions of the middle surface of the band, which are called into play by the tendency to the contrary curvature in the direction of the breadth, keep this curvature in check, so that the strained form never deviates appreciably from that of a cylinder.

Lamb's solution is reproduced below in a somewhat modified form.

---

<sup>5</sup> Lamb, H., On the Flexure of a Flat Elastic Spring, Phil. Mag. Ser. 5, Vol. 31, 1891, pp. 182-188.

For other treatments of the same problem see also:  
Love, A.E.H., Mathematical Theory of Elasticity, Dover 1944, pp. 553-557.

Green, A.E., and Zerna, W., Theoretical Elasticity, Oxford, 1954, pp. 435-437.





Consider an element cut out of a plate, of width  $b$  and thickness  $d$ , which is subjected to a longitudinal curvature produced by uniform moments  $M_y$  applied to two opposite edges which lie in the  $x$ - $z$  plane as shown in Figure 1.2. It is assumed the weight of the plate can be neglected.

The moments and the forces are measured per unit length. Because the  $x$  and  $y$  axes have been chosen to lie in the principal directions of bending, the forces and moments in these directions are principal values and will be denoted by a single subscript.

The equilibrium of the element will now be considered.

#### Force Equilibrium

$$\sum F_x = 0$$

$$\left[ N_x + \frac{\partial N_x}{\partial x} dx \right] dy - N_x dy = 0$$

or,

$$\frac{\partial N_x}{\partial x} dx dy = 0$$

and since  $dx dy$  is completely arbitrary this becomes

$$\frac{\partial N_x}{\partial x} = 0$$

or

$$N_x = f(y)$$

and is independent of  $x$ . However, at the edges  $x = \pm b/2$  there are no surface forces and thus  $N_x$  must be zero at these edges. But if  $N_x$  is zero at the edges and is independent of  $x$ , then it must be zero everywhere. Thus,

$$N_x = 0 \quad \text{for all } x \quad 1.1$$

$$\sum F_z = 0$$

$$\left[ Q_x + \frac{\partial Q_x}{\partial x} dx \right] dy - Q_x dy + N_y dx \sin(d\theta) = 0$$



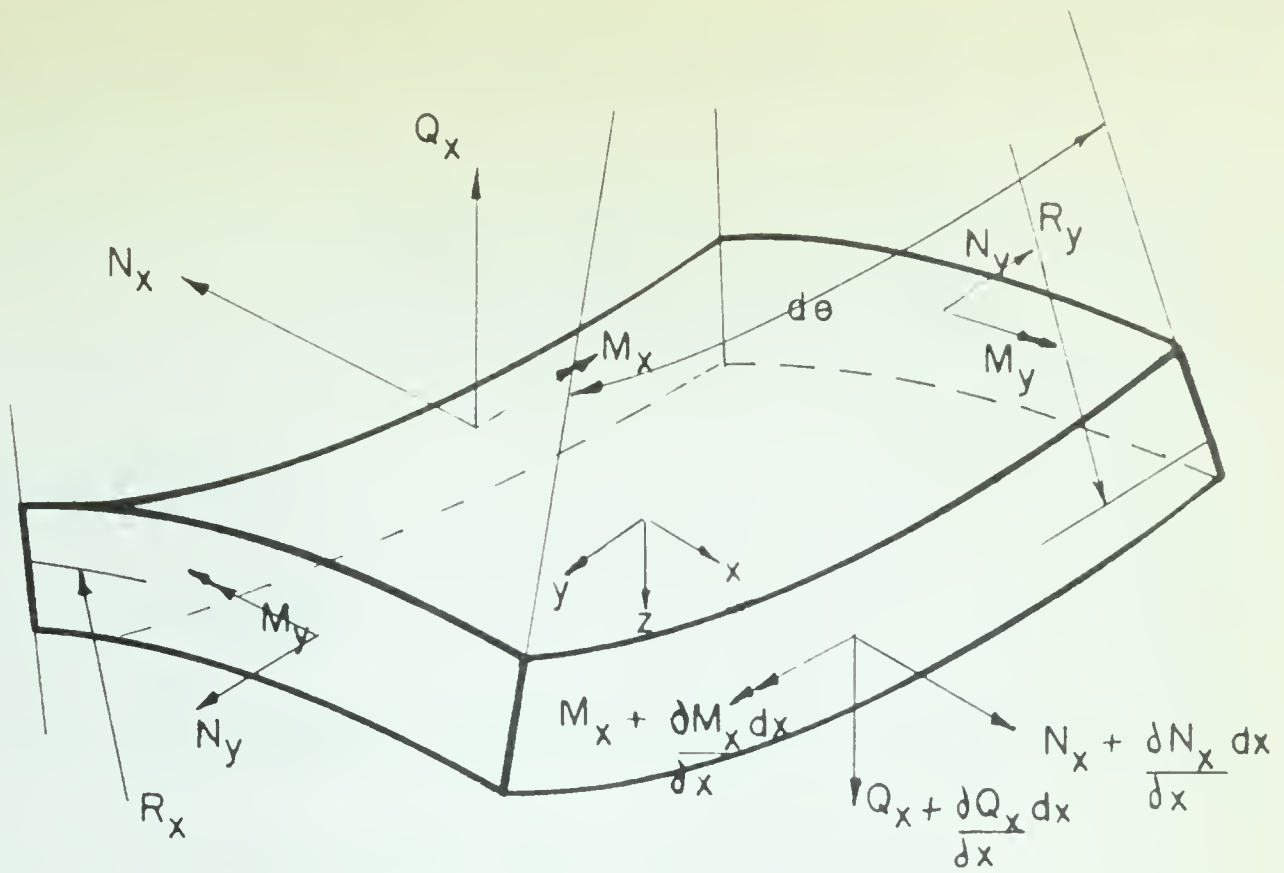


FIGURE 1.2 PLATE ELEMENT

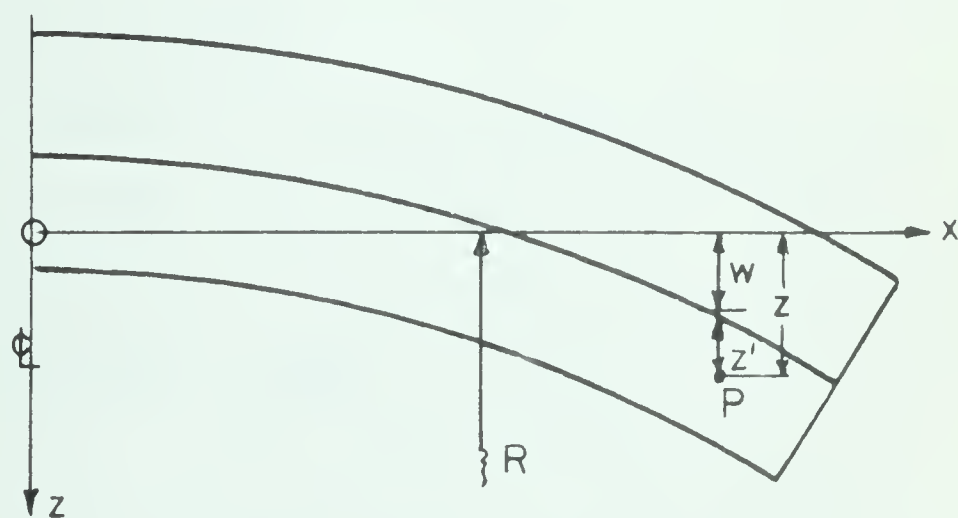


FIGURE 1.3 PLATE TRANSVERSE SECTION



but because  $d\theta$  is small,  $\sin d\theta \doteq d\theta$ , and since  $R_y d\theta = dy$ , this equation reduces to

$$\frac{\partial Q_x}{\partial x} + \frac{N_y}{R_y} = 0, \quad 1.2$$

### Moment Equilibrium

$\sum M = 0$  in y-direction

$$\left[ M_x + \frac{\partial M_x}{\partial x} dx \right] dy - M_x dy - \left[ Q_x + \frac{\partial Q_x}{\partial x} dx \right] dx dy = 0$$

and neglecting second order terms this becomes,

$$\frac{\partial M_x}{\partial x} - Q_x = 0. \quad 1.3$$

Eliminating  $Q_x$  from equations 1.2 and 1.3 yields

$$\frac{\partial^2 M_x}{\partial x^2} + \frac{N_y}{R_y} = 0. \quad 1.4$$

### Stress Strain Relationships

It is assumed the stress in the z-direction is negligible compared to the other stresses. From Hooke's law and the principle of superposition the stress strain relationships in the x and y directions become

$$Ee_x = \sigma_x - \nu\sigma_y$$

$$Ee_y = \sigma_y - \nu\sigma_x$$

or,

$$\sigma_x = \frac{E}{(1-\nu^2)} (e_x + \nu e_y) \quad 1.5$$

$$\sigma_y = \frac{E}{(1-\nu^2)} (e_y + \nu e_x). \quad 1.6$$



### Geometric Relationships

Due to the uniform moments applied along the edges  $y = \pm$  constant, a bending strain will be produced which will be proportional to the curvatures at the point under consideration. That is,

$$\epsilon_x = - \frac{z'}{R_x} \quad , \quad \epsilon_y = - \frac{z'}{R_y} \quad 1.7$$

where  $z'$  is the distance measured from the middle surface to any arbitrary point P in the plate cross section, and from Figure 1.3,  $z' = z - w$ , where  $w$  is the radial displacement in the  $z$ -direction measured from the  $x$ -axis to the midline of the transverse cross section. Therefore, the moment in the  $x$ -direction is

$$M_x = \int_{-d/2}^{d/2} z' \sigma_x dz'$$

and from equations 1.5 and 1.7 this becomes

$$M_x = - D \left[ \frac{1}{R_x} + \frac{\nu}{R_y} \right] \quad 1.8$$

where the flexural rigidity of the plate is defined as

$$D = \frac{Ed^3}{12(1 - \nu^2)} .$$

The strains given by equation 1.7 are bending strains only. Membrane strains will also occur when the transverse cross section begins to distort as shown in Figure 1.3. The total strain in the  $y$ -direction at an arbitrary point P will be given by

$$\epsilon_y = - \frac{z' + w}{R_y} = - \frac{z'}{R - w} - \frac{w}{R - w} . \quad 1.9$$

The first term on the right hand side is the strain caused by





bending as shown above; the second term is the membrane strain caused by the stretching (or contraction) of the middle fibers. The membrane forces induced by this stretching are given by

$$N_Y = \int_{-d/2}^{d/2} \sigma_Y dz' \quad 1.10$$

and,

$$N_X = \int_{-d/2}^{d/2} \sigma_X dz'. \quad 1.11$$

But, the membrane force in equation 1.11 is equal to the stress at the middle surface (i.e., at  $z' = 0$ ) multiplied by the thickness  $d$ . Therefore,

$$N_X = (d) \left[ \sigma_X \right]_{z'=0},$$

and from equations 1.1 and 1.5

$$N_X = 0 = \frac{Ed}{(1-\nu^2)} \left[ e_X + \nu e_Y \right]_{z'=0},$$

therefore

$$\left[ e_X + \nu e_Y \right]_{z'=0} = 0. \quad 1.12$$

Using equation 1.12 in equation 1.10 yields

$$N_Y = E \int_{-d/2}^{d/2} \left[ e_Y \right]_{z'=0} dz' = - E \int_{-d/2}^{d/2} \left[ \frac{w}{R-w} \right] dz'$$

and,

$$N_Y = - \frac{Ewd}{R-w}. \quad 1.13$$

Substituting equations 1.8 and 1.13 into the equilibrium equation 1.4 it follows, assuming  $D$  is a constant

$$D \frac{\partial^2}{\partial x^2} \left[ \frac{1}{R_x} + \frac{\nu}{R-w} \right] + \frac{Ewd}{(R-w)^2} = 0 \quad 1.14$$



For a given transverse strip,  $w$  is a function of  $x$  only, and the partial derivatives of equation 1.14 may be replaced with total derivatives. The exact expression for the curvature in the  $x$ -direction can be shown to be

$$\frac{1}{R_x} = \frac{\frac{d^2 w}{dx^2}}{\left[1 + \left(\frac{dw}{dx}\right)^2\right]^{3/2}} .$$

Since the slopes  $\frac{dw}{dx}$  are very much less than one, their squares may be neglected. Thus

$$\frac{1}{R_x} = \frac{d^2 w}{dx^2} ,$$

and equation 1.14 becomes

$$D \frac{d^2}{dx^2} \left[ \frac{d^2 w}{dx^2} + \frac{\nu}{R-w} \right] + \frac{Ewd}{(R-w)^2} = 0$$

or,

$$\frac{d^4 w}{dx^4} + \frac{\nu}{(R-w)^2} \frac{d^2 w}{dx^2} + \frac{2\nu}{(R-w)^3} \left[ \frac{dw}{dx} \right]^2 + \frac{12(1-\nu^2)w}{d^2(R-w)^2} = 0 . \quad 1.15$$

This equation is a non-linear, fourth order differential equation. Before an attempt is made to solve it there are certain negligible terms which can be eliminated, thus making the equation more manageable. It can be argued a posteriori that the third term is a negligible quantity.\* It can be shown the second term is also negligible. Using the approximation

$$R - w \doteq R$$

---

\* The maximum slope for any given curve occurs at the edge  $x = \pm b/2$  and increases with increased  $b^2/Rd$ . For a  $b^2/Rd$  of 320.0 the third term in equation 1.15 is smaller than the fourth term by a factor of approximately  $10^5$ .



and the notation

$$4\alpha^4 = \frac{12(1-\nu^2)}{R^2 d^2} \quad 1.16$$

the characteristic equation of equation 1.15 is

$$m^4 + \frac{\nu}{R^2} m^2 + 4\alpha^4 = 0$$

or

$$2m^2 = -\frac{\nu}{R^2} \pm \left[ \frac{\nu^2}{R^4} - 16\alpha^4 \right]^{1/2}.$$

In order to determine whether the second derivative term is significant or not, it is required to show that

$$\frac{\nu}{R^2} \ll 4\alpha^2. \quad 1.17$$

From equation 1.16, for  $\nu = 1/3$ , it follows that

$$\frac{d^2}{R^2} \ll 384.$$

For an aluminum plate having a yield stress of 67,000 psi and a modulus of elasticity of  $10.4 \times 10^6$  psi, the yield strain will be 6440  $\mu$ in. per in. The maximum strain in a plate bent by end couples applied along the edges  $y = \pm$  constant will be at the surface in the longitudinal direction; that is,

$$\left[ e_y \right]_{\max} = \frac{d}{2R}$$

and if the plate is allowed to bend to its maximum without yielding, then

$$\frac{d}{R} = 2(6440 \times 10^{-6})$$

or

$$\frac{d^2}{R^2} = 0.000169$$

and thus the inequality in 1.17 is justified. The expression for





$m^2$  then reduces to

$$m = \pm \left[ \frac{-v}{2R^2} \pm 2\alpha^2 i \right]^{1/2}$$

where  $i = (-1)^{1/2}$ . Setting the expression on the right hand side to  $(a + ib)$ , squaring, and evaluating the real and imaginary coefficients  $a$  and  $b$ , it follows that

$$m = \pm \left\{ \left[ \frac{-v}{4R^2} \pm \left[ \frac{v^2}{16R^4} + \alpha^4 \right]^{1/2} \right]^{1/2} + i \left[ \frac{v}{4R^2} \pm \left[ \frac{v^2}{16R^4} + \alpha^4 \right]^{1/2} \right]^{1/2} \right\}$$

and by virtue of the inequality in 1.17 this reduces to

$$m = \pm \left\{ \left[ \frac{-v}{4R^2} \pm \alpha^2 \right]^{1/2} + i \left[ \frac{v}{4R^2} \pm \alpha^2 \right]^{1/2} \right\}$$

which further reduces to

$$m = \pm (1 \pm i)\alpha.$$

Thus the contribution of the second derivative in equation 1.15 can be neglected, and the characteristic equation is simplified to

$$m^4 + 4\alpha^4 = 0 \quad 1.18$$

which has four roots, as shown above, equal to  $\pm(1+i)\alpha$ ,  $\pm(1-i)\alpha$ .

The solution of this equation is then

$$w = C_1 e^{(1+i)\alpha x} + C_2 e^{-(1+i)\alpha x} + C_3 e^{(1-i)\alpha x} + C_4 e^{-(1-i)\alpha x},$$

which can be rewritten in the form

$$w = A \cosh \alpha x \cos \alpha x + B \cosh \alpha x \sin \alpha x \\ + C \sinh \alpha x \sin \alpha x + D \sinh \alpha x \cos \alpha x, \quad 1.19$$

where the constants  $A, B, C, D$  are real.



### Boundary Conditions

At the free edge of the plate (i.e., at  $x = \pm b/2$ ) the moments and shear forces are zero. Therefore,

$$V_x = Q_x + \frac{\partial}{\partial y} (M_{xy}) = 0 \text{ at } x = \pm b/2$$

or,

$$V_x = D \frac{\partial}{\partial x} (\nabla^2 w) + \frac{\partial}{\partial y} \left[ -D(1+\nu) \frac{\partial^2 w}{\partial x \partial y} \right] .$$

Since  $w$  is a function of  $x$  only for a given transverse strip, the condition for zero shear at the free edge of the plate reduces to

$$V_x = -D \frac{d^3 w}{dx^3} = 0$$

or,

$$\left[ \frac{d^3 w}{dx^3} \right]_{x=\pm b/2} = 0 . \quad 1.20$$

The condition for zero moment at the free edge of the plate is given by equation 1.8

$$M_x = -D \left[ \frac{d^2 w}{dx^2} + \frac{\nu}{R_y} \right] = 0 .$$

Using the approximation  $R_y = R - w \doteq R$ , it follows, that at the edge of the plate

$$\frac{d^2 w}{dx^2} = -\frac{\nu}{R} \text{ at } x = \pm b/2 . \quad 1.21$$

From equation 1.19 it follows that

$$\begin{aligned} \frac{dw}{dx} = & \alpha A (\sinh \alpha x \cos \alpha x - \cosh \alpha x \sin \alpha x) \\ & + \alpha B (\sinh \alpha x \sin \alpha x + \cosh \alpha x \cos \alpha x) \\ & + \alpha C (\cosh \alpha x \sin \alpha x + \sinh \alpha x \cos \alpha x) \\ & + \alpha D (\cosh \alpha x \cos \alpha x - \sinh \alpha x \sin \alpha x) \end{aligned} \quad 1.22$$



$$\begin{aligned} \frac{d^2 w}{dx^2} = & - 2\alpha^2 A \sinh \alpha x \sin \alpha x + 2\alpha^2 B \sinh \alpha x \cos \alpha x \\ & + 2\alpha^2 C \cosh \alpha x \cos \alpha x - 2\alpha^2 D \cosh \alpha x \sin \alpha x \end{aligned} \quad 1.23$$

$$\begin{aligned} \frac{d^3 w}{dx^3} = & - 2\alpha^3 A (\sinh \alpha x \cos \alpha x + \cosh \alpha x \sin \alpha x) \\ & + 2\alpha^3 B (\cosh \alpha x \cos \alpha x - \sinh \alpha x \sin \alpha x) \\ & + 2\alpha^3 C (\sinh \alpha x \cos \alpha x - \cosh \alpha x \sin \alpha x) \\ & - 2\alpha^3 D (\sinh \alpha x \sin \alpha x + \cosh \alpha x \cos \alpha x) . \end{aligned} \quad 1.24$$

Substituting equation 1.24 into equation 1.20 yields

$$\begin{aligned} 0 = & - A \left( \sinh \frac{\alpha b}{2} \cos \frac{\alpha b}{2} + \cosh \frac{\alpha b}{2} \sin \frac{\alpha b}{2} \right) \\ & + B \left( \cosh \frac{\alpha b}{2} \cos \frac{\alpha b}{2} - \sinh \frac{\alpha b}{2} \sin \frac{\alpha b}{2} \right) \\ & + C \left( \sinh \frac{\alpha b}{2} \cos \frac{\alpha b}{2} - \cosh \frac{\alpha b}{2} \sin \frac{\alpha b}{2} \right) \\ & - D \left( \sinh \frac{\alpha b}{2} \sin \frac{\alpha b}{2} + \cosh \frac{\alpha b}{2} \cos \frac{\alpha b}{2} \right) \end{aligned} \quad 1.25$$

and

$$\begin{aligned} 0 = & A \left( \sinh \frac{\alpha b}{2} \cos \frac{\alpha b}{2} + \cosh \frac{\alpha b}{2} \sin \frac{\alpha b}{2} \right) \\ & + B \left( \cosh \frac{\alpha b}{2} \cos \frac{\alpha b}{2} - \sinh \frac{\alpha b}{2} \sin \frac{\alpha b}{2} \right) \\ & - C \left( \sinh \frac{\alpha b}{2} \cos \frac{\alpha b}{2} - \cosh \frac{\alpha b}{2} \sin \frac{\alpha b}{2} \right) \\ & - D \left( \sinh \frac{\alpha b}{2} \sin \frac{\alpha b}{2} + \cosh \frac{\alpha b}{2} \cos \frac{\alpha b}{2} \right) . \end{aligned} \quad 1.26$$

Adding equations 1.25 and 1.26 yields

$$\begin{aligned} B \left( \cosh \frac{\alpha b}{2} \cos \frac{\alpha b}{2} - \sinh \frac{\alpha b}{2} \sin \frac{\alpha b}{2} \right) = \\ D \left( \sinh \frac{\alpha b}{2} \sin \frac{\alpha b}{2} + \cosh \frac{\alpha b}{2} \cos \frac{\alpha b}{2} \right) \end{aligned} \quad 1.27$$

and subtracting them, yields





$$A(\sinh \frac{\alpha b}{2} \cos \frac{\alpha b}{2} + \cosh \frac{\alpha b}{2} \sin \frac{\alpha b}{2}) =$$

$$C(\sinh \frac{\alpha b}{2} \cos \frac{\alpha b}{2} - \cosh \frac{\alpha b}{2} \sin \frac{\alpha b}{2}) . \quad 1.28$$

Substituting equation 1.23 into equation 1.21 yields

$$\frac{-v}{R} = -2\alpha^2 A \sinh \frac{\alpha b}{2} \sin \frac{\alpha b}{2} + 2\alpha^2 B \sinh \frac{\alpha b}{2} \cos \frac{\alpha b}{2}$$

$$+ 2\alpha^2 C \cosh \frac{\alpha b}{2} \cos \frac{\alpha b}{2} - 2\alpha^2 D \cosh \frac{\alpha b}{2} \sin \frac{\alpha b}{2} \quad 1.29$$

and

$$\frac{-v}{R} = -2\alpha^2 A \sinh \frac{\alpha b}{2} \sin \frac{\alpha b}{2} - 2\alpha^2 B \sinh \frac{\alpha b}{2} \cos \frac{\alpha b}{2}$$

$$+ 2\alpha^2 C \cosh \frac{\alpha b}{2} \cos \frac{\alpha b}{2} + 2\alpha^2 D \cosh \frac{\alpha b}{2} \sin \frac{\alpha b}{2} . \quad 1.30$$

Adding equations 1.29 and 1.30 gives

$$\frac{-v}{R} = -2\alpha^2 A \sinh \frac{\alpha b}{2} \sin \frac{\alpha b}{2} + 2\alpha^2 C \cosh \frac{\alpha b}{2} \cos \frac{\alpha b}{2} \quad 1.31$$

and subtracting them gives

$$B = \frac{\cosh \frac{\alpha b}{2} \sin \frac{\alpha b}{2}}{\sinh \frac{\alpha b}{2} \cos \frac{\alpha b}{2}} D , \quad 1.32$$

Substituting equation 1.32 into equation 1.27 gives, after simplification

$$D(\sin \alpha b - \sinh \alpha b) = 0 .$$

Since the expression in brackets can never be zero, for  $b$  greater than zero, it follows that

$$D = B = 0 . \quad 1.33$$

Substituting equation 1.28 into equation 1.29 gives, after simplification



$$\bar{A} = \frac{-\nu}{\alpha^2 R} \frac{\sinh \frac{\alpha b}{2} \cos \frac{\alpha b}{2} - \cosh \frac{\alpha b}{2} \sin \frac{\alpha b}{2}}{\sinh \alpha b + \sin \alpha b} \quad 1.34$$

and,

$$\bar{B} = \frac{-\nu}{\alpha^2 R} \frac{\sinh \frac{\alpha b}{2} \cos \frac{\alpha b}{2} + \cosh \frac{\alpha b}{2} \sin \frac{\alpha b}{2}}{\sinh \alpha b + \sin \alpha b} \quad 1.35$$

where A and C have been replaced by  $\bar{A}$  and  $\bar{B}$  respectively.

Therefore, the final expression for the transverse deflection becomes, from equation 1.19

$$w = \bar{A} \cosh \alpha x \cos \alpha x + \bar{B} \sinh \alpha x \sin \alpha x . \quad 1.36$$

In evaluating the constants of integration an alternative approach is to recognize that the deflected form in the transverse direction should be symmetrical about the origin. This would then admit only even functions of x in the general expression for the deflection which would require that the constants B and D be zero.

A detailed discussion of equation 1.36 is given in Section 1.2.

#### 1.1.5 Searle

In 1908 Searle published a book<sup>6</sup> on experimental elasticity in which he discussed the changes in the cross section of a bar due to bending. Apparently, at the time of this publication, he was unaware of Lamb's solution, for he remarked "The exact solution for finite bending has not yet been found by any

---

<sup>6</sup> Searle, G.F.C., Experimental Elasticity, Cambridge, 1908, pp. 38-58.



mathematician." However, his approach to the problem of the distortion of the transverse cross section is interesting in that he follows the reasoning initiated by Kelvin and Tait.

In the notation of the previous section,  $b$  is the width and  $d$  the depth of the cross section. The member is assumed to be sufficiently long so that the manner in which the loads are applied to the ends  $y = \pm \text{constant}$  does not affect a central transverse strip. Let these loads be a force per unit area denoted by  $\sigma$ . Such loads will bend the member to a radius  $R$ , where  $R$  is the radius of curvature of the neutral surface in the longitudinal direction. From Figure 1.4 it can be seen that the applied forces have a resultant force per unit area in the  $z$ -direction of magnitude equal to  $2\sigma \sin \theta/2$ . If  $s$  is the arc length of the middle surface between the sides of area  $A$  upon which the stresses  $\sigma$  act, and if  $\theta$  is chosen to be small, then the resultant force acting in the  $z$ -direction is equal to  $\sigma As/R$ ; or,  $\sigma/R$  is a force per unit volume and can be considered as a "body force". Searle points out that it is the presence, or lack thereof, of this body force which determines the shape of the transverse cross section. In his discussion he assumes that the sides of the longitudinal fibers are stress free but he notes that in order to fulfil this condition and maintain equilibrium

...it may be necessary to apply to each element of the rod a force like that due to gravity, which may be regarded as acting at a distance.





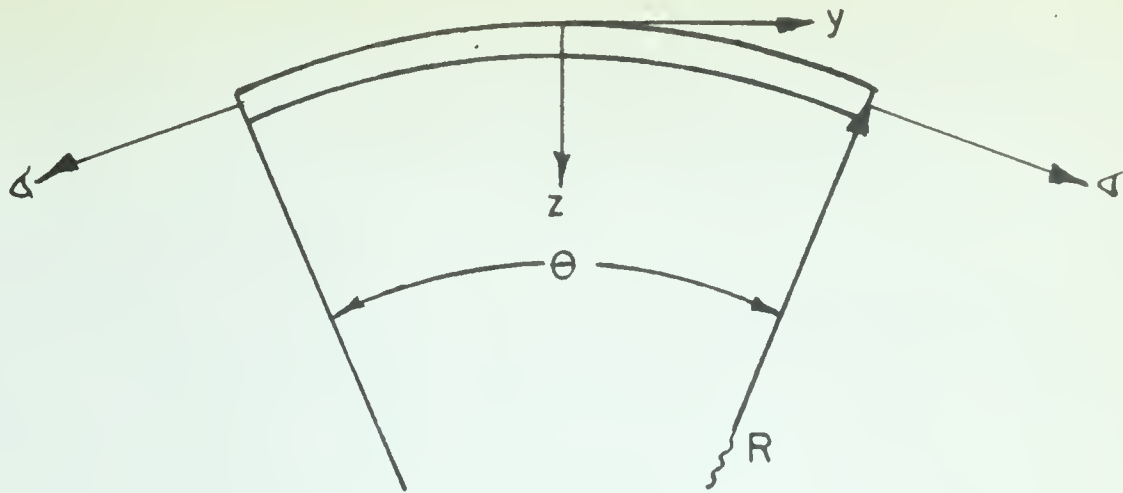


FIGURE 1.4 LONGITUDINAL SECTION

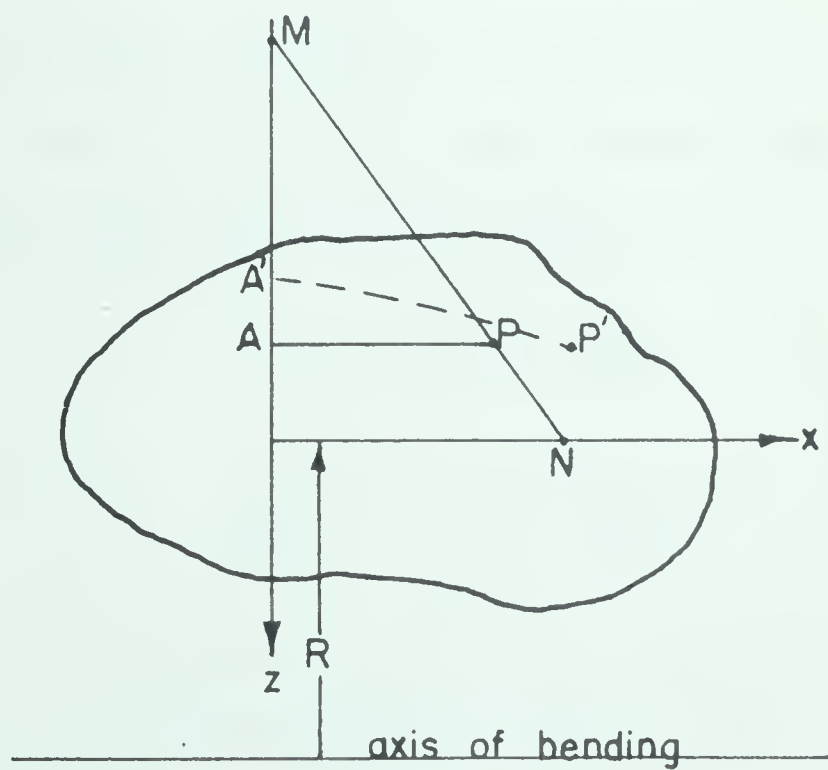


FIGURE 1.5 TRANSVERSE SECTION



### Deformation of Cross Section

Consider in Figure 1.5 the cross section of a rod whose middle fiber has been bent to a radius  $R$  in the longitudinal direction. The width of the rod is assumed to be the same order of magnitude as its depth.

The strain at point  $P$  is  $-z/R$  perpendicular to the plane of the paper. The corresponding strain in the  $x$ -direction will be  $\nu z/R$ . The longitudinal fibers above  $OX$  undergo a lateral contraction, while those below  $OX$  undergo a lateral extension. Let  $P'A'$  be the arc length of a transverse fiber which becomes the straight line  $PA$  when the longitudinal fibers are bent to a radius  $R$ . The transverse strain can be written as

$$e_x = \frac{\nu z}{R} = \frac{PA - P'A'}{P'A'} = \frac{x}{P'A'} - 1$$

or 
$$\frac{x}{P'A'} - \frac{\nu z}{R} = 1$$

where the length of  $PA$  is equal to  $x$  since  $PA$  is parallel to  $OX$ .

Let  $P'A'$  be an arc of a circle whose center is a distance  $R''$  measured along the  $z$ -axis, then the  $x$ -coordinate of  $P'$  will be

$$x' = R'' \sin \frac{P'A'}{R''}$$

or, approximately

$$\frac{x'}{P'A'} = 1 - \frac{1}{6} \left[ \frac{P'A'}{R''} \right]^2,$$

Searle argues, with regard to this last equation, if  $P'A'$  is less than  $R''/10$ , the difference between  $x'$  and  $P'A'$  will be less than  $P'A'/600$  and can be neglected. Therefore, a straight line in the transverse cross section, before bending, given by the equation

$$x' = \text{constant},$$



may be expressed in the deformed condition by the equation

$$\frac{x'}{P'A'} - \frac{vz}{R} = 1 ,$$

provided

$$P'A' < \frac{R''}{10} .$$

All straight lines, originally parallel to the z-axis, in the deformed state will intersect the z-axis at a common point (point M in Figure 1.5). From the above equation at  $x' = 0$  it is seen that this straight line cuts the z-axis at  $-R/v$ . Therefore,

$$OM = \frac{R}{v}$$

and let

$$R' = \frac{R}{v} .$$

It is seen that straight lines originally perpendicular to OX become inclined, intersecting the z-axis at M; or stated another way, straight lines parallel to OX before bending become arcs of circles of radius  $R'$  in the strained condition.

It is interesting to observe the restriction that Searle placed on the above analysis. That is, in order that the anticlastic curvature have a constant radius  $R'$ , the inequality

$$P'A' < \frac{R''}{10}$$

must be valid. This can be written in terms of the dimensions of the plate by noting that the limiting length of  $P'A'$  is half the width of the plate. Also, when  $z$  is small compared with  $R$ , the radius of curvature  $R''$  is approximately equal to  $R'$ . Thus, the inequality can be rewritten as

$$\frac{b}{R} < \frac{1}{5v}$$





Now Searle left the inequality in this form, but it can be written in a more useful form by noting, in the above derivation, that it was assumed that the width of the beam was of the same order of magnitude as its depth. Thus, if the left hand side of the inequality is multiplied by  $b/d$  the right hand side is unchanged in magnitude, and it follows for  $\nu = \frac{1}{3}$ , that

$$\frac{b^2}{Rd} < 0.6 . \quad 1.37$$

### Centroidal Axis of Cross Section

Searle also noted that the cross section will deform about the x-axis so that the x-axis remains the centroidal axis.

The resultant force acting on a cross section is

$$F = \int_A \sigma dA$$

where 
$$\sigma = Ee = - \frac{Ez}{R} , \quad 1.38$$

therefore, 
$$F = - \frac{E}{R} \int_A z dA .$$

For  $F$  to be zero, as it must be, and excluding the trivial case when  $R$  is infinite, it follows that

$$\int_A z dA = 0$$

which by definition, identifies the x-axis as the centroidal axis.



### Removal of "body forces"

Searle investigates the effects on the cross section when the "body force" is removed. It has been shown above that the "body force" is of the form  $\sigma/R$ . Let  $Y$  be the value of this force at an arbitrary point  $P$  in the cross section (see Figure 1.6a). From equation 1.38 then

$$Y = \frac{\sigma}{(R-z)} = - \frac{Ez}{R(R-z)} . \quad 1.39$$

Consider a small element of cross section  $(dx)(dz)$ , located at the point  $P(x,z)$ , bounded by two planes an angle  $d\theta$  apart. The volume of this element is  $(R-z)(d\theta)(dx)(dz)$ , and the radial component of the force acting on this element is

$$dF = - \frac{Ez}{R} d\theta dx dz . \quad 1.40$$

This force is proportional to  $z$  and can act upward or downward depending on whether  $P$  is below or above the  $x$ -axis.

Considering an element of width  $dx$  and height  $d$ , the depth of the cross section, it follows from Figure 1.6b that when  $ab > bc$  there is a resultant downward force on the strip, while if  $ab < bc$  there is a resultant upward force on the strip. Thus, when the transverse cross section begins to distort anticlastically,  $ab < bc$  near the origin while  $ab > bc$  near the edge of the cross section, giving the result of an equilibrated couple applied to the cross section tending to prevent this anticlastic curvature as shown in Figure 1.6C.



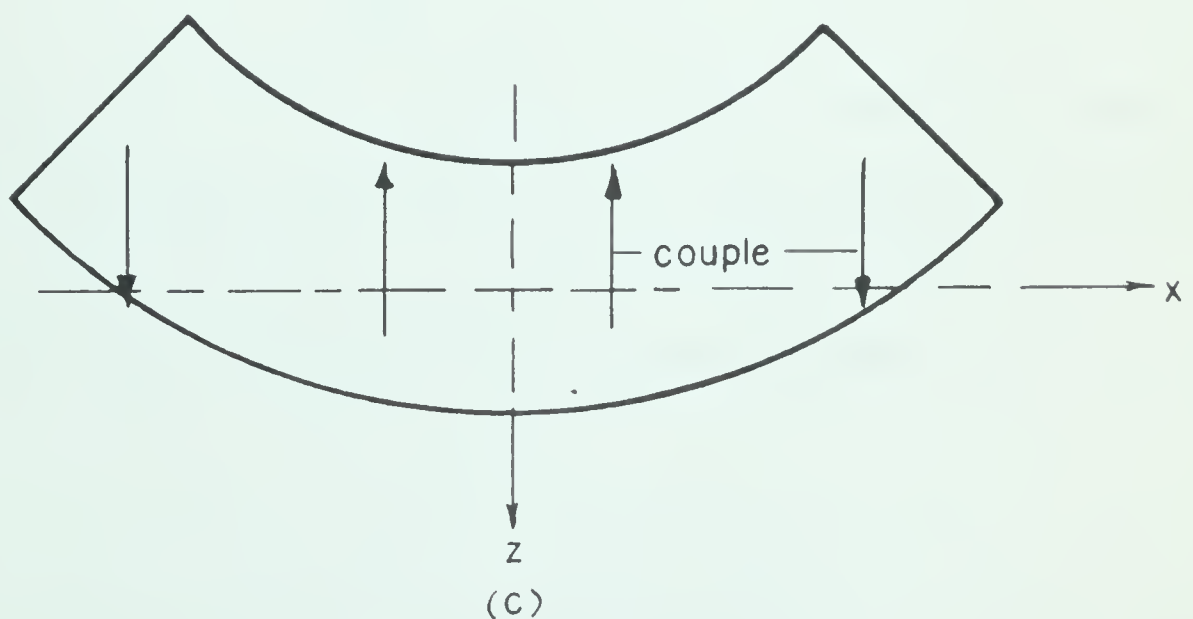
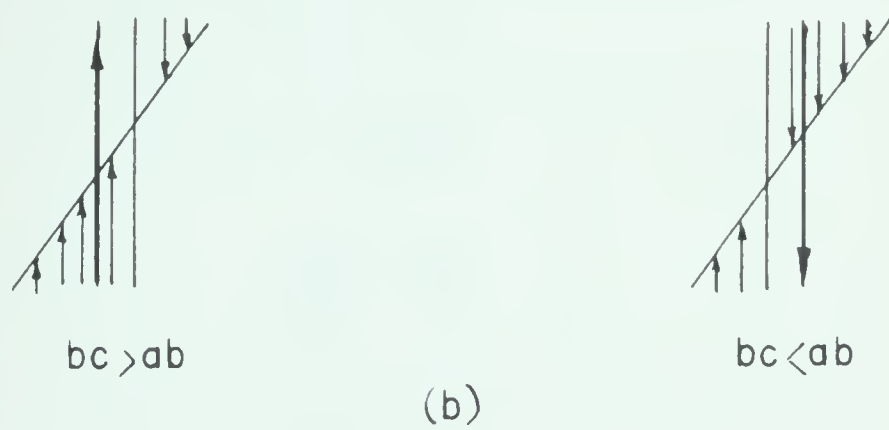
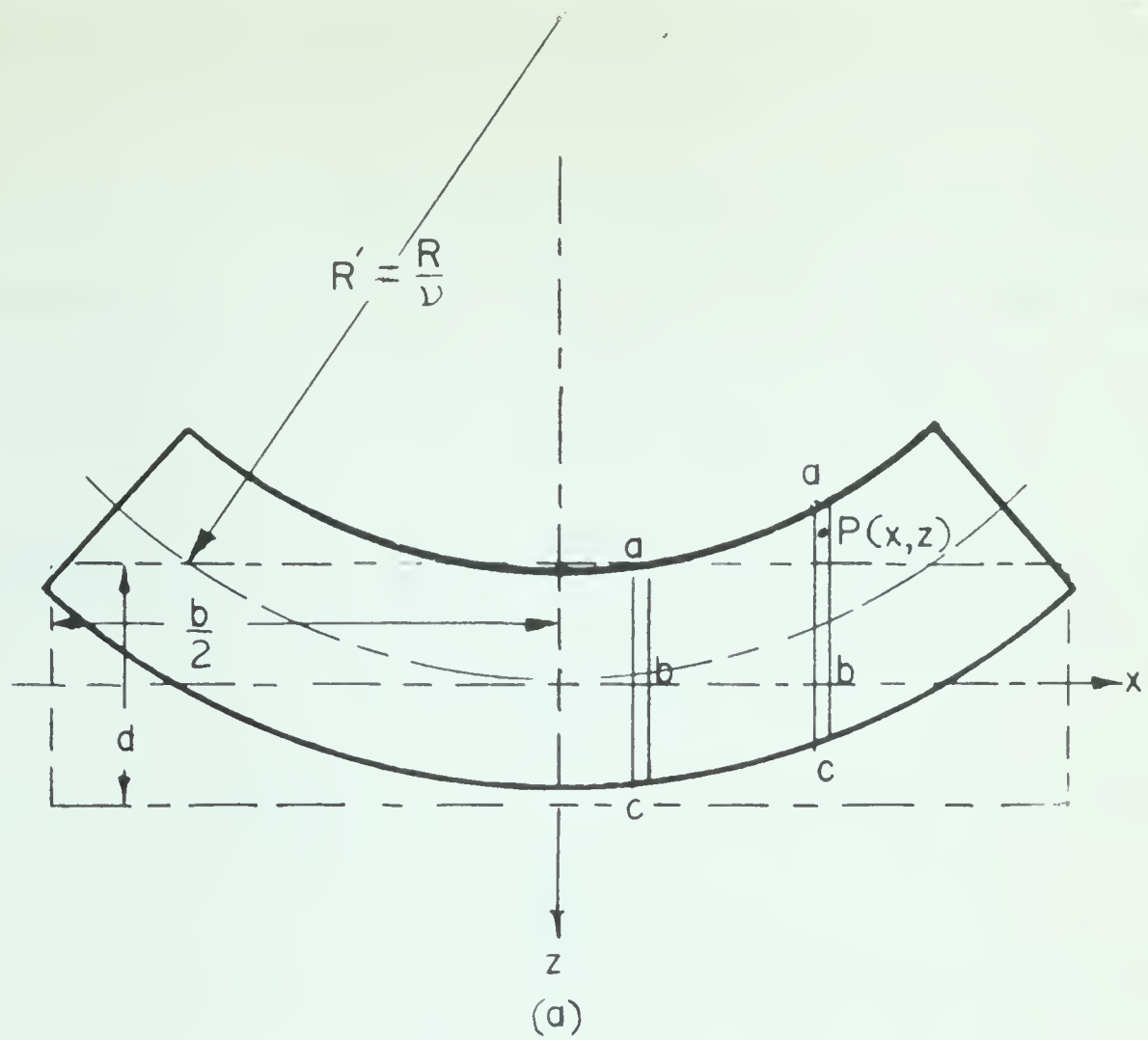


FIGURE 1.6 FORCES ON CROSS SECTION





Beam

In the case of a beam bent into an anticlastic surface, the maximum deflection of the transverse cross section occurs at the edge and is equal to

$$\delta = R'(1 - \cos \alpha)$$

or approximately,

$$\delta = \frac{R'\alpha^2}{2}$$

but

$$R'\alpha = \frac{b}{2} ,$$

and therefore, this becomes

$$\delta = \frac{b^2}{8R'} . \quad 1.41$$

Searle concludes if  $\delta$  is small then the effect of the bending moment caused by the body forces is negligible, that is, anti-clastic curvature will prevail if

$$\delta < \frac{d}{2}$$

or

$$\frac{b^2}{8R'} < \frac{d}{2}$$

and for  $\nu = \frac{1}{3}$

$$\frac{b^2}{Rd} < 12 . \quad 1.42$$

It will be noted that this inequality differs from the expression in 1.37. But the expression 1.37 is for the transverse section to have a constant curvature; in expression 1.42 this is not necessarily the case, although the curvature must still be anti-clastic.



## Plate

When the width of a cross section is large compared to its depth it is commonly called a plate\*. Searle investigated the deformation of the cross section when the width is large compared to the depth.

In Figure 1.7 two possible configurations for the deformed cross section are shown. The x-axis is the centroidal axis for the curve ABC. Let OB be the distance measured from this axis to the midline of ABC at the origin. In terms of OB the equation of the curve ABC is

$$OB - w = R'(1 - \cos \alpha)$$

or approximately

$$OB - w = \frac{R'\alpha^2}{2}$$

where as before, w is the deflection measured from the x-axis to the midline of the cross section. Since  $x = R'\alpha$  for small curvatures, then

$$w = OB - \frac{x^2}{2R'} \quad 1.43$$

Since the x-axis is the centroidal axis it is evident that

$$\begin{aligned} 0 &= \int_A w dA \\ &= \int_{-b/2}^{b/2} w(d) dx \end{aligned}$$

and using equation 1.43 this yields

$$OB = \frac{b^2}{24R'} \quad 1.44$$

---

\* It will be evident from later sections of this thesis that such a criterion is not necessarily valid.



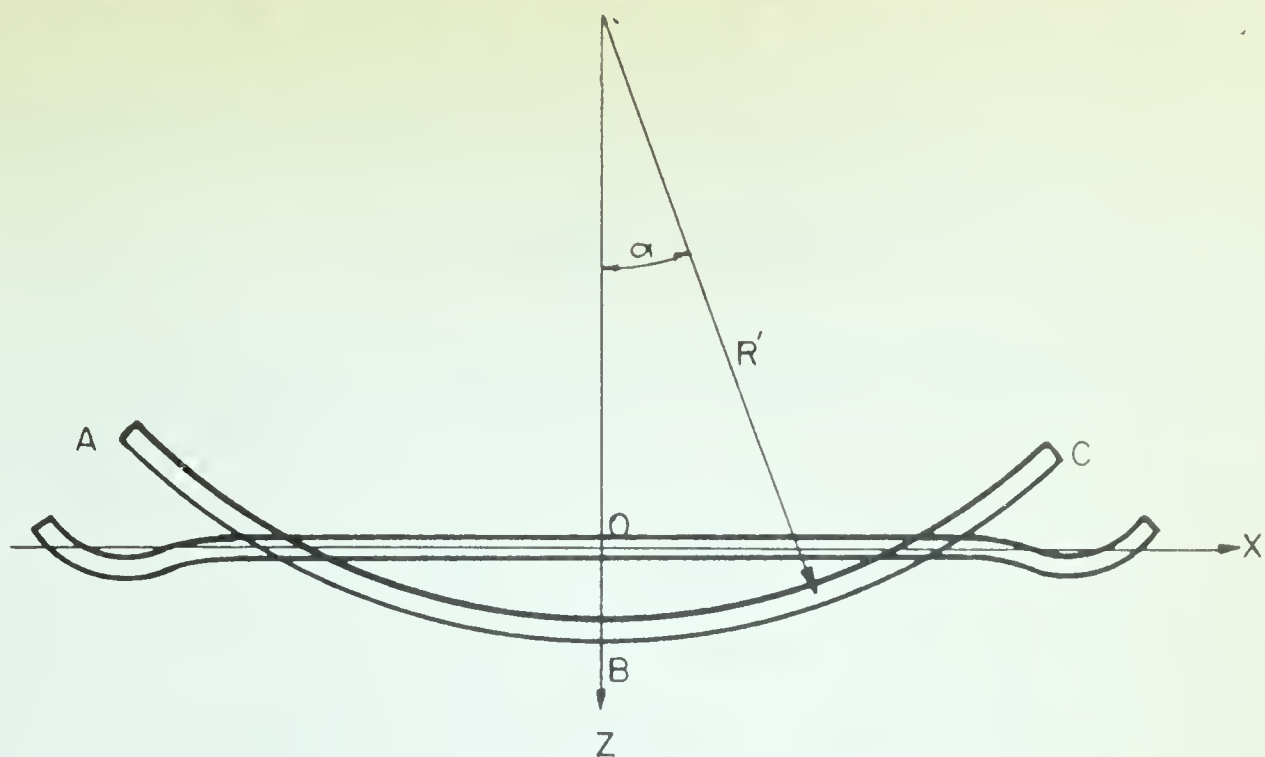


FIGURE I.7 TWO MODES OF DEFORMED CROSS SECTION

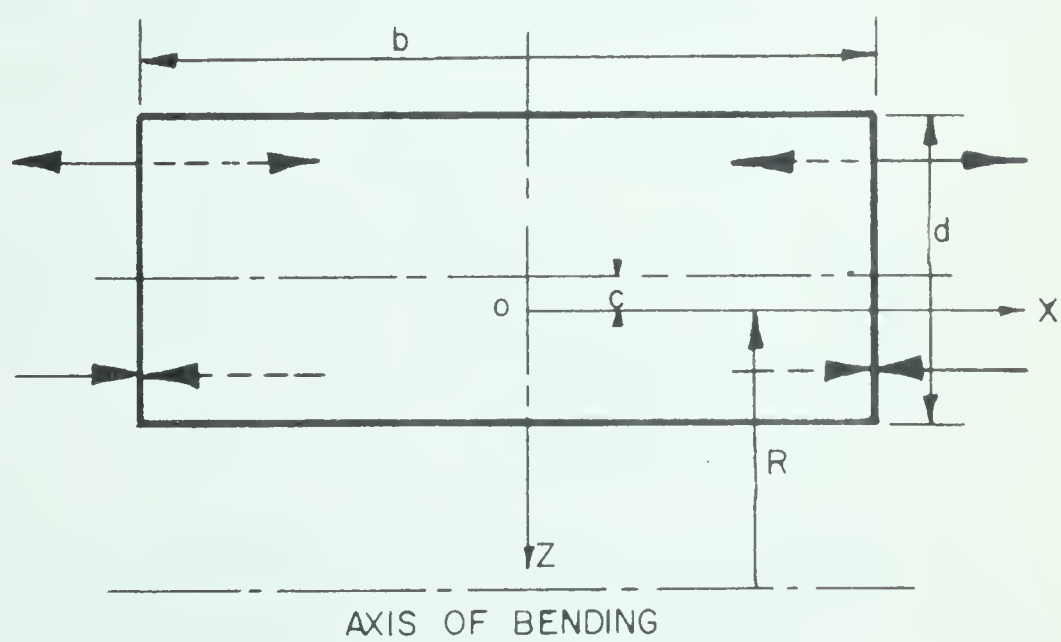


FIGURE I.8 PLATE TRANVERSE SECTION





and from equations 1.43 and 1.44 it follows that

$$w = \frac{b^2}{24R'} - \frac{x^2}{2R'} \quad . \quad 1.45$$

The "body force" acting on an element  $(d)(dx)$  produces a moment  $M$  about the  $y$ -axis, that is

$$dM = - x dF$$

and letting  $z = w$  in equation 1.40, which means the strain at the midline is considered, this bending moment becomes, with the aid of equation 1.45

$$M = \frac{Ewd(d\theta)}{RR'} \int_0^{b/2} \left[ \frac{b^2x}{24} - \frac{x^3}{2} \right] dx \quad .$$

Integrating and simplifying leads to the final result

$$M = - \frac{Ed(d\theta)b^4}{384 RR'} \quad . \quad 1.46$$

Assuming the shape of the element  $(d)(dy)$  is approximately a right angle, the second moment of area of the element about the  $y$ -axis is

$$I = \frac{dy d^3}{12} = \frac{Rd\theta d^3}{12}$$

and substituting this result into equation 1.46 gives

$$M = - \frac{EIb^4}{32R^2R'd^2} \quad . \quad 1.47$$

The effect of this moment is to reduce the anticlastic curvature. Let  $1/\rho$  be the curvature caused by  $M$ , where  $1/\rho$  represents a decrease in curvature. Then

$$\frac{1}{\rho} = - \frac{M}{EI} \quad 1.48$$



and from equation 1.47 this becomes

$$\frac{1}{\rho} = \frac{b^4}{32R^2R'd^2} \quad 1.49$$

and thus, anticlastic curvature will be neutralized when

$$\frac{1}{\rho} \geq \frac{1}{R'}$$

For this to be true, from equation 1.49, then

$$\frac{b^4}{32R^2R'd^2} \geq \frac{1}{R'}$$

or

$$\frac{b^2}{Rd} \geq 6 \quad 1.50$$

### Bending of a Very Wide and Thin Plate

Searle notes that when a plate is very wide compared to its depth, the cross section does not become anticlastic but remains essentially flat when subjected to a large longitudinal curvature. Since the ordinary theory developed for beams is no longer valid for this case, Searle outlines "... a fresh investigation."

Consider a cross section in a plate of depth  $d$ , width  $b$ . The plate is assumed to be bent to a uniform curvature  $1/R$  in the longitudinal direction. It is further assumed that all transverse fibers remain parallel to the axis of bending. Searle justifies this assumption by calling attention to the bending behaviour of thin metal sheets, such that, when uniformly bent, the deflected shape "...does not differ appreciably from part of a circular cylinder, however great the curvature may be...." Let  $(dx)(dz)$  be a small element in the cross section



at a point  $P(x,z)$ . Searle argues that since the cross section remains flat it is reasonable to assume that the sides  $x = \pm b/2$  remain perpendicular to the axis of bending (see Figure 1.8) and thus the strain  $e_x$  is constant for all transverse fibers. From Hooke's law it follows

$$\begin{aligned} Ee_x &= \sigma_x - \nu\sigma_y \\ Ee_y &= \sigma_y - \nu\sigma_x \\ Ee_z &= -\nu(\sigma_x + \sigma_y) \end{aligned}$$

assuming  $\sigma_z = 0$ . But  $e_z$  is also zero, therefore, these equations become

$$\begin{aligned} \sigma_x &= \frac{E}{1-\nu^2} \left[ e_x - \frac{\nu z}{R} \right] \\ \sigma_y &= \frac{E}{1-\nu^2} \left[ -\frac{z}{R} + \nu e_x \right] \end{aligned} \quad 1.51$$

where,

$$e_y = -\frac{z}{R}$$

Because of the assumed uniform bending conditions the resultant force perpendicular to the cross section must be zero. If  $c$  is the distance from the neutral surface to the middle surface then, for zero resultant force

$$\int_{-c-d/2}^{-c+d/2} \sigma_y b \, dz = 0$$

and using equation 1.51 this becomes, upon integration

$$\frac{Eb}{(1-\nu^2)} \left[ -\frac{z^2}{2R} + \nu e_x z \right]_{-c-d/2}^{-c+d/2} = 0,$$

and

$$e_x = \frac{-c}{\nu R} \quad 1.52$$





The distance  $c$  will be zero if the sides  $z = \pm d/2$  remain parallel to OX. Searle shows that  $c$  is negligible and can be neglected, and as a result,  $e_x = 0$ . Now the bending moment about OX is given by

$$M_Y = \int_{-c-d/2}^{-c+d/2} \sigma_Y z' b \, dz' ,$$

and using equations 1.51 and 1.52 this becomes

$$\begin{aligned} M_Y &= \frac{Eb}{R(1-\nu^2)} \int_{-c-d/2}^{-c+d/2} (-z^2 - cz) \, dz \\ &= - \frac{Ebd^3}{12(1-\nu^2)R} \\ &= - \frac{EI}{R(1-\nu^2)} \end{aligned} \quad 1.53$$

where

$$I = \frac{bd^3}{12} .$$

In his argument Searle states that the stress  $\sigma_x$ , in reality, does not exist at the edges  $x = \pm b/2$ . From equation 1.51 and 1.52 it follows that

$$\sigma_x = \frac{E}{(1-\nu^2)R} \left[ \frac{-c}{\nu} - \nu z \right] ,$$

and if  $z$  is negative,  $\sigma_x$  is tensile, and if  $z > c/\nu^2$ ,  $\sigma_x$  is compressive\*. These stresses are shown at the edges in Figure 1.8. To correct this inconsistency Searle suggests applying reverse stresses at these edges (shown dotted) and, according to him

---

\* For the bending condition considered,  $c$  will be very small.



These reversed tensions will tend to change the section of the blade, but as soon as the section is changed the changed tension in the longitudinal filaments near the edge of the blade will give rise to radial forces tending to counteract the effects of the reversed tensions. Experiment shows that any distortion which the section may suffer near the edges...is exceedingly small and that it cannot be made appreciable by increasing the curvature of the longitudinal filaments.

### Change of Type of Bending

In conclusion, Searle makes the interesting observation that there will be a smooth transition from beam action governed by the equation

$$M = -\frac{EI}{R} ,$$

when the bending is very slight, to plate action governed by the equation

$$M = -\frac{EI}{(1-\nu^2)R}$$

when the ratio  $b^2/Rd$  is large.

### 1.1.6 Timoshenko

In 1923 Timoshenko published a short note<sup>7</sup> emphasizing the influence of radial forces on the deflected shape of the transverse cross section. His argument follows much the same lines as Searle's, but unlike Searle he was aware of Lamb's solution. He notes that the bending moment equation for beams

---

<sup>7</sup> Timoshenko, S.P., "Determination of the Modulus of Elasticity," Mechanical Engineering, 1923, 45(4), pp. 259-260.

See also: Timoshenko, S.P., Collected Papers, McGraw Hill, 1953, pp. 366-370.



can be related to the bending equation for plates by a factor  $k$  which is related to the curvature  $1/R$ , the width  $b$ , and the thickness  $d$ . That is

$$M = -\frac{EI}{R} \left[ \frac{1-k\nu^2}{1-\nu^2} \right] , \quad 1.54$$

such that for plates  $k = 0$ , and for beams  $k = 1$ . Timoshenko gives a table of  $k$  values for different  $\beta b$  values where the latter is defined by

$$\beta b = b \left[ \frac{3(1-\nu^2)}{R^2 d^2} \right]^{1/4} . \quad 1.55$$

Equation 1.55 is similar to equation 1.16 developed in connection with Lamb's work. It is not too difficult to see how the value  $k$  is determined from the moment applied to the edges  $y = \pm$  constant. The total applied moment is made up from the bending moment  $M_y$  plus the moment due to the axial forces  $N_y$  acting at a distance  $w(x)$ , where  $w(x)$  is the displacement of the mid-line measured from the centroidal axis ( $x$ -axis). This gives

$$M = -M_y - wN_y ,$$

but these are moments per unit length, therefore, the total applied moment to a member of width  $b$  becomes

$$M = - \int_{-b/2}^{b/2} M_y dx - \int_{-b/2}^{b/2} wN_y dx , \quad 1.56$$

where the sign convention is used such that a bending moment is positive if it produces tension on a positive face. Also, similar to equation 1.8 it follows that

$$M_y = -D \left[ \frac{1}{R_y} + \frac{\nu}{R_x} \right] ,$$





and assuming the approximation  $R_y = (R - w) \doteq R$  and using equation 1.13 in equation 1.56 gives

$$M = D \int_{-b/2}^{b/2} \left[ \frac{1}{R} + \frac{v d^2 w}{dx^2} \right] dx + \frac{Ed}{R} \int_{-b/2}^{b/2} w^2 dx, \quad 1.57$$

and with the aid of equation 1.36 this becomes

$$M = \frac{Db}{R} + 2v\alpha^2 D \int_{-b/2}^{b/2} (\bar{B} \cosh \alpha x \cos \alpha x - \bar{A} \sinh \alpha x \sin \alpha x) dx \\ + \frac{Ed}{R} \int_{-b/2}^{b/2} (\bar{A} \cosh \alpha x \cos \alpha x + \bar{B} \sinh \alpha x \sin \alpha x)^2 dx.$$

Upon integration this becomes,

$$M = \frac{Db}{R} + 2v\alpha^2 D \left[ \frac{\bar{B}}{2\alpha} (\sinh \alpha x \cos \alpha x + \cosh \alpha x \sin \alpha x) \right. \\ \left. - \frac{\bar{A}}{2\alpha} (\cosh \alpha x \sin \alpha x - \sinh \alpha x \cos \alpha x) \right]_{-b/2}^{b/2} \\ + \frac{Ed}{R} \left\{ \frac{\bar{A}^2}{16\alpha} \left[ 4\alpha x + \sinh 2\alpha x (2 + \cos 2\alpha x) + \sin 2\alpha x (2 + \cosh 2\alpha x) \right. \right. \\ \left. \left. + \frac{2\bar{A}\bar{B}}{16\alpha} \left[ \cosh 2\alpha x \sin 2\alpha x - \sinh 2\alpha x \cos 2\alpha x \right] \right. \right. \\ \left. \left. + \frac{\bar{B}^2}{16\alpha} \left[ 4\alpha x + \sinh 2\alpha x (\cos 2\alpha x - 2) + \sin 2\alpha x (\cosh 2\alpha x - 2) \right] \right\}_{-b/2}^{b/2} \\ M = \frac{Db}{R} + 2v\alpha D \left[ \bar{B} \left( \sinh \frac{\alpha b}{2} \cos \frac{\alpha b}{2} + \cosh \frac{\alpha b}{2} \sin \frac{\alpha b}{2} \right) \right. \\ \left. - \bar{A} \left( \cosh \frac{\alpha b}{2} \sin \frac{\alpha b}{2} - \sinh \frac{\alpha b}{2} \cos \frac{\alpha b}{2} \right) \right] \\ + \frac{Ed}{R} \left\{ \frac{\bar{A}^2}{16\alpha} \left[ 4\alpha b + 2\sinh \alpha b (2 + \cos \alpha b) + 2\sin \alpha b (2 + \cosh \alpha b) \right] \right. \\ \left. + \frac{\bar{A}\bar{B}}{4\alpha} \left[ \cosh \alpha b \sin \alpha b - \sinh \alpha b \cos \alpha b \right] \right. \\ \left. + \frac{\bar{B}^2}{16\alpha} \left[ -4\alpha b + 2\sinh \alpha b (2 - \cos \alpha b) + 2\sin \alpha b (2 + \cosh \alpha b) \right] \right\}$$



$$M = \frac{Db}{R} + 2v\alpha D \left[ \sinh \frac{\alpha b}{2} \cos \frac{\alpha b}{2} (\bar{B} + \bar{A}) + \cosh \frac{\alpha b}{2} \sin \frac{\alpha b}{2} (\bar{B} - \bar{A}) \right] \\ + \frac{Ed}{8\alpha R} \left[ 2b\alpha (\bar{A}^2 - \bar{B}^2) + \sinh \alpha b \cos \alpha b (\bar{A}^2 - 2\bar{A}\bar{B} - \bar{B}^2) \right. \\ \left. + 2(\bar{B}^2 + \bar{A}^2)(\sinh \alpha b + \sin \alpha b) + \cosh \alpha b \sin \alpha b (\bar{A}^2 + 2\bar{A}\bar{B} - \bar{B}^2) \right] .$$

This can be rewritten in a simpler form

$$M = \frac{Db}{R} + 2v\alpha D f(\alpha b) + \frac{Ed}{8\alpha R} g(\alpha b) ,$$

and if  $I = \frac{bd^3}{12}$  this becomes

$$M = \frac{EI}{R} \left[ \frac{1}{1-v^2} + \frac{2v\alpha R}{(1-v^2)b} f(\alpha b) + \frac{3}{2\alpha d^2 b} g(\alpha b) \right] , \quad 1.58$$

where,

$$f(\alpha b) = (\bar{B} + \bar{A}) \sinh \frac{\alpha b}{2} \cos \frac{\alpha b}{2} + (\bar{B} - \bar{A}) \cosh \frac{\alpha b}{2} \sin \frac{\alpha b}{2} \quad 1.59$$

and

$$g(\alpha b) = 2\alpha b (\bar{A}^2 - \bar{B}^2) + \sinh \alpha b \cos \alpha b (\bar{A}^2 - 2\bar{A}\bar{B} - \bar{B}^2) \\ + 2 (\bar{B}^2 + \bar{A}^2)(\sinh \alpha b + \sin \alpha b) \\ + \cosh \alpha b \sin \alpha b (\bar{A}^2 + 2\bar{A}\bar{B} - \bar{B}^2) . \quad 1.60$$

From equations 1.54 and 1.58 it follows that

$$k = \frac{2\alpha R}{bv} \left[ f(\alpha b) + \frac{\alpha^2 R}{4v} g(\alpha b) \right] . \quad 1.61$$

In Section 1.3 numerical results are given for equation 1.61.



### 1.1.7 Case

In an appendix to his book<sup>8</sup> Case treats the problem of anticlastic curvature. Like Searle it is assumed that Case was unaware of the work of Lamb in 1891 since he makes no mention of the differential equation developed by Lamb which leads to the solution of the problem.

In connection with the problem of the transition of beam behaviour to plate behaviour, Case says,

If we apply a continuously increasing bending moment to such a blade, at first anticlastic curvature will be present, but a critical stage will be reached when the type of bending will change, the blade becoming flat except near the edges -- another one of those very frequent instances where continuous quantitative change brings about a discontinuity in quality. \*

It is shown in Section 1.2.2 that the transition is continuous.

### 1.1.8 Ashwell

An alternative method of developing the governing differential equation was given by Ashwell in 1950<sup>9</sup>. Ashwell takes the "body force" described by Searle (see Section 1.15) which is

$$\frac{\sigma A s}{R} ,$$

---

8 Case, J., Strength of Materials, Arnold, 1938, pp. 546-554.

\* The emphasis is that of Case.

9 Ashwell, D.G., "The anticlastic curvature of rectangular beams and plates," Royal Aeronautical Society Journal, 1950, Vol. 54, pp. 708-715.

See also: Flugge, W., Handbook of Engineering Mechanics McGraw Hill 1962, Sections 45.1-45.8, contributed by Ashwell.





and, because  $A = d(dx)$ , he relates this to a force per unit length in the transverse direction

$$P = pw \quad ,$$

where

$$p = \frac{Esd}{R^2} \quad , \quad 1.62$$

where  $s$  is the width in the  $y$ -direction of the transverse strip under consideration. Isolating this transverse strip under the action of the pressure  $p$  is analogous to a beam on an elastic foundation, since the force  $P$  per unit length is proportional to the deflection  $w$ .

Consider a beam of negligible weight acting on an elastic foundation whose spring constant is  $p$ . It follows from variational calculus that the total potential energy of such a beam is given by the expression,\*

$$U = \frac{1}{2} \int_{-b/2}^{b/2} \frac{EI}{(1-\nu^2)} \left[ \frac{d^2 w}{dx^2} \right]^2 dx - \frac{1}{2} \int_{-b/2}^{b/2} pw^2 dx \quad , \quad 1.63$$

where the first term represents the strain energy of the beam and the second the energy of the elastic support. The principle of minimum of potential energy states that of all admissible displacement functions  $w$  the one which satisfies the equilibrium equations will make the potential energy  $U$  an absolute minimum. It can be shown that minimizing the integral in equation 1.63 is equivalent to solving the Euler-Lagrange differential equation

$$\frac{\partial L}{\partial w} + \frac{d^2}{dx^2} \left[ \frac{\partial L}{\partial w''} \right] = 0 \quad , \quad 1.64$$

---

\* In Ashwell's paper he did not derive the differential equation for a beam on an elastic foundation. To be complete it is derived here.



where

$$L = \frac{EI \ddot{w}^2}{2(1-\nu^2)} + \frac{pw^2}{2} , \quad 1.65$$

and,

$$\ddot{w} = \frac{d^2 w}{dx^2} .$$

Thus, using equations 1.64 and 1.65 it follows that

$$pw + \frac{d^2}{dx^2} \left[ \frac{EI \ddot{w}}{(1-\nu^2)} \right] = 0 ,$$

and for EI constant this reduces to

$$\frac{d^4 w}{dx^4} + \frac{p}{EI} (1-\nu^2) w = 0 , \quad 1.66$$

and from equation 1.62 this becomes

$$\frac{d^4 w}{dx^4} + \frac{12(1-\nu^2)}{d^2 R^2} w = 0 , \quad 1.67$$

where

$$I = \frac{sd^3}{12} .$$

It is seen that equation 1.67 agrees with the differential equation 1.18 developed by Lamb.

In a manner slightly different from Timoshenko, Ashwell relates the bending moment between beam and plate action by the quantity  $\emptyset$ , that is,

$$M = -\frac{EI\emptyset}{R} , \quad 1.68$$

where for beams

$$\emptyset = 1 ,$$

and for plates

$$\emptyset = \frac{1}{1-\nu^2} .$$

Obviously, from equation 1.54

$$\emptyset = \frac{1-\nu^2 k}{1-\nu^2} . \quad 1.69$$



Ashwell observed that for large  $b^2/Rd$  values the maximum deflection, which occurs at the edge, tends to a constant value. To illustrate this it is noted that for  $b^2/Rd$  large,  $\alpha b$  is also large. That is, from equation 1.16

$$\alpha b = \left[ 3(1-\nu^2) \right]^{1/4} \left[ \frac{b^2}{Rd} \right]^{1/2},$$

$$\text{and } \cosh \alpha b = \frac{e^{\alpha b} - e^{-\alpha b}}{2} \doteq \frac{e^{\alpha b}}{2} \doteq \sinh \alpha b,$$

also  $\cosh \alpha x \doteq \frac{e^{\alpha x}}{2}$  near the edges. Now from equation 1.36 the deflection is approximately

$$w = \frac{e^{\alpha x}}{2} (\bar{A} \cos \alpha x + \bar{B} \sin \alpha x),$$

and for large  $b^2/Rd$  the constants  $\bar{A}$ ,  $\bar{B}$  become

$$\bar{A} = \frac{-\nu}{\alpha^2 R} \left[ \frac{e^{\alpha b/2} \cos \alpha b/2 - e^{\alpha b/2} \sin \alpha b/2}{e^{\alpha b} + 2 \sin \alpha b} \right]$$

$$\bar{B} = \frac{-\nu}{\alpha^2 R} \left[ \frac{e^{\alpha b/2} \cos \alpha b/2 + e^{\alpha b/2} \sin \alpha b/2}{e^{\alpha b} + 2 \sin \alpha b} \right].$$

But  $2 \sin \alpha b$  will be very small compared with  $e^{\alpha b}$  and thus the deflection reduces to the approximate formula

$$\frac{w}{d} = \frac{-\nu e^{(\alpha b/2) + \alpha x}}{2\alpha^2 R d e^{\alpha b}} \left[ \left( \cos \frac{\alpha b}{2} - \sin \frac{\alpha b}{2} \right) \cos \alpha x \right. \\ \left. + \left( \cos \frac{\alpha b}{2} + \sin \frac{\alpha b}{2} \right) \sin \alpha x \right],$$

$$\text{or } \frac{w}{d} = \frac{-\nu e^{\alpha(x-b/2)}}{2\alpha^2 R d} \left[ \cos \alpha \left( x - \frac{b}{2} \right) + \sin \alpha \left( x - \frac{b}{2} \right) \right]. \quad 1.70$$





Now let  $X$  be the distance measured from the edges  $x = \pm b/2$ , then

$$X = b/2 - x \quad 1.71$$

Hence from equations 1.70 and 1.71 it follows

$$\frac{w}{d} = \frac{-ve^{-\alpha X}}{2\alpha^2 R d} \left[ \cos \alpha X - \sin \alpha X \right] \quad 1.72$$

At  $x = + b/2$ ,  $X = 0$ , therefore the deflection at the edges tends to a maximum value

$$\frac{w}{d} = \frac{-v}{2\alpha^2 R d} = \frac{-v}{2 \left[ 3(1-v^2) \right]^{1/2}}$$

and for  $b^2/Rd = 100$  and  $v = 1/3$  this becomes

$$w = -0.102d$$

#### 1.1.9 Fung and Wittrick

In discussing the transverse shape for  $b^2/Rd$  greater than 100, Ashwell<sup>10</sup> plotted  $w/d$  versus  $\frac{b}{(Rd)^{1/2}} \left[ \frac{X}{b} \right]$  evaluated from equation 1.72 above. Although apparently missed at first by Ashwell, Fung and Wittrick<sup>11</sup> noted from this graph that for large  $b^2/Rd$  ratios the distortion of the transverse strip is confined to a narrow region along the edge and the

10 Loc. cit.

11 Fung, Y.C., and Wittrick, W.H., "A Boundary Layer Phenomenon in the Large Deflection of Thin Plates," Quart. Journal Mech. and Applied Math., 1955, Vol. VIII, Part 2, pp. 191-210.

See also: Ashwell, D.G., "The Equilibrium Equations of the Inextensional Theory for Thin Flat Plates," Quart. Journal Mech. and Applied Math., 1957, Vol. X, Part 2, pp. 169-182.



width of this region is of the order  $(Rd)^{1/2}$ . They conclude that for large  $b^2/Rd$  ratios a plate will bend into a developable surface except for this finite boundary layer.

From equation 1.72 it can be seen that for  $w$  to be zero, the first two values of  $\alpha X$  are  $\pi/4$  and  $5\pi/4$ . Therefore, for  $\nu = 1/3$  it follows that

$$X = 0.611 (Rd)^{1/2} ,$$

$$\text{and} \quad X = 3.055 (Rd)^{1/2} , \quad 1.73$$

where  $X$  is measured from the edges  $x = \pm b/2$ .

#### 1.1.10 Concluding Remarks

Kelvin and Tait were the first to realize that the shape of the transverse section depends on the parameter  $b^2/Rd$  and further, that anticlastic bending will occur providing

$$\frac{b^2}{Rd} < 3 .$$

It is unknown how these philosophical mathematicians arrived at such a remarkable conclusion. They posed the problem, which in its present form, was given an exact solution by Lamb.

Searle provided the physical insight into the problem although, as noted, he apparently was unaware of Lamb's solution. He improved on the criterion for beam action, noting if

$$\frac{b^2}{Rd} < 0.6 , \quad 1.37$$

"pure beam action" would result. He also estimated that if

$$\frac{b^2}{Rd} < 12 ,$$



anticlastic curvature would prevail throughout the entire width of the plate.

The next major contribution was made by Timoshenko in a single short note in which he calculated the bending moment that had to be applied to a plate in order to produce a given curvature. He related this moment to the  $b^2/Rd$  ratio.

Case remarked that the transition from beam behaviour to plate behaviour involved some kind of discontinuity. In Section 1.2.2 it is shown that no such discontinuity exists.

Ashwell summarized the work of Lamb and Searle. He presented the Lamb solution by considering the transverse strip as acting like a beam on an elastic foundation. This was not the first time such a problem was thus considered for, according to Timoshenko<sup>12</sup>, H. Scheffler in 1859 recognized that a strip taken from a cylindrical shell is in the same condition as a beam on an elastic foundation.

Comparing the approaches of Lamb and Searle to the problem, it appears that the one of Lamb is more correct; it only requires to be tested by experiment. In Section 1.2 it is shown that Lamb's solution gives the deflected form, as a function of  $x$ , for beam action, for the transition between beam and plate action, and for plate action. But Searle argued the problem on the basis of two solutions; one for beams and one for plates, and directed his efforts to finding the limits within which either of the solutions are valid. Although Lamb's

---

12 Timoshenko, S.P., Strength of Materials, Van Nostrand, 1956, Vol. 2, p. 126.







approach seems to be more valid, Searle cannot be criticized for he certainly supplied the physical reasoning for the problem.

## 1.2 COMPUTER RESULTS OF LAMB'S SOLUTION

### 1.2.1 Governing Equations for Deflection

In Section 1.1.4 the solution to the governing differential equation was found to be

$$w = \bar{A} \cosh \alpha x \cos \alpha x + \bar{B} \sinh \alpha x \sin \alpha x \quad 1.36$$

$$\text{where } \bar{A} = \frac{-\nu}{\alpha^2 R} \frac{\sinh \alpha b/2 \cos \alpha b/2 - \cosh \alpha b/2 \sin \alpha b/2}{\sinh \alpha b + \sin \alpha b}$$

$$\bar{B} = \frac{-\nu}{\alpha^2 R} \frac{\sinh \alpha b/2 \cos \alpha b/2 + \cosh \alpha b/2 \sin \alpha b/2}{\sinh \alpha b + \sin \alpha b} .$$

Dividing both sides of equation 1.36 by the plate thickness will put it in a non-dimensional form, thus getting

$$\frac{w}{d} = \frac{-\nu}{[3(1-\nu^2)]^{1/2}} \left[ \frac{\cosh \alpha x \cos \alpha x [\sinh \alpha b/2 \cos \alpha b/2 - \cosh \alpha b/2 \sin \alpha b/2]}{\sinh \alpha b + \sin \alpha b} + \frac{\sinh \alpha x \sin \alpha x [\sinh \alpha b/2 \cos \alpha b/2 + \cosh \alpha b/2 \sin \alpha b/2]}{\sinh \alpha b + \sin \alpha b} \right] . \quad 1.74$$

The terms on the right hand side of equation 1.74 containing  $x$  could also be put in a non-dimensional form by writing instead of  $x$ ,  $(x/b)b$ , but this is obviously unnecessary.



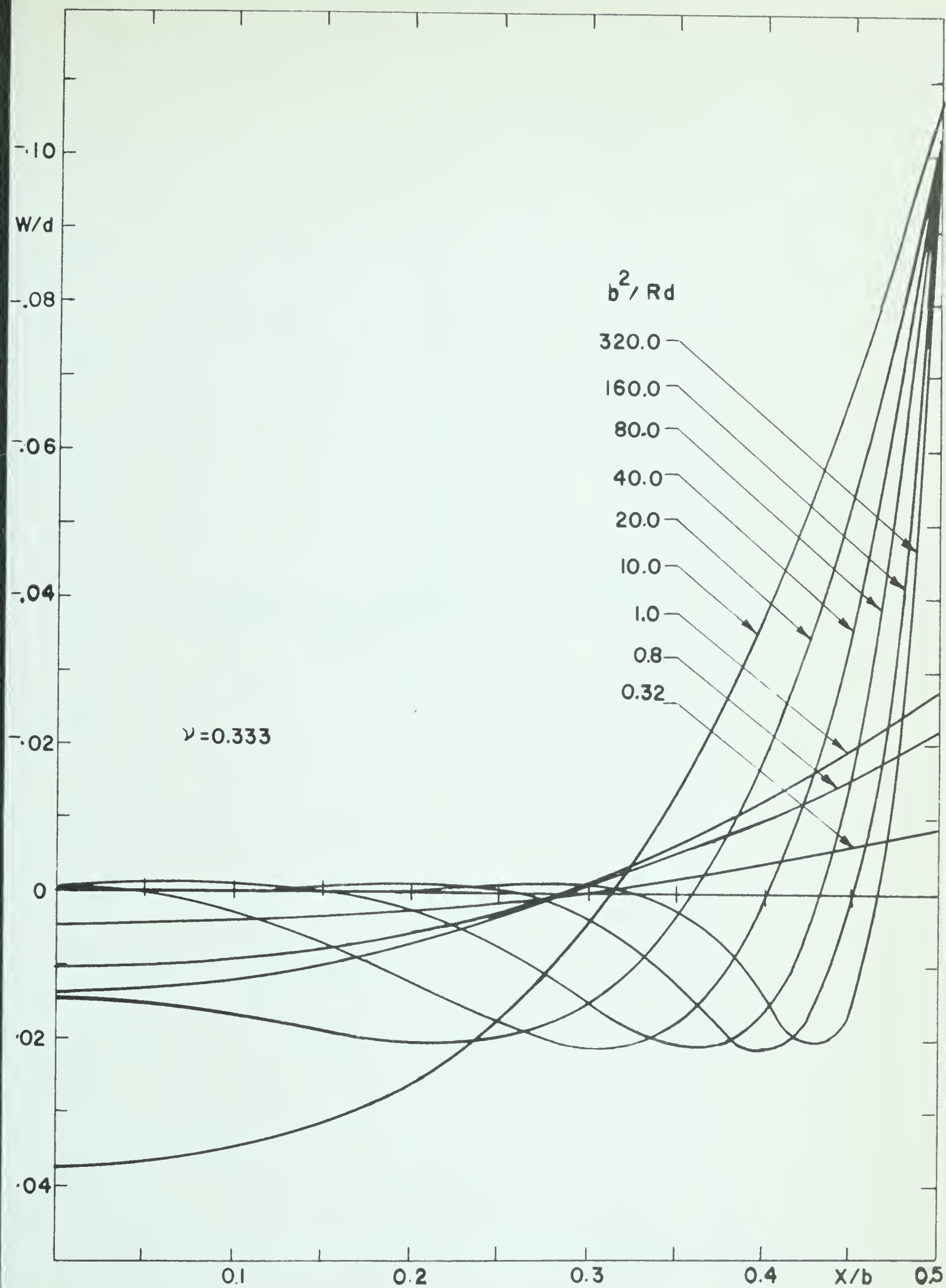


FIGURE I.9 TRANSVERSE DEFLECTION (LAMB'S THEORY)



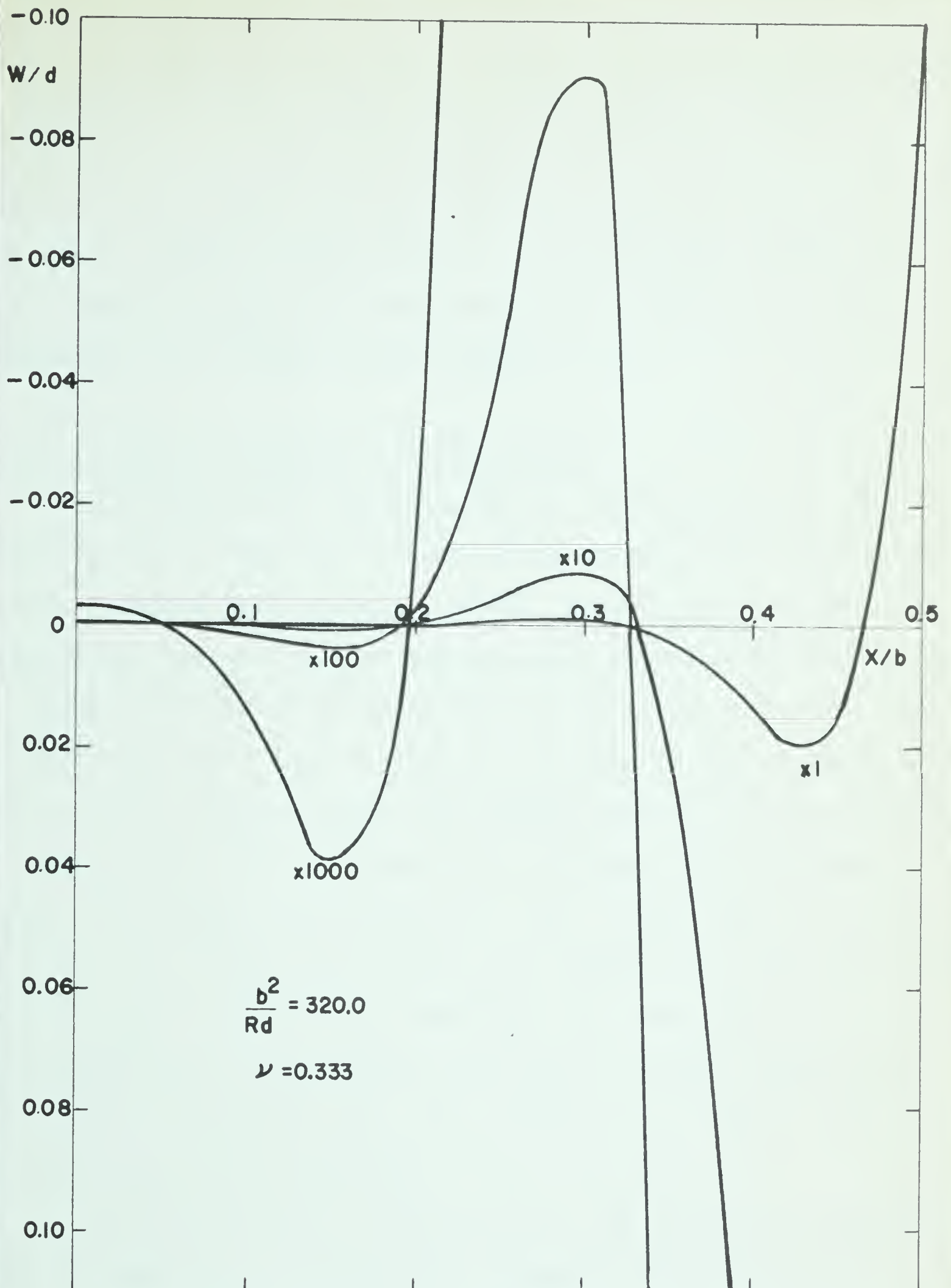


FIGURE 1.10 TRANSVERSE DEFLECTION (ENLARGED SCALES)





In Appendix I a computer tabulation is given for equation 1.74 with the results tabled for  $b^2/Rd$  ratios from 0.320 to 320.0. A few of these results are plotted in Figure 1.9 and 1.10. Figure 1.10 is shown with very enlarged scales to show that with the ratio  $b^2/Rd$  as high as 320.0, the transverse deflection curve undulates even near the centerline of the plate. These curves are for Poisson's ratio equal to  $1/3$ .

### 1.2.2 Remarks on Case's "Discontinuity"

In Figure 1.11 seven curves of  $w/d$  versus  $x/b$  have been plotted to show how the deflected shape of the transverse section changes with changing  $b^2/Rd$  values. For  $b^2/Rd$  less than 13.06 (curve 5) it is observed that the transverse curvature is always negative, that is, always anticlastic, while for  $b^2/Rd$  greater than 14.22 (curve 3) the transverse curvature is positive over a small central region and changes from positive to negative at about  $0.10b$  from the centerline. Between these two curves there is a gradual transformation. For  $b^2/Rd$  equal to 13.62 (curve 4) it appears the curvature is almost zero near the centerline.\* Thus it can be concluded that the transition of the deflected form from one whose curvature is always negative to one whose curvature changes sign, occurs at a  $b^2/Rd$  ratio of 13.62. This is for a Poisson's ratio of 0.333.

The deflection at the origin is not zero even though the mode of transverse curvature has changed as described above.

---

\* To see exactly how much change occurs near the centerline, reference is made to the tabulated values in Appendix I.



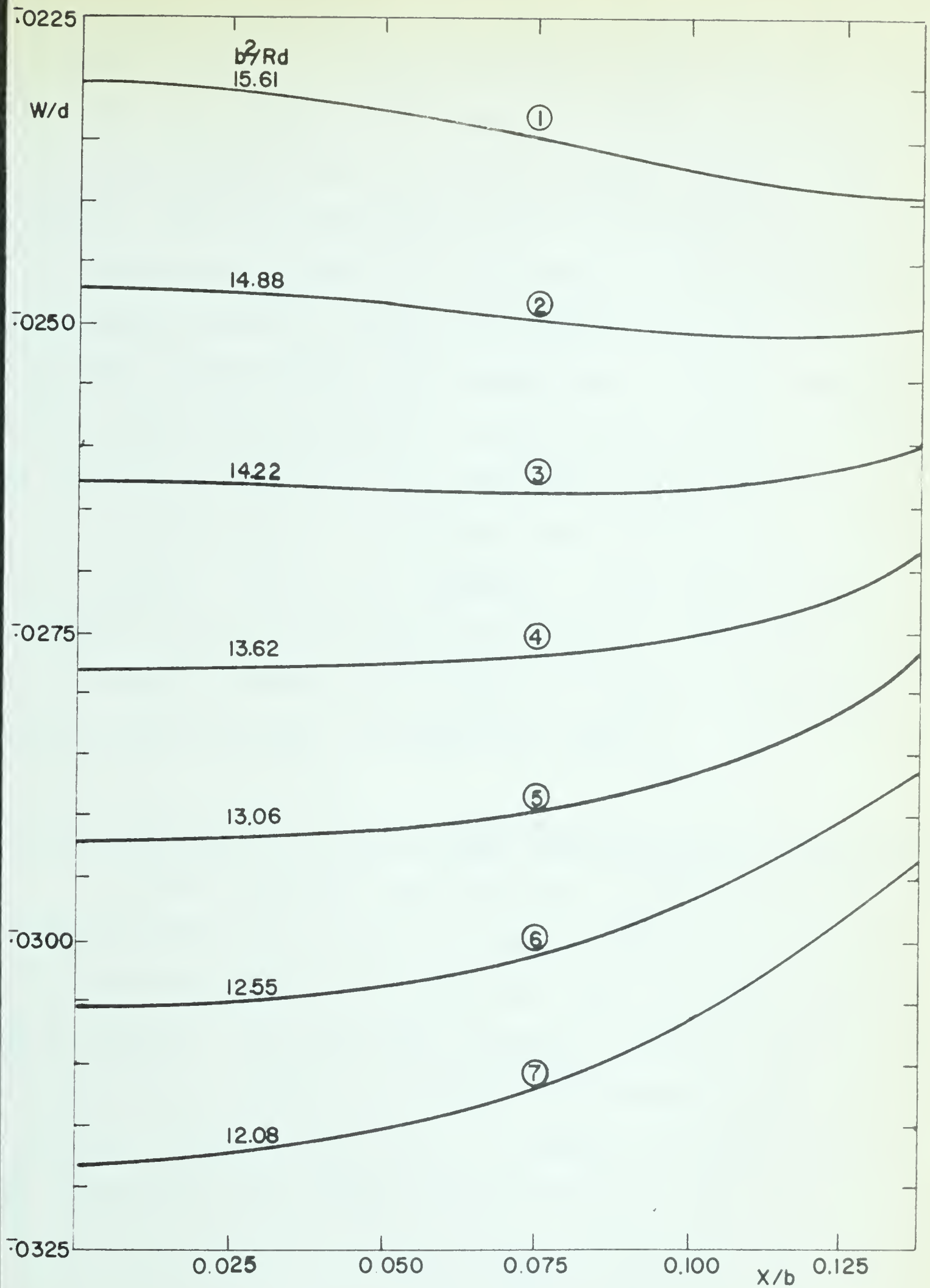


FIGURE 1.11 TRANSITION FROM ANTICLASTIC TO  
SYNCLASTIC BEHAVIOUR AT CENTERLINE



From Figure 1.9 it is observed, that as the ratio  $b^2/Rd$  is increased, there is a gradual decrease in the centerline deflection until it reaches almost zero at a  $b^2/Rd$  value of 35.55 and remains essentially zero for all higher  $b^2/Rd$  values. Actually, from the tabulated results in Appendix I the centerline deflection is never zero but alternates between positive and negative values. However, the centerline deflection is small for  $b^2/Rd$  large; for example, for a  $b^2/Rd$  value of 160 the centerline deflection ( $w/d$ ) is only  $0.76 \times 10^{-4}$  which is negligible compared to the edge deflection ( $w/d$ ) of  $-0.102$ .

On the basis of the theoretical solution, and the foregoing remarks, there is no evidence, or any remote tendency, for a discontinuity in deflected form to occur. The transition from an anticlastic surface to one which is almost cylindrical, except near the edges, is completely smooth.

### 1.2.3 Comparison of Results With Those of Earlier Investigators

It was discussed above that for  $b^2/Rd$  ratios less than 13.62 the deflected transverse shape is entirely anticlastic. This does not necessarily define the limits of the so-called "beam theory". To check this, consider the edge deflection of a beam bent to a radius  $R$  in the longitudinal direction. From equation 1.45 the deflection at the edge  $x = \pm b/2$  relative to the centroidal axis ( $x$ -axis) is given by

$$w = \frac{-b^2}{12R},$$

or 
$$w = \frac{-\nu b^2}{12R},$$





and dividing each side by the thickness, gives

$$\frac{w}{d} = \frac{-\nu}{12} \left[ \frac{b^2}{Rd} \right] . \quad 1.75$$

In Table 1.1 a few values of  $w/d$  calculated from equation 1.75 are compared to the edge deflection as given from Lamb's solution and tabulated in Appendix I.

FIGURE 1.1 COMPARISON OF BEAM THEORY WITH LAMB'S SOLUTION

$\frac{b^2}{Rd}$	$w/d$ for $\nu = 1/3$	
	"Beam" Theory	Lamb's Solution
0.4	0.01111	0.01107
0.8	0.02222	0.02193
1.0	0.02778	0.02723
1.6	0.04444	0.04235
3.2	0.08889	0.07457
4.0	0.11111	0.08574
8.0	0.22222	0.10708
10.0	0.27778	0.10772
16.0	0.44444	0.10424
20.0	0.55556	0.10267
32.0	0.88889	0.10171

It is seen from the above table, that the "beam" theory agrees reasonably well with Lamb's solution for  $b^2/Rd$  ratios less than 1.0 or even 1.6. For larger values of  $b^2/Rd$  the two theories disagree markedly. This is demonstrated graphically in



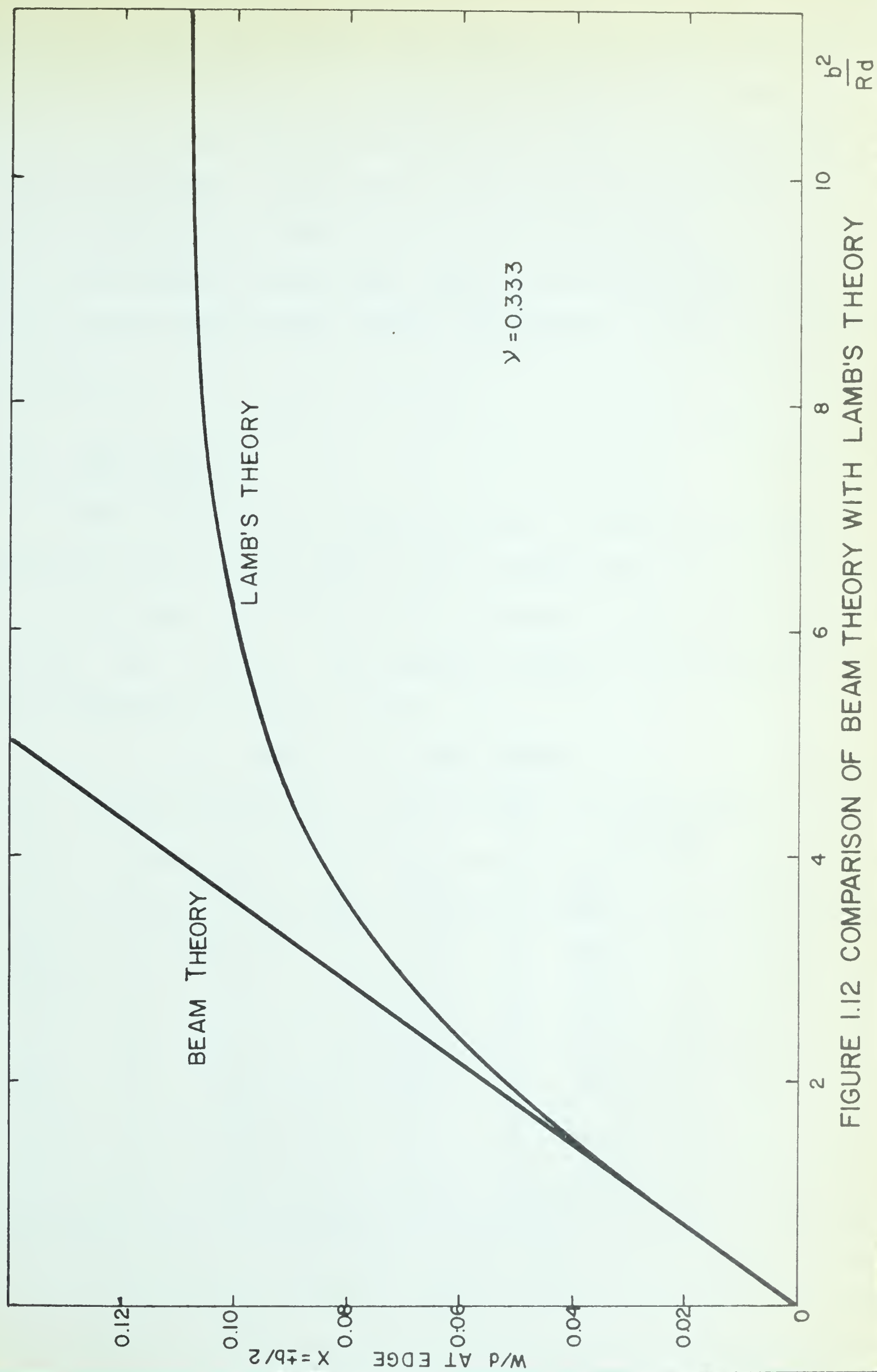


FIGURE 1.12 COMPARISON OF BEAM THEORY WITH LAMB'S THEORY



Figure 1.12 where the values from Table 1.1 have been plotted. It will be remembered from Section 1.1.3 that Kelvin and Tait predicted that anticlastic bending would exist providing  $b^2/Rd$  is less than three. Also, Searle predicted the limit for anticlastic bending was  $b^2/Rd$  less than 0.6 (see Section 1.1.5). These investigators, especially Searle, came remarkably close to the correct value which speaks most highly of their physical reasoning.

#### 1.2.4 Edge Effect

With reference to Figure 1.9 let  $X$  be the distance measured from the plate edge (at  $x = \pm b/2$ ) inward to the centerline. The first two values of  $X$ , closest to the plate edge, for which  $w/d$  is zero, are listed in Table 1.2 for various  $b^2/Rd$  ratios.

TABLE 1.2 EDGE EFFECT

$\frac{b^2}{Rd}$	X for $w/d = 0$		$\frac{X}{b} \left[ \frac{b^2}{Rd} \right]^{1/2}$	
	1st	2nd	1st	2nd
320	0.65	3.42	.5811	3.063
160	0.95	4.85	.6009	3.068
107	1.17	5.90	.6060	3.050
80	1.36	6.80	.6079	3.040
64	1.52	7.70	.6080	3.080
40	1.94	9.10	.6130	2.876





The values  $\frac{x}{b} \left[ \frac{b^2}{Rd} \right]^{1/2}$  have been calculated in order to compare with the coefficients of the equation 1.73. The edge effect is usually taken as the distance, from the edge, to the second point at which  $w/d = 0$ . From equation 1.73 the coefficient is 3.055 which is in reasonable agreement with the values in Table 1.2 for a  $b^2/Rd$  greater than or equal to 64; the difference between the two values is less than one per cent. Thus in using equation 1.73 the approximation amounts to neglecting terms of magnitude  $10 \times 10^{-4}$  and smaller in evaluating the hyperbolic sines and cosines. In conclusion, equation 1.73 is valid for  $b^2/Rd$  greater than or equal to 64.

### 1.3 CURVATURE, BENDING MOMENT RELATION

#### 1.3.1 Computer Solution of Timoshenko Relation

The equations for the bending moment applied along the edges  $y = \pm$  constant to produce a given curvature  $1/R$  were given in Section 1.1.6. It was shown that the bending moment had the form

$$M = \frac{EI}{R} \left[ \frac{1}{1-\nu^2} + \frac{2\sqrt{3}\nu}{\alpha b(1-\nu^2)^{1/2}db} f(\alpha b) + \frac{3}{2\alpha b d^2} g(\alpha b) \right], \quad 1.76$$

but  $f(\alpha b)$  has a common factor  $-\nu/\alpha^2 R$  in all terms arising from the constants  $\bar{A}$  and  $\bar{B}$ , and  $g(\alpha b)$  has a common factor  $\nu^2/\alpha^4 R^2$  in all terms arising from the constants  $\bar{A}^2$  and  $\bar{B}^2$ , therefore, factoring these terms out define the following



$$f(\alpha b) = \frac{-v}{\alpha^2 R} F(\alpha b) \quad 1.77$$

$$g(\alpha b) = \frac{v^2}{\alpha^4 R^2} G(\alpha b) , \quad 1.78$$

where,

$$F(\alpha b) = (A' + B') \sinh \frac{\alpha b}{2} \cos \frac{\alpha b}{2} + (B' - A') \cosh \frac{\alpha b}{2} \sin \frac{\alpha b}{2} ,$$

and

$$\begin{aligned} G(\alpha b) = & 2\alpha b(A'^2 - B'^2) + 2(A'^2 + B'^2)(\sinh \alpha b + \sin \alpha b) \\ & + (A'^2 - 2A'B' - B'^2) \sinh \alpha b \cos \alpha b \\ & + (A'^2 + 2A'B' - B'^2) \cosh \alpha b \sin \alpha b , \end{aligned}$$

$$\text{where,} \quad A' = \frac{\sinh \frac{\alpha b}{2} \cos \frac{\alpha b}{2} - \cosh \frac{\alpha b}{2} \sin \frac{\alpha b}{2}}{\sinh \alpha b + \sin \alpha b}$$

$$\text{and,} \quad B' = \frac{\sinh \frac{\alpha b}{2} \cos \frac{\alpha b}{2} + \cosh \frac{\alpha b}{2} \sin \frac{\alpha b}{2}}{\sinh \alpha b + \sin \alpha b} .$$

Substituting equations 1.77 and 1.78 into 1.76 the bending moment simplifies to

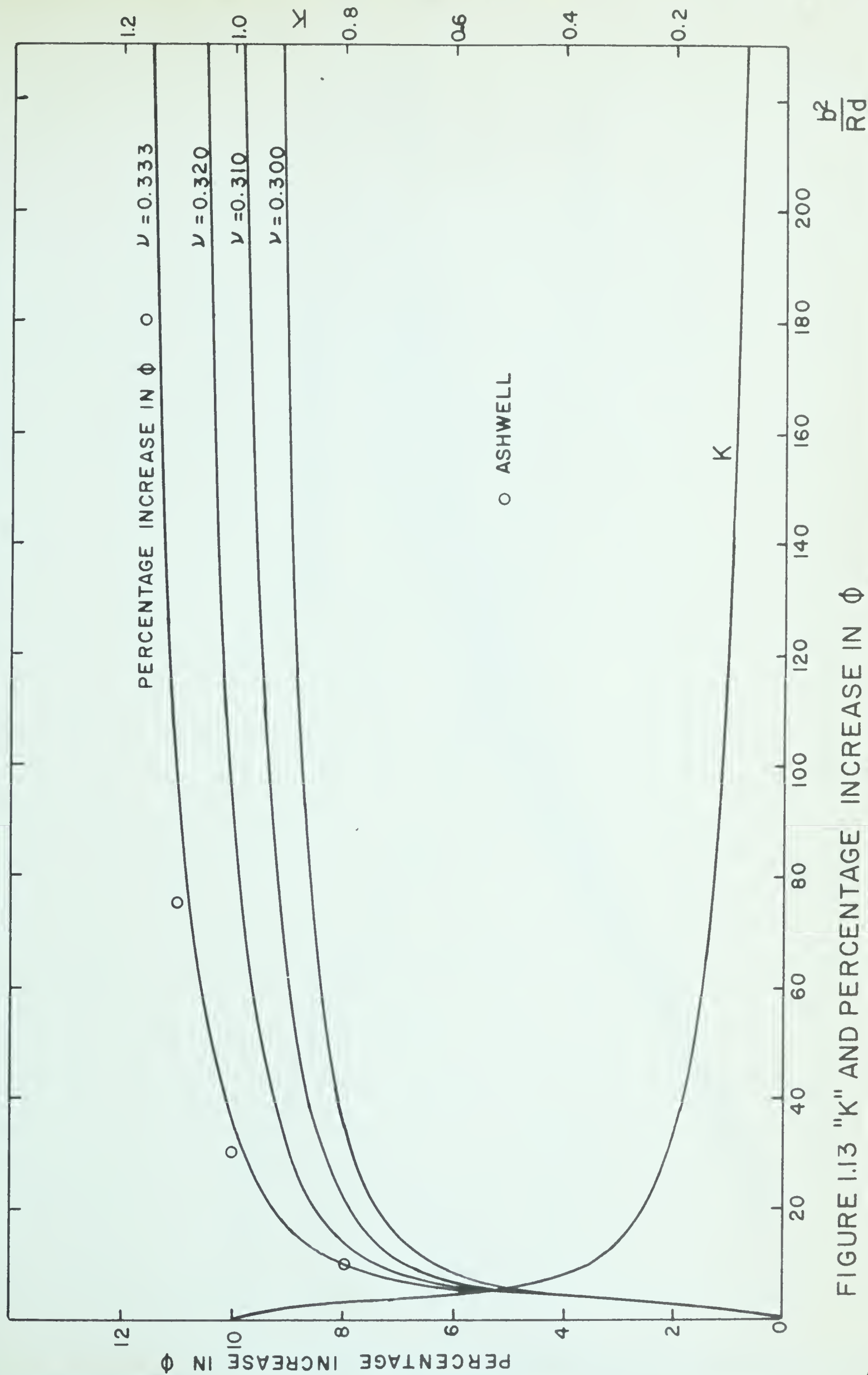
$$M = \frac{EI}{R} \left[ \frac{1}{1-v^2} - \frac{2v^2}{\alpha b(1-v^2)} F(\alpha b) + \frac{v^2}{2\alpha b(1-v^2)} G(\alpha b) \right] . \quad 1.79$$

Equating the bracketed expression to  $(1-kv^2)/(1-v^2)$  gives the value of  $k$  which, it is suggested, was known by Timoshenko in 1923, that is

$$k = \frac{1}{\alpha b} \left[ 2F(\alpha b) - \frac{1}{2} G(\alpha b) \right] . \quad 1.80$$

In Appendix II a computer program has been written to evaluate equation 1.80, the value of  $\emptyset$  from equation 1.69, and the "percentage increase" in  $\emptyset$ . The results are plotted



FIGURE 1.13 "K" AND PERCENTAGE INCREASE IN  $\phi$





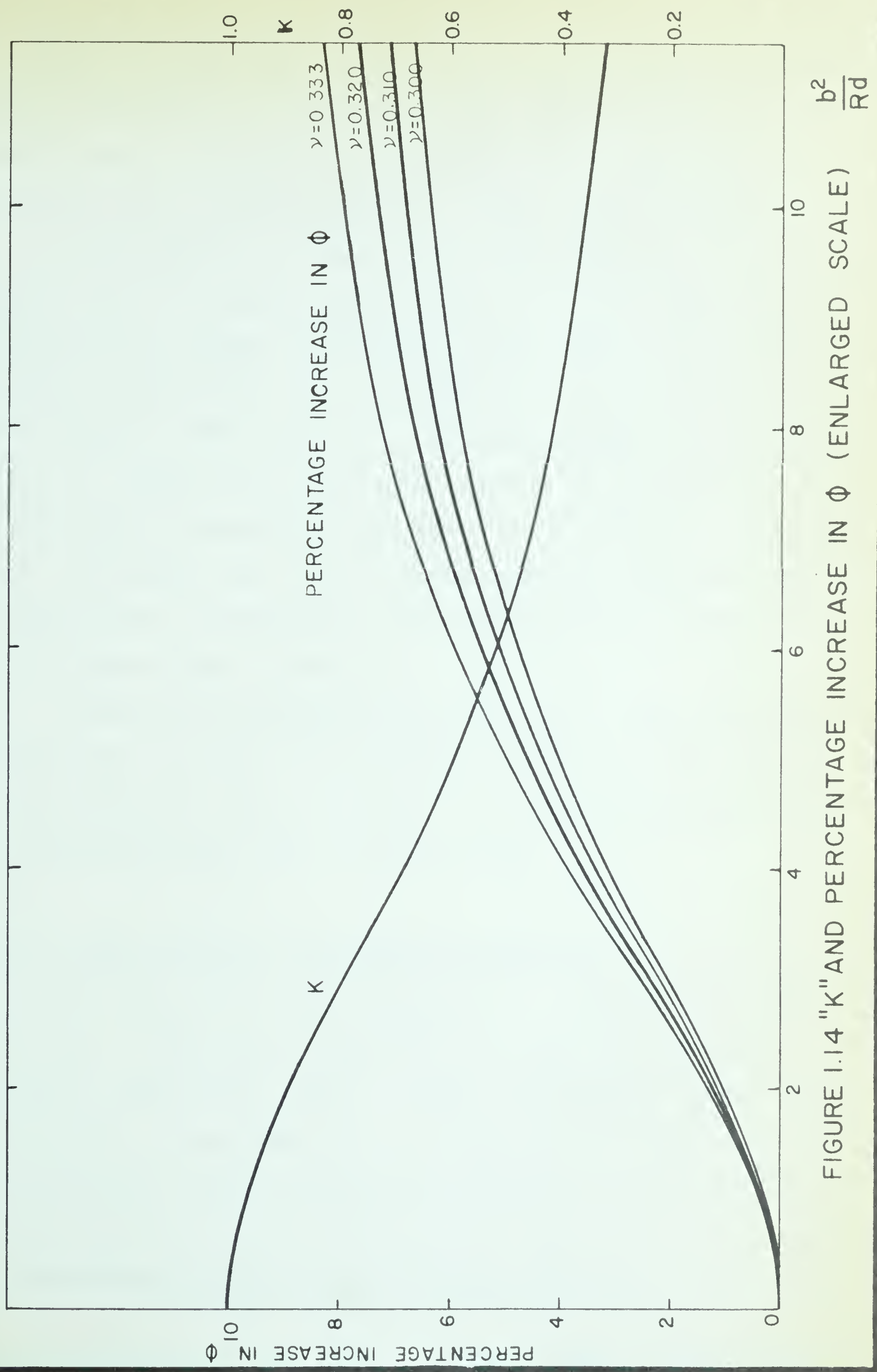


FIGURE 1.14 "K" AND PERCENTAGE INCREASE IN  $\phi$  (ENLARGED SCALE)



in Figures 1.13 and 1.14. Figure 1.14 is plotted on an enlarged scale to show that  $k$  approaches 1.0 asymptotically as  $b^2/Rd$  tends to zero. Similarly, the "percentage increase" in  $\phi$  approaches 0.0 asymptotically as  $b^2/Rd$  tends to zero.

From Figures 1.13 and 1.14 or the tabulated values in Appendix II, it is quite apparent that  $k$  is not affected significantly by a change in Poisson's ratio, whereas  $\phi$ , or the percentage increase in  $\phi$ , are affected. In particular, for a  $b^2/Rd$  value of 900 and an 11 percent increase in Poisson's ratio,  $k$  changes by 0.60 percent, whilst  $\phi$  changes by 2.3 percent and the "percentage increase" in  $\phi$  changes by 26.4 percent. It follows that  $k$  is a more realistic parameter than  $\phi$  to describe the transformation from beam action to plate action in the bending moment equation.

Although the difference is small, it is apparent from the tabulated results in Appendix II and equation 1.68 that increasing Poisson's ratio increases the effective stiffness ( $EI\phi$ ) of the plate for the same curvature  $1/R$ .

### 1.3.2 Comparison with Timoshenko and Ashwell

In Figure 1.15 the value of  $k$  is plotted versus  $\beta b$  where  $\beta b$  is defined in equation 1.55 using the tabulated results in Appendix I. There is some disagreement between the curve and the values tabulated by Timoshenko<sup>13</sup> in 1923. It only can be surmised, that in calculating equation 1.80, Timoshenko

---

<sup>13</sup> Timoshenko, Mechanical Engineering, loc. cit.



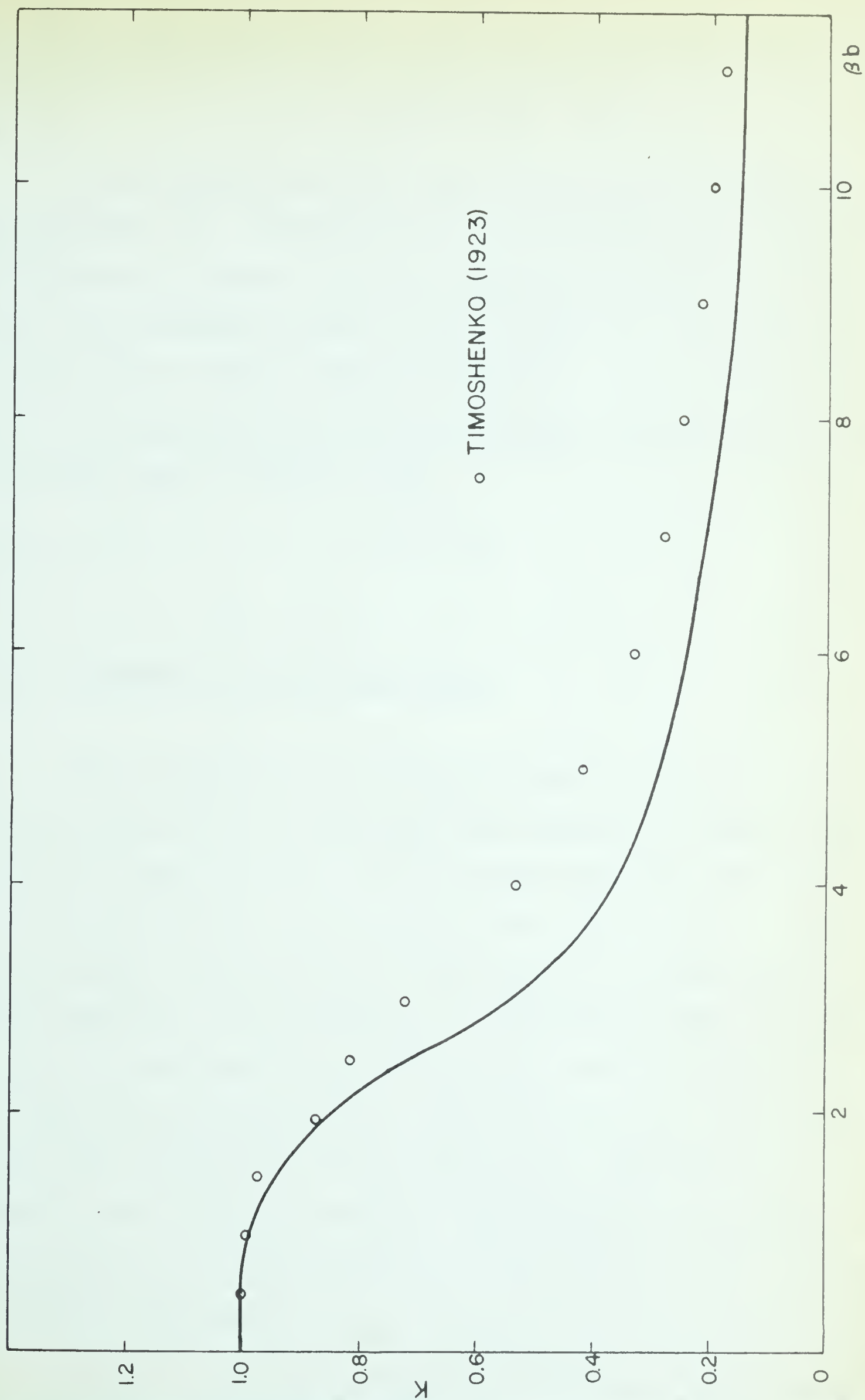


FIGURE 1.15 "K", BENDING MOMENT CURVATURE RELATIONSHIP





discarded those higher order terms which he believed were insignificant, but which this analysis shows, can affect the final result.

Since Ashwell did not tabulate any of his results for the parameter  $\emptyset$ , comparison can only be made with his graph<sup>14</sup>. Superimposed on Figure 1.13 are a few points taken from Ashwell's graph for a Poisson's ratio of  $1/3$ . There is a reasonable agreement but not as good as might be expected. Since Ashwell's solution is the same as that given in equation 1.76 the discrepancy is probably due to scaling only.

#### 1.4 PROBLEM OF CYLINDRICAL SHELL

The differential equation developed in Section 1.1.4, equation 1.18, which is analogous to a beam on an elastic foundation, is restricted only by the assumptions that the transverse slope be small and the shear force  $Q_y$  is zero. In a similar manner to Section 1.1.4 the solution of this differential equation can be applied to a cylindrical shell of radius  $R$ . In the undeformed state the curvature in the  $x$ -direction is zero and the curvature in the  $y$ -direction is  $1/R$ . After deformation the curvature in the  $x$ -direction is, approximately,  $d^2w/dx^2$  while in the  $y$ -direction the curvature now becomes

---

14 Ashwell, loc. cit.



$1/(R-w)$ . Thus the moments producing the deformation can be written as

$$M_x = -D \left\{ \frac{d^2 w}{dx^2} + \nu \left[ \frac{1}{R} - \frac{1}{R-w} \right] \right\} ,$$

and since  $w$  is very small compared with  $R$  this expression becomes

$$M_x = -D \frac{d^2 w}{dx^2} ,$$

and, 
$$M_y = \nu M_x . \quad 1.81$$

Timoshenko<sup>15</sup> has solved the problem outlined above for a shell subjected to edge moments  $M_o$ , see Figure 1.16. Thus, from equation 1.80 the boundary conditions become

$$\frac{d^2 w}{dx^2} = \frac{-M_o}{D} \quad \text{at } x = \pm b/2 , \quad 1.82$$

$$\frac{d^3 w}{dx^3} = 0 \quad \text{at } x = \pm b/2 .$$

Using these boundary conditions to evaluate the differential equation 1.18, Timoshenko arrives at the following equation for the deflection at the edge  $x = \pm b/2$

$$w = \frac{-2M_o \alpha^2 R^2}{Ed} \frac{\sinh \alpha b - \sin \alpha b}{\sinh \alpha b + \sin \alpha b}$$

or, 
$$w = \frac{-2M_o \alpha^2 R^2}{Ed} \chi_2 (\alpha b) , \quad 1.83$$

where, 
$$\chi_2 (\alpha b) = \frac{\sinh \alpha b - \sin \alpha b}{\sinh \alpha b + \sin \alpha b} .$$

Timoshenko has a table of  $\chi_2 (\alpha b)$  values for  $(\alpha b)$  from 0.20 to 5.0.

---

15 Timoshenko, S.P., and Woinowsky-Krieger, S., Theory of Plates and Shells, McGraw-Hill, 1959, pp. 478-479.



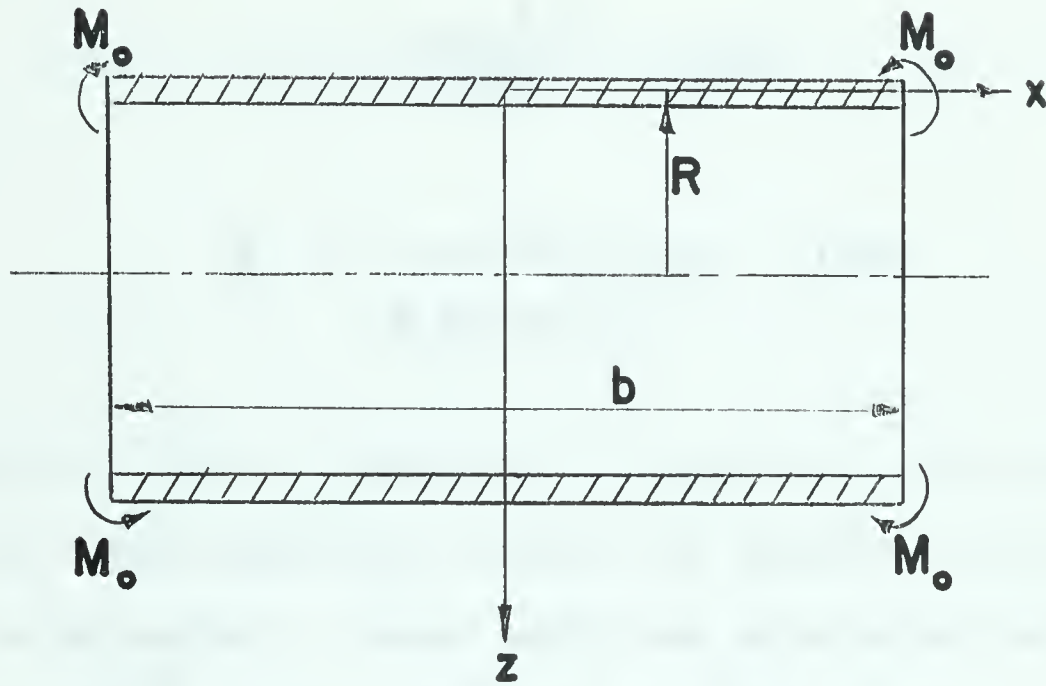


FIGURE 1.16 SECTION OF A CYLINDRICAL SHELL

If a plate is bent by a moment  $M_y = -M$  to a curvature  $\frac{1}{R}$ , and the surface is to remain cylindrical, then moments must be applied along the edges  $x = \pm b/2$  to prevent distortion; that is

$$M_x = \frac{-\nu D}{R}.$$

Now, for the plate problem under consideration the edges  $x = \pm b/2$  have no moments acting on them. Therefore, edge moments equal to  $\frac{+\nu D}{R}$  must be added to the problem above\*. But this is equivalent to the problem solved by Timoshenko, where

$$M_o = \frac{\nu D}{R}. \quad 1.84$$

\* Acknowledgement is given to H.D. Conway for outlining this approach.





Using equation 1.84 in equation 1.83 it follows that the edge deflection is given by,

$$w = \frac{-2\nu D \alpha^2 R^2}{R E d} \chi_2(\alpha b)$$

or, 
$$\frac{w}{d} = \frac{-\nu}{2 \left[ 3(1-\nu^2) \right]^{1/2}} \chi_2(\alpha b) \quad 1.85$$

Equation 1.85 is identical to equation 1.36 evaluated at  $x = \pm b/2$ . The numerical values for equation 1.85, which are listed in Appendix I, agree with the tabulated values in Timoshenko's book<sup>16</sup> for the same  $\beta b$  or  $b^2/Rd$  ratios.

---

16 Loc. cit.



## CHAPTER II

### EXPERIMENTAL METHODS IN DETERMINING SMALL TRANSVERSE DEFLECTIONS

This chapter describes some methods which may be used to measure small deflections. The results of previous experimental work in measuring transverse deflections of plates is discussed. A detailed development is given for the measurement of deflections from electrical resistance strain gauges. It is shown, using a numerical integration procedure, how a programmed digital data processor and a digital computer are combined to speed up computation of the deflections and yield reasonably accurate results. The experimental apparatus used for testing rectangular plates under large longitudinal curvatures is also given.

#### 2.1 PREVIOUS EXPERIMENTAL WORK

##### 2.1.1 General Remarks

In 1891 Lamb<sup>17</sup> concluded the paper on the plate problem, with the following remarks;

At the edge (of the plate) itself the deviation from the cylindrical form is comparable with  $(d/2)$ , but it rapidly diminishes as we pass inwards, at the same time fluctuating in sign. The latter result may perhaps be unexpected, but a little consideration will show that it is intimately bound up with the supposition we have made, that there is no resultant force on the ends of the band. The amplitudes of the fluctuations diminish, however, so rapidly that it is not likely that this feature of the strain could ever be made the subject of observation.

---

17 Lamb, loc. cit.



The object of this chapter is to describe an adequate means of observing these "fluctuations".

The type of experiment that is conducted will depend on the apparatus and measuring equipment available. From the theoretical solution it is obvious that whatever plate size is chosen, two opposite edges must be free, and a uniform bending moment must be applied to the other two edges. On the choice of a suitable plate size, Searle<sup>18</sup> remarked

...success will largely depend upon a proper choice of the section of the blade and upon the use of a sensitive and accurate instrument for measuring the displacement.... The bending of the blade under its own weight should be made as small as possible by the use of a short blade and by a proper choice of the distance between knife edges.

### 2.1.2 Ashwell and Greenwood

In 1950 Ashwell and Greenwood<sup>19</sup> described an experimental method designed to check the validity of Lamb's solution. A mild steel plate  $1/8 \times 15 \times 96$  in. was supported on knife edges 4 ft apart. Bending moments were applied by placing weights on the overhangs. This size of plate was chosen in order that  $b^2/Rd$  values up to 16 could be obtained and still remain below the yield point. The importance of measuring at locations sufficiently far removed from the support and loading regions was noted and it was suggested the distance between supports should be between three and four times the width of the plate.

---

18 Searle, loc. cit.

19 Ashwell, D.G., and Greenwood, E.D., "The Pure Bending of Rectangular Plates," Engineering, 21st and 28th July, 1950., pp. 51-53, and pp. 76-78.







The distortion of the transverse section was measured, at first, with a dial gauge placed at  $1/2$  in. intervals across the breadth of the plate. However, it was found that the pressure of the dial gauge plunger was sufficient to produce an additional deflection of the plate which was not negligible compared with the deflection being measured. Notwithstanding this deficiency, it was shown, for a  $b^2/Rd$  ratio of 11.8, the transverse deflection was of the same form as the theoretical curve. The longitudinal curvature was determined by measuring, with a scale, the distance between the plate at its midline and a string stretched between the supports.

In a series of tests (the results were not recorded) it was found that the plate deflected unsymmetrically, especially for large longitudinal curvatures. Ashwell and Greenwood found that this effect could be "cured by leaving (the plate) for two days and nights fairly heavily loaded."

In a second set of experiments Ashwell and Greenwood<sup>20</sup> used an "Angle Dekkor", a type of auto-collimator capable of measuring small angle changes with an accuracy of one minute. The angle changes along a transverse direction of the plate were observed by placing mirrors  $1-1/8 \times 11/16$  in. at  $3/4$  in. intervals across the width of the plate. These mirrors were "secured" to the plate "by small lumps of Plasticene".

The results obtained using the "Angle Dekkor" were compared with the theory for  $b^2/Rd$  ratios up to 7.75. The

---

20 Ashwell, D.G., and Greenwood, E.D., "Measuring Small Changes in Curvature with an Angle Dekkor," Machinery, Dec. 1948, pp. 835-836.



disagreement between theory and experiment was attributed to initial stresses in the plate and it was emphasized that the final deflected form would be influenced by the presence of these stresses; "This is a fact that must always make experiments of this type rather difficult...."

### 2.1.3 Experiments at the University of Alberta

An alternative method to that of Ashwell and Greenwood was used by the author<sup>21</sup> to show that the transverse deflection could be computed accurately from electrical resistance strain gauges bonded to the top and bottom surfaces of a plate in a transverse direction.

Using strain gauges the author attempted to investigate the transverse deflection of plates for  $b^2/Rd$  ratios as high as 191. Several plates were tested with widths from 10 in. to 36 in., the distance between supports being kept constant at 36 in. for all plates. The transverse deflection of plates 18 in. and wider was extremely distorted; in fact, becoming synclastic for large  $b^2/Rd$  values.

The plates chosen for these experiments were of 75 ST-6 Alclad aluminum. Aluminum was used rather than steel because, for the same curvature, the loads required are about one third less.

Despite the abnormal distortion for large  $b^2/Rd$  values it was concluded that  $b^2/Rd$  represented a true physical ratio

---

21 Bellow, D.G., Transverse Curvature of Plates under Large Deflections, Unpublished M.Sc. Thesis, University of Alberta, 1960.





and that its magnitude described the mode of transverse bending. It was found for  $b^2/Rd$  less than 16 the transverse curvature was anticlastic, while for  $b^2/Rd$  greater than 22 the transverse curvature was essentially synclastic.

In an effort to determine the influence of the supports and loading hangers on the transverse deflection, strain gauges were placed longitudinally along the centerline between the transverse gauges and the support. It was then believed that if the longitudinal strains were identical, the assumption of a uniform bending moment would be justified. If however, the readings from these gauges varied appreciably then it would be assumed these readings were influenced by the method of loading or by the local disturbance caused by the supports. As expected, the longitudinal strains did not differ appreciably from one another and it was concluded that the supports did not influence the transverse curvature.

Also, if the experimental values are correct, and if the differential equation is correct, then a possible reason for the discrepancy between experiment and theory is that the boundary conditions of the differential equation are incorrect. It was recommended that an attempt be made to determine the true boundary conditions.

#### 2.1.4 Discussion and Summary

There are advantages and disadvantages in all of the experimental methods described above. While the accuracy of the "Angle Dekkor" used by Ashwell and Greenwood is satisfactory, the





disadvantage of this method lies in observing the slope, not at a point, but averaged over  $11/16$  in. Also, reliance must be placed on the fixity of the Plasticene. Alternatively, if the mirrors were bonded to the plate with adhesive a certain reinforcing effect would result. With the method used by the author there is no reinforcing effect from the strain gauges although they are intimately bonded to the metal surface. Also, with small gauges there is very little averaging of strains.

Ashwell and Greenwood compared the experimental slopes as measured by the "Angle Dekkor" with the theoretical slopes. No comparison was made with the theoretical deflections except as noted with the use of dial gauges.

The published results of Ashwell and Greenwood and the M.Sc. thesis of the author indicated that more experimental results are required, especially at large  $b^2/Rd$  values, for experimental verification of Lamb's solution for all modes of deformation from beam to plate behaviour.

At the present time it appears that no one has performed a successful experiment to determine a value of  $k$  or  $\phi$  (see Section 1.3); although in 1908, Searle<sup>22</sup> said "It would be interesting to endeavour to detect experimentally the change in the product (MR) as the bending proceeds." The difficulty in performing an experiment of this type is that  $k$  varies from one to zero ( $\phi$  varies from one to  $9/8$ ) and the effect of such a small variation will be extremely difficult to detect even with

---

22 Searle, loc. cit.



the most elaborate test equipment. If however, good agreement between experiment and theory can be obtained for the transverse deflection, then this will verify the differential equation and justify the assumed boundary conditions, which are used in determining the theoretical value of  $k$  (see Section 1.1.6).

## 2.2 MEASUREMENT OF TRANSVERSE DEFLECTIONS BY MEANS OF ELECTRICAL RESISTANCE STRAIN GAUGES

### 2.2.1 Basic Assumptions

When using electrical resistance strain gauges in applications where great accuracy is required, certain precautions must be taken in the selection and application of these gauges. Once these precautions have been taken it is usual to assume the following;

1. The effect of the thickness of the adhesive plus the strain gauge backing material is negligible so that the strain recorded by the gauge is the same as that for the test material immediately underneath the gauge.
2. The variation of strain along the length of the grid is small compared with the measured strain. That is, the value of strain recorded from a gauge of finite length (which is an average value) can be considered to be the strain at a point.



3. The transverse sensitivity coefficient is sufficiently small so that a strain gauge placed in a two dimensional strain field is unaffected by strains perpendicular to its length.

These assumptions are discussed in more detail in Section 2.4.3. They are mentioned here because of their importance in the numerical analysis of the following sections.

### 2.2.2 Analysis of Strains to Obtain Deflections

The curvature in the transverse direction is given by the expression

$$\frac{1}{R_x} = \frac{\frac{d^2 w}{dx^2}}{\left[1 + \left(\frac{dw}{dx}\right)^2\right]^{3/2}} .$$

If the slopes are small, then the squares of the slopes are negligible compared with unity, and the above expression can be written as

$$\frac{1}{R_x} \doteq \frac{d^2 w}{dx^2} .$$

Integrating this expression twice with respect to the transverse direction  $x$  yields

$$w(x) = \int_{c_1}^x \int_{c_2}^x \frac{d^2 w}{dx^2} dx dx \quad 2.1$$

where  $c_1$  and  $c_2$  are arbitrary constants.

Consider a transverse strip, sufficiently removed from the supports and loading regions, with curvature  $1/R_{x_i}$  at a point  $x_i$ . Let the values recorded from two strain gauges, mounted on the top and bottom of the strip, be denoted by  $e_{T_i}$  and  $e_{B_i}$  respectively. The strain at a point in a fiber, a







distance  $z$  from the neutral surface, is directly proportional to the curvature at that point; that is

$$e = -\frac{z}{R_x} \quad 2.2$$

providing plane sections remain plane. It is possible the strains recorded from the gauges  $e_{T_i}$  and  $e_{B_i}$  include membrane as well as bending strains. To eliminate the membrane strains, since the curvature depends only on the bending strains, it is required to subtract the average value of  $e_{T_i}$  and  $e_{B_i}$  from either of these strains. Therefore,

$$\begin{aligned} e_{av_i} &= \frac{e_{T_i} + e_{B_i}}{2} \\ (e_{bending})_i &= e_{B_i} - e_{av_i} = - (e_{T_i} - e_{av_i}) \\ &= \frac{e_{T_i} - e_{B_i}}{2}, \end{aligned} \quad 2.3$$

but, from equation 2.2 the bending strain at the surface of a strip of thickness  $d$  is given by

$$(e_{bending})_i = \frac{d}{2R_{x_i}},$$

and substituting this result into equation 2.3 gives

$$\frac{1}{R_{x_i}} = \frac{e_{T_i} - e_{B_i}}{d} \quad 2.4$$

where "i" denotes a particular position along the transverse strip. It is seen from this equation that the sign of the curvature depends on the signs of the strains as well as their magnitudes. For anticlastic bending  $e_{T_i}$  is compressive,  $e_{B_i}$  is



tensile, and  $1/R_{x_i}$  is negative. This agrees with the sign convention adopted in Chapter I.

Equation 2.4 is used, in the numerical analysis of Section 2.2.5, to determine the transverse slopes.

### 2.2.3 Numerical Methods of Integration

A numerical integration of a set of tabulated values  $f(x)$  consists in finding a suitable interpolating function which passes through several adjacent points and then integrating this interpolating function.

Two simple methods of numerical integration are the trapezoidal rule and Simpson's rule; the former consists in passing a straightline through two adjacent points and finding the area of the resulting trapezoid, the latter consists in passing a parabola through three adjacent points and finding the area of the enclosed region. Simpson's rule requires three points in the integrating process while the trapezoidal rule only requires two. It will be shown in the following paragraphs that it is required to compute the area of a curve between two adjacent points; this precludes the use of Simpson's rule. Thus, the trapezoidal rule is used as the integration method.

### 2.2.4 Trapezoidal Rule<sup>23</sup>

In Figure 2.1 a portion of a curve  $f(x)$  is shown with ordinates  $f_i$  and  $f_{i+1}$  at  $x_i$  and  $x_{i+1}$  respectively.

---

23 Crandall, S.H., Engineering Analysis, McGraw-Hill, 1956, Problem 3-45, p. 162.



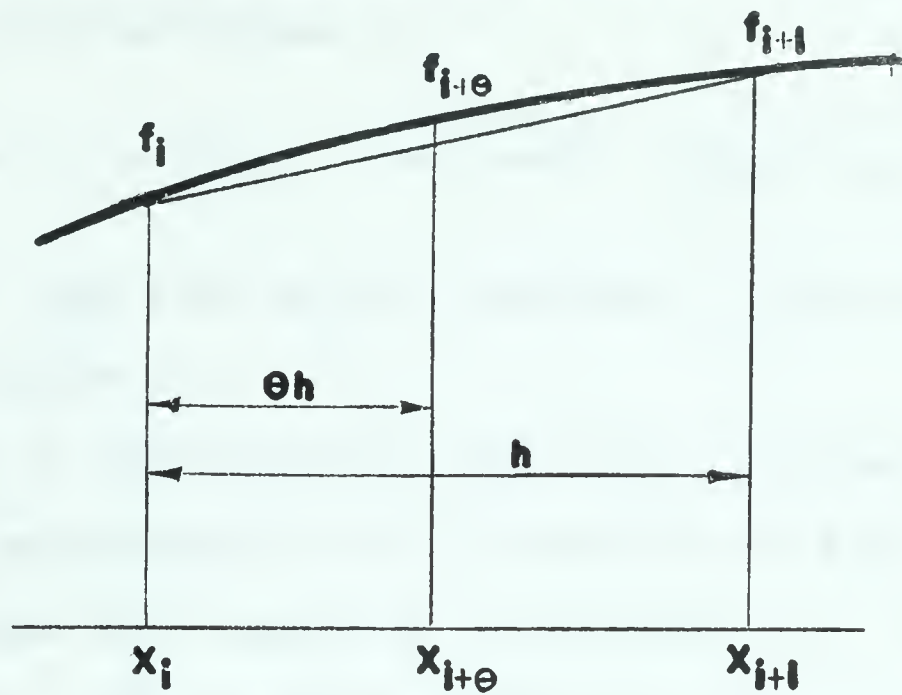


**FIGURE 2.1 STRAIGHT LINE INTERPOLATION**

Let  $x_{i+1} - x_i = h$

and  $x_{i+\theta} - x_i = h\theta$

where  $0 \leq \theta \leq 1$ .

Introducing the notation

$$f(x_i + \theta h) = f_{i+\theta}$$

and expanding the left hand side in a Taylor series gives

$$f(x_i + \theta h) = f(x_i) + \theta h f'(x_i) + \frac{(\theta h)^2}{2!} f''(x_i) + \dots \quad 2.5$$

For  $\theta = 1$  equation 2.5 becomes

$$f_{i+1} = f(x_i) + h f'(x_i) + \frac{h^2}{2!} f''(x_i) + \dots, \quad 2.6$$

and for  $\theta = 0$

$$f_i = f(x_i)$$







as defined earlier. Multiplying equation 2.6 by  $h$  and adding  $hf(x_i)$  to each side reduces to

$$\frac{h}{2} (f_{i+1} + f_i) = hf(x_i) + \frac{h^2 f'(x_i)}{2} + \frac{h^3}{2 \cdot 2!} f''(x_i) + \dots, \quad 2.7$$

where the left hand side of this equation is the area of the trapezoid in Figure 2.1.

To get an expression for the error involved, in using a straight line approximation, it is required to find the exact value of the area and compare it to equation 2.7. The exact expression can be obtained by multiplying equation 2.5 by  $h$  and integrating term by term with respect to  $\theta$  over the interval zero to one. This gives

$$\int_0^1 hf(x_i + \theta h) d\theta = hf(x_i) + \frac{h^2}{2} f'(x_i) + \frac{h^3}{6} f''(x_i) + \dots \quad 2.8$$

Subtracting equation 2.7 from 2.8 gives the truncation error, which is

$$\int_0^1 hf(x_i + \theta h) d\theta - \frac{h}{2} (f_{i+1} + f_i) = -\frac{h^3}{12} \left[ \frac{d^2 f}{dx^2} \right]_i + \dots \quad 2.9$$

For measuring stations  $1/2$  in. apart the leading term of the truncation error is

$$\frac{1}{96} \left[ \frac{d^2 f}{dx^2} \right]_i \text{ in.}^2 \quad 2.10$$

In the evaluation of the experimental results, expression 2.10 is used to check the error.



### 2.2.5 Application of the Trapezoidal Rule to Obtain Deflections

The values of  $R_{x_i}$  are evaluated at the measuring points  $x_i$  from equation 2.4. The difference in slopes between points  $x_{i+1}$  and  $x_i$  is given by

$$\left[ \frac{dw}{dx} \right]_{i+1} - \left[ \frac{dw}{dx} \right]_i = \int_{x_i}^{x_{i+1}} \frac{1}{R_x} dx \quad . \quad 2.11$$

Using the trapezoidal rule, the right hand side of equation 2.11 is evaluated as follows

$$\left[ \frac{dw}{dx} \right]_{i+1} - \left[ \frac{dw}{dx} \right]_i = \frac{1}{2} \left[ \frac{1}{R_{x_{i+1}}} + \frac{1}{R_{x_i}} \right] (x_{i+1} - x_i) \quad . \quad 2.12$$

Since the slope at  $x_0$  is zero ( $x = 0$ ) the slope at the point  $x_i$  can be evaluated from the values of equation 2.4 by addition. The numerical integration, in each case, is started at the center of the plate.

Once the slopes have been evaluated a similar procedure is followed to determine the deflections. The difference in deflections between points  $x_{i+1}$  and  $x_i$  is given by

$$w_{i+1} - w_i = \int_{x_i}^{x_{i+1}} \frac{dw}{dx} dx \quad . \quad 2.13$$

Using the trapezoidal rule the right hand side of equation 2.13 is evaluated as follows

$$w_{i+1} - w_i = \frac{1}{2} \left\{ \left[ \frac{dw}{dx} \right]_{i+1} + \left[ \frac{dw}{dx} \right]_i \right\} (x_{i+1} - x_i) \quad . \quad 2.14$$

The deflection at  $x_0$  is taken as zero. By starting the numerical integration at  $x_0$ , that is, at the centerline of the



plate, the deflection at any point along the transverse strip can be obtained by a repeated application of equation 2.14.

The deflections obtained from equation 2.14 are relative to  $w = 0$  at  $x_0$ . These are not the true deflections since it was shown in Chapter I that a necessary condition for the resultant force  $N_y$  integrated over the entire plate width to be zero, is that the  $x$ -axis coincide with the centroidal axis of the cross section. The calculation of the centroid is discussed in Section 2.2.6.

#### 2.2.6 Calculation of Centroidal Axis

To calculate the position of the centroidal axis a straight line interpolation is used between adjacent points on the curve  $w$  versus  $x$ . The length of this line is given by

$$\left[ h^2 + (w_{i+1} - w_i)^2 \right]^{1/2},$$

where  $h$  is the distance between  $x_i$  and  $x_{i+1}$  measured along the  $x$ -axis. The moment of this line about this axis is equivalent to

$$\left[ \frac{w_{i+1} + w_i}{2} \right] \left[ h^2 + (w_{i+1} - w_i)^2 \right]^{1/2}.$$

Now the greatest possible difference of  $w$  between any two adjacent measuring points of the plate will be less than one-tenth the thickness of the plate. Thus, it follows for a plate thickness of  $1/8$  in.

$$(w_{i+1} - w_i)^2 \doteq \frac{1}{6400} \text{ in.}^2$$

and for measuring stations  $1/2$  in. apart it is seen that





$$(w_{i+1} - w_i)^2 \ll h^2$$

and thus the length of the line connecting  $w_i$  to  $w_{i+1}$  can be taken as  $h$ . Consequently the moment of this line is

$$\frac{h}{2} (w_{i+1} + w_i) .$$

The centroid of the deflected transverse cross section is given by

$$\bar{w}b = \int_{-b/2}^{b/2} w dx$$

where  $b$  is the plate width. By using a straight line interpolation  $\bar{w}$  will be given by

$$\bar{w}b = \frac{h}{2} \left[ (w_0 + w_1) + (w_1 + w_2) + \dots (w_{n-1} + w_n) \right] .$$

If  $n$  is the number of measuring stations, and noting that the width of the plate can be expressed by

$$b = (n - 1)h ,$$

then it follows that

$$\bar{w} = \frac{1}{2(n-1)} (w_0 + \sum_{m=2}^n 2w_{m-1} + w_n) . \quad 2.15$$

The true position of the  $w$  curve relative to the centroidal axis will be given by equations 2.14 and 2.15, that is

$$w_{\text{true}} = w - \bar{w}$$

The foregoing analysis indicates that the evaluation of  $\bar{w}$  is another application of the trapezoidal rule.



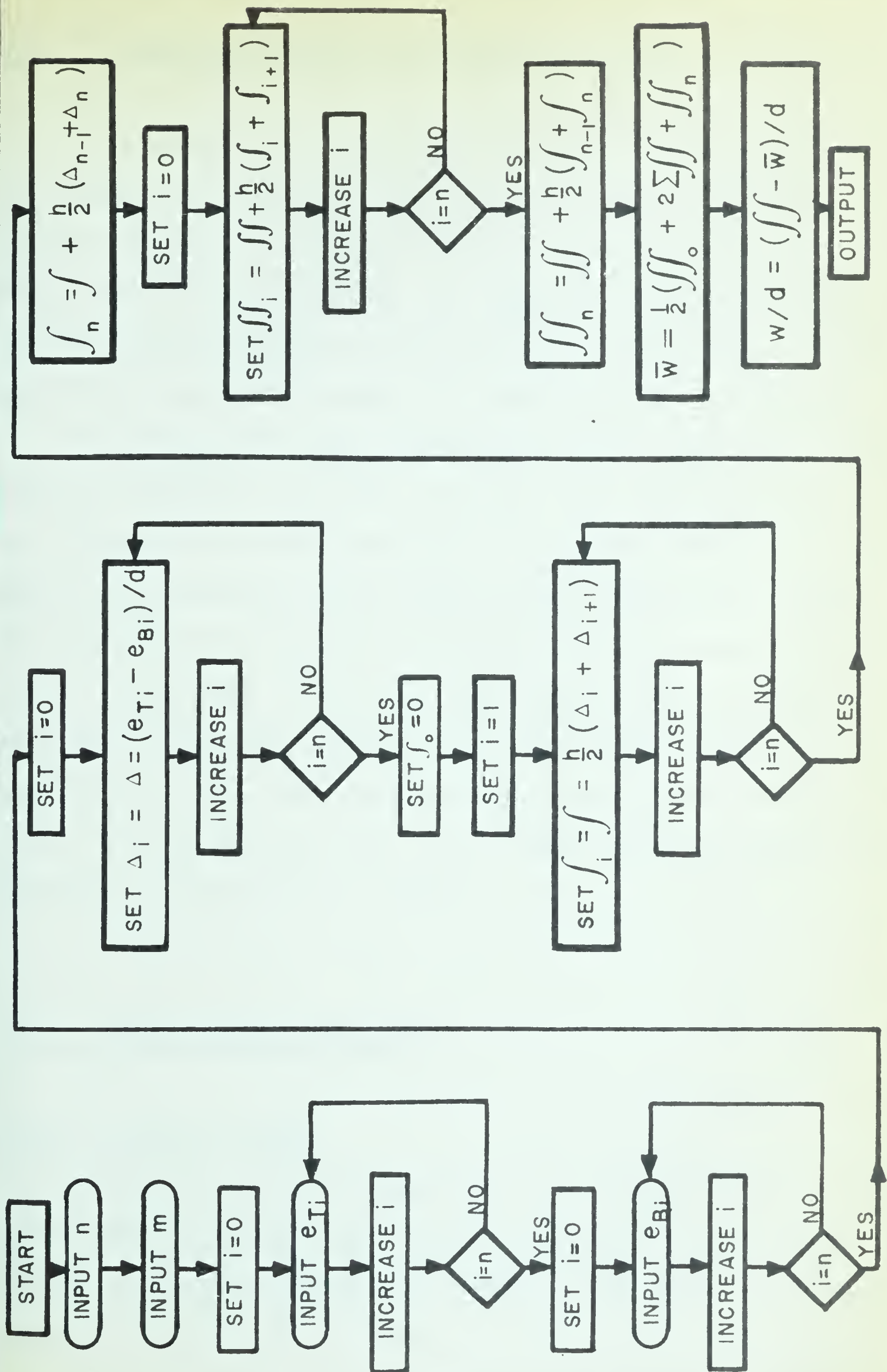


FIG. 2.2 COMPUTER CALCULATION OF DEFLECTIONS FROM STRAINS



## 2.3 COMPUTER ANALYSIS OF EXPERIMENTAL DATA

A McBee LGP-30 computer was used in the determination of the transverse deflection from the strain readings using the trapezoidal rule. Transverse strains recorded on a perforated tape were fed directly into the computer. The flow diagram of the main program is shown in Figure 2.2. The entire program, written in machine language, is reproduced in Appendix III.

It was found from preliminary tests, that the cantilever bridge assemblies (see Section 4.2.2) were not sensitive enough to achieve a null corresponding to zero load condition. This meant the recorded strains could not be considered absolute. A special conversion program was written to overcome this difficulty. This program subtracts the initial strains, recorded for zero load condition, from the strains recorded for any other loading condition (see Appendix III). The output of this program, which is on perforated tape, is fed into the main program for the multiple integration calculation.

## 2.4 EXPERIMENTAL APPARATUS

### 2.4.1 Loading Frame

For the current experimental testing, the loading frame used in the author's M.Sc. thesis was modified from a fixed span length to one of variable span length. The reasons for this were;







1. In order to obtain more conclusive results it was decided a wider plate would be necessary. This would enable more strain gauges to be placed across the width of the plate and, in effect, reduce the truncation error in the subsequent numerical analysis.
2. In anticipation of the experimental work discussed in Chapter III it was decided the frame should be adjustable so that it could accommodate various span lengths. The frame was therefore modified to have an adjustable span length of 1.5 to 6.0 ft.

The previous method of applying loads to a plate consisted in bolting a load hanger assembly to the plate. This had the disadvantage that at large curvatures the hanger assembly not only exerted a force at the point of application but also a moment, the latter of which was difficult to evaluate. Consequently the loading system was changed so that at the point of application only a force was applied. This was accomplished by loading on freely swinging hangers which always acted in a vertical plane as shown in Figure 2.3. To prevent these slipping off the plate, two small screws were inserted into the plate at the ends. Figure 2.4 shows the plate under load on the test frame for a  $b^2/Rd$  value of 55.

#### 2.4.2 Plate Size

In the author's M.Sc. thesis several combinations of plate widths and thicknesses were individually loaded and their transverse curvatures recorded in order to determine if the ratio





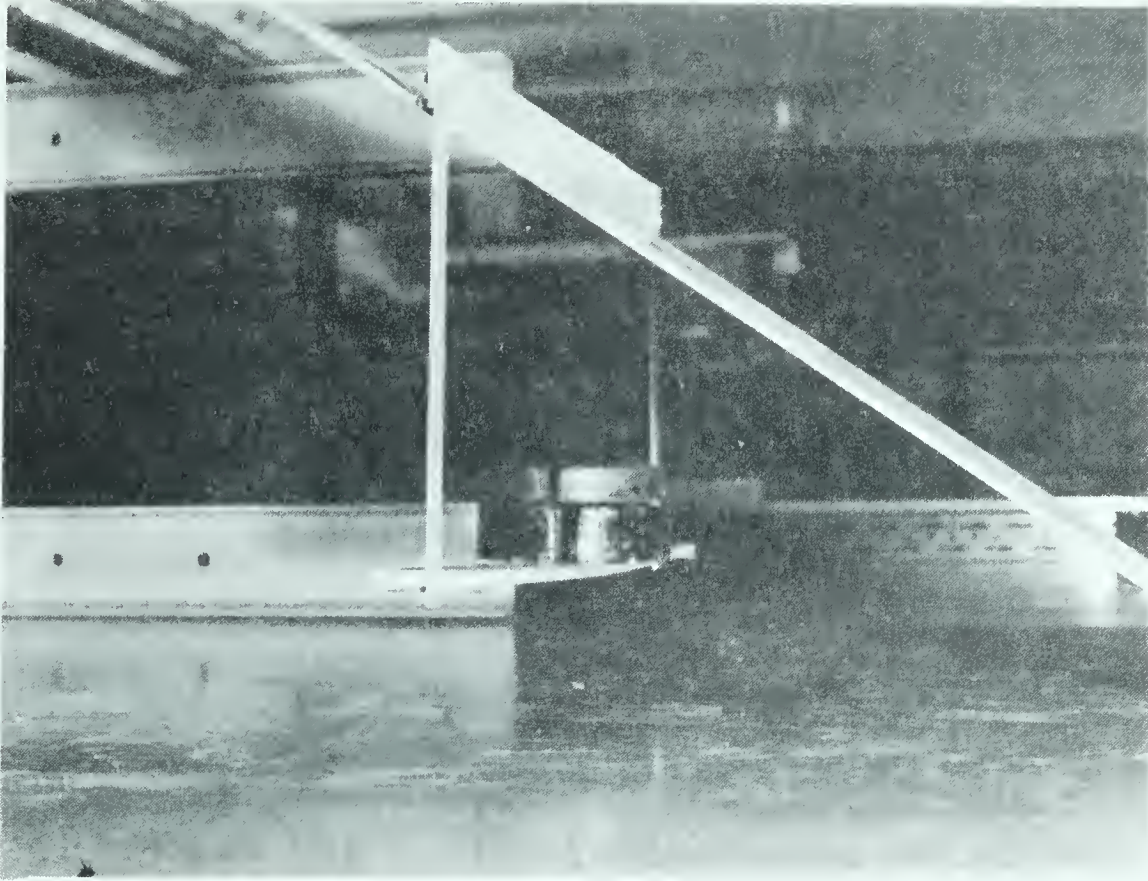


FIGURE 2.3 LOAD HANGER ASSEMBLY

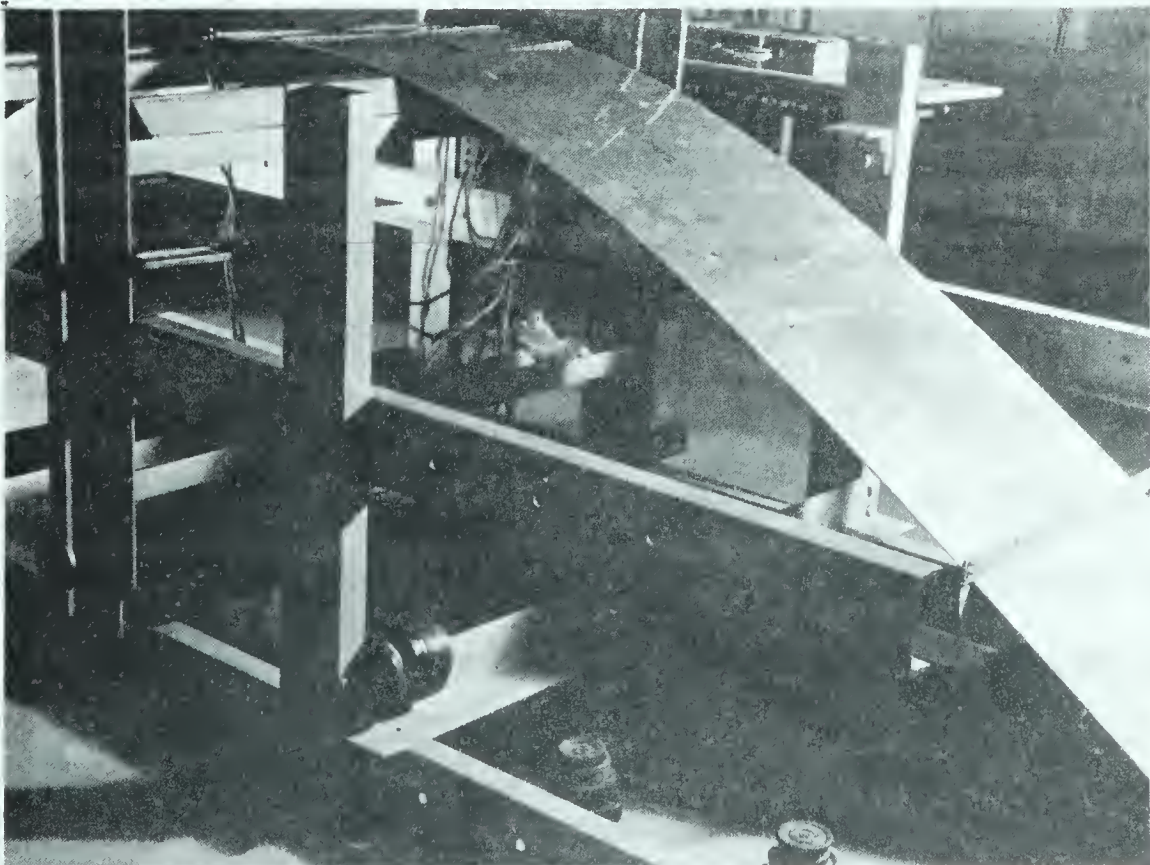


FIGURE 2.4 PLATE UNDER LOAD ON TEST FRAME





$b^2/Rd$  was truly independent of plate size. It was found from these tests that the  $b^2/Rd$  ratio determines the mode of transverse curvature. On the basis of these results it was decided it would be unnecessary to test more than a single plate since the curves  $w$  versus  $x$  can be made non-dimensional if desired, by dividing by the depth in the case of the ordinate  $w$ , and dividing by the width in the case of the abscissa  $x$ .

As in the previous experimental work of the author an aluminum sheet was chosen because lower loads would be required to produce a given curvature than if the sheet were of steel. The sheet chosen was cut from a rolled sheet of Alclad 75 ST-6. The finished dimensions were  $1/8 \times 18 \times 144$  in.

#### 2.4.3 Strain Gauges

Baldwin-Lima-Hamilton SR-4 strain gauges, type A-5-1, were used in the previous experimental work of the author. The A-5-1 is a wire-wound paper backed gauge, with a grid length of 0.5 in. and an overall length (trimmed) of 1.0 in. With this gauge, strains could not be measured at intervals less than 1.0 in. Also, paper plus glue thickness sometimes resulted in the gauge being up to 0.011 in. away from the mounting surface. Although these factors are of no consequence in many strain gauge applications, they were critical in the present application. Consequently, a smaller thinner strain gauge was required.

In recent years considerable improvements have been made in the strain gauge field. One of the most significant advances





was the development of the metal film, etched, or printed circuit strain gauge. The advantages of this gauge over the bonded filament type are the wide range of available sizes, temperature compensation, close electrical tolerances, large power-handling capability, thinness of backing material, and low transverse sensitivity. Disadvantages of these gauges are the higher cost and difficulty of application. The technique in applying metal film gauges, despite the claims of the manufacturers, is not simple and requires considerable experience, time, and patience. Standard metal film strain gauges can be obtained with gauge lengths of 0.015 in. It can be appreciated the application of these small gauges is difficult.

Considering all the disadvantages and advantages it was decided to use "Budd Instruments" metal film strain gauges, type C12-121, for the measuring stations across the plate. These gauges are temperature compensated for aluminum and have a grid length of 0.125 in. and an overall length of 0.250 in. The gauges were placed at 1/2 in. intervals across the plate. Closer grouping of these gauges was possible but if this were done the number of channels to be measured and recorded would be greater than the capacity of DIDAP\*.

It was required to obtain the strain at the edges  $x = \pm b/2$  on the top and bottom surfaces of the plate. This would require a gauge of zero length. To obtain as close an

---

\* Abbreviation adopted in this text for the much longer title of "Multi-Channel Digital Data Processor" of which a complete description is found in Chapter IV.



approximation to this as possible type Cl2-111 gauges were placed at the edges of the plate. These gauges have a grid length of 0.063 in. and are temperature compensated for aluminum. The center of the grid is 0.0315 in. from the edge, or the center to center distance to the adjacent gauge is 0.4635 in. This will contribute a small error into the numerical analysis which assumes a constant interval of 0.5 in. between gauges. In addition, this gauge will record a lower value of strain than if it were placed exactly at the edge.

#### 2.4.4 Transverse Sensitivity

An electrical resistance strain gauge is a sensing device made up of a finely wound wire, or foil grid, of a special alloy. Any change in length of the grid results in a proportional change in resistance. The constant of proportionality is called the gauge factor. If a gauge is placed in a two-dimensional strain field the change in length will be due to first, the longitudinal change in length of the gauge, and second, the effect of the strain field perpendicular to the gauge. This secondary effect is known as transverse sensitivity. It is caused by numerous factors such as; Poisson's ratio of the grid material, grid configuration, grid dimensions, and gauge backing material.<sup>24</sup> The ideal strain gauge is one with a zero transverse sensitivity coefficient. If a gauge has some transverse

---

24 Wu, C.T., "Transverse Sensitivity of Bonded Strain Gauges," Experimental Mechanics, Nov. 1962, pp. 338-344.





sensitivity, and it is significant, it must be taken into account when an accurate analysis is required. The magnitude of the error, in neglecting the transverse sensitivity, depends on the transverse sensitivity coefficient and the magnitude of the strain perpendicular to the direction in which the strain is being measured.

The manufacturers use an empirical approach to transverse sensitivity. The change in resistance of a gauge is assumed to be proportional to a linear combination of the strains in the axial and transverse directions. That is,

$$\frac{\delta R}{R} = F_a (e_a + c e_t) \quad 2.16$$

where,  $F_a$  is the axial strain sensitivity of a gauge for zero transverse strain,  $e_a$  is the axial strain,  $e_t$  is the transverse strain, and  $c$  is the transverse sensitivity coefficient.<sup>25</sup> The gauge factor  $k$  is defined as

$$k = \frac{\delta R/R}{\delta L/L} = \frac{\delta R/R}{e_a} \quad 2.17$$

Eliminating  $\delta R/R$  from equations 2.16 and 2.17 yields

$$e_a = \frac{c F_a e_t}{k - F_a} \quad 2.18$$

Strain gauges are calibrated by the manufacturer using nickel-plated steel specimens ( $\nu = 0.285$ ) subject to uniaxial loading.

---

25 Baumberger, R., and Hines, F., "Practical Reduction Formulas for Use on Bonded Wire Strain Gages in Two-Dimensional Stress Fields," Proc., Soc. Exp. Stress Analysis, 1944, pp. 113-147.





Using the fact that  $-v_o e_a = e_t$  in equation 2.18 gives

$$F_a = \frac{k}{1 - cv_o} \quad . \quad 2.19$$

But if  $e_c$  is the apparent strain, then

$$e_c = \frac{\delta R/R}{k} \quad 2.20$$

From equations 2.16, 2.19 and 2.20 it follows that

$$e_c = \frac{e_a + ce_t}{1 - cv_o} \quad 2.21$$

or

$$e_x = \frac{(1 - cv_o)(e_x' - ce_y')}{1 - c^2} \quad , \quad 2.22$$

and

$$e_y = \frac{(1 - cv_o)(e_y' - ce_x')}{1 - c^2} \quad 2.23$$

where the primes indicate apparent strains and the unprimed quantities refer to the true values. With equations 2.22 and 2.23 corrections can be made for transverse sensitivity, where  $v_o = 0.285$  is given by the strain gauge manufacturer.

In the analysis of the plate problem the strain  $e_T$  on the top surface was subtracted from the strain  $e_B$  on the bottom surface. If  $\Delta$  is the true difference and  $\Delta'$  the apparent difference, it follows from equation 2.21 that

$$\Delta = \frac{1 - cv_o}{1 - c^2} \left[ \Delta' - c[e_{y_T}' - e_{y_B}'] \right] \quad 2.24$$

The effect of equation 2.24 can be observed by considering the typical values and the calculated results in Table 2.1.



TABLE 2.1 TRANSVERSE SENSITIVITY OF STRAIN GAUGES

STRAIN GAUGE	A-5-1	C12-111 AND C12-121
c	3.5%	0.25%
$e_{Y_T}' - e_{Y_B}'$	500 $\mu$ in. per in.	500 $\mu$ in. per in.
$\Delta'$	100 $\mu$ in. per in.	100 $\mu$ in. per in.
$\Delta$	81.7 $\mu$ in. per in.	98.7 $\mu$ in. per in.
Percent diff.	18.3	1.3

It is seen that the transverse sensitivity for the C12-111 and C12-121 type strain gauges is very much less than the A-5-1. The error involved in neglecting the transverse sensitivity for the C12 series gauges amounts to neglecting two or three micro inches per inch while for the A-5-1 the error is multiplied by ten. The accuracy of the measuring equipment (DIDAP) is discussed in Section 4.7.2 and is found to be within  $\pm 6 \mu$ in. per in. Therefore the error in neglecting the transverse sensitivity for the C12 series strain gauges is less than the accuracy of the measuring equipment.

#### 2.4.5 Adhesive, Wire, Solder, Waterproofing

With the introduction of the metal film gauges an excellent adhesive was introduced called Eastman "910".<sup>26</sup> This adhesive is a pressure sensitive cement, along with a special

---

26 "Instruction Manual BG-3100," Budd Instruments Division, 1960.



catalyst, which develops sufficient bond strength within one minute. The advantage is that it does not require solvent evaporation in the development of its bond strength as with most adhesives used with the paper backed gauges. Also, the "910" is quite inviscid before application which gives a very thin glue line. The combination of the metal film gauge and the "910" cement results in a grid to surface distance of only 0.0028 in. with a glue line of 0.0013 in.

In applying the metal film gauge with the "910" cement the manufacturer's recommendations were followed. In addition, it was found desirable, for increased bond strength, to lightly abrade the back of the strain gauge with fine sandpaper. Also, there was less gauge wastage if the drying time of the catalyst was increased from four minutes to ten minutes.

Because of the delicacy of the metal film gauge it is quite difficult to attach lead wires. These gauges are not available with the lead wires attached. When soldering the lead wires a special low temperature solder was used to minimize gauge wastage. This solder is called 63-37 tin-lead, and has a melting and solidifying temperature of 361 F (compared to 430 F for ordinary solders).

The wire used to connect the strain gauges to the junction boxes was No. 28 AWG multistrand. This wire was light and flexible and thus did not impede the movement of the plate under test.

To prevent corrosion and resulting electrical instability, the final process in the installation of the strain gauge was the water proofing. Many water proofing compounds were evaluated,







some of which hardened upon drying, others of which remained pliable. It was found that the best waterproofing compound is GW-1. This is a Dow Corning, air drying, silicon resin which remains pliable upon drying. A minor disadvantage of this compound was that it required several coats before a sufficient thickness covered the gauge and the soldered connections.

#### 2.4.6 Application of DIDAP to the Plate Problem

Two factors were important in the adaptation of DIDAP to the plate problem under consideration;

1. The integration as discussed in Section 2.2.5 was started at the centerline of the plate and proceeded to either edge  $x = \pm b/2$ .
2. The LGP-30 computer required the data to be complete with sign (+ or -), followed by the end of word code (').

The junction boxes of DIDAP were wired so that strains would be recorded on one half the plate at a time, first along the top, then along the bottom. The procedure was repeated for the other half of the plate. The plug board of the program unit was wired to enable the strains to be recorded in the form  $xxx \pm'$ . When the tape perforator was in operation, the channel number was not recorded because this information was not required by the computer.



## 2.5 SUMMARY

In this chapter the previous experimental work of Ashwell and Greenwood, and the author, concerning the transverse deflections of rectangular plates, was discussed. It was concluded that more experimental work was required, especially for large  $b^2/Rd$  ratios, before Lamb's solution could be verified completely. A detailed description was given on the use of electrical resistance strain gauges in calculating the transverse deflections. This method was used in the experimental work presented in Chapter III.



## CHAPTER III

### EXPERIMENTAL RESULTS OF A RECTANGULAR PLATE UNDER LARGE LONGITUDINAL CURVATURES

This chapter presents the experimental results of the transverse deflection using the strain gauge method described in Chapter II. For each test the results are compared with Lamb's theory as described in Chapter I. It is shown for  $b^2/Rd$  ratios up to 55 there is generally good agreement between experiment and theory. The poorer agreement for low  $b^2/Rd$  ratios is explained in terms of initial imperfections in the plate and experimental error.

#### 3.1 GENERAL REMARKS

The first series of tests (Series I) were conducted with a fixed span length, between supports, of 6.0 ft. The overhanging portion of the plate was 3.0 ft at either end. The plate was tested with side A facing up and then turned over and tested with side B facing up so as to evaluate symmetry and initial imperfections in the plate.\*

In the second series of tests (Series II), tests were conducted with various span lengths of 6.0 ft to 1.5 ft to investigate the influence of the support and loading conditions and, consequently, load the plate at higher  $b^2/Rd$  values.

---

\* The manufacturer's name and plate specification was stencilled on one side of the plate (side B), the other side was unmarked (side A).





## 3.2        SERIES I

### 3.2.1    Testing Procedure

Before testing the plate under load it was first placed flat on a table and the initial strains were recorded for each channel. Actually the cantilever bridge assemblies (see Section 4.2.2) were balanced to as near a null condition as possible when the plate was sitting flat on the table, but to ensure that the strains recorded for each loaded condition were absolute, an initial set of readings were recorded. These initial strains were subtracted from the strains recorded for a loaded condition using the LGP-30 computer. The plate was then set on the supports for which conditions another set of readings was recorded. The load hanger assemblies were then attached to the plate and weights were added to these hangers one at a time. For each loaded condition the transverse strains were recorded simultaneously on the tape perforator and the typewriter. If a set of readings were abnormal, which was easily observed from the typewritten page, the corresponding tape was rejected. In this way no computer time was wasted in calculating unacceptable data. For each loaded condition the transverse deflections were obtained from the LGP-30 computer which was programmed to use the trapezoidal method described in Chapter II.

The  $b^2/Rd$  ratio was recorded for each loaded condition. The longitudinal radius of curvature was obtained by means of two longitudinally placed strain gauges, one on top, the other on the bottom of the plate.



### 3.2.2 Experimental Results

The experimental results for test Series I are plotted in Figures 3.1 to 3.20 (pages 115 to 124). In these figures the experimental values are the small circles. The solid lines are the theoretical curves as obtained from Lamb's solution. The  $b^2/Rd$  ratio was varied from 0 to 18. Higher  $b^2/Rd$  ratios, for a span of 6.0 ft, were not possible because the plate lifted off the roller and was carried by the channel section which supported the roller. This induced membrane stresses into the plate which adversely affected the transverse deflections.

The plate was tested with side A up and then turned over and tested with side B up. This checked whether the plate deflected in the same manner irrespective of which side was facing up.

Figures 3.1 and 3.2 are shown for  $b^2/Rd$  equal to zero. This is in agreement with the fact when the plate was sitting symmetrically on the simple supports, so that the overhanging portion of the plate was equal to half the distance between supports, the bending moment at the centerline, due to the dead weight of the plate alone, was zero. Thus the curvature  $1/R_y$  at the midline was zero. It was found for side A up, Figure 3.1, the  $b^2/Rd$  ratio was -1.34, and for side B up, the  $b^2/Rd$  ratio was 0.89. To bring the  $b^2/Rd$  ratios into agreement for the zero moment condition these initial values were algebraically subtracted from the recorded values, corresponding to which side was facing up, as shown in Table 3.1. The left hand column is the load in pounds which was applied to the overhangs of the





plate. It is seen that, correcting for the zero moment condition, the adjusted  $b^2/Rd$  values are in very close agreement. The adjusted  $b^2/Rd$  ratios were used in Figures 3.1 to 3.20.

TABLE 3.1 ADJUSTMENT OF  $b^2/Rd$  RATIOS

LOAD IN POUNDS	$b^2/Rd$			
	SIDE A UP		SIDE B UP	
	Recorded	Adjusted	Recorded	Adjusted
0	0.85	0	-1.35	0
0.61	2.41	1.56	0.18	1.53
1.61	4.85	4.00	2.77	4.12
2.61	7.17	6.32	5.20	6.55
3.61	9.36	8.51	7.45	8.80
4.61	11.49	10.64	9.63	10.98
5.61	13.55	12.70	11.63	12.98
6.61	15.43	14.58	13.64	14.99
7.61	17.13	16.28	15.45	16.80
8.61	18.85	18.00	17.13	18.48

### 3.2.3 Symmetry

It was found from the experimental results that for small  $b^2/Rd$  ratios the plate deflected symmetrically about the y-axis as expected, but as this ratio was increased there was a noticeable antisymmetry in the deflected form of the transverse strip. This was observed by comparing the results from the strain gauges placed on one half the plate (Row I) with the gauges on the other





half of the plate (Row II). Rows I and II were collinear along the midline of the plate. Figure 3.43 shows the location of the strain gauges and the support locations.

The possibility was considered that the loads were not placed on the plate symmetrically, and as a result, were producing a twisting moment. To check this for a  $b^2/Rd$  ratio of 18.48 the plate was loaded by applying the weights on the centerline of the hangers and the strains were recorded. The weights were then shifted on the hangers so that they appeared to act at the corners diagonally opposite one another. The strains were again recorded. The same procedure was followed with the weights shifted to the opposite corners. From each set of data recorded the transverse deflections were calculated. The comparison of these results showed negligible variation between one test and another (less than 2 percent at the edges). Therefore, it was concluded that the manner in which the loads were applied did not affect the transverse curvature. Further, the assumption that the loads produced a twisting moment was concluded to be false. The results plotted in Figures 3.1 and 3.20 are the values averaged from Rows I and II.

#### 3.2.4 Comparison with Theory

In Figures 3.1 to 3.20 the axes have been made dimensionless by dividing by  $b$ , the width of the plate, in the case of the abscissa  $x$ , and dividing by  $d$ , the thickness, in the case of the ordinate  $w$ . The actual plate tested was 18 in. wide, with strain gauges mounted across the width of the plate every 0.5 in.



Although only a single point was plotted for each measuring station, each loaded condition was tested at least six times, and sometimes nine or ten times. It was found, for a given  $b^2/Rd$  ratio, that all tests coincided almost exactly with one another and the difference could not be observed from the plotted results.

The theoretical curve from Lamb's solution is shown for each set of experimental values corresponding to the experimental  $b^2/Rd$  ratio and Poisson's ratio of 0.333. Except for Figure 3.3 which agreed exactly ( $b^2/Rd = 1.56$ , side A up), there is some discrepancy between theory and experiment for small  $b^2/Rd$  ratios. This difference decreases as  $b^2/Rd$  increases, and for Figures 3.12 to 3.20 the agreement between theory and experiment is good. It is evident from the plotted results, irrespective of which side was facing up, that the experimental curves are flatter, or less curved, than the corresponding theoretical curves. In most cases there is slightly better agreement between theory and experiment for side A up than for side B up. However, there was very little difference between the experimental results, irrespective of which side was facing up, for  $b^2/Rd$  greater than 4.





### 3.3        SERIES II

#### 3.3.1    Testing Procedure

To investigate the influence of the supports on the transverse deflection, calculated along the midline of the plate, additional rows of strain gauges were placed 6 in. on either side and parallel to Row I. These rows were labeled III and IV (see Figure 3.43). If the supports or loading hangers influenced the deflected form in the transverse direction then it was believed that the computed deflections from Rows III and IV would disagree appreciably from Rows I and II.

Four additional sets of longitudinal strain gauges were mounted along the centerline of the plate 2.75 in. and 5.38 in. on either side of the midline. Readings from each of the five sets of longitudinal gauges were used to calculate the curvatures.

The loading and recording procedure was the same as described in Section 3.2.1 above. However, instead of a fixed span length, tests were conducted with span lengths of 6.0, 3.0, 2.0, and 1.5 ft. For each test, four rows of strain gauges and five sets of longitudinal strain gauges (a total of 162 strain gauges) were recorded.

All of the tests in Series II were conducted with side A facing up. In view of the results of Section 3.2.4 it was believed unnecessary to test the plate with side B facing up. The zero load condition was taken with the plate resting flat on the table. The various tests that were carried out in this series are listed below.





### 1. Test (6-3)

The distance between supports was 6 ft and the load hangers were applied on the overhangs 3 ft from the supports as in the tests of Series I. Eight separate tests were recorded for each of six different loaded conditions.

### 2. Test (3-3)

The distance between supports was moved in to 3 ft and the hangers were placed so that they acted 3 ft away from the supports as in test (6-3) above. Five separate tests were recorded for each of six different loaded conditions.

### 3. Test (3-1.5)

The distance between supports was unchanged at 3 ft but the hangers were placed on the overhangs 1.5 ft from the supports. This was done to see if any change in the transverse deflections could be detected because in this set, for a given curvature, twice the load was required than for test (3-3) above. Three separate tests were recorded for each of seven different loaded conditions.

### 4. Test (2-3.4)

The distance between supports was 2 ft and the load hangers were applied on the overhangs 3.4 ft away from the supports. Three separate tests were recorded for each of five different loaded conditions.

### 5. Test (1.5-3.7A)

The distance between supports was 1.5 ft and the load hangers were applied on the overhangs 3.7 ft away from the supports. Three separate tests were recorded for each of four different loaded conditions.



## 6. Test (1.5-3.7B)

For this set of tests an additional row (Row V) of strain gauges was mounted collinear with Row IV and parallel and on the same side of the plate as Row II (see Figure 3.43). This was carried out to give a further check on the symmetry of the deflected form. The total number of gauges recorded was 198. The support and loading hanger distances were the same as in test (1.5-3.7A) above. Three separate tests were recorded for each of three different loaded conditions.

The loads that were applied to the plate in each of the above tests were chosen so that the range of  $b^2/Rd$  values for each set would overlap those of an adjacent set. This was a further check to investigate the loading and support conditions on the deflected form.

### 3.3.2 Experimental Results

The results from the four rows of gauges in test (6-3) were identical to those plotted in Series I, Figures 3.1 to 3.20. Therefore, they are not repeated here.

The results from test (3-3) are plotted in Figures 3.21 to 3.26 (pages 125 to 127). The  $b^2/Rd$  ratio varied from 23.88 to 41.68.

In the Figures 3.27 to 3.33 (pages 128 to 131) the results from test (3-1.5) are plotted. The  $b^2/Rd$  ratios varied from 24.05 to 42.37.

The results from test (2-3.4) are plotted in Figures 3.34 to 3.38 (pages 131 to 133). The  $b^2/Rd$  ratios varied from 32.54 to 48.95.





In Figures 3.39 to 3.42 (pages 134 to 135 ) the results from test (1.5-3.7) are plotted. The  $b^2/Rd$  ratios varied from 37.04 to 54.77.

In all the results plotted for Series II (Figures 3.21 to 3.42) the  $b^2/Rd$  values are the recorded values. These values were not adjusted, as in Series I, because the difference made in the  $b^2/Rd$  ratio was not sufficient to cause any significant change in the theoretical curves.

### 3.3.3 Symmetry

In Section 3.2.3 it was mentioned that the deflections computed from Row I differed from those of Row II. The results recorded from Rows III and IV, which were parallel and on the same side of the plate as Row I, agreed with the results from Row I. This seemed to indicate that one side of the plate was distorting more than the other. In test (1.5-3.7B) an additional row of strain gauges (Row V) were placed parallel and on the same side as Row II. The results from Row V agreed with those of Row II. Therefore, it was surmised that the lack of symmetry was due to initial imperfections in the plate and these were not confined to the central region in the vicinity of Rows I and II.

For test (1.5-3.7B),  $b^2/Rd$  ratio equal to 54.77, the loads were placed on the plate in an unsymmetrical manner using the method described in Section 3.2.2. The computed deflections were compared with those in which the loads were placed symmetrically on the loading hangers. Again it was found that there was negligible difference in the results whether or not the loads





were placed symmetrically. It was concluded that the manner in which the loads were applied did not affect the transverse deflection which was recorded 3 in. from the supports. This is equivalent to saying for a span to width ratio as low as  $1/3$ , the method of loading did not influence the transverse deflections.

As in Series I the results plotted in Figures 3.21 to 3.42 are the values averaged from Rows I and II.

### 3.3.4 Comparison with Theory

#### 1. Test (6-3)

The results recorded in this series of tests were identical with those in Series I. For a discussion on the agreement between theory and experiment see Section 3.2.4.

#### 2. Test (3-3)

Figures 3.21 to 3.25 show good agreement between experiment and theory. In Figure 3.26 ( $b^2/Rd = 41.68$ ) a slight difference between experiment and theory is observed.

#### 3. Test (3-1.5)

Good agreement between experiment and theory is seen in Figures 3.27 to 3.32. For Figure 3.33 ( $b^2/Rd = 42.37$ ) there is some disagreement. Comparing the results of this test with test (3-3) it was shown that, for a given longitudinal curvature and given deflected form obtained in test (3-3), the plate required twice the load as in test (3-1.5). As an example, in test (3-3), Figure 3.24, a load of 4 lbs was required to produce a  $b^2/Rd$  ratio of 33.92 while in test (3-1.5)



Figure 3.32 a load of 8 lbs was required to produce a  $b^2/Rd$  ratio of 34.09. The experimental values plotted in Figures 3.24 and 3.32 are almost identical with one another and with the theory. Similar comparisons can be made for other  $b^2/Rd$  ratios.

#### 4. Test (2-3.4)

In this test good agreement between experiment and theory was obtained in Figures 3.34 to 3.38. There was some disagreement in Figures 3.34 and 3.35.

#### 5. Test (1.5-3.7A)

In Figures 3.39 to 3.42 the results of this test show reasonable agreement between experiment and theory. Greater discrepancies, although small, between theory and experiment were noted for this test when compared to the other tests.

Considering all the experimental data in Series II, Figures 3.21 to 3.42, there was good agreement between experiment and theory for  $b^2/Rd$  ratios from 23.86 to 54.77. Although some discrepancies were noted, these were small. It appears that the transverse deflections are unaffected by the support conditions and the method of loading. Further, the longitudinal strain gauge readings were almost identical for every loaded condition. This indicated a constant longitudinal curvature existed between Rows III and IV (see Figure 3.43).



### 3.4 EXPERIMENTAL ERROR

Inaccuracies in the computed transverse deflections arose from three sources; calibration error, measurement (DIDAP) error, and truncation error.

#### 3.4.1 Calibration Error

It is an often repeated remark that the accuracy of any strain gauge measurement is no better than the initial calibration. The calibration error was made up from the variation in resistance of the strain gauge, the variation in the gauge factor, and the variation in the shunt or calibration resistance. For the strain gauges Type C12-121 used in this work, the variation in gauge resistance was  $\pm 0.17$  percent and the variation in gauge factor was  $\pm 0.5$  percent. A "General Radio" decade resistance box, with an accuracy of  $\pm 0.05$  percent, was used as the shunt resistance. Summing all these errors, the calibration error was found to be within  $\pm 0.72$  percent.

#### 3.4.2 Measurement Error

The measurement (DIDAP) error is fully discussed in Section 4.7.2 and was found to be  $\pm 0.6$  percent full scale. Therefore, the measurement error depends on the magnitude of strain being measured. Since the strains across the transverse strip vary anywhere from zero to large negative and positive values it is difficult to assess an accuracy value for the entire transverse strip. The inaccuracies in the strain measurements







are large (up to 100 percent) near the centerline of the plate. However, the ordinates  $w/d$  in this region are small so that the overall effect on the entire transverse deflection curve is small. Towards the edge of the plate where the ordinates  $w/d$  are large, the inaccuracies in strain measurements are quite small (less than 1 percent).

### 3.4.3 Truncation Error

The truncation error was estimated from the first term of equation 2.9, that is

$$\frac{h^3}{12} \left[ \frac{d^2 w}{dx^2} \right]_i$$

where  $h$  is the distance between adjacent measuring stations.

Noting that the curvature is proportional to the change in slopes between two points  $x_{i+1}$  and  $x_i$ , this can be written as

$$\frac{h^2}{12} \left[ \frac{dw}{dx}_{i+1} - \frac{dw}{dx}_i \right]$$

or, 
$$\frac{1}{48} \left[ \frac{dw}{dx}_{i+1} - \frac{dw}{dx}_i \right] \text{ in.}^2$$

where the distance between  $x_{i+1}$  and  $x_i$  is 0.5 in.

It was observed from the experimental data that the greatest change in slope occurred approximately at the quarter points of the transverse section; the change in slope being more pronounced for large  $b^2/Rd$  values. To consider a particular case, the strains recorded for a  $b^2/Rd$  of 18 were analyzed in the following way. First, the curvature was computed from



the strains for each station and a graph was plotted  $1/R$  versus  $x$ . From this graph the maximum change in slope over a  $1/2$  in. interval was found to be  $1.6 \times 10^{-5} \text{ in.}^{-2}$ , or the truncation error in computing the slopes  $dw/dx$  amounted to  $3.33 \times 10^{-7}$ . If it is assumed this error is constant, which it is not, the total error accumulated in measuring nineteen stations amounted to  $6.33 \times 10^{-6}$ . The maximum slope  $dw/dx$  occurring at the edge of the plate was found to be  $14750 \times 10^{-6}$ . Thus the truncation error in computing slopes was less than 0.04 percent.

Second, in a similar manner to the curvatures, the maximum change in slope of the plotted curve  $dw/dx$  versus  $x$  was found to be  $8.7 \times 10^{-5} \text{ in.}^{-1}$  making the truncation error in computing  $w$  from  $dw/dx$   $1.81 \times 10^{-6} \text{ in.}$  Assuming again a constant truncation error of this amount, the total error in calculating the edge deflection of  $58000 \times 10^{-6} \text{ in.}$  amounted to less than 0.06 percent.

Finally, from the deflection curve  $w$  versus  $x$ , the trapezoidal rule was used to calculate the position of the centroidal axis of the deflected transverse strip. From the curve  $w$  versus  $x$  the maximum change in slope was found to be  $4.18 \times 10^{-4}$  making the truncation error  $8.7 \times 10^{-6} \text{ in.}^2$ . Noting from equation 2.15 that  $\bar{w}$  is computed by dividing the first moment of area by half the width of the plate, the total error in computing  $\bar{w}$ , for nineteen measuring stations, was  $1.85 \times 10^{-5} \text{ in.}$  For a  $b^2/Rd$  ratio of 18,  $\bar{w}$  was computed to be  $1.6 \times 10^{-2} \text{ in.}$  Thus, the truncation error was less than 0.11 percent.





By assuming a constant truncation error over the width of the plate the above errors are larger than they would actually be. Summing the errors it was found the computation of the values  $(w - \bar{w})$  versus  $x$ , using the trapezoidal rule, incurred an error of less than 0.21 percent.

#### 3.4.4 Summary

The total error of measurement of the deflection  $w$  was found to be within  $\pm 0.93$  percent plus the error in strain measurement.

### 3.5 GENERAL DISCUSSION

The results plotted in Figures 3.1 to 3.42 indicate that better agreement is obtained between theory and experiment for large values of  $b^2/Rd$ . The greatest discrepancies between experiment and theory occurred in the range of  $b^2/Rd$  values from 0 to 10.98 (Figures 3.1 to 3.12), test Series I. This disagreement between theory and experiment caused considerable concern. A check on the accuracy of the  $b^2/Rd$  ratio showed it could be in error by  $\pm 5$  percent due to the variations in plate thickness and width. When this tolerance was applied to any of the theoretical curves it was found that the change in these curves was unnoticeable.





Another possible source of error was the value of Poisson's ratio used in determining the theoretical curves. The handbook<sup>27</sup> value of Poisson's ratio is  $1/3$ . This was checked experimentally and was found to be correct. However, if a lower value, say 0.300 was used, it had the effect of flattening all the theoretical curves, thus bringing experiment and theory into better agreement. No justification could be found for using the lower value, therefore, Poisson's ratio was taken equal to  $1/3$ .

It will be remembered that Ashwell and Greenwood<sup>28</sup> found disagreement between experiment and theory. They attributed this to residual stresses in their plate and found, by assuming a particular initial transverse curvature, the theory could be made to agree with the experiment. The results they presented are for one particular loading. It is not clear whether they applied the same correction to other loadings and still obtained good agreement between experiment and theory.

At first it was believed the discrepancies between theory and experiment in Figures 3.1 to 3.20 could also be explained in terms of an initial transverse curvature. However, a thorough investigation failed to show any justification for such an explanation. Of course, any one or two sets of experimental values could be made to agree with the theory by a judicious choice of an initial transverse curvature, but invariably this led to greater discrepancies in the other sets of experimental values.

---

27 Alcoa Aluminum Handbook, 1956, Aluminum Company of America.

28 Ashwell, D.G. and Greenwood, loc. cit.



The aluminum plate as delivered from the manufacturer was presumably free from initial curvatures. Certainly there were no perceptible initial curvatures. It was believed that the discrepancies between theory and experiment, especially in test Series I, were due to unaccountable initial imperfections in the plate.

The lack of symmetry in the deflected form in test Series II was also attributed to these initial imperfections. The possibility was considered that a variation in plate thickness was causing the antisymmetry. A thickness gauge was constructed to measure the variation in plate thickness across the width of the plate. This gauge indicated the plate thickness did not vary appreciably across the width, and if anything, was thicker along the portion (Row II and V) which distorted the most.

Since the agreement between experiment and theory was much better for test Series II than test Series I this was probably due to the higher strains, and resulting greater accuracy, recorded in the Series II. It can be seen from Figures 3.1 to 3.42, as the  $b^2/Rd$  ratio was increased, generally the agreement between theory and experiment was improved.

In the M.Sc. of the author it was believed the distorted results observed were possibly caused by the supports being too close to the strain gauges which were used to measure the transverse deflections. The experimental results of this chapter showed that the supports, when placed as close as 3 in. from the transverse strain gauges, did not affect the transverse





deflections. This was equivalent to a span to width ratio of  $1/3$ . Therefore the distortions observed in the M.Sc. thesis were probably due to some other cause. It is suggested the manner in which the loads were applied, coupled with the initial imperfections in the plate, caused the distortions. Similarly, in the work of Ashwell and Greenwood the discrepancies they observed might have been due to their knife edge supports and they were quite justified in saying that a span to width ratio greater than three was required to eliminate the effect of the supports. It was observed in conducting the experiments of this chapter that if the plate lifted off the roller and was carried by the channel iron supporting the roller, which was equivalent to a knife edge, there was distortion in the recorded strains. As a result, care was taken in all tests to ensure the plate rested on the roller at all times.

In Section 2.1.4 the difficulty was mentioned in performing an experiment to determine  $\phi$  or  $k$ , the factor which relates the moment and curvature to the stiffness. Since the effect sought is so small the test equipment used in this thesis was inadequate for its detection. One of the greatest difficulties is in measuring the moment because, as the plate was loaded, the deflections at the ends were large enough to move the supports closer together, by virtue of the plate acting on the roller, and also change the moment arm of the loads acting on the overhangs. Basically the difficulty with the experiment is that  $\phi$  changes from 1 to  $9/8$  or by 12.5 percent while the measurement of  $R$ ,  $E$  and  $I$  together could be out by 20 percent. However, it has been



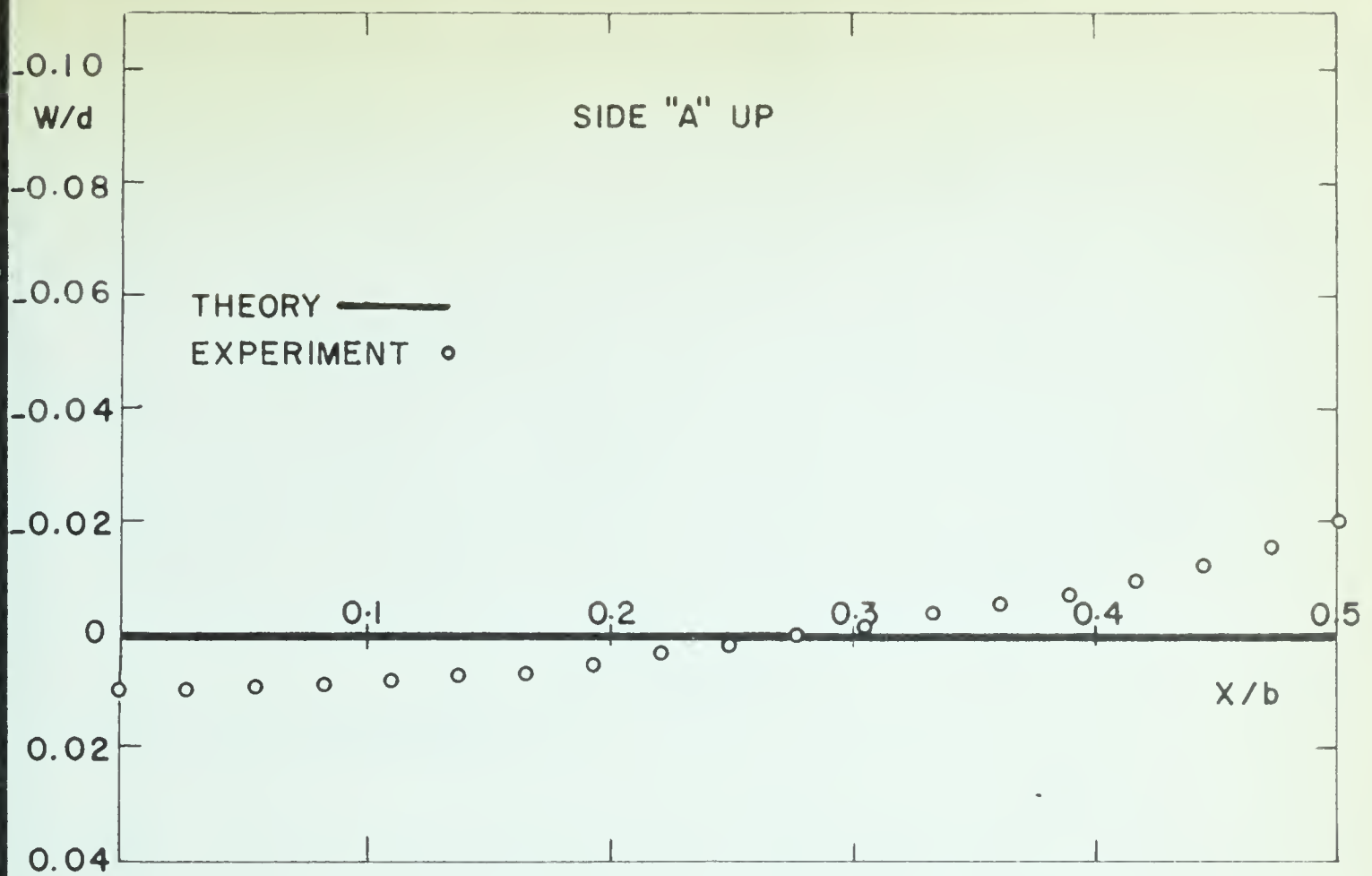
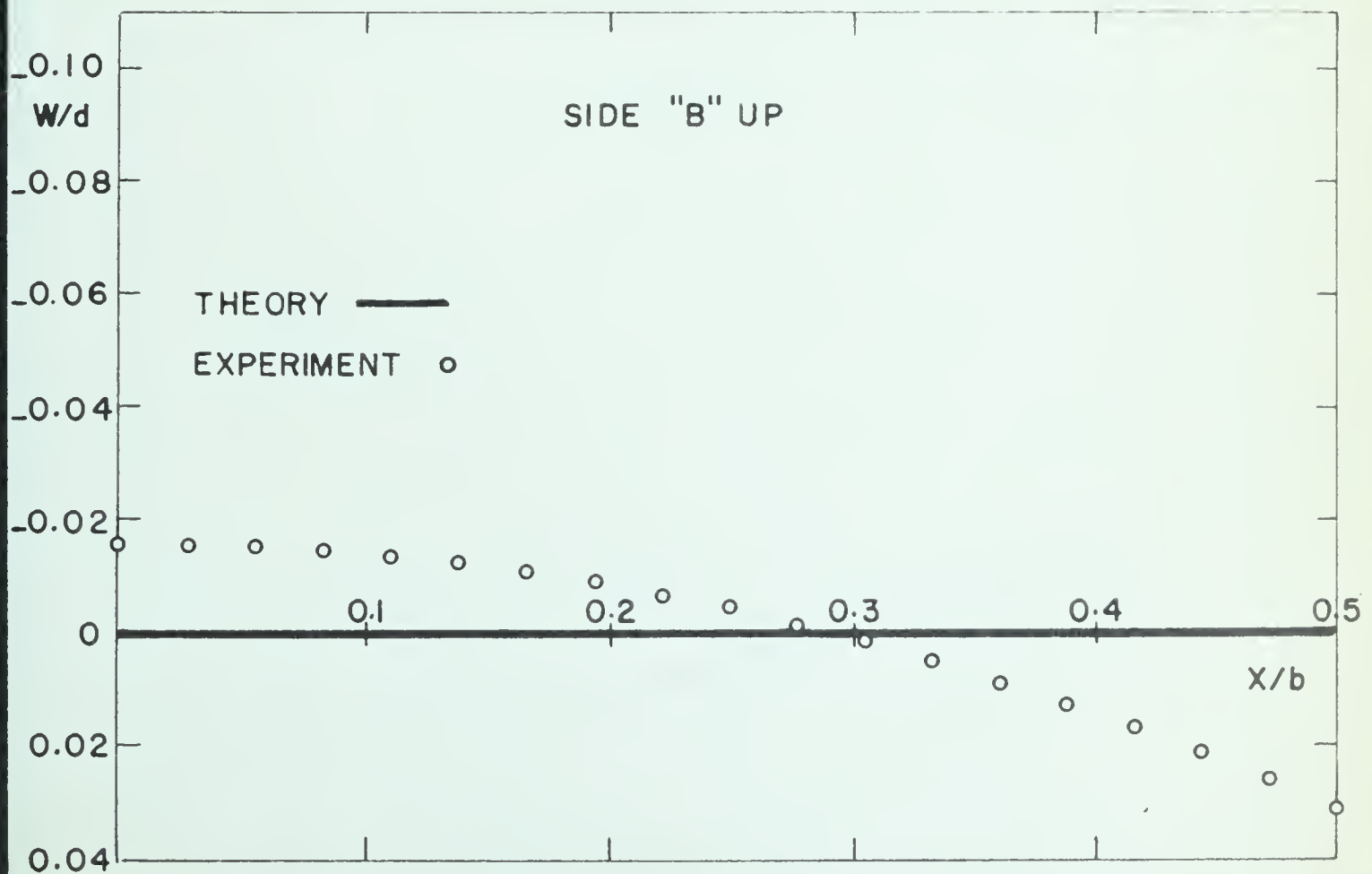


shown the experimental values of the transverse deflection agree quite closely with theory and therefore the theoretical solution of Lamb is valid. Since there exists a theoretical expression for  $k$  or  $\phi$  derived from Lamb's solution it must follow that also the theoretical values of  $k$  and  $\phi$  are justified.

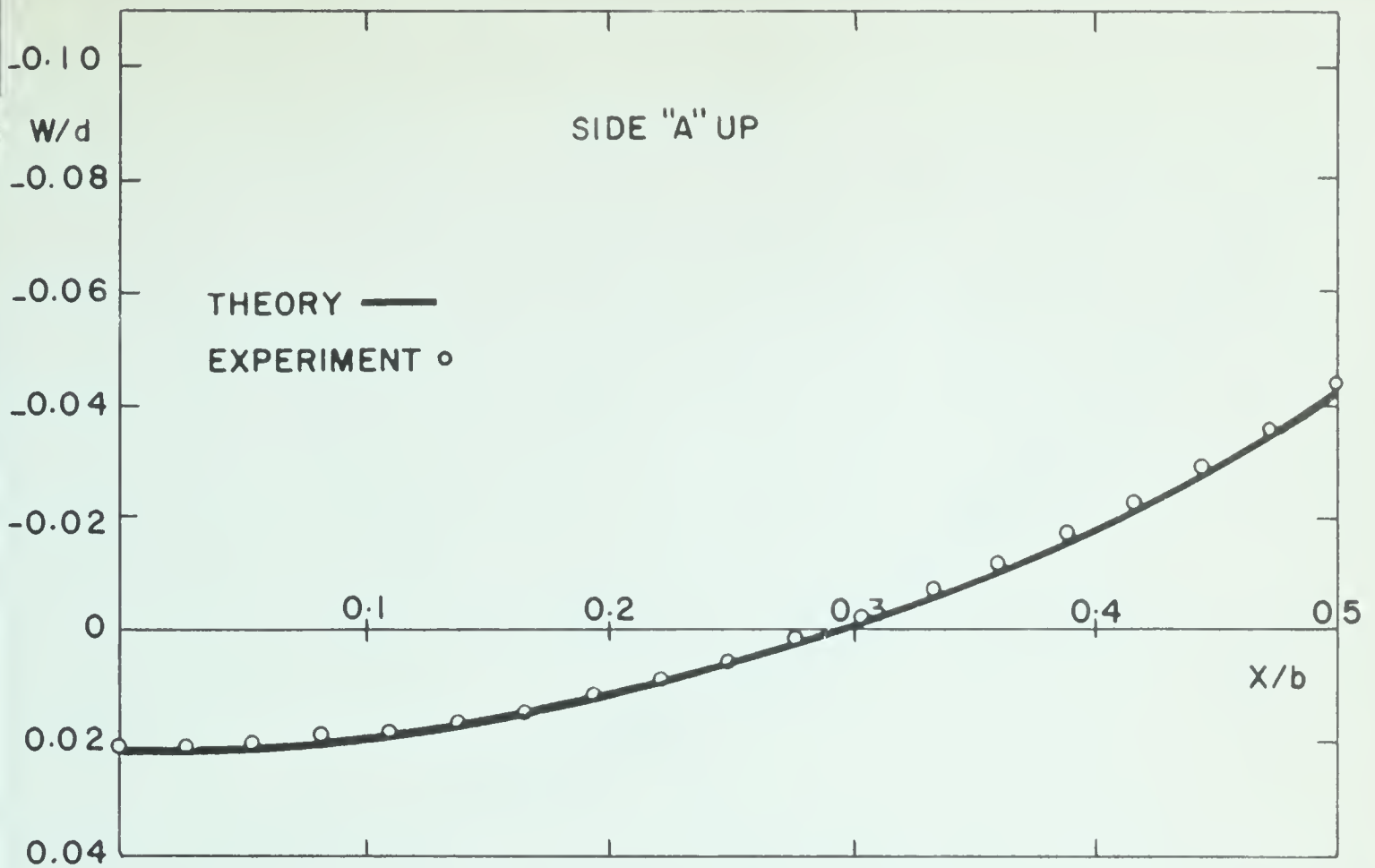
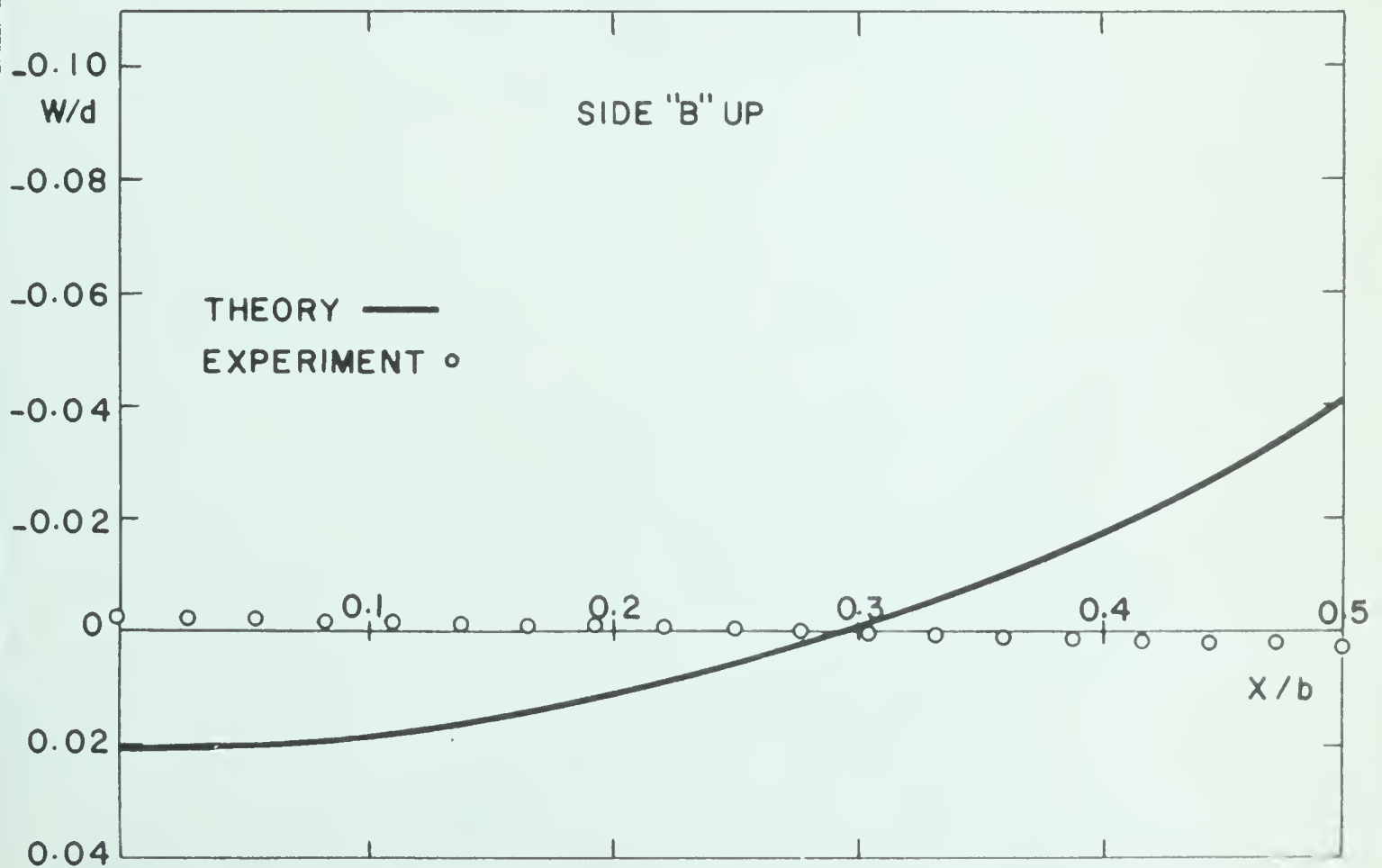
### 3.6 CONCLUSIONS

1. Experiment generally agreed with theory as the transverse deflection passed from beam action, through the transition region and into the beginning of plate behaviour, for  $b^2/Rd$  values up to 54.77. Discrepancies noted at low  $b^2/Rd$  values were probably due to error of measurement and initial imperfections in the plate.
2. No snap through behaviour of any kind was observed as the transverse deflection passed through the transition region from anticlastic to synclastic bending at the centerline. This verified the prediction of Lamb's theory.
3. The support conditions and method of loading the plate did not affect the mode of transverse deflection even when the supports were placed as close as 3 in. from the transverse strain gauges. Thus no distortion was experienced for an equivalent span to width ratio of  $1/3$ .
4. Strain gauges give a good means of determining curvatures.
5. The trapezoidal rule is adequate for determining deflections from strain gauge readings.



FIGURE 3.1 TRANSVERSE DEFLECTION FOR  $b^2/Rd=0.00$ FIGURE 3.2 TRANSVERSE DEFLECTION FOR  $b^2/Rd=0.00$



FIGURE 3.3 TRANSVERSE DEFLECTION FOR  $b^2/Rd=1.56$ FIGURE 3.4 TRANSVERSE DEFLECTION FOR  $b^2/Rd=1.53$





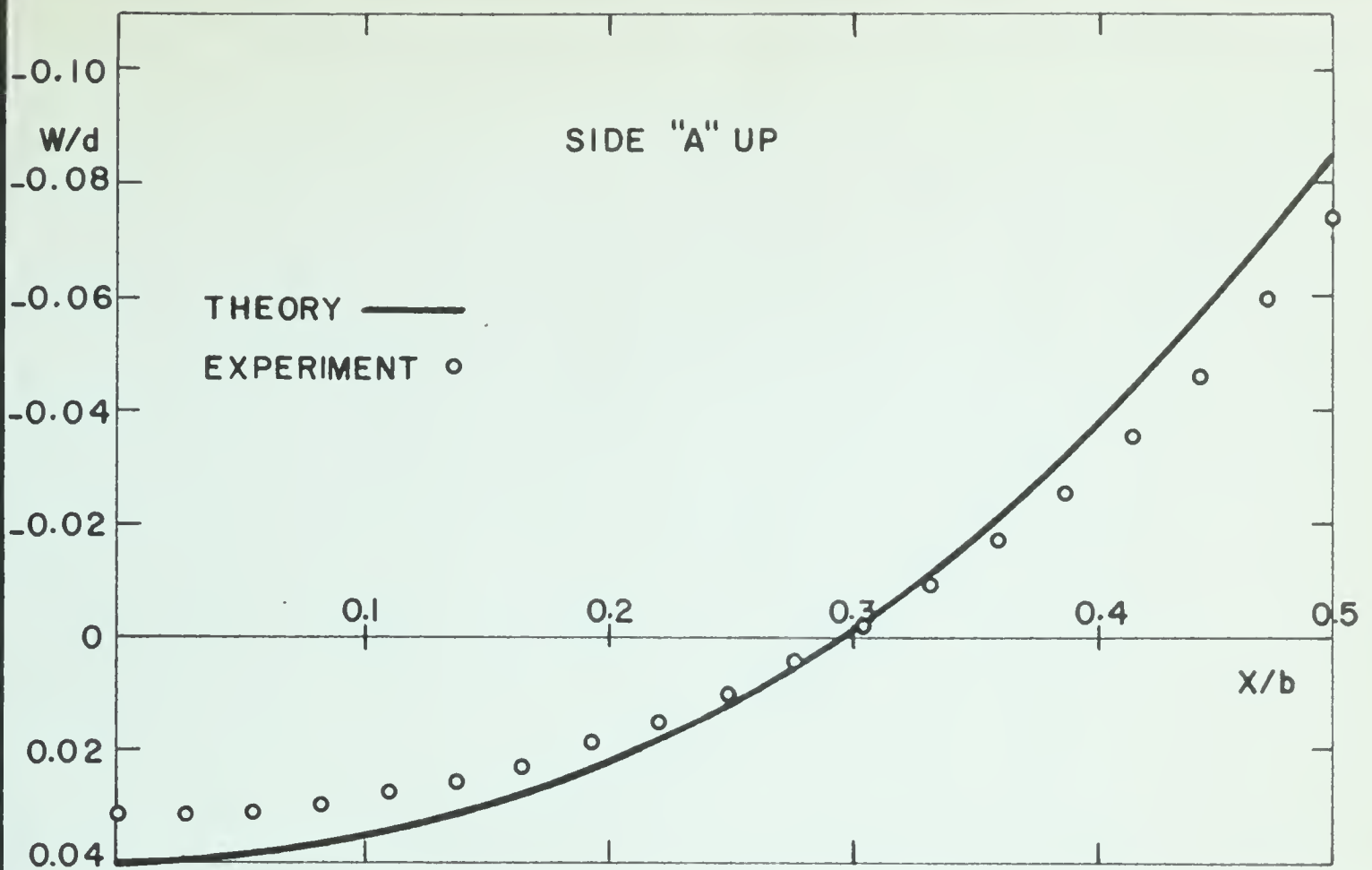


FIGURE 3.5 TRANSVERSE DEFLECTION FOR  $b^2/Rd=4.00$

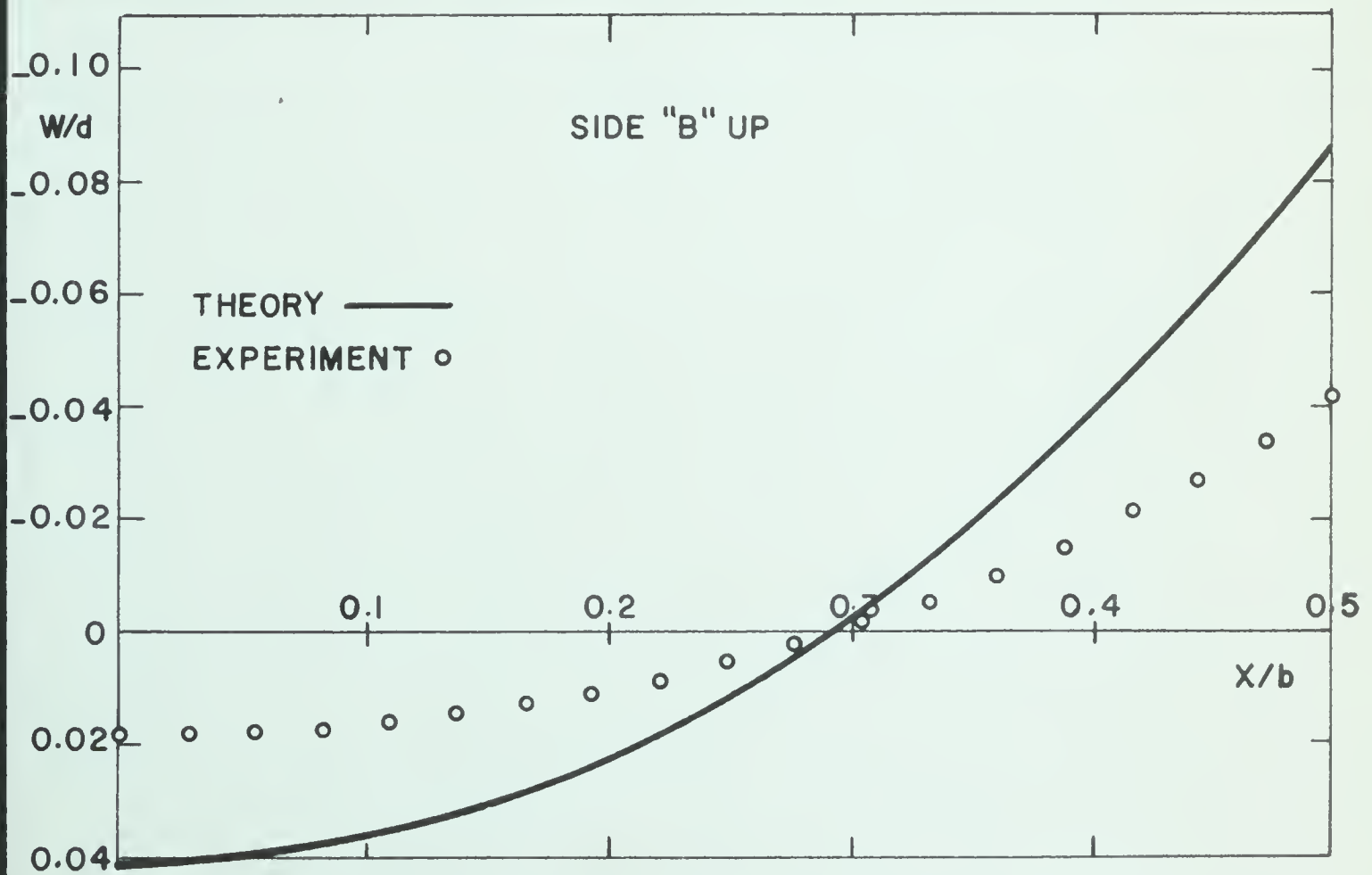
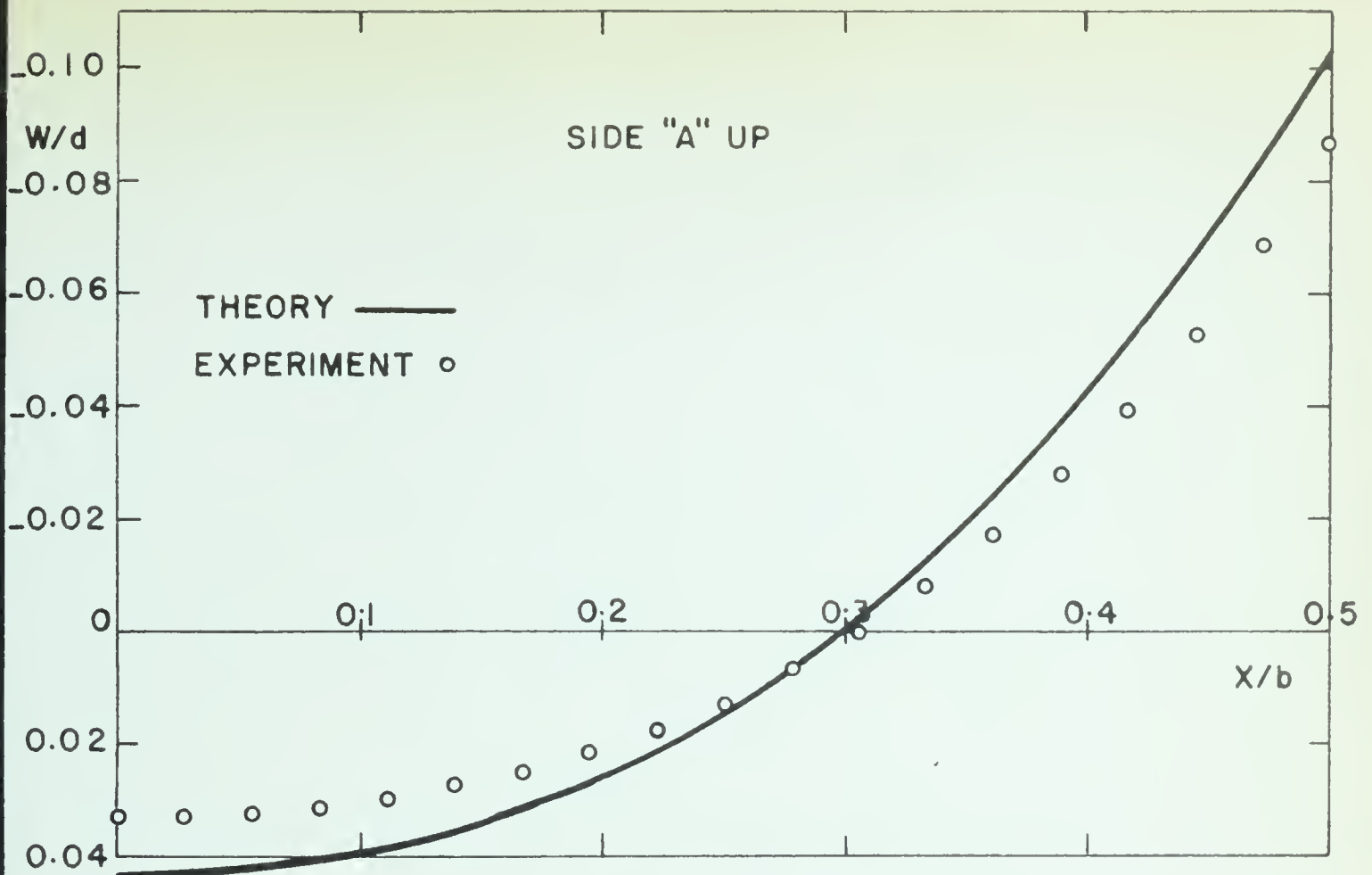
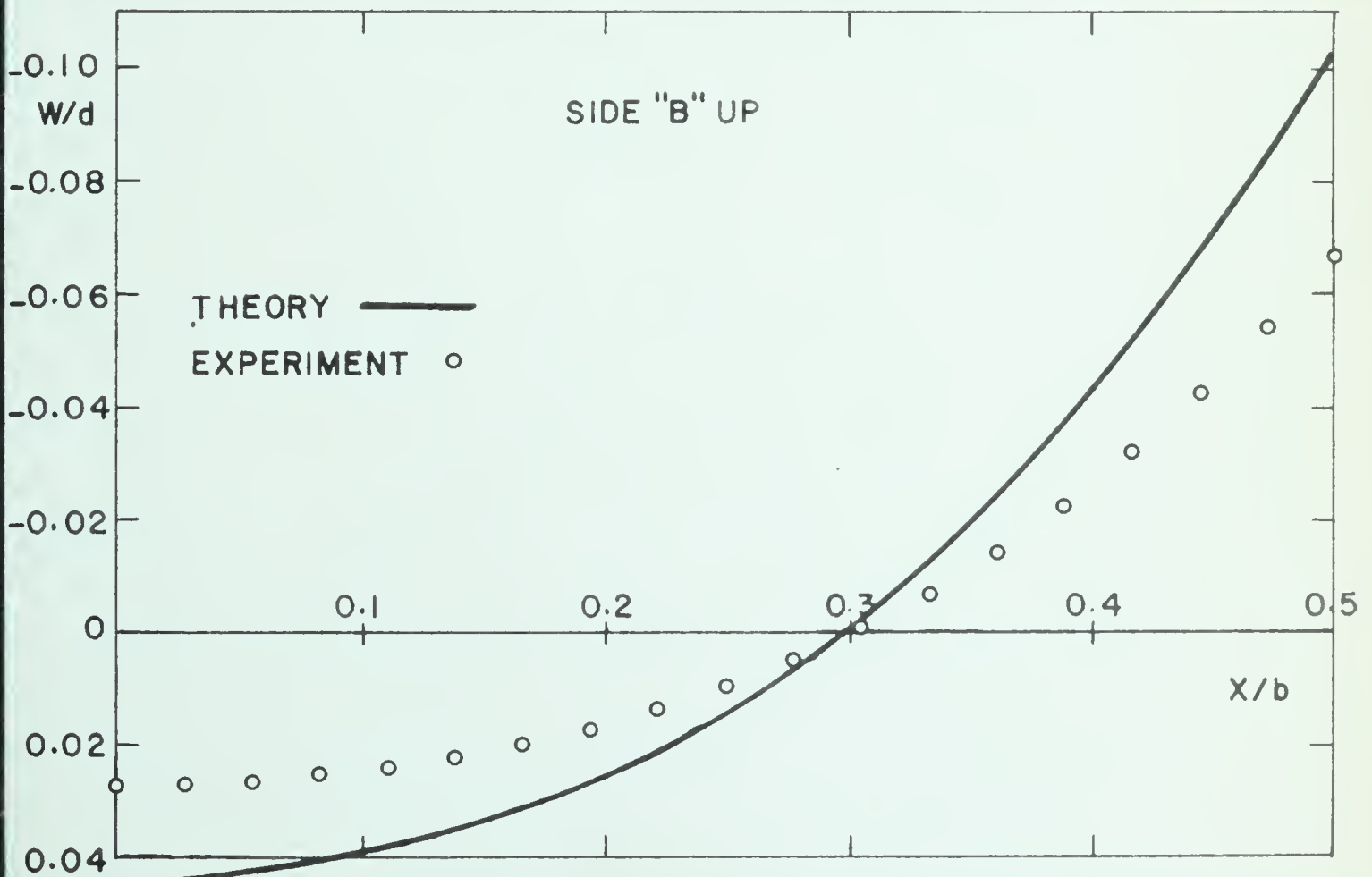


FIGURE 3.6 TRANSVERSE DEFLECTION FOR  $b^2/Rd=4.12$



FIGURE 3.7 TRANSVERSE DEFLECTION FOR  $b^2/Rd=6.32$ FIGURE 3.8 TRANSVERSE DEFLECTION FOR  $b^2/Rd=6.55$



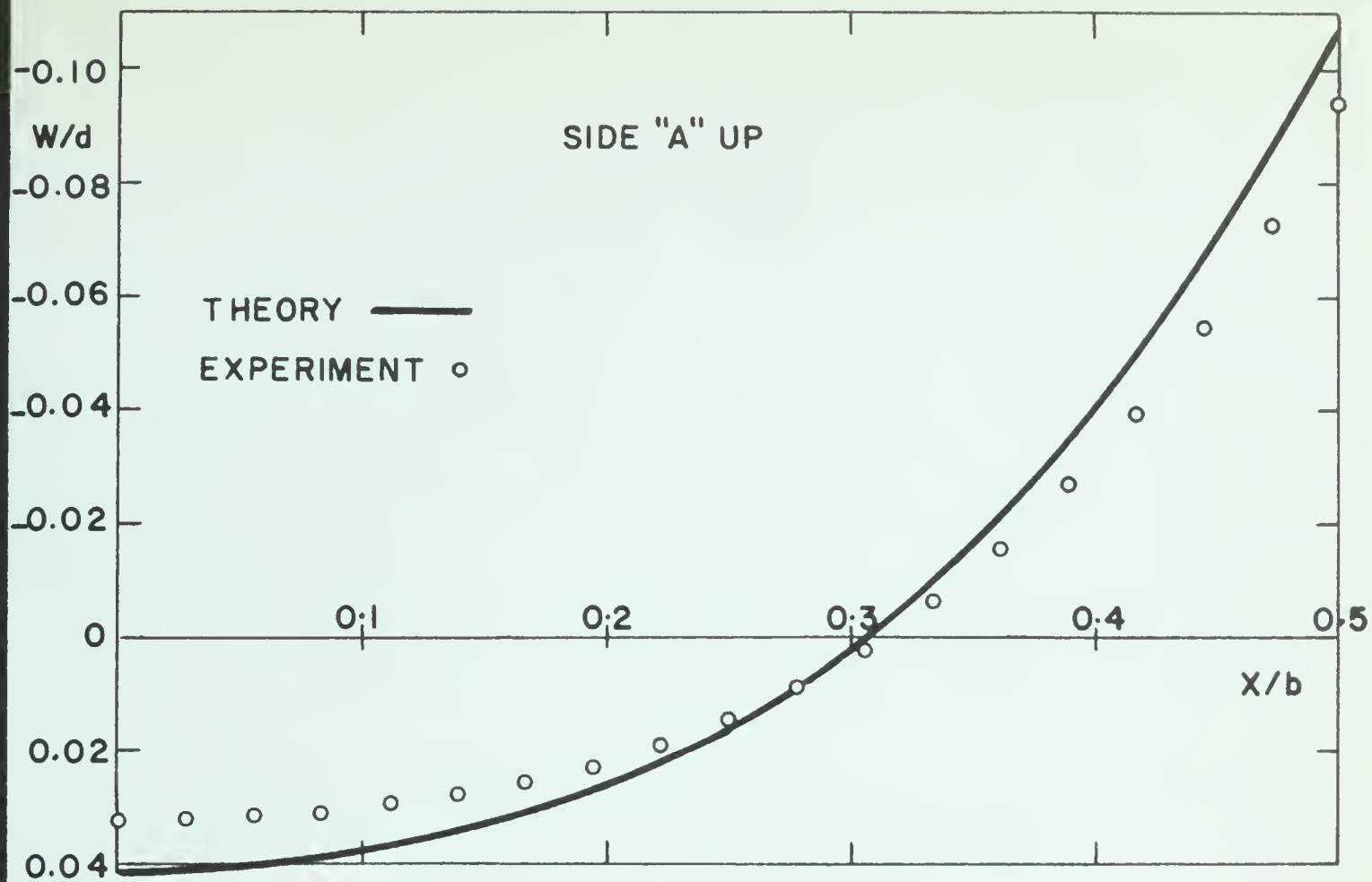


FIGURE 3.9 TRANSVERSE DEFLECTION FOR  $b^2/Rd=8.51$

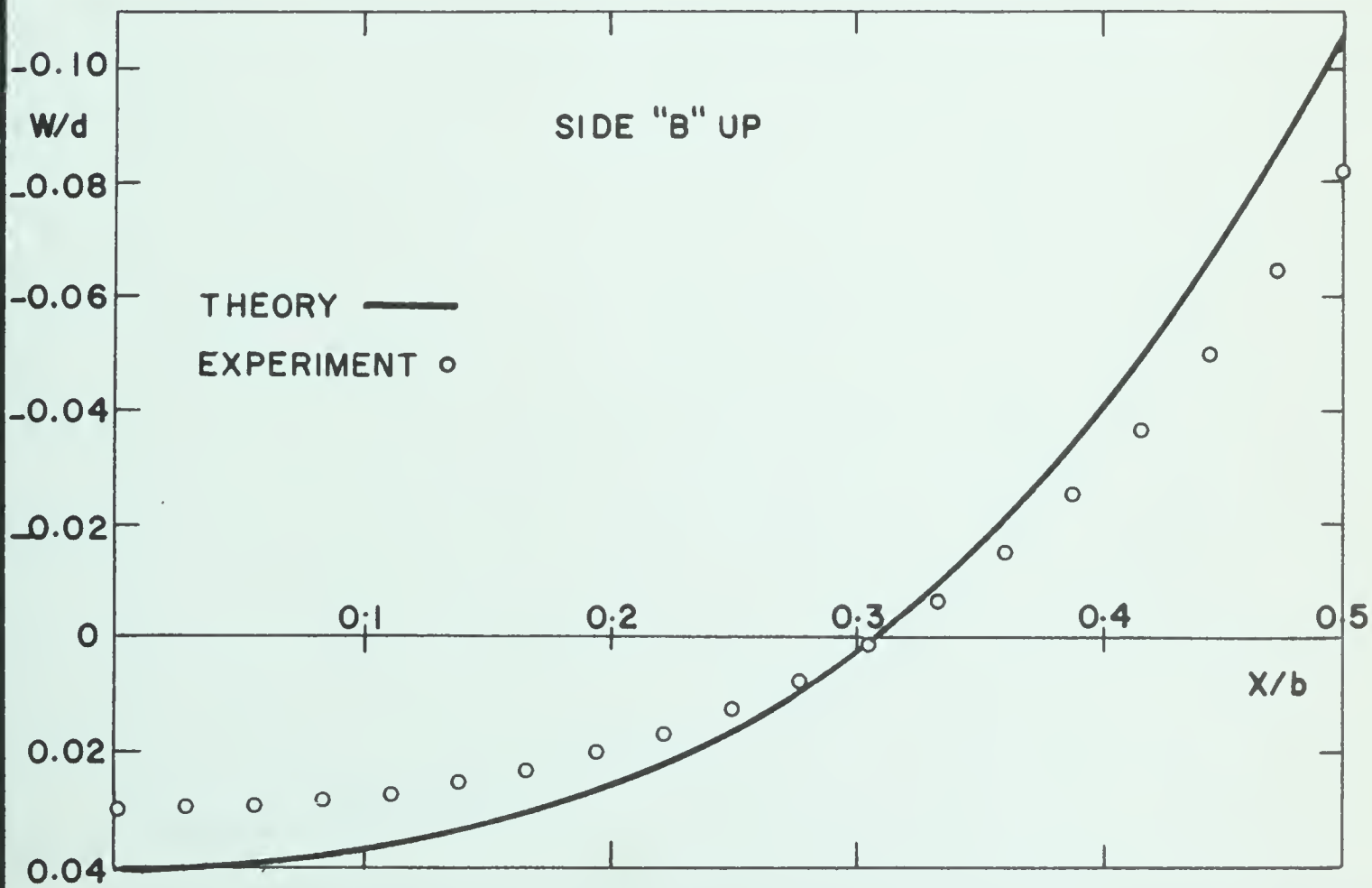


FIGURE 3.10 TRANSVERSE DEFLECTION FOR  $b^2/Rd=8.80$





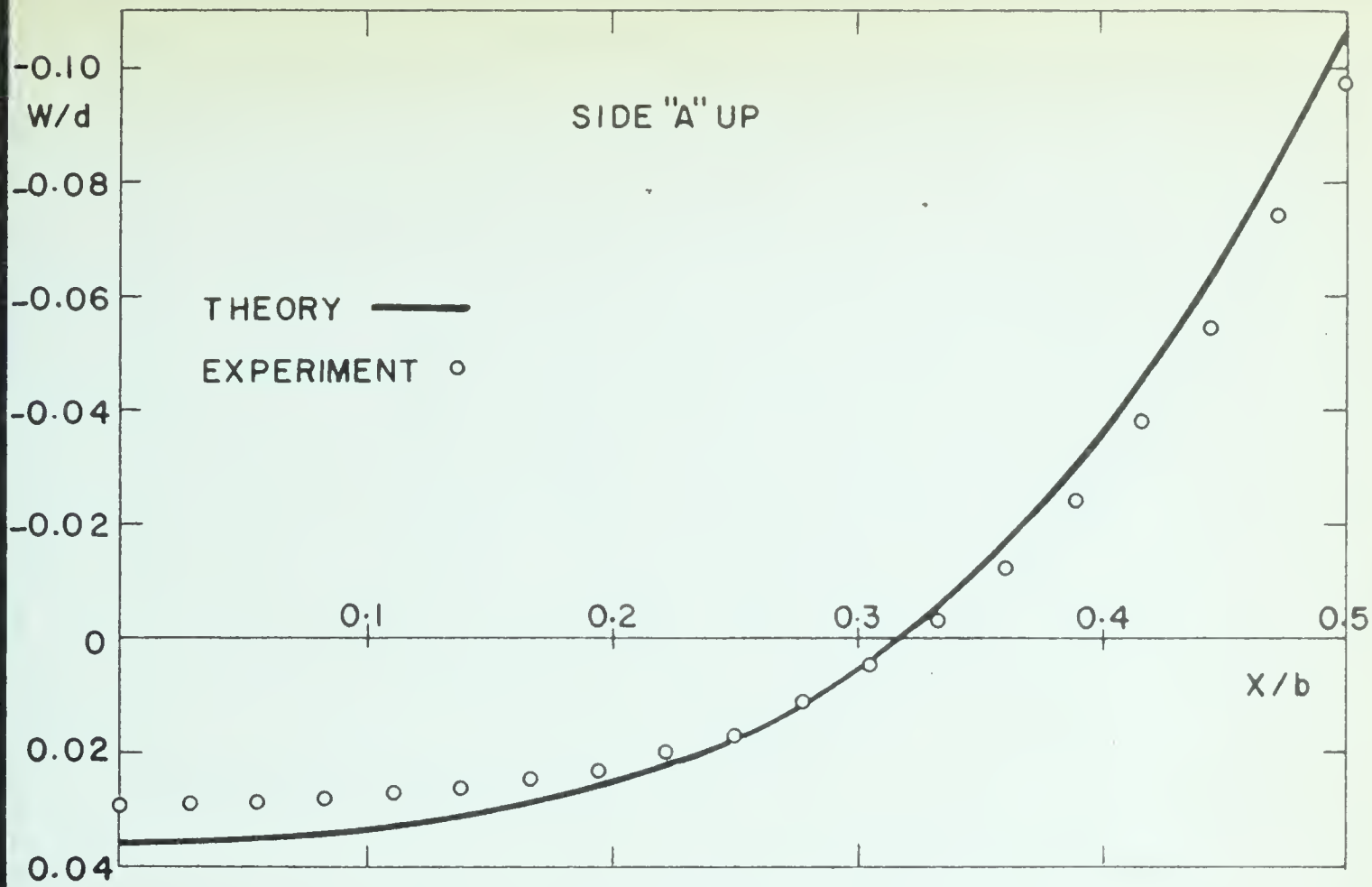


FIGURE 3.11 TRANSVERSE DEFLECTION FOR  $b^2/Rd=10.64$

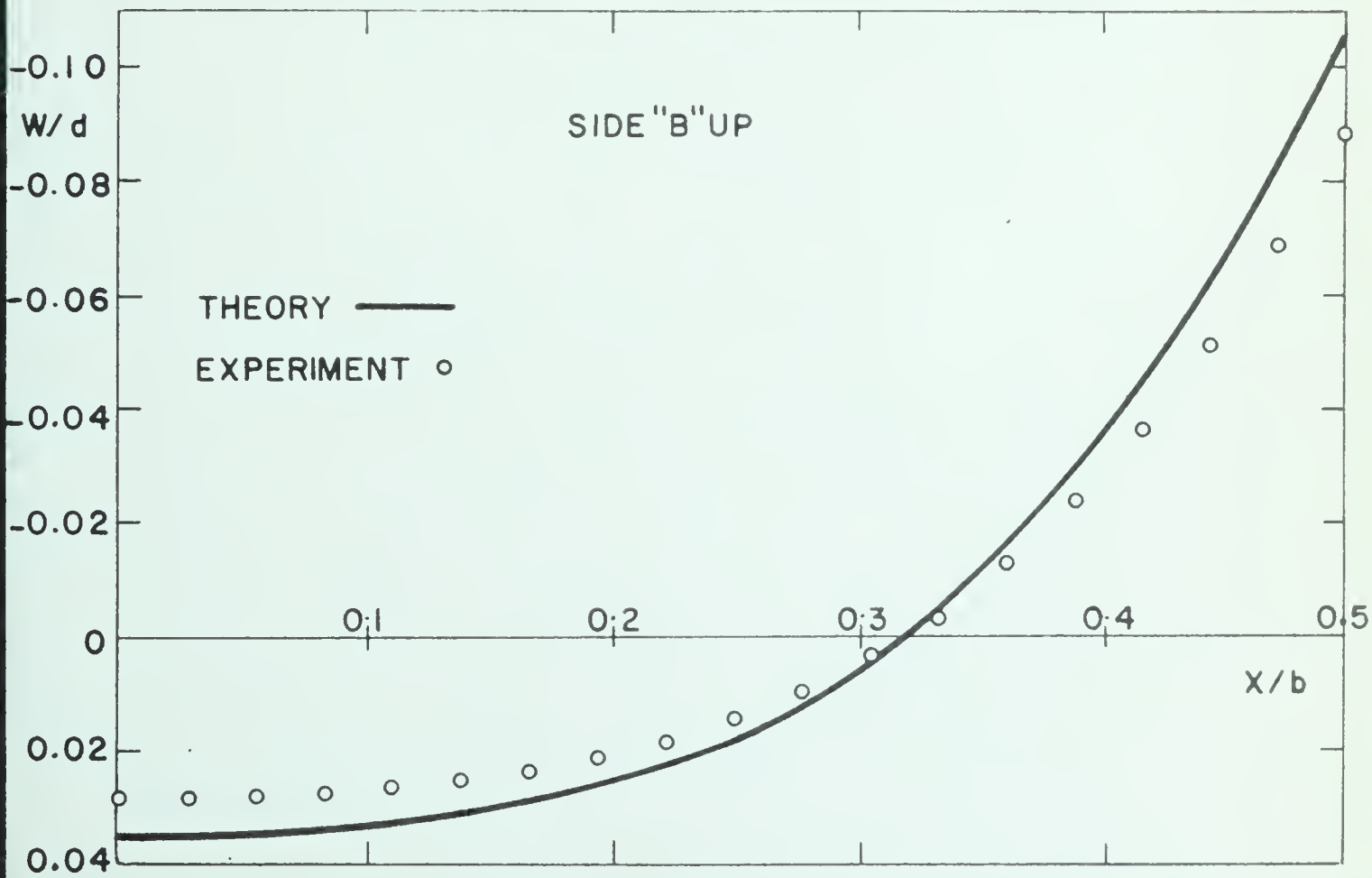
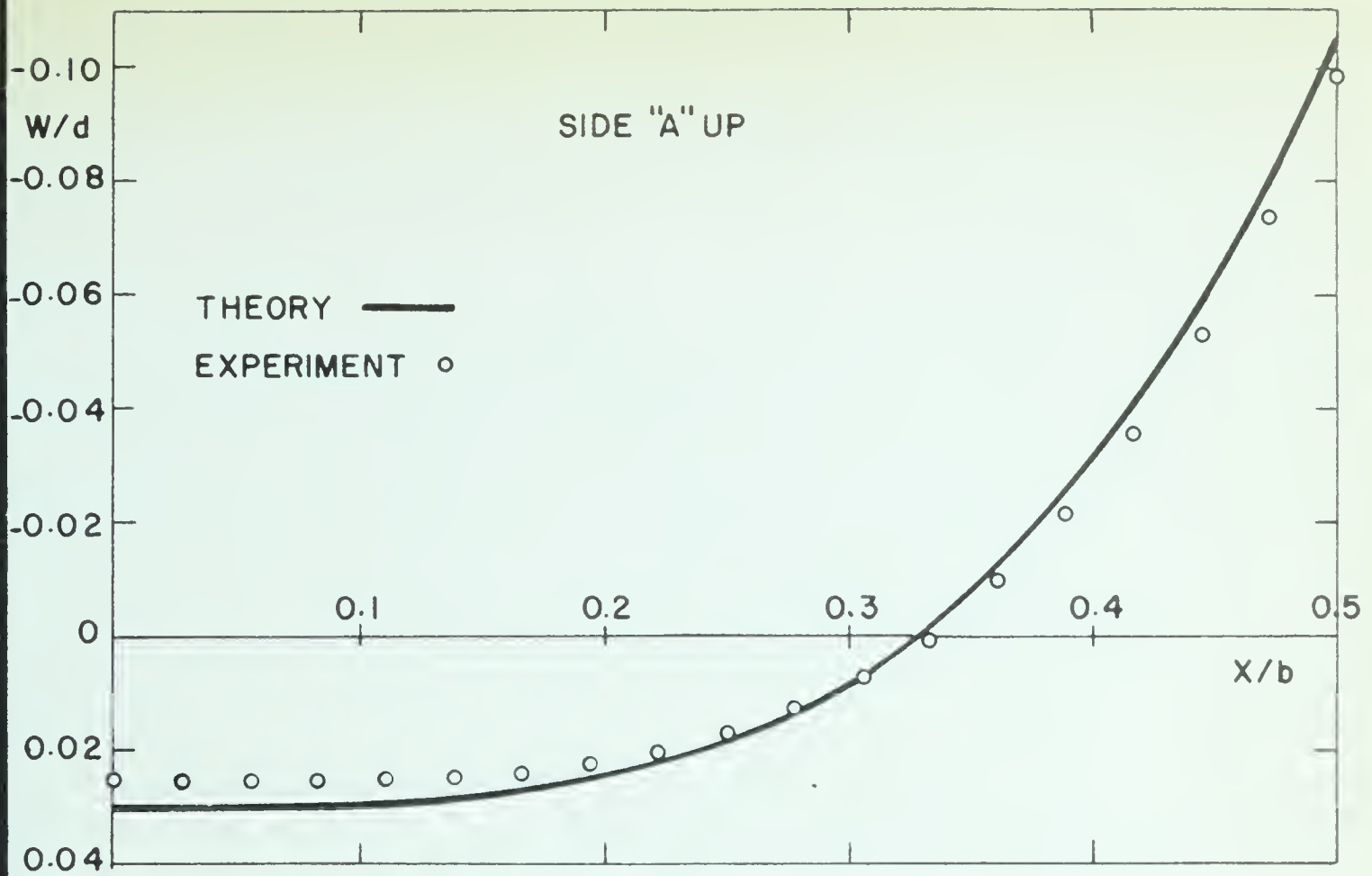
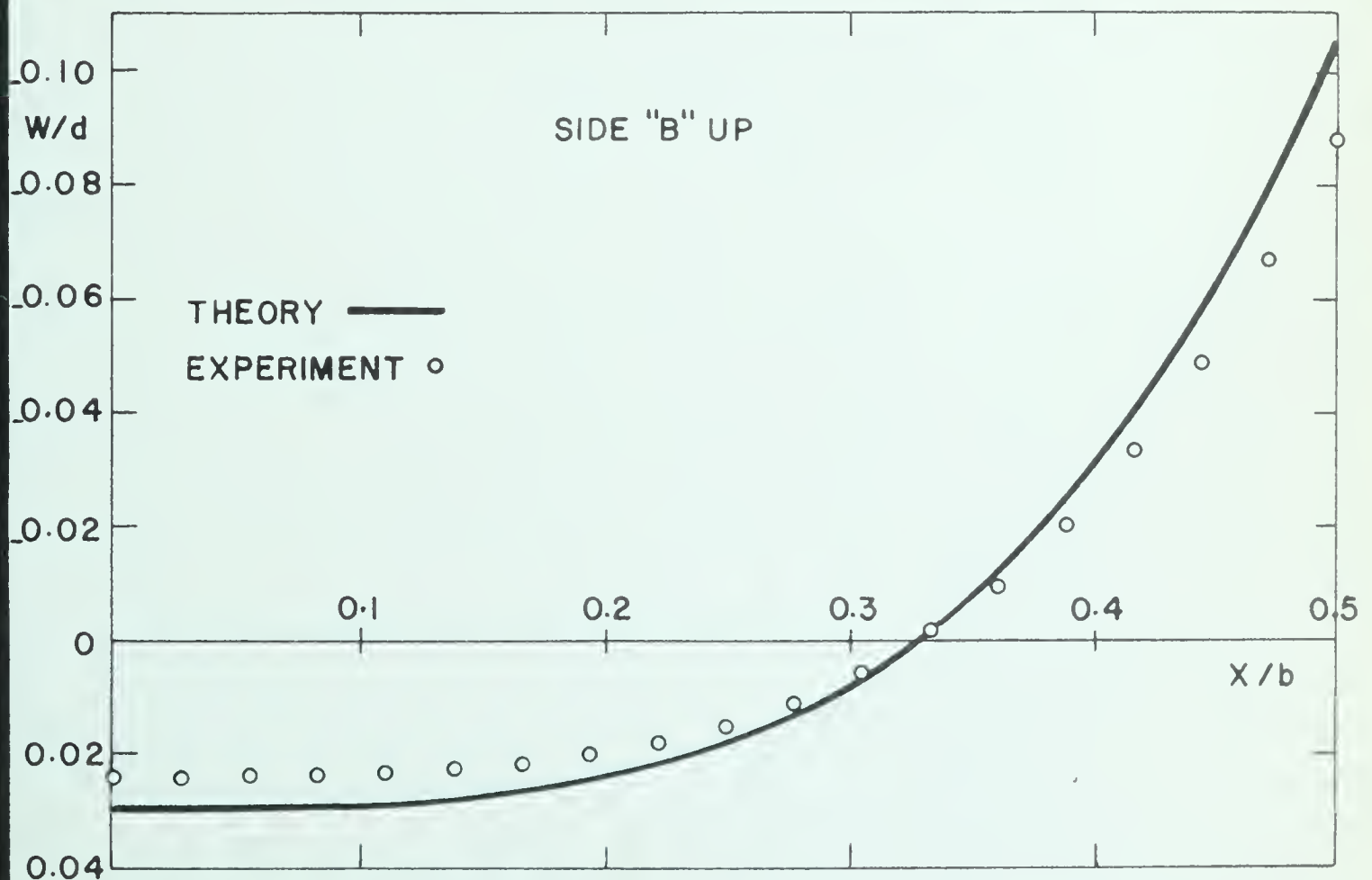


FIGURE 3.12 TRANSVERSE DEFLECTION FOR  $b^2/Rd=10.98$



FIGURE 3.13 TRANSVERSE DEFLECTION FOR  $b^2/Rd=12.70$ FIGURE 3.14 TRANSVERSE DEFLECTION FOR  $b^2/Rd=12.98$



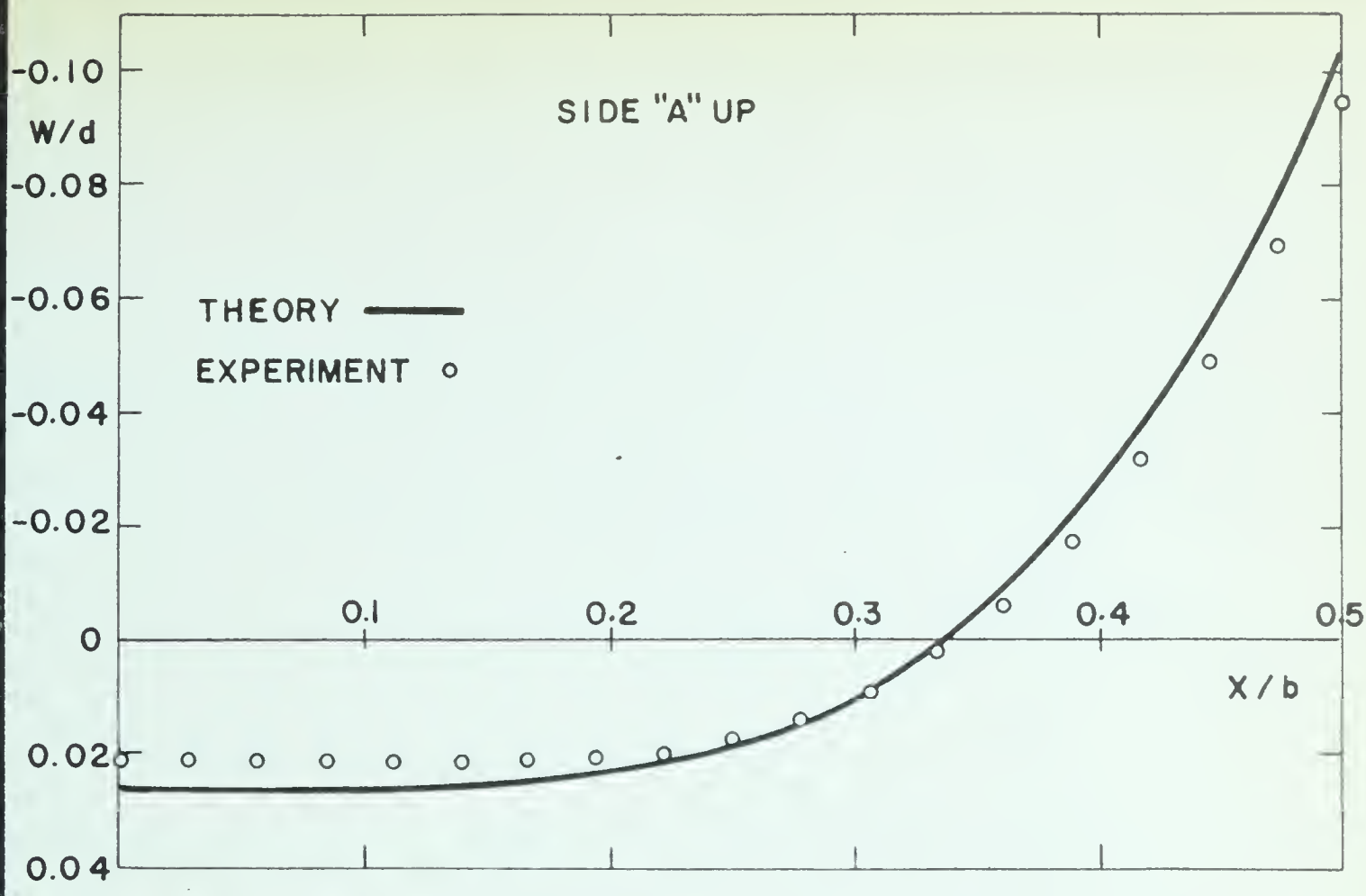


FIGURE 3.15 TRANSVERSE DEFLECTION FOR  $b^2/Rd=14.58$

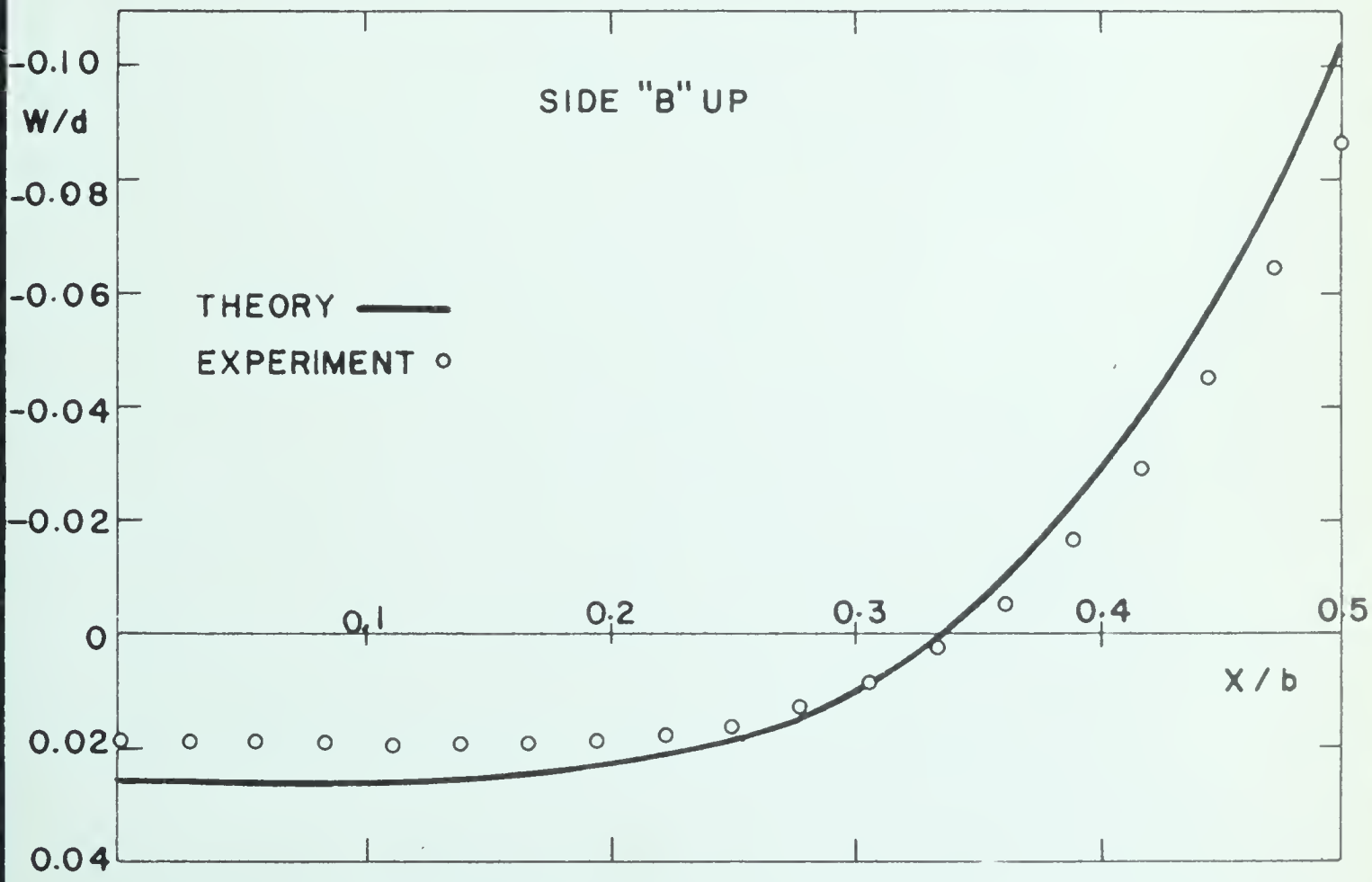


FIGURE 3.16 TRANSVERSE DEFLECTION FOR  $b^2/Rd=14.99$





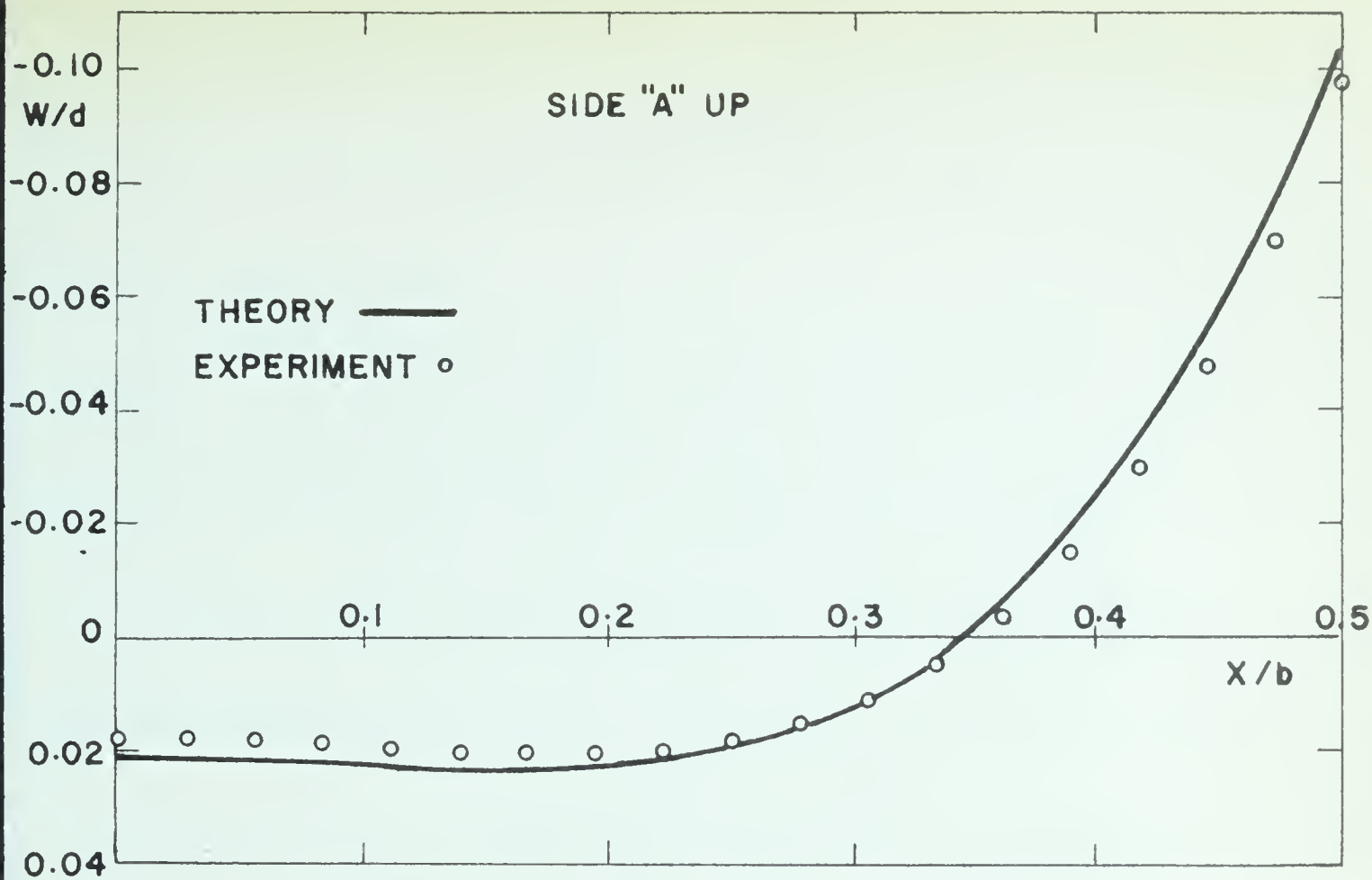


FIGURE 3.17 TRANSVERSE DEFLECTION FOR  $b^2/Rd=16.28$

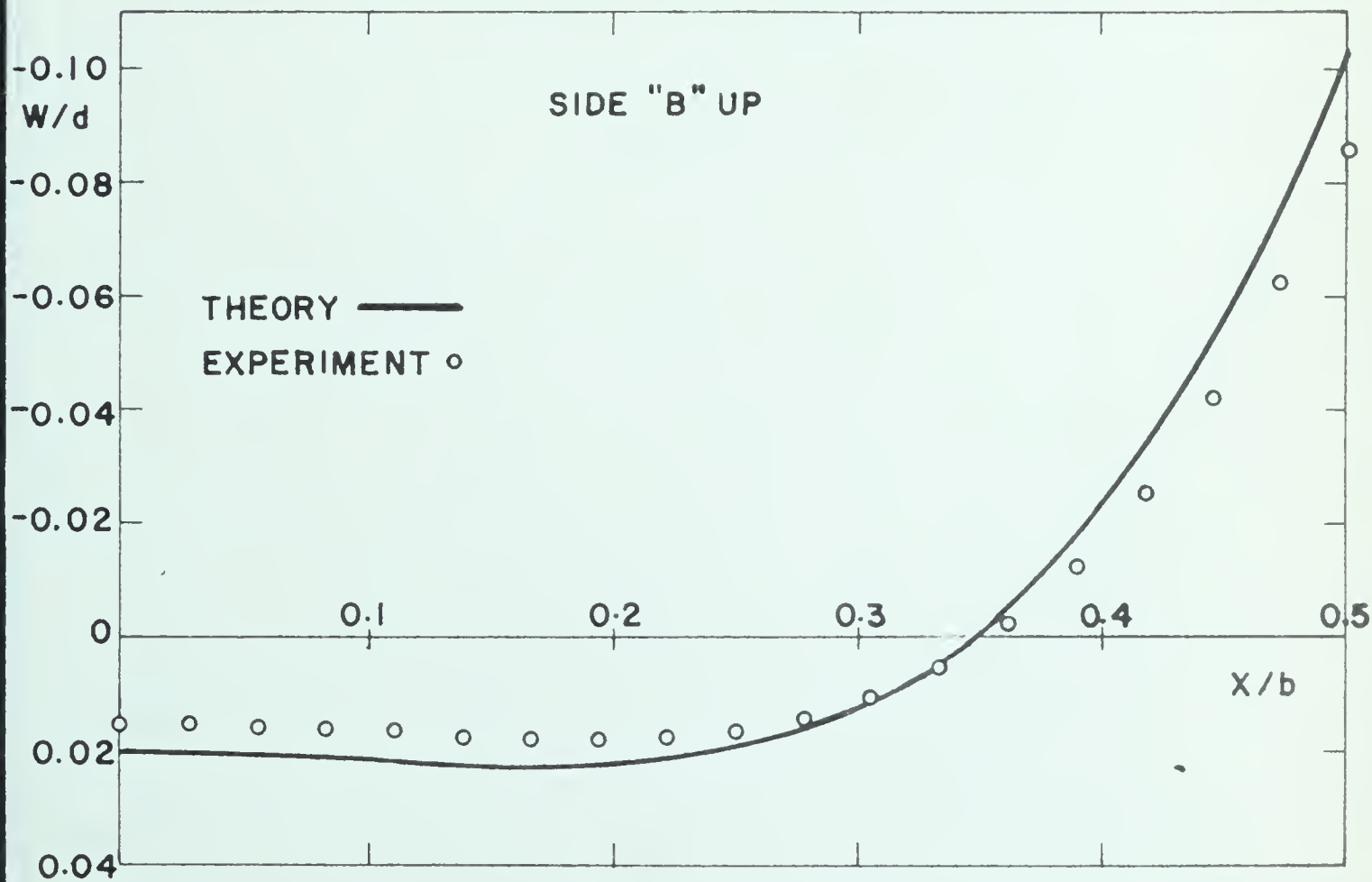


FIGURE 3.18 TRANSVERSE DEFLECTION FOR  $b^2/Rd=16.80$



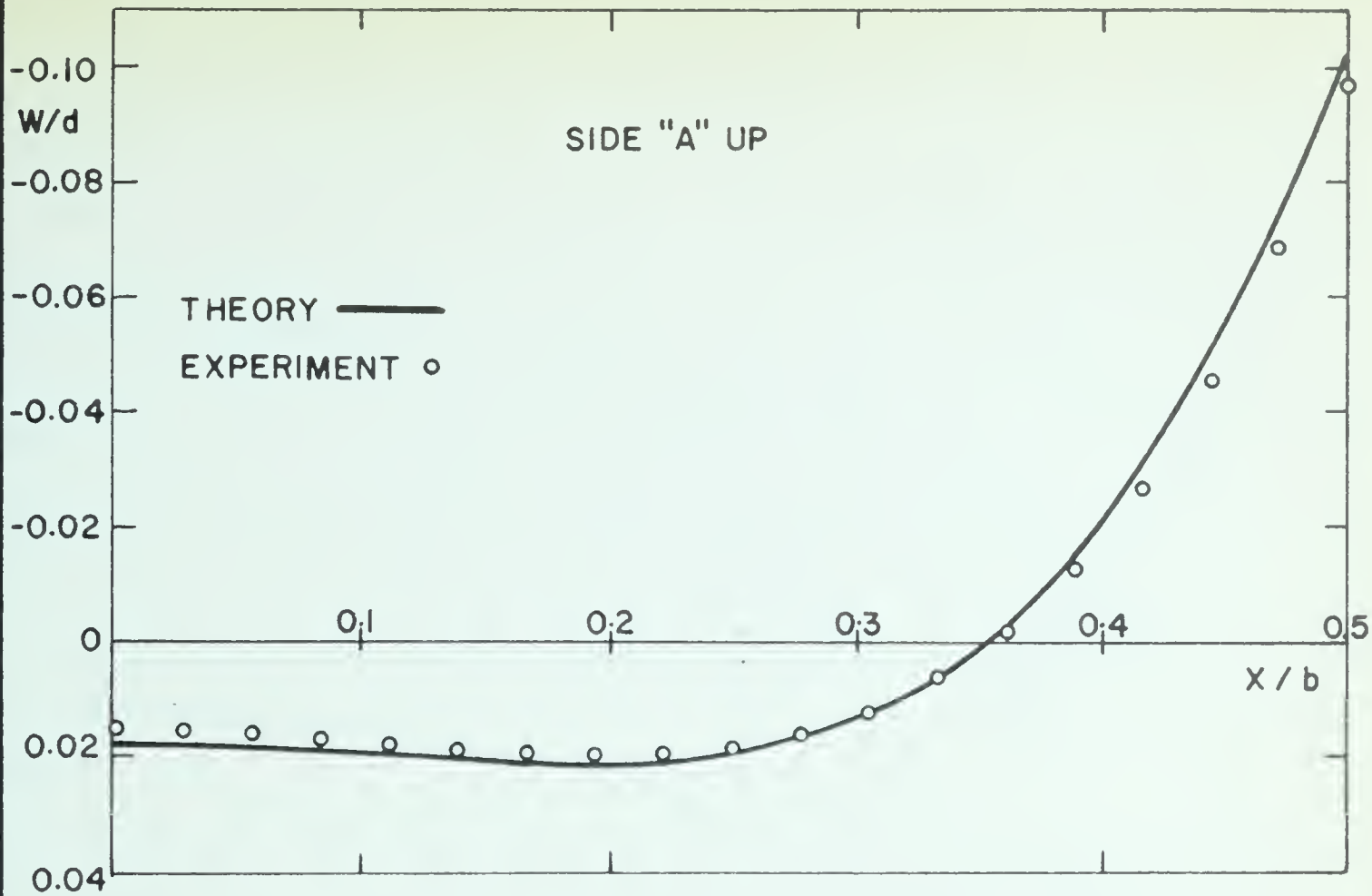


FIGURE 3.19 TRANSVERSE DEFLECTION FOR  $b^2/Rd=18.00$

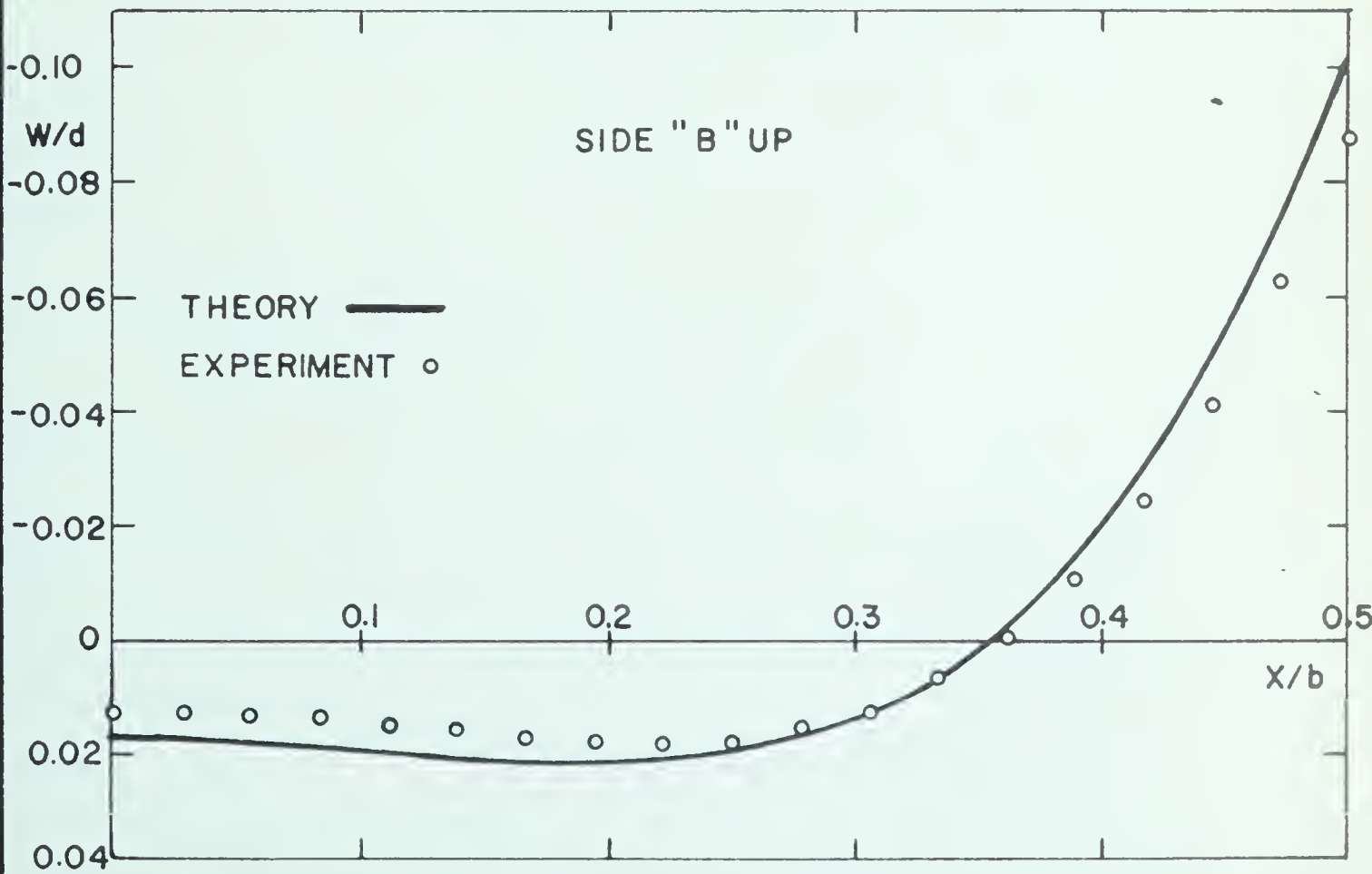


FIGURE 3.20 TRANSVERSE DEFLECTION FOR  $b^2/Rd=18.48$



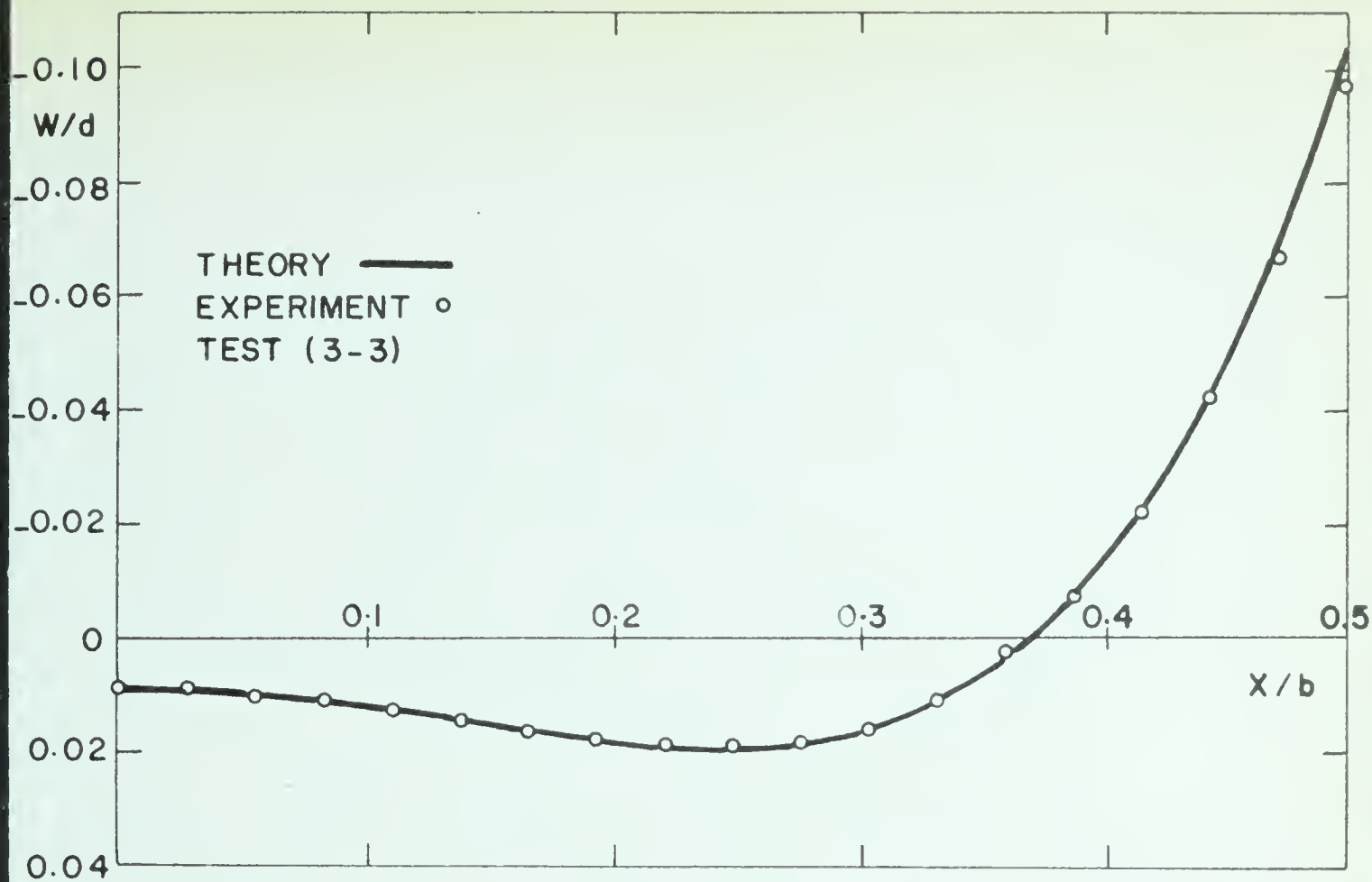


FIGURE 3.21 TRANSVERSE DEFLECTION FOR  $b^2/Rd=23.88$

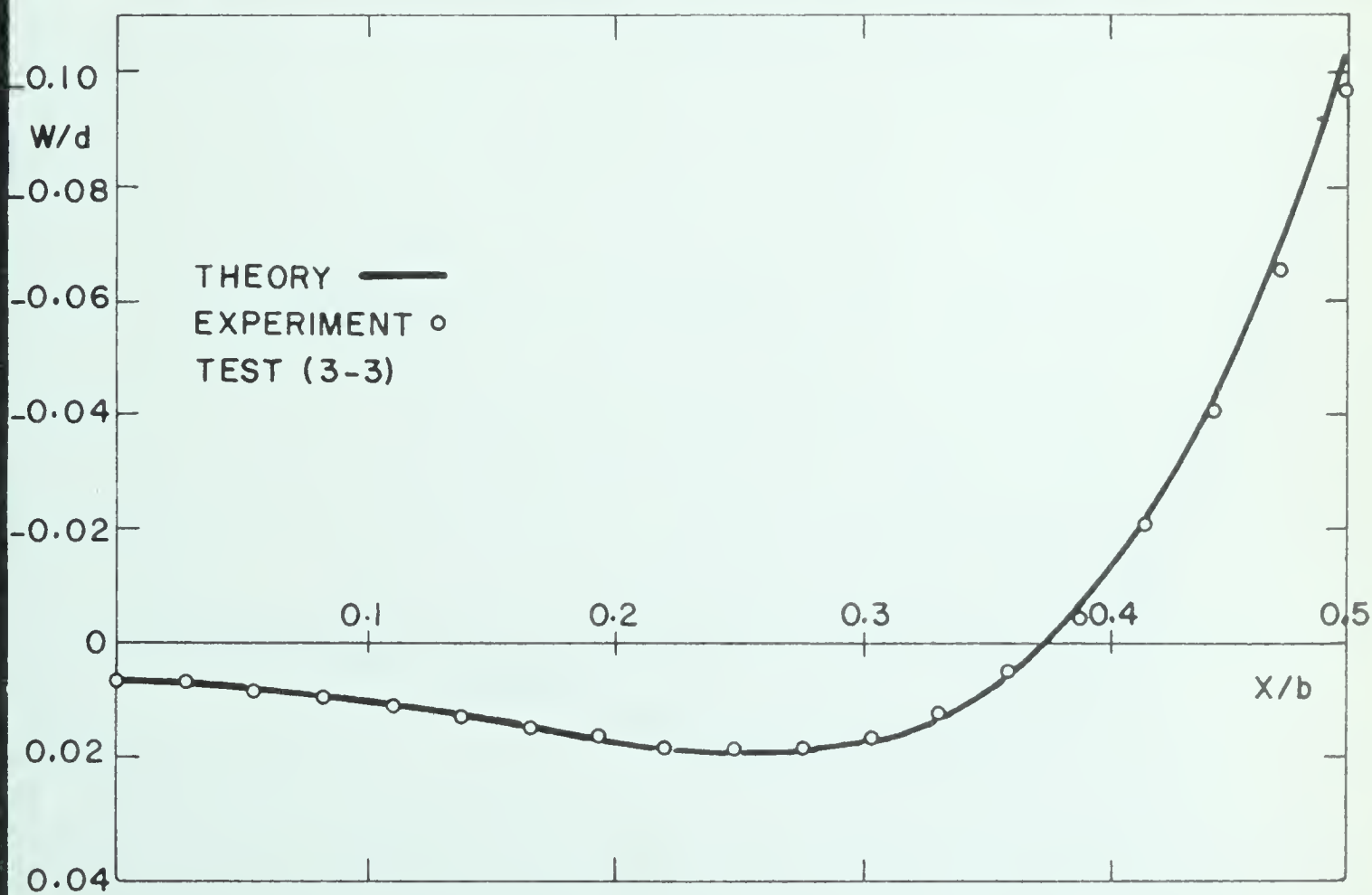
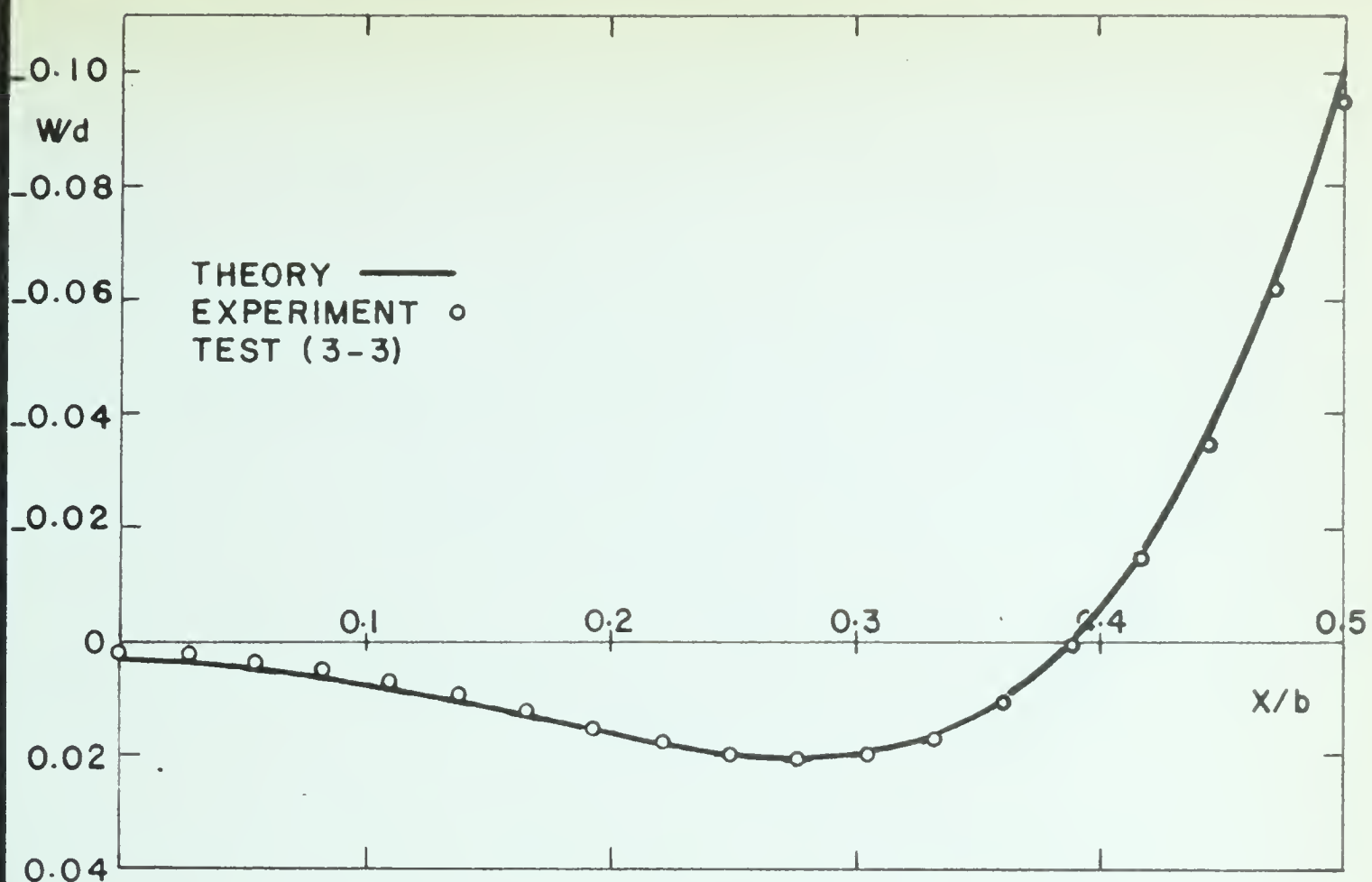
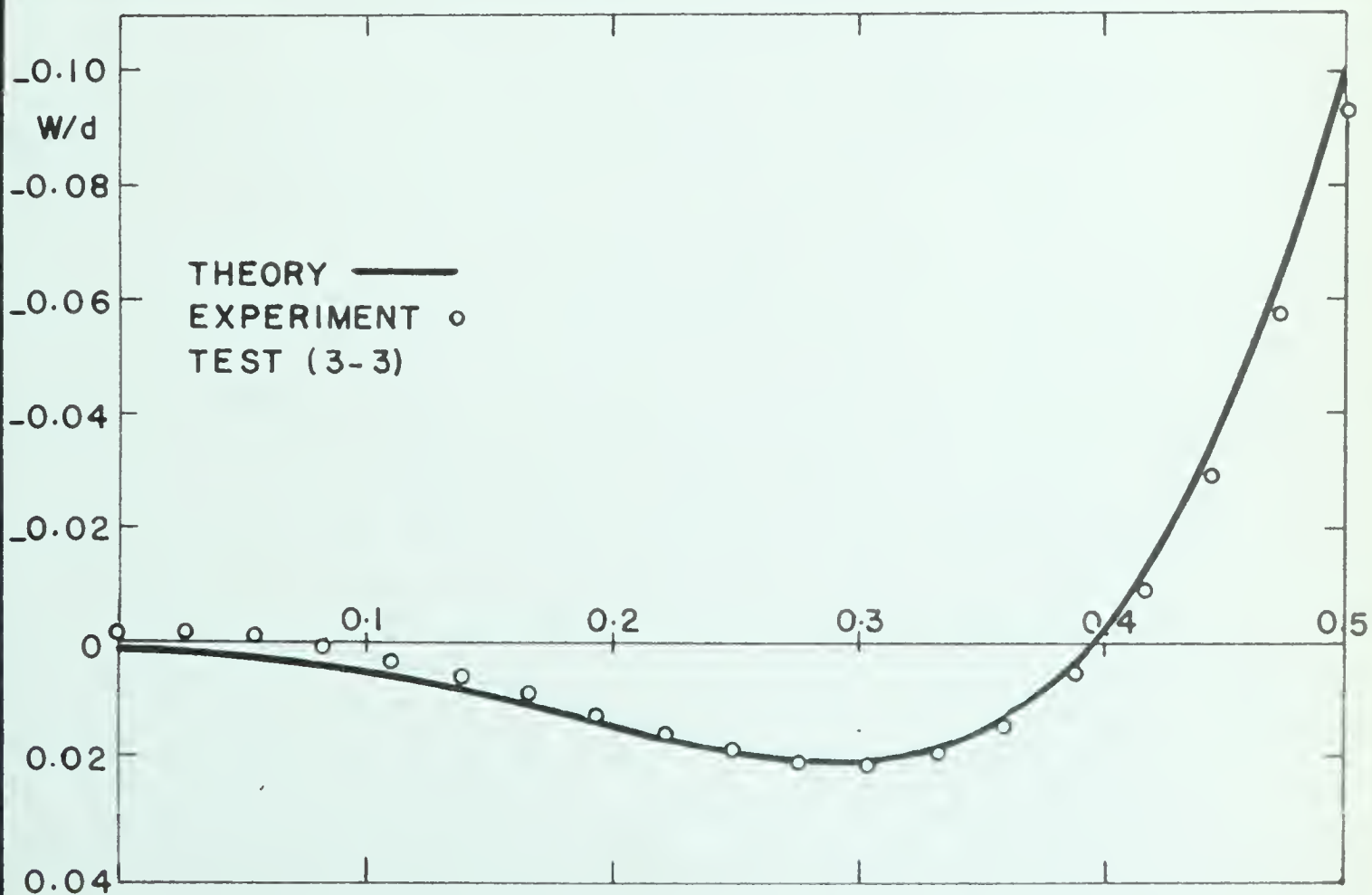


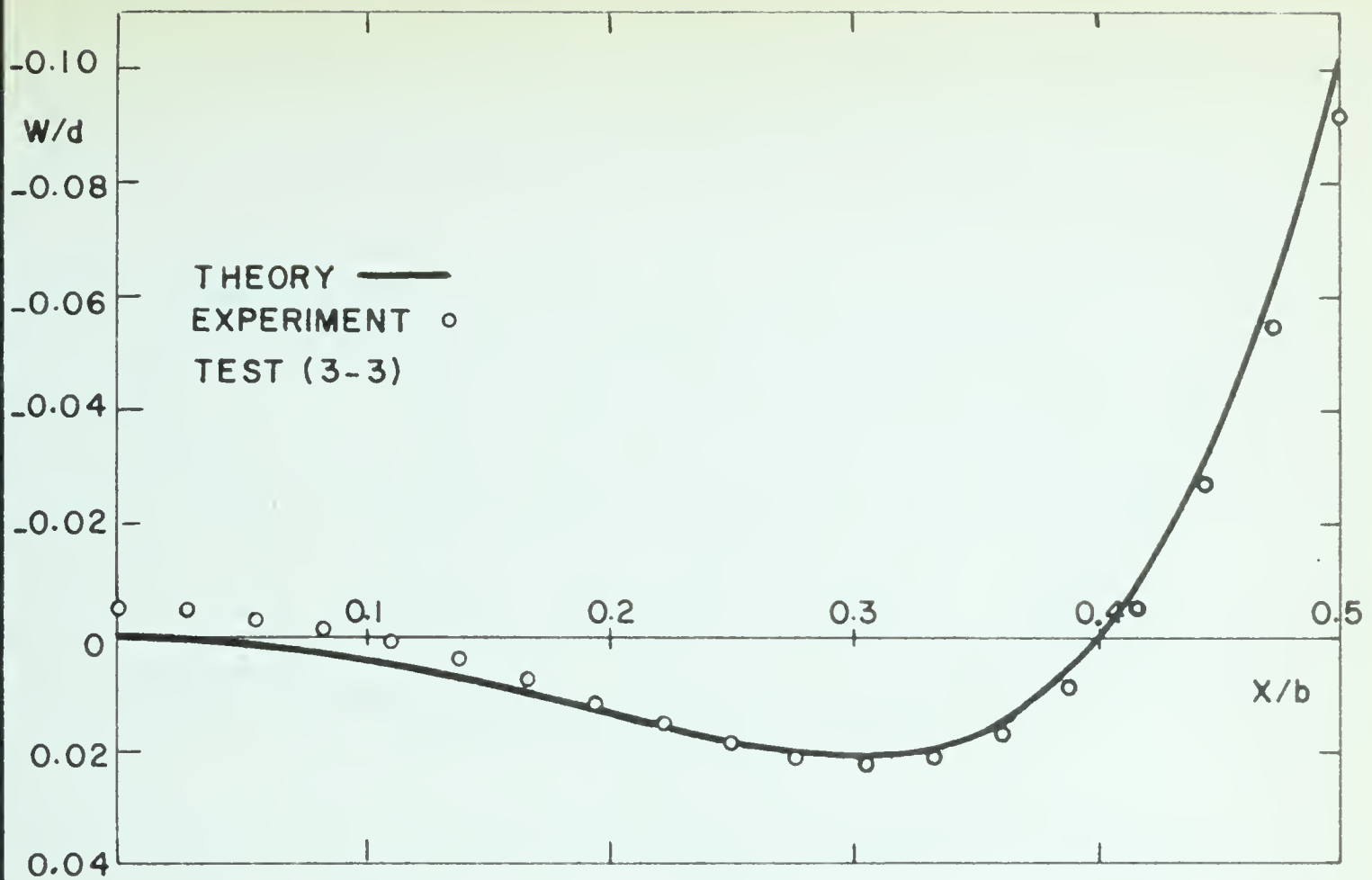
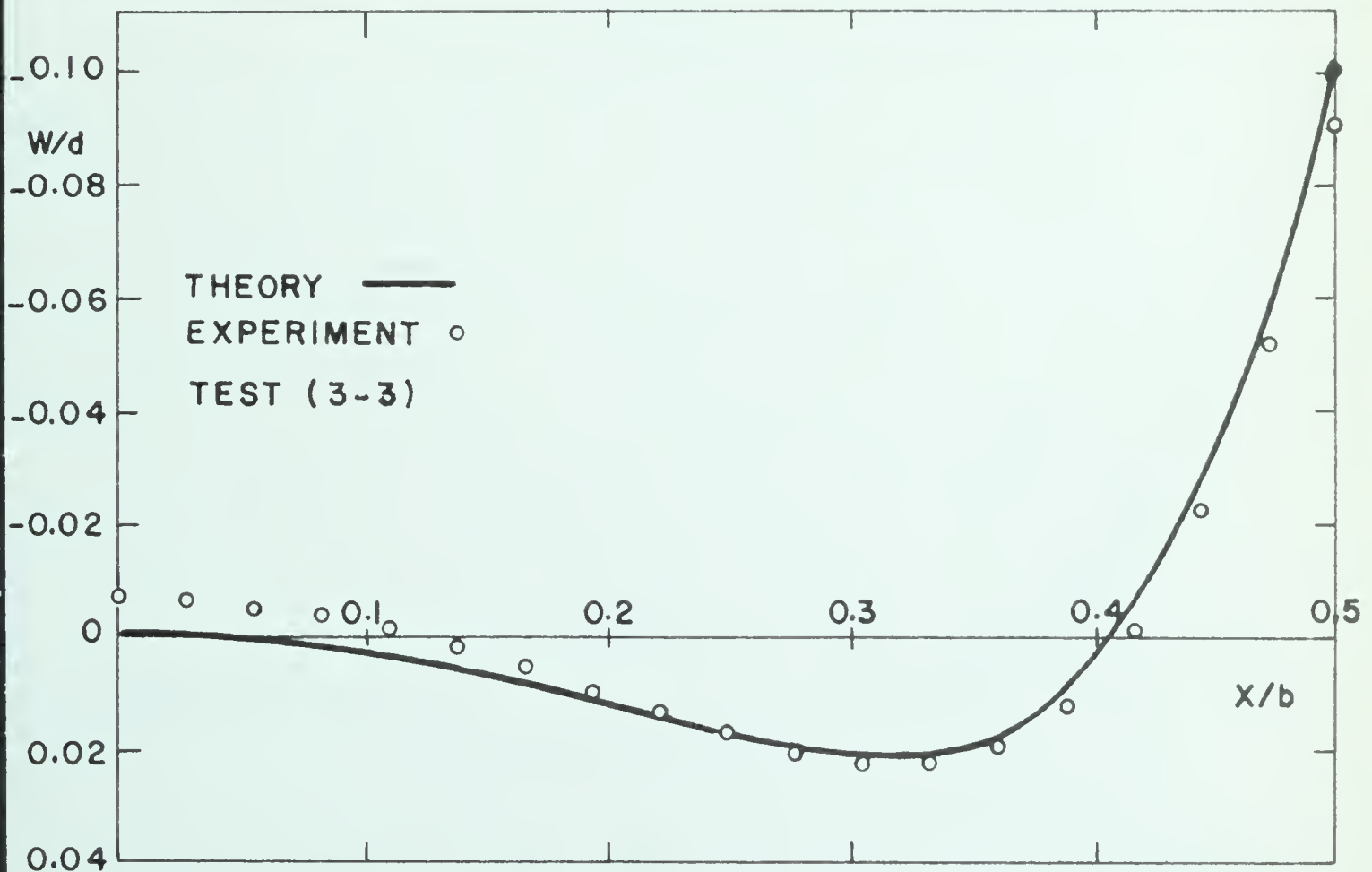
FIGURE 3.22 TRANSVERSE DEFLECTION FOR  $b^2/Rd=25.38$



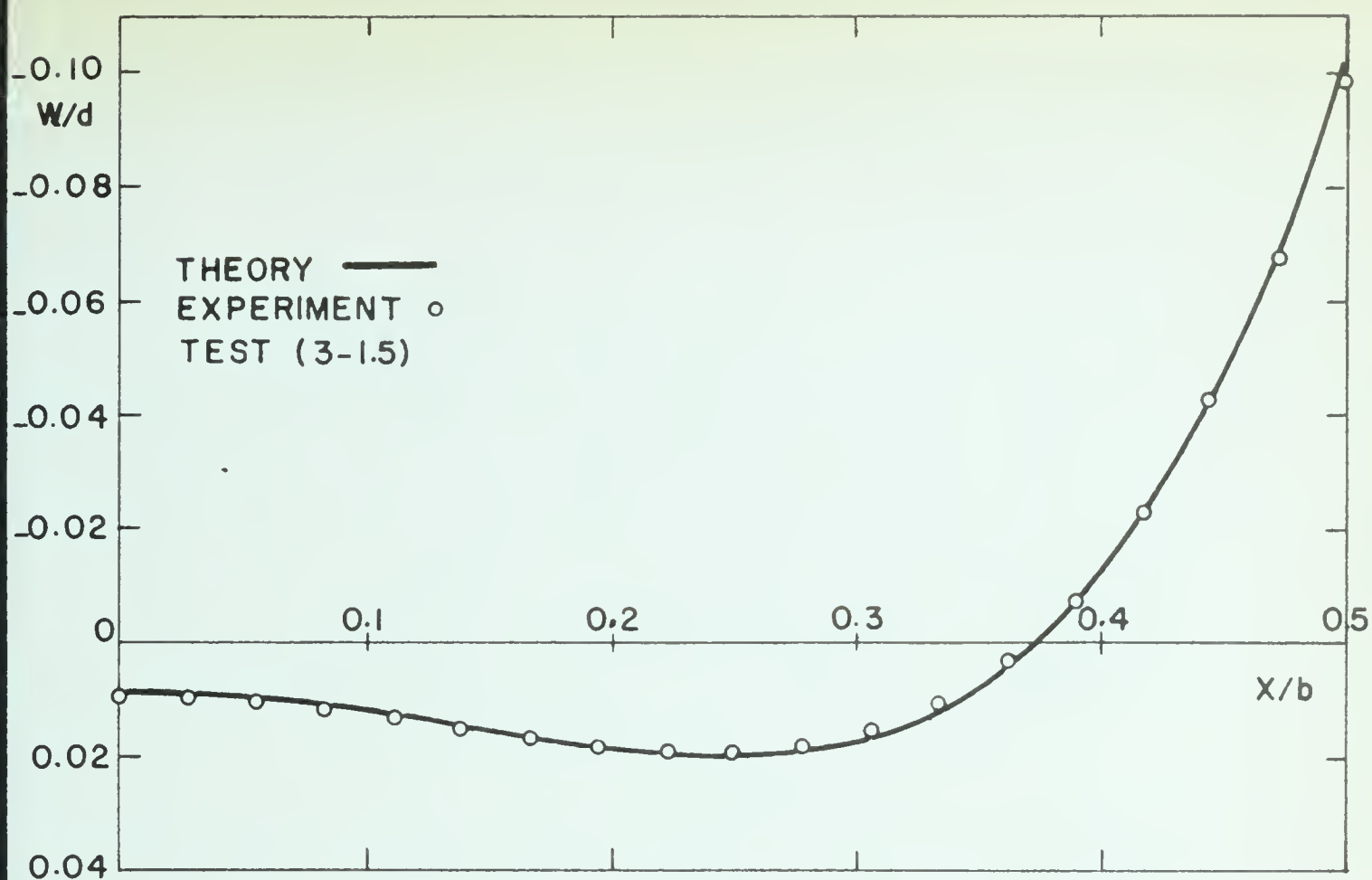
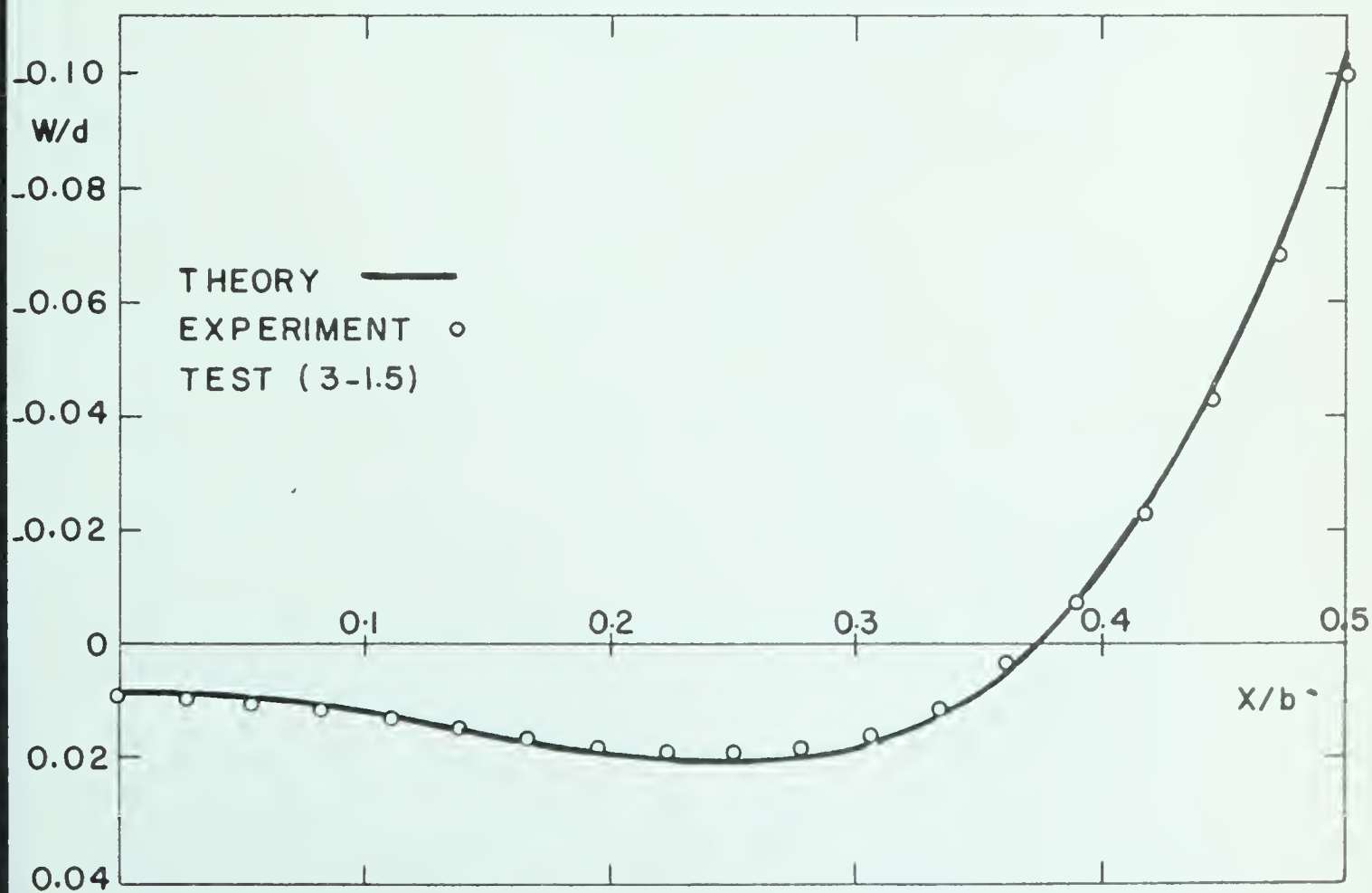


FIGURE 3.23 TRANSVERSE DEFLECTION FOR  $b^2/Rd = 29.78$ FIGURE 3.24 TRANSVERSE DEFLECTION FOR  $b^2/Rd = 33.92$



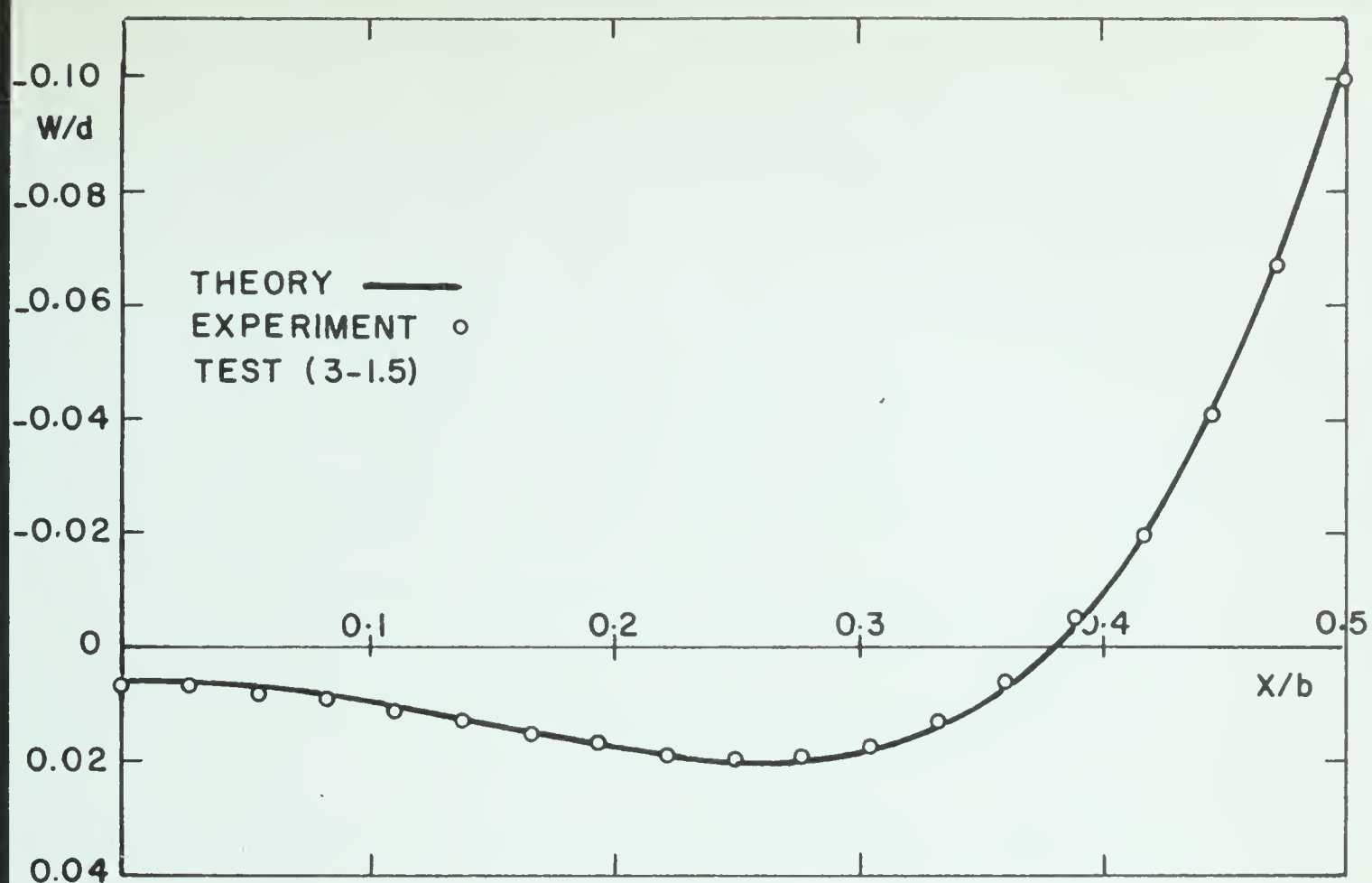
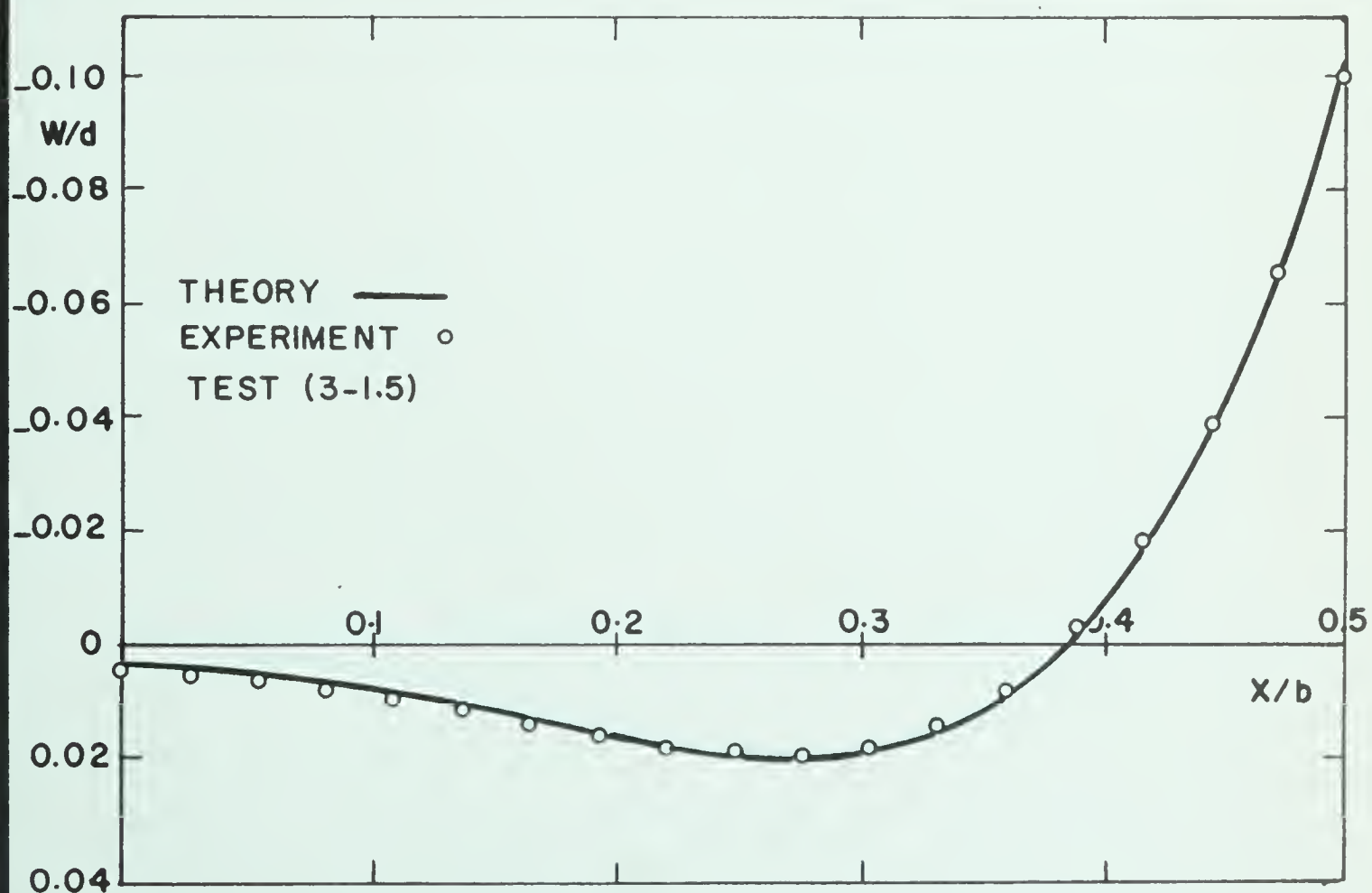
FIGURE 3.25 TRANSVERSE DEFLECTION FOR  $b^2/Rd=37.87$ FIGURE 3.26 TRANSVERSE DEFLECTION FOR  $b^2/Rd=41.68$



FIGURE 3.27 TRANSVERSE DEFLECTION FOR  $b^2/Rd=24.05$ FIGURE 3.28 TRANSVERSE DEFLECTION FOR  $b^2/Rd=24.83$





FIGURE 3.29 TRANSVERSE DEFLECTION FOR  $b^2/Rd=27.20$ FIGURE 3.30 TRANSVERSE DEFLECTION FOR  $b^2/Rd=29.57$



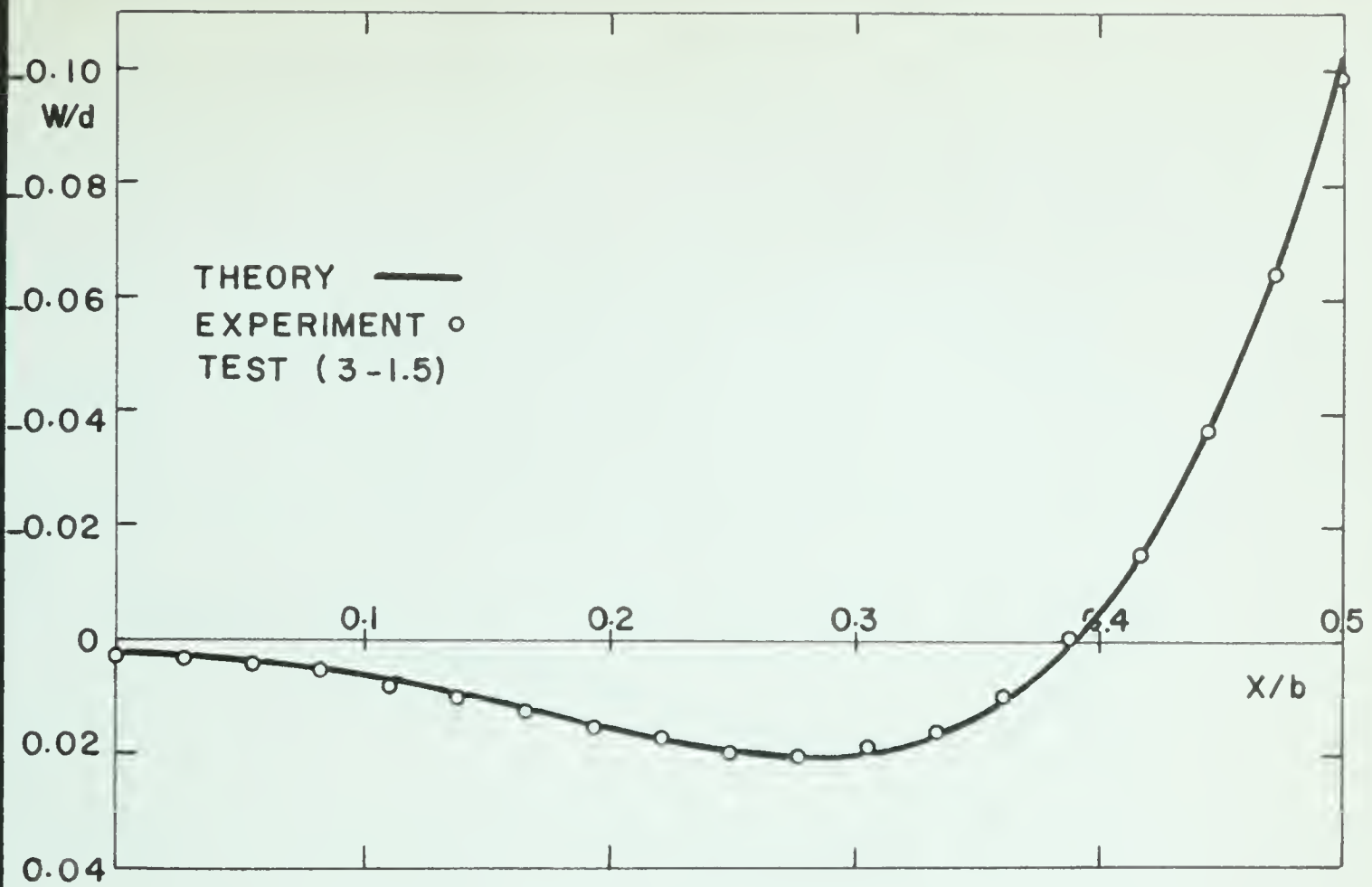


FIGURE 3.31 TRANSVERSE DEFLECTION FOR  $b^2/Rd=31.80$

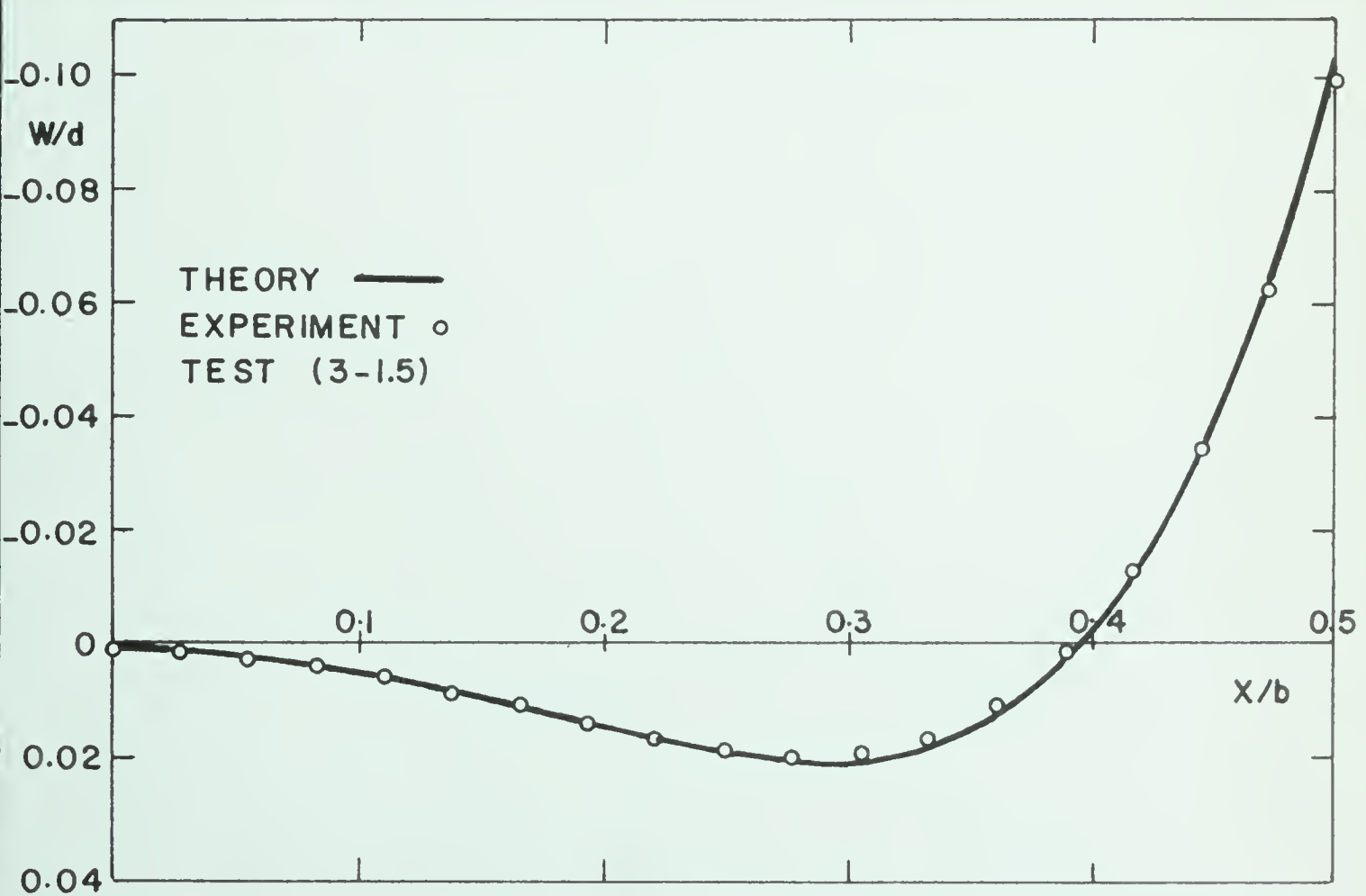
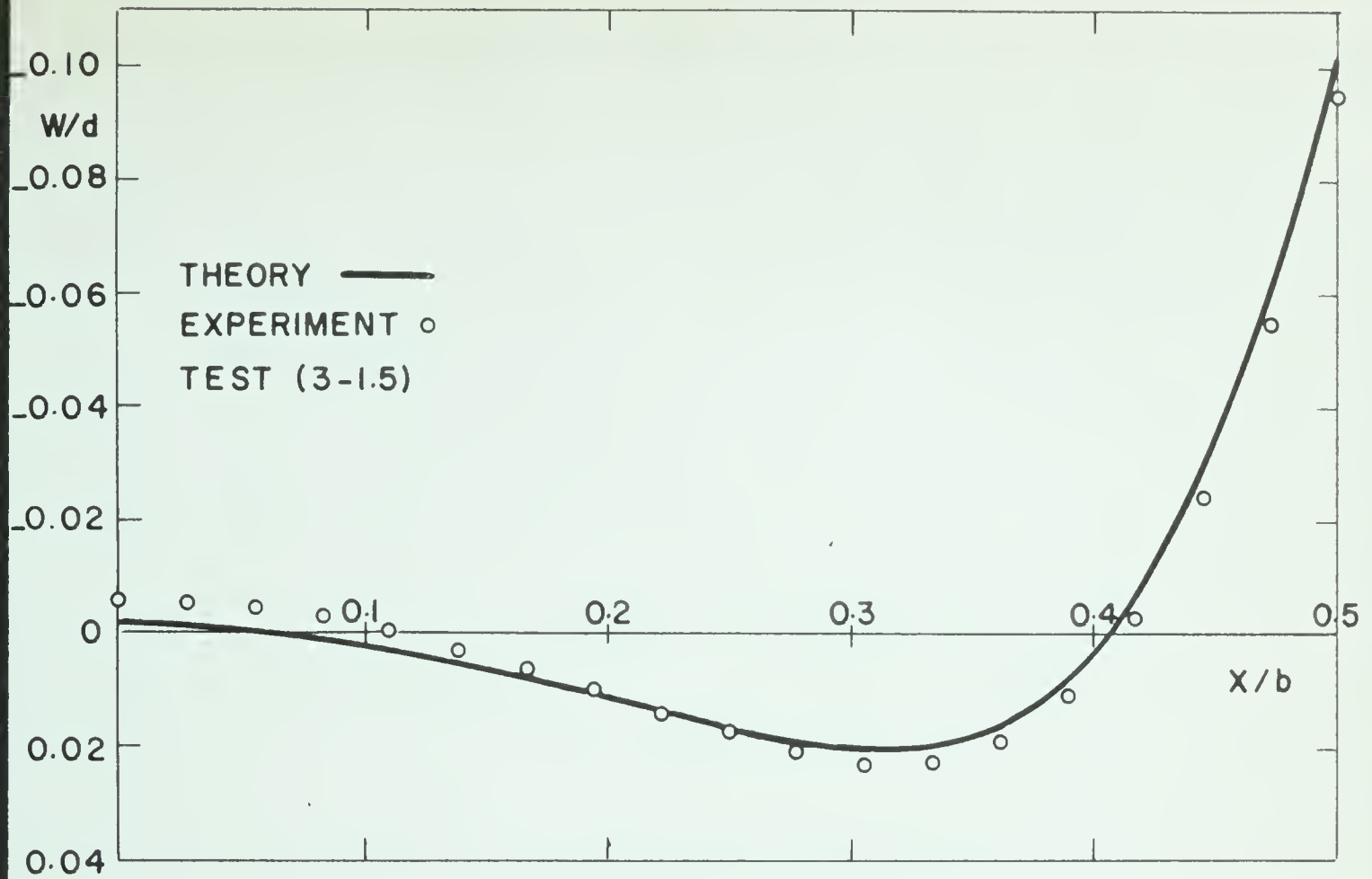
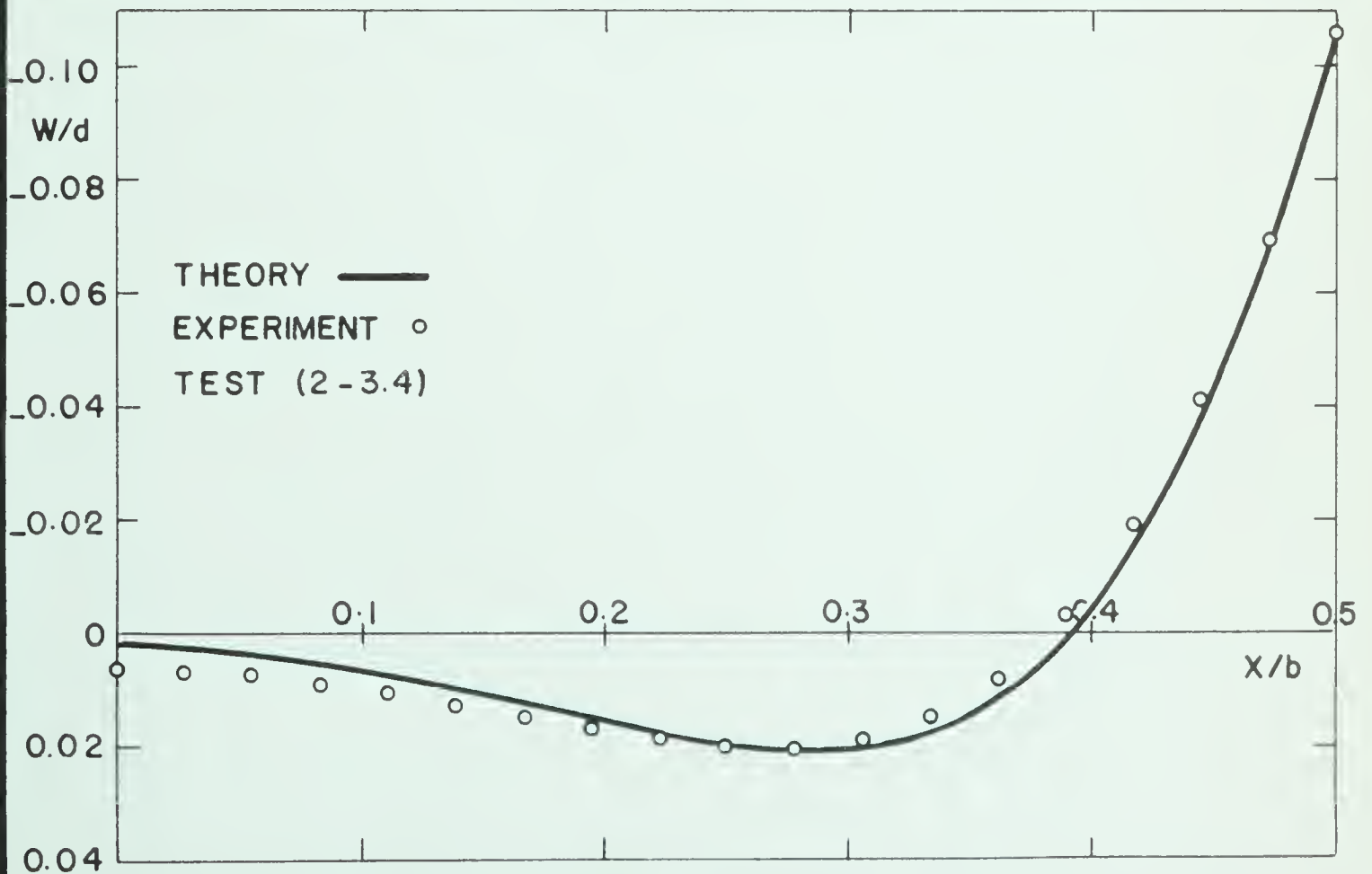


FIGURE 3.32 TRANSVERSE DEFLECTION FOR  $b^2/Rd=34.09$



FIGURE 3.33 TRANSVERSE DEFLECTION FOR  $b^2/Rd=42.37$ FIGURE 3.34 TRANSVERSE DEFLECTION FOR  $b^2/Rd=32.54$





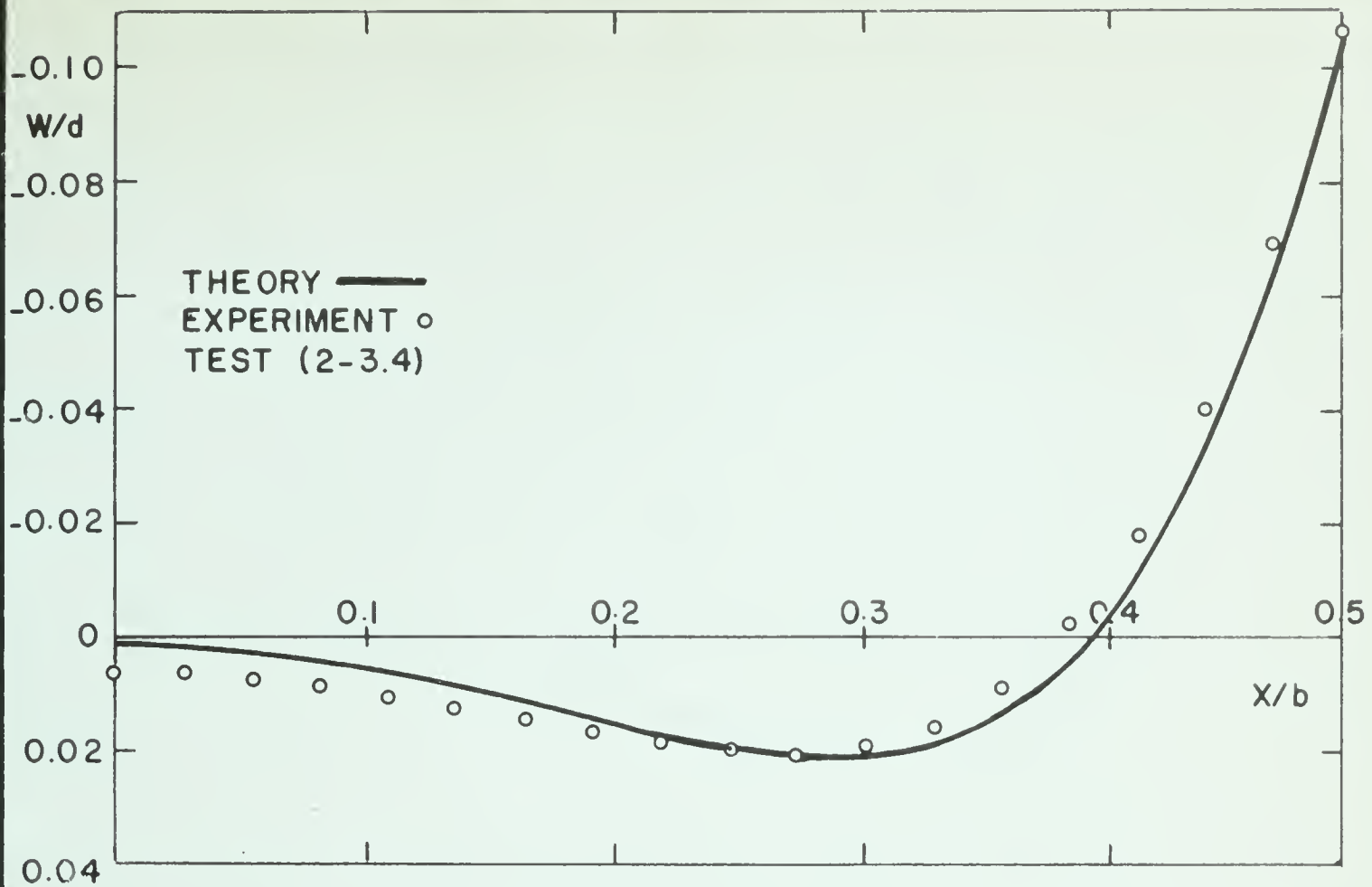


FIGURE 3.35 TRANSVERSE DEFLECTION FOR  $b^2/Rd=34.15$

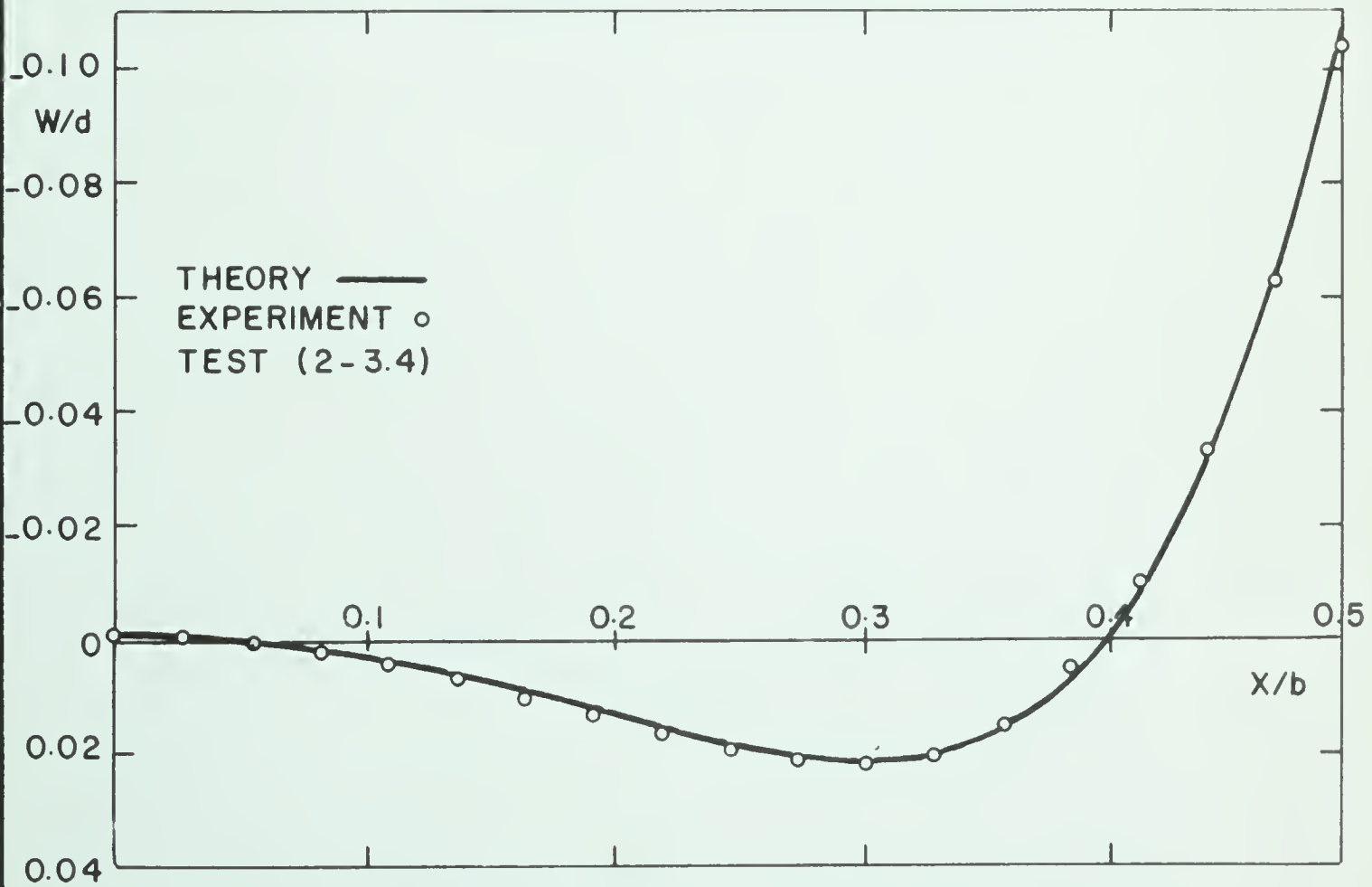


FIGURE 3.36 TRANSVERSE DEFLECTION FOR  $b^2/Rd=39.39$



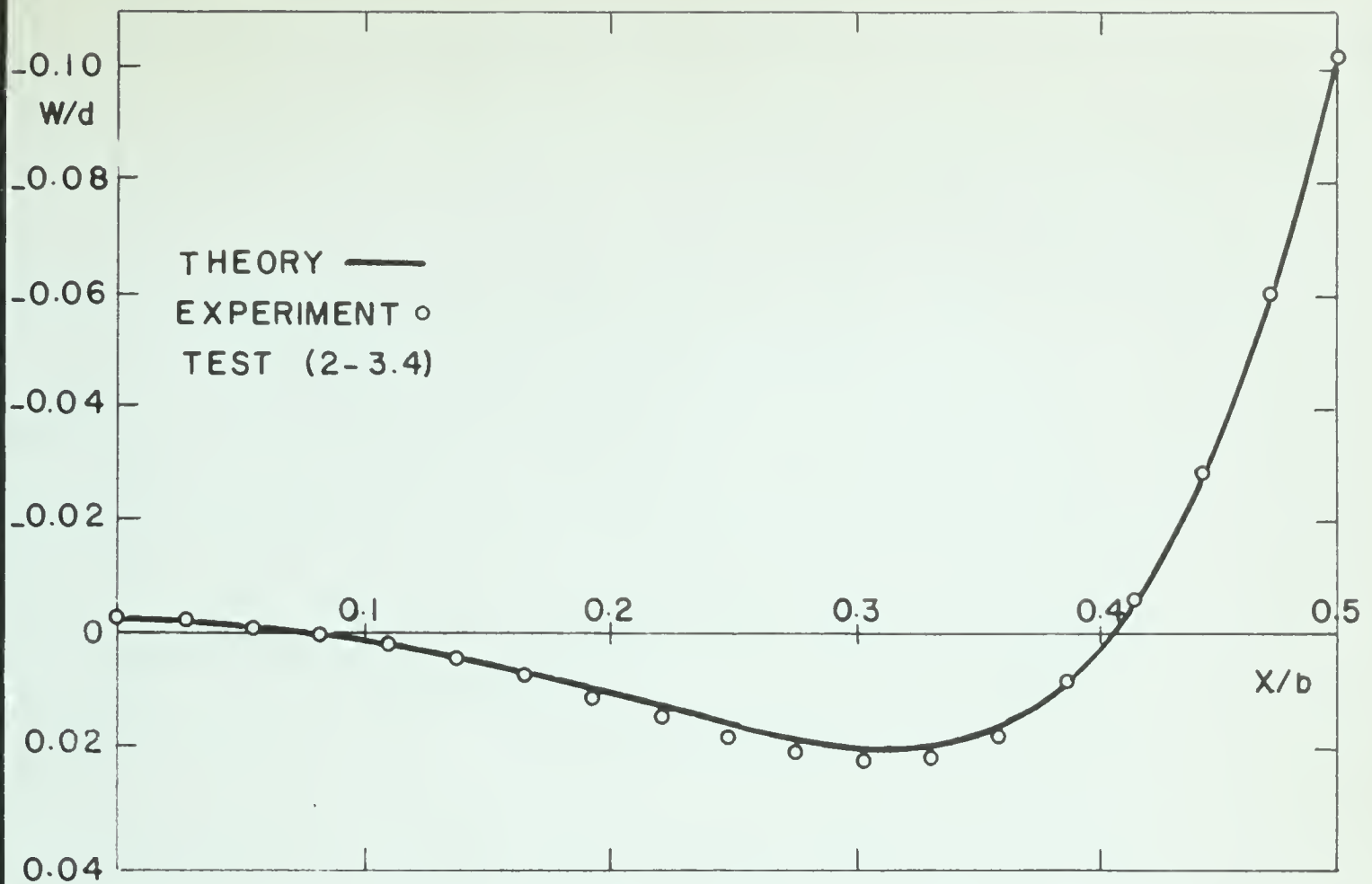


FIGURE 3.37 TRANSVERSE DEFLECTION FOR  $b^2/Rd = 44.62$

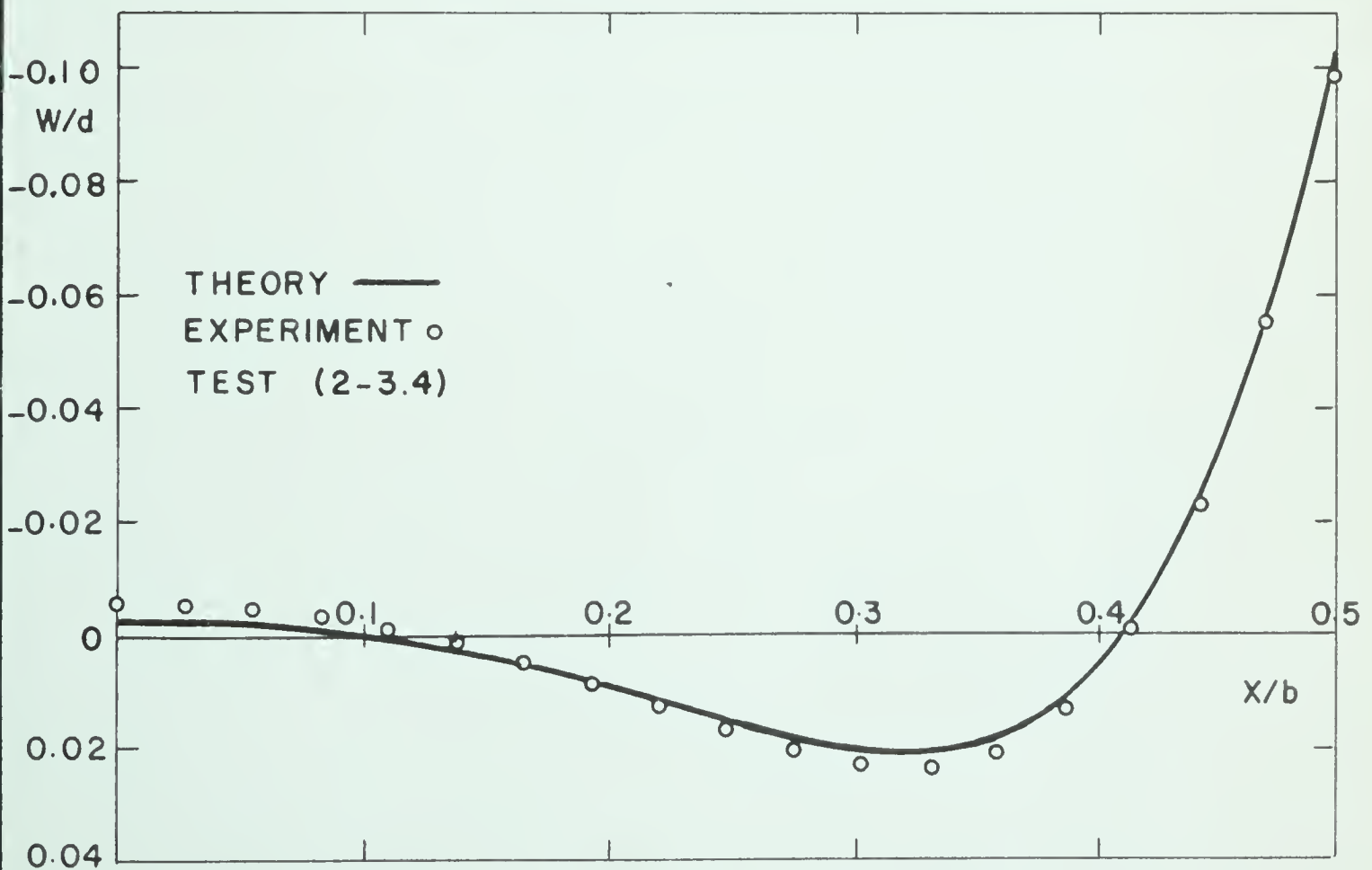


FIGURE 3.38 TRANSVERSE DEFLECTION FOR  $b^2/Rd = 48.95$



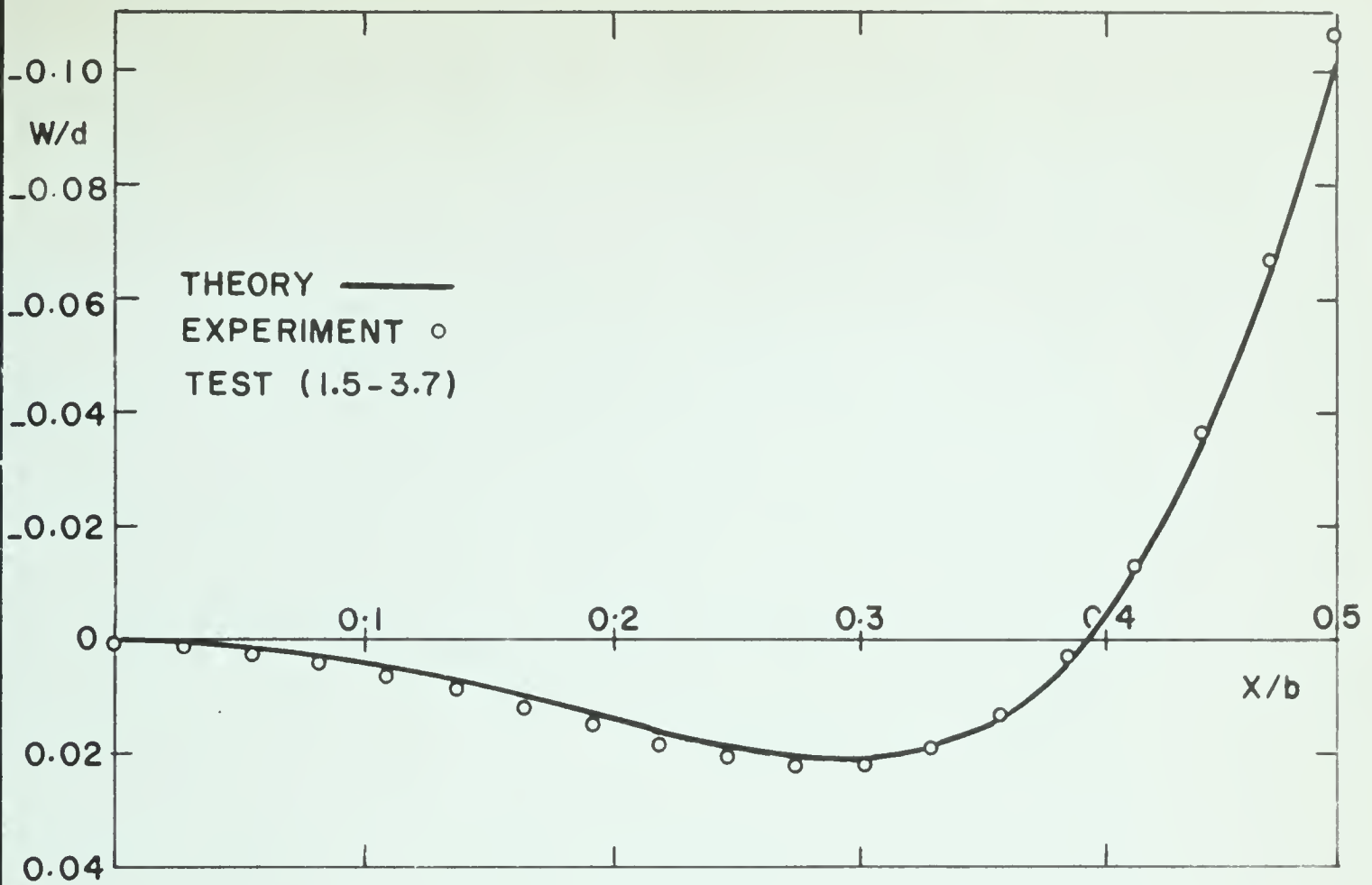


FIGURE 3.39 TRANSVERSE DEFLECTION FOR  $b^2/Rd=37.04$

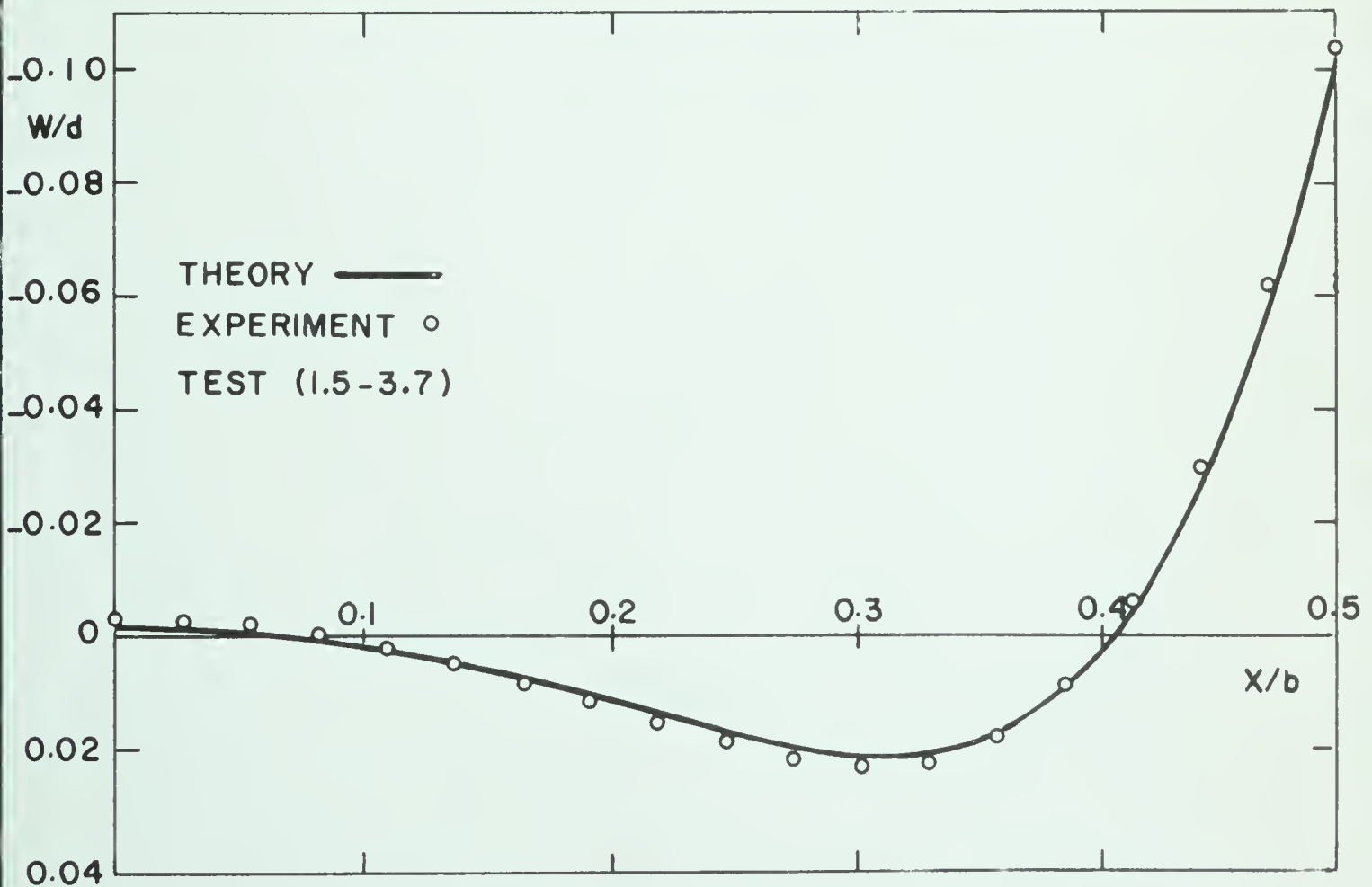


FIGURE 3.40 TRANSVERSE DEFLECTION FOR  $b^2/Rd=44.39$





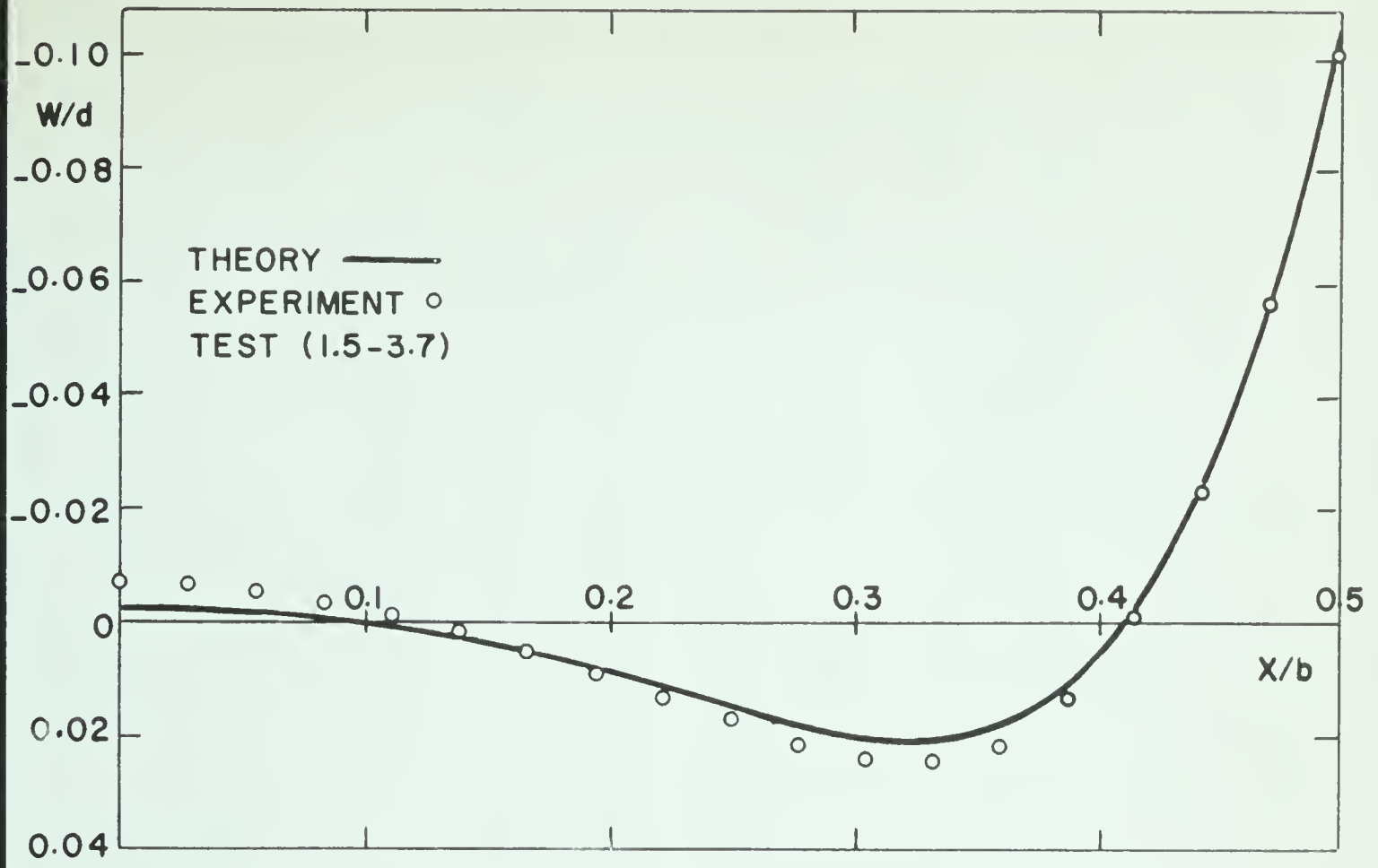


FIGURE 3.41 TRANSVERSE DEFLECTION FOR  $b^2/Rd=49.71$

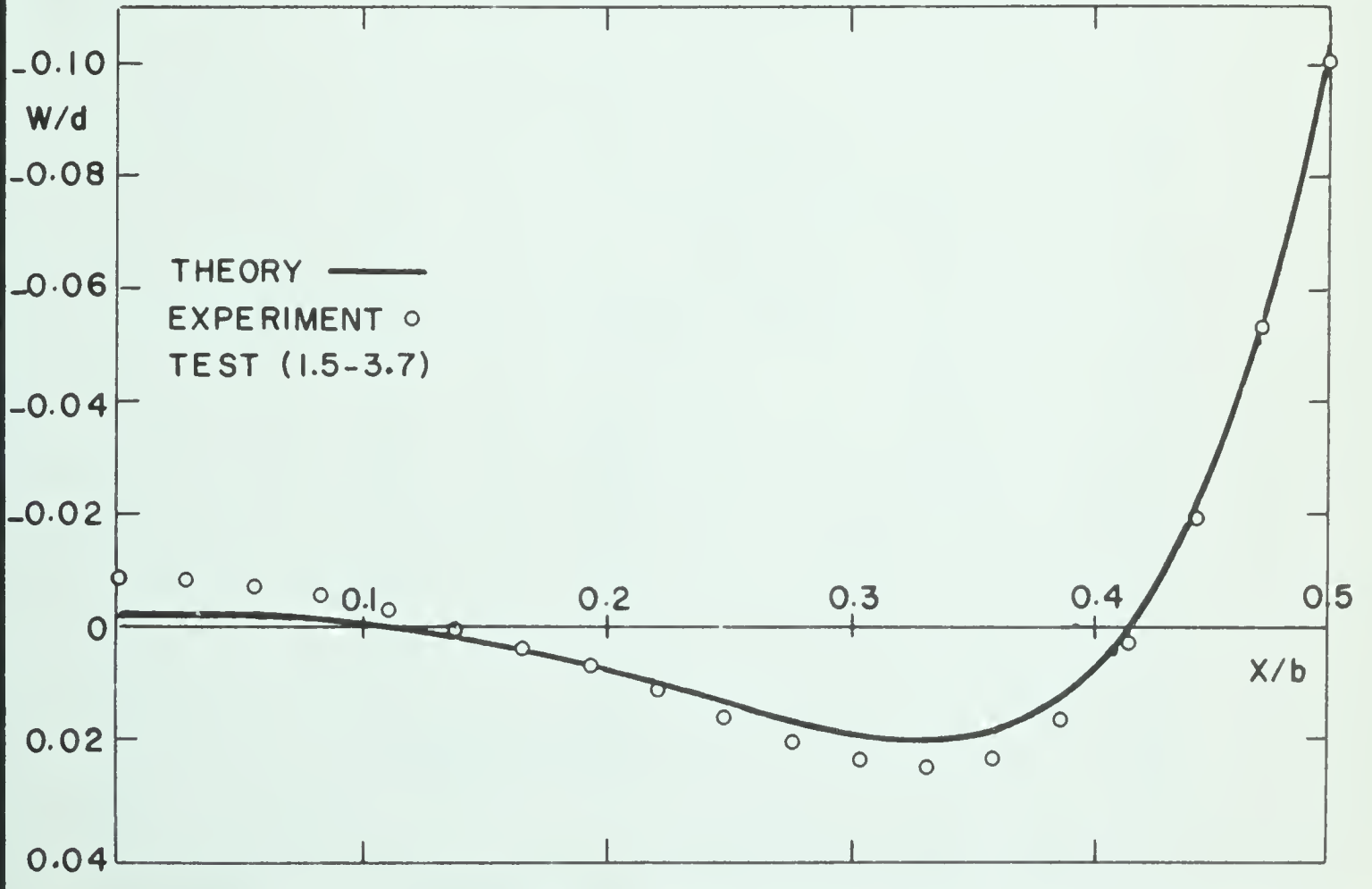


FIGURE 3.42 TRANSVERSE DEFLECTION FOR  $b^2/Rd=54.77$



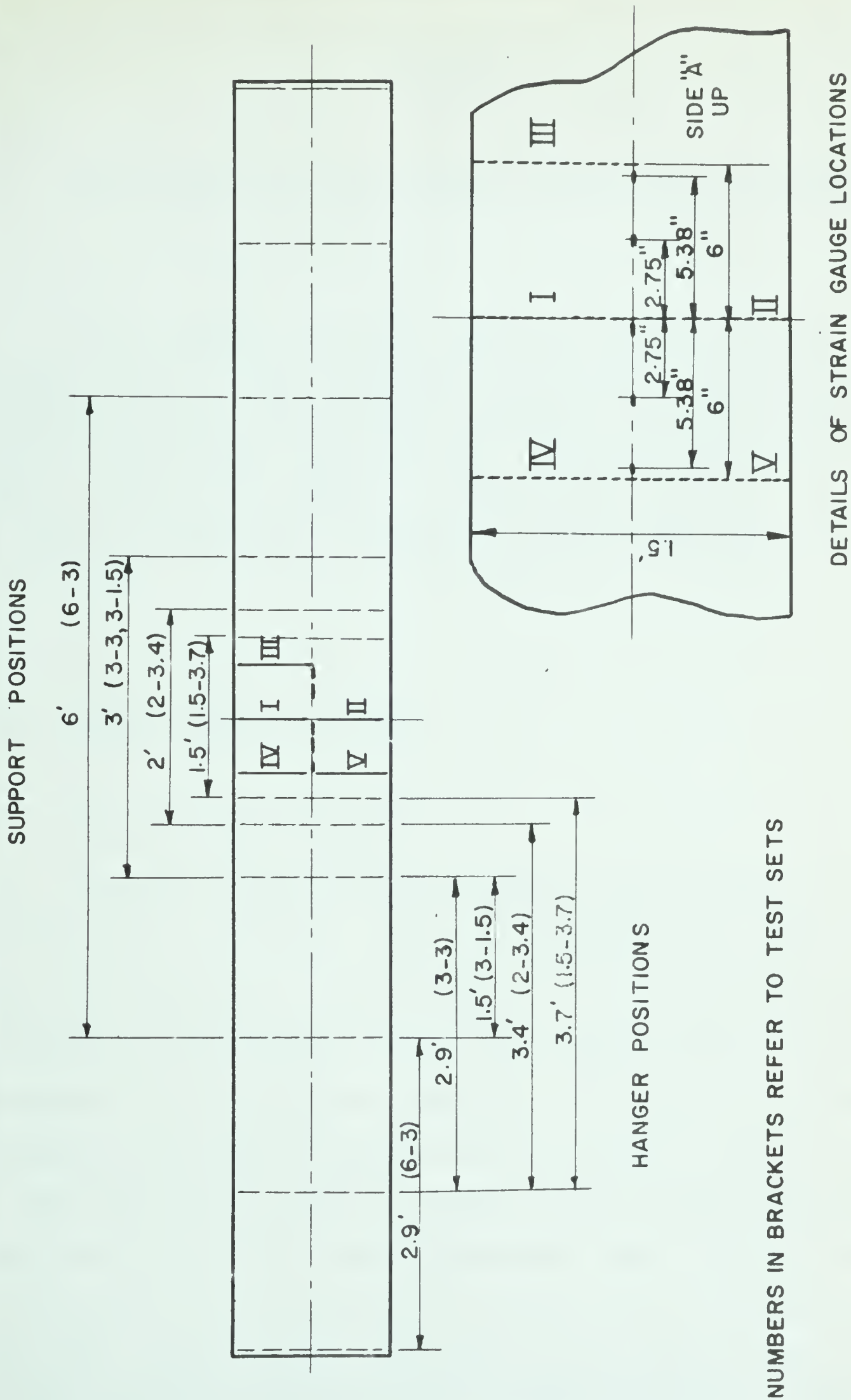


FIGURE 3.43 LOCATION OF STRAIN GAUGES, SUPPORTS, AND LOADING HANGERS



## CHAPTER IV

### DEVELOPMENT OF MULTI-CHANNEL DIGITAL DATA PROCESSOR

This chapter describes the multi-channel digital data processor built at the University of Alberta. It is shown that this apparatus is built around a Wheatstone bridge circuit with automatic devices for switching and recording the unknown voltages as indicated by transducers\*. Problems encountered in the construction of this apparatus such as noise and drift are discussed. An overall accuracy of measurement figure is given and the speed of operation is examined. Advantages and disadvantages are discussed for this and other competitive systems.

#### 4.1 DESIGN CONSIDERATIONS

##### 4.1.1 Preliminary Remarks

It was evident from the author's M.Sc. thesis that a more efficient method was required to measure the output from electrical resistance strain gauges. It was also considered desirable to use a method whereby the recorded data could be fed directly into a digital computer. Although the numerical procedures developed in Chapter II are simple, they are tedious and time consuming if done by hand or with a desk calculator. It was anticipated that the experimental work on the transverse

---

\* The term transducers is used here in the broad sense to include any device which produces a small voltage or change in voltage when subjected to time, temperature, load, strain, or displacement variations.





deflections of plates would result in thousands of readings, which discouraged the use of any manual recording system. In addition, when the number of transducers to be recorded is large, say forty or more, the time to switch, balance, and record all of the readings manually in the conventional manner will probably exceed the time interval for which the conditions producing the readings can be held reliably constant. To avoid this situation it is necessary to record the data in as short a time as possible.

It was decided to construct a system in the Department of Mechanical Engineering capable of switching and balancing large quantities of transducer signals and permanently recording these values so that they may be fed directly into a computer. In subsequent sections of this chapter the design and operation of this equipment is described.

#### 4.1.2 National Aeronautical Establishment

In correspondence with the Structures Laboratory of the National Aeronautical Establishment at Ottawa it was learned that they had constructed a 500 channel digital output strain gauge recorder. This system incorporated a unique method of zero balancing which could be built inexpensively.

After consulting various electronic manufacturers it was decided to use the basic design developed by the National Aeronautical Establishment. One of the advantages this system had over other proposed systems was that the initial cost was low and the apparatus could be built in steps, yet be useful for gathering data at any time in the building process.



## 4.2 CONSTRUCTION

### 4.2.1 General Remarks

The basic measuring circuit used with transducers is a Wheatstone bridge. Figure 4.1 shows the circuit which is used for a single channel.\* The transducer in this case is an electrical resistance strain gauge where

$R_g$  = resistance of active or measuring strain gauge,

$R_d$  = resistance of temperature compensating gauge, sometimes referred to as a dummy gauge,

$R_c$  = resistance of variable resistor used to obtain initial balance of the bridge,

$E_v$  = excitation voltage of the bridge.

When the bridge is balanced, the potential at X equals the potential at Y and no current flows through A. If a change in parameter changes the resistance of the active gauge  $R_g$  then an unbalanced condition exists, producing a current flow through A due to a difference in potential between X and Y. The amount of resistance required to restore balance in conventional recorders is indicated on a dial calibrated in micro-inches per inch. A balanced condition is indicated by a null reading on a meter placed at A.

The Wheatstone bridge circuit can be used in an automatic system. A balancing potentiometer or voltmeter capable of converting analog readings to digital readings is placed at A.

---

\* Channel is used synonymously with channel of information, or transducer signal.



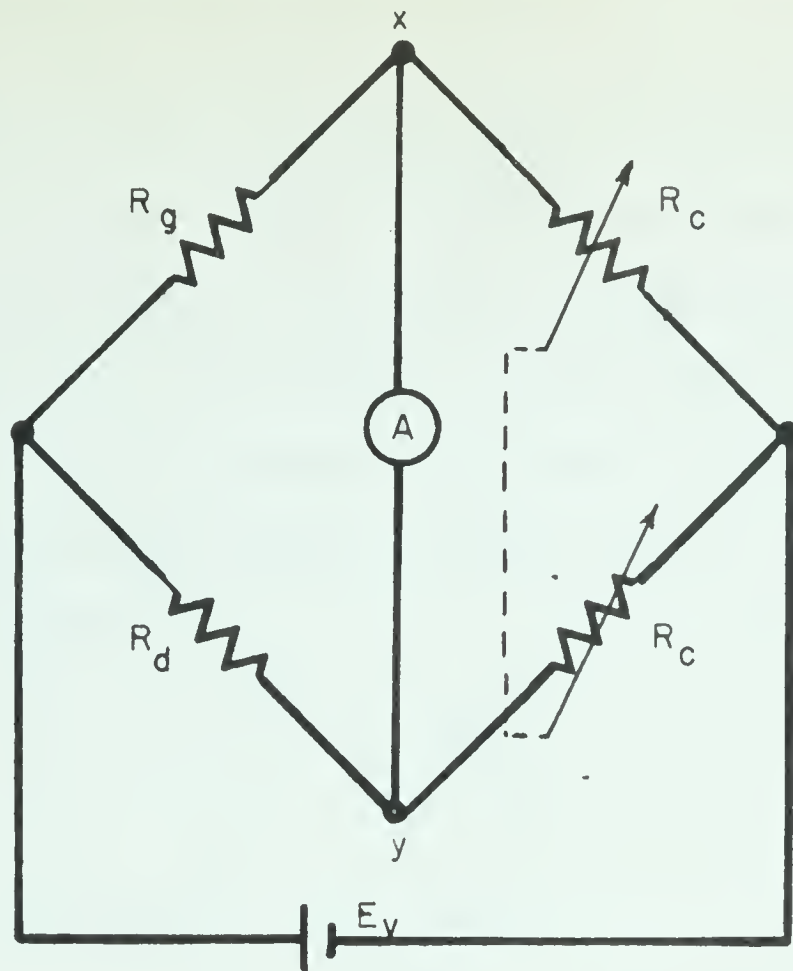


FIGURE 4.1 WHEATSTONE BRIDGE

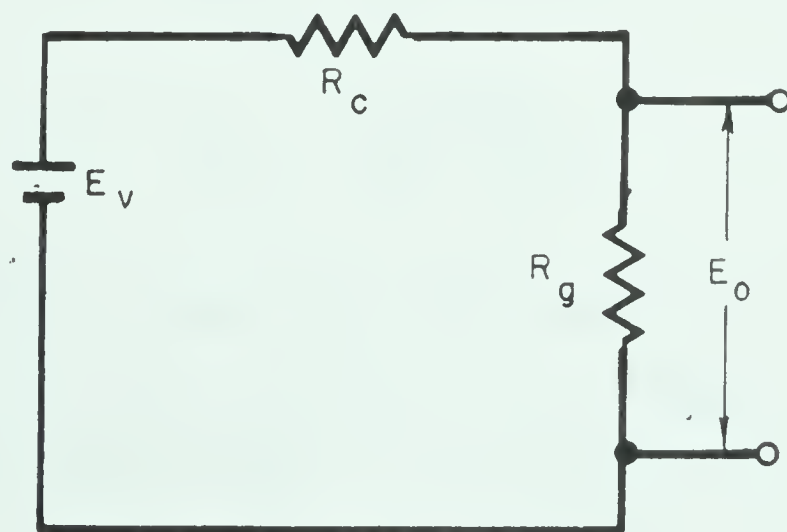


FIGURE 4.2 SIMPLIFIED CIRCUIT





Instead of balancing the bridge the ADVM (analog digital voltmeter) reads out the potential difference between X and Y.

The only arm of the Wheatstone bridge which will change resistance, relative to the others, is the active strain gauge  $R_g$ . The top half of the circuit in Figure 4.1 can be replaced by the equivalent circuit shown in Figure 4.2. The current in the circuit is  $I$ , where

$$I = \frac{E_v}{R_g + R_c},$$

and the voltage drop across  $R_g$  becomes

$$E_o = \frac{R_g E_v}{R_g + R_c}. \quad 4.1$$

The relationship between the change in output voltage caused by a change in gauge resistance is given by

$$\frac{dE_o}{dR_g} = \frac{E_v R_c}{(R_g + R_c)^2}$$

or,

$$dE_o = \frac{I R_c dR_g}{(R_c + R_g)}. \quad 4.2$$

Equations 4.1 and 4.2 assume the ADVM produces no load on the circuit. This is a valid assumption if the impedance of the ADVM is high. The gauge factor  $k$  of strain gauges is defined as

$$k = \frac{dR_g/R_g}{e}, \quad 4.3$$

where  $e$  is the strain. Substituting equation 4.3 into 4.2 gives



$$dE_o = \frac{R_c R_g I_{ke}}{(R_c + R_g)} \quad 4.4$$

and, if  $R_c = R_g$ , then

$$dE_o = \frac{1}{2} (R_g I_{ke}) . \quad 4.5$$

Assuming the following typical values

$$k = 2.0$$

$$e = 1000 \text{ } \mu\text{in. per in.}$$

$$E_v = 2.0 \text{ v}$$

$$E_g = 120.0 \text{ ohms}$$

the output will be

$$dE_o = 1000 \text{ } \mu\text{v} .$$

Obviously if 1000  $\mu\text{in. per in.}$  is to represent a full scale reading, the ADVm must have a full scale reading of 1000  $\mu\text{v}$ . If the lowest full scale range of the ADVm is 10,000  $\mu\text{v}$ , then an amplifier must be used ahead of the input to the ADVm so that 1000  $\mu\text{v}$  can be amplified to represent a full scale reading on the ADVm.

An obvious method of increasing the gauge output, for a given strain, would be simply to increase the bridge voltage  $E_v$ . This is an undesirable solution. If the lowest full scale output is 10,000  $\mu\text{v}$  the gauge output needs to be increased by a factor of 10. Thus,  $E_v$  would be increased to 20 v, but, this would heat the strain gauge causing excessive drift. It has been found that the safe operating power level for metal film strain gauges is approximately 15 watts per sq in. of grid area. The power level is lowered to 4 watts per sq in. for wire wound strain gauges. Now for a single channel bridge circuit using



metal film gauges whose grid area is 0.015 sq in. per gauge, or a total grid area of 0.060 sq in. for the four gauges, the maximum power that can be dissipated without drift is 0.90 watts. However, a bridge supply of 20 v draws 1.7 watts and hence, in this example, drift in the strain gauge readings would be experienced. Therefore, increasing the bridge voltage is an unsatisfactory method in obtaining increased gauge output. The only other solution is to use an amplifier ahead of the ADVM.

#### 4.2.2 Circuit Design

The block diagram of Figure 4.3 shows the general layout of the digital-data-processor system (DIDAP). For every channel a pair of wires lead into one of the four junction boxes. When a compensating gauge is used for every active gauge, another pair of wires lead into the junction box for each channel. In this box, one lead of the compensating gauge is attached to the positive terminal, the other lead is joined to one lead of the active gauge and connected to the common terminal. The other lead of the active gauge is connected to the negative terminal (see Figure 4.4). If a single compensating gauge is used it is wired directly into the scanning unit as shown in Figure 4.5 (in the experimental work on this thesis one compensating gauge was used to service up to 198 active gauges).

Two 50 channel balancing units follow from the junction boxes. The unique idea of these units was suggested by the Structures Laboratory of the National Aeronautical Establishment in Ottawa. Figure 4.6 shows the detail of the balancing





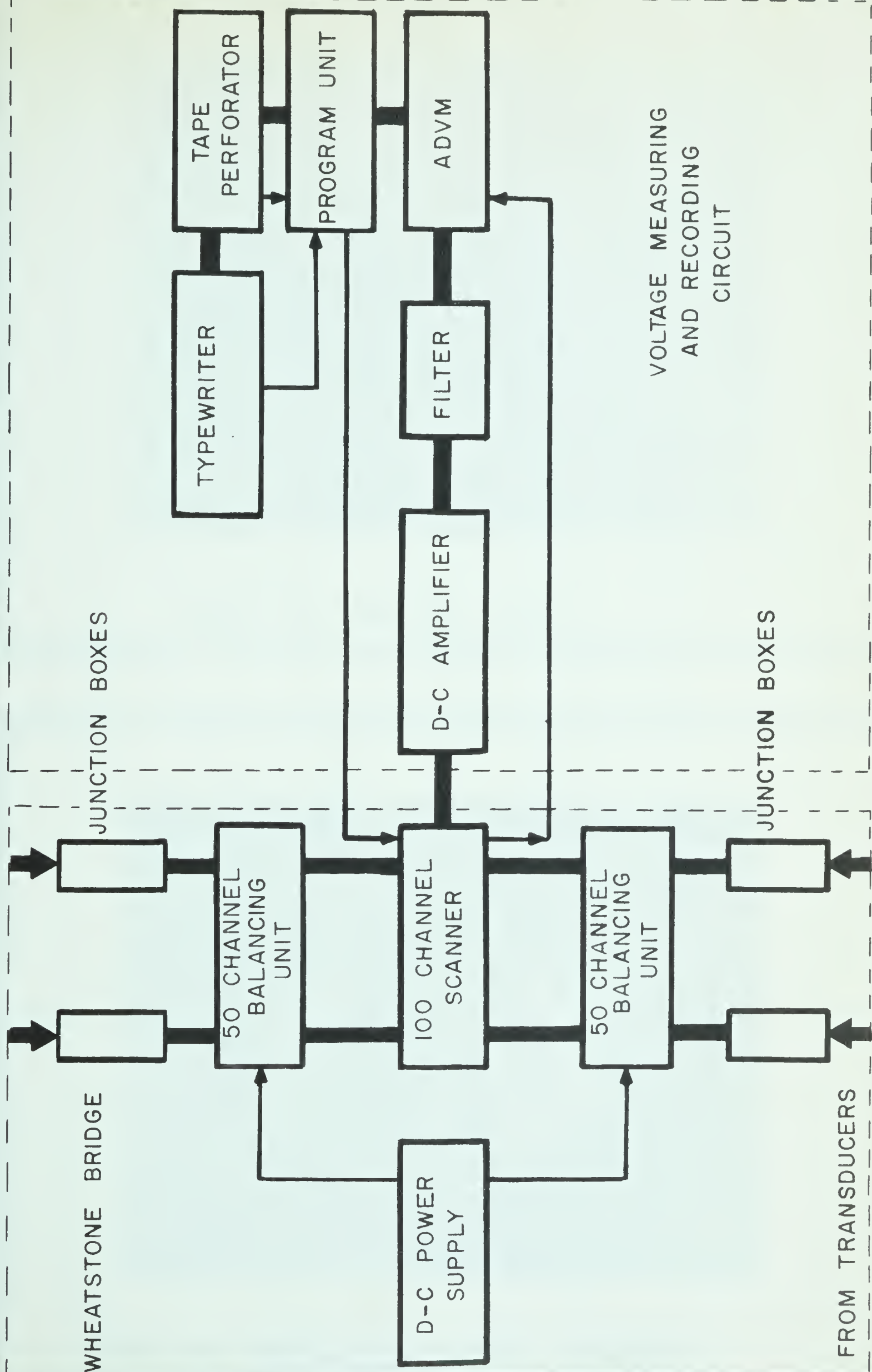


FIGURE 4.3 BLOCK DIAGRAM OF DIDAP



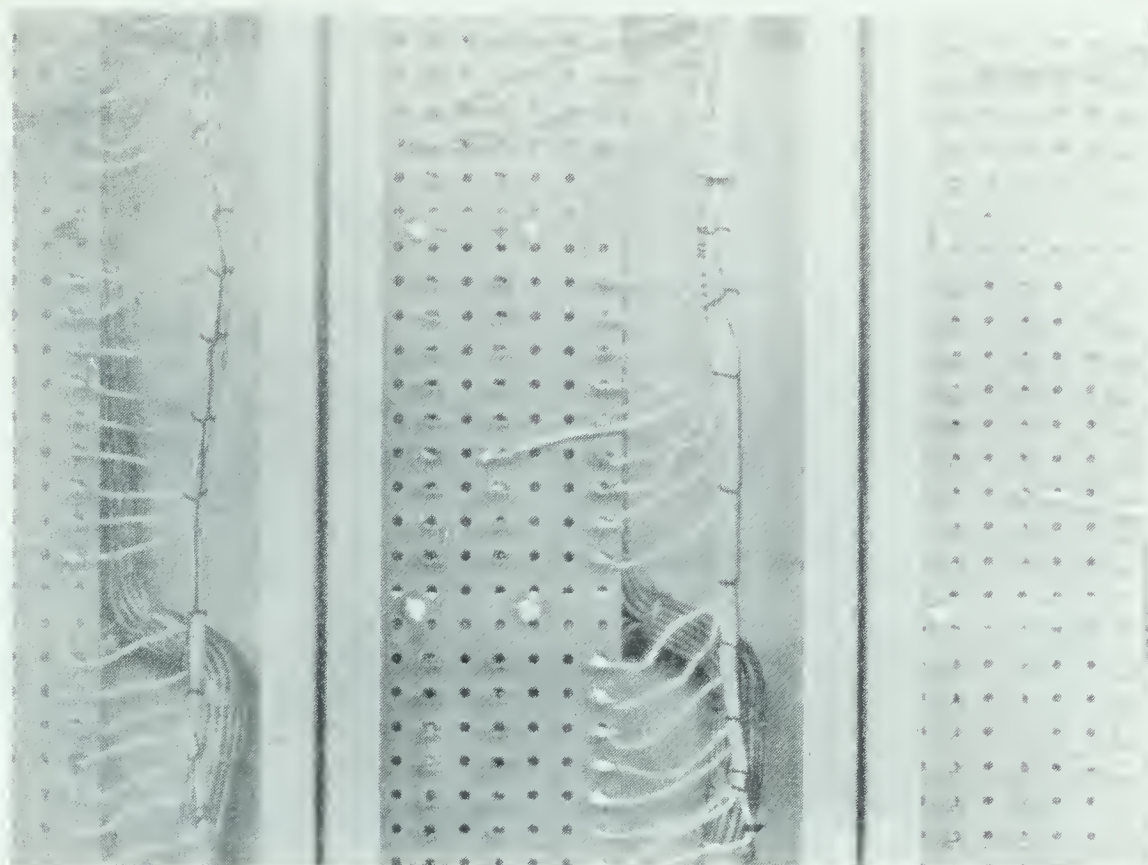


FIGURE 4.4 JUNCTION BOXES

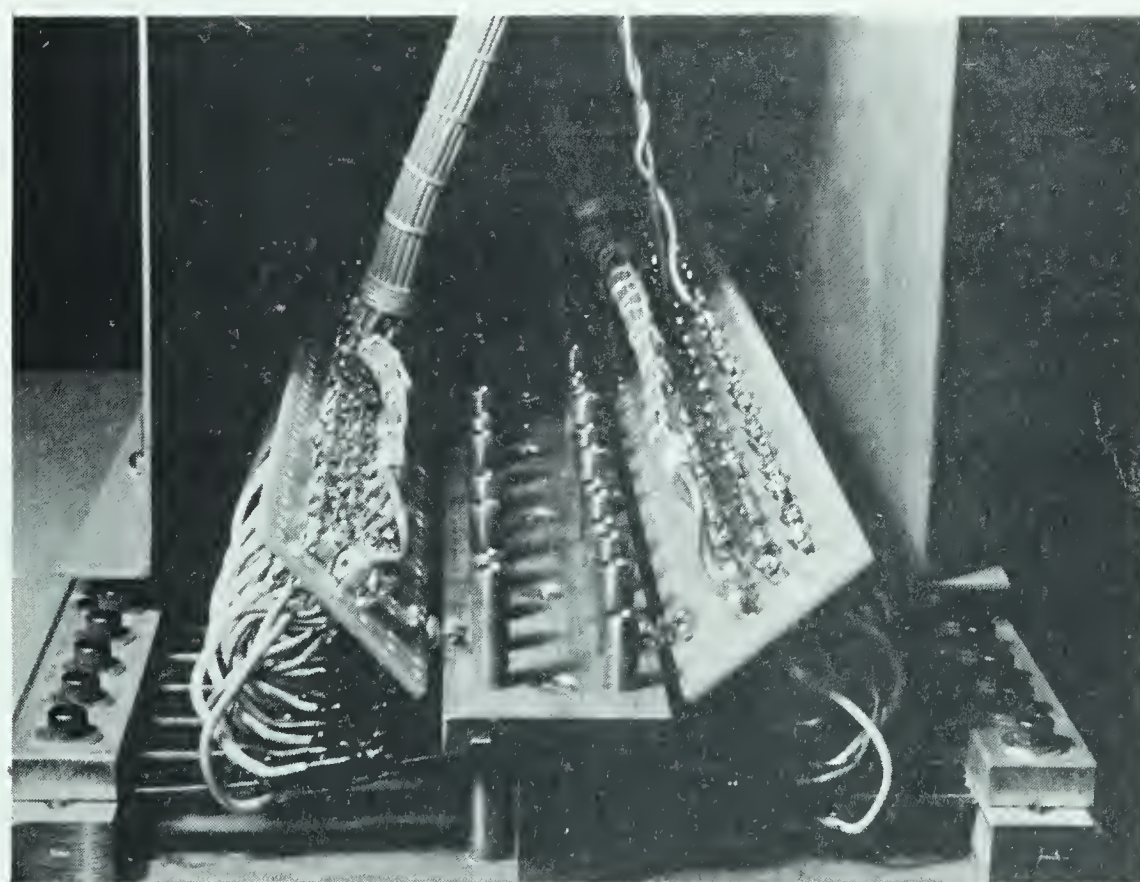
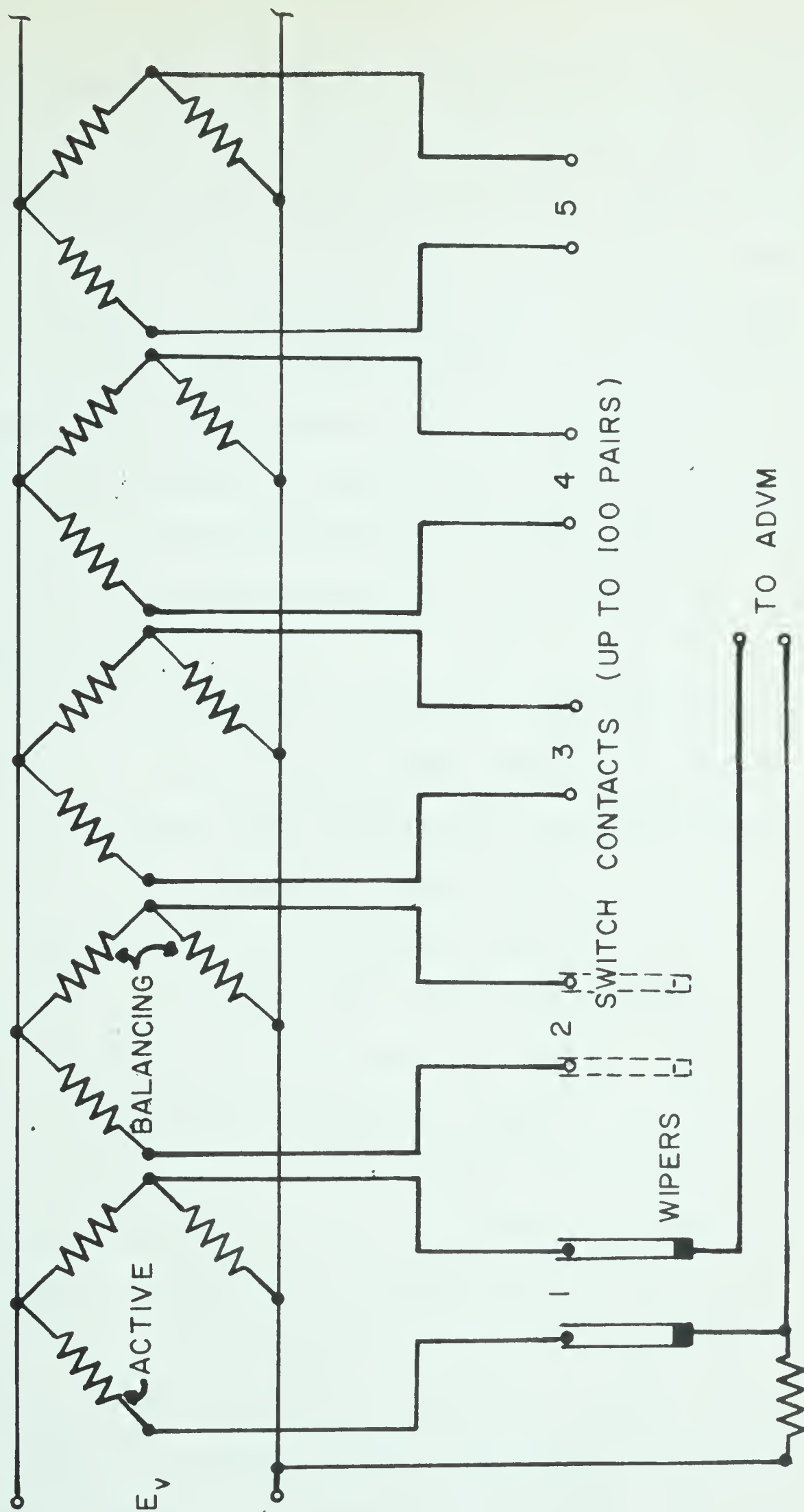


FIGURE 4.6 CANTILEVER BRIDGE ASSEMBLY







SINGLE  
COMPENSATING GAUGE

FIGURE 4.5 CIRCUIT FOR SINGLE COMPENSATING GAUGE





units. These units consist of banks of cantilever bridge assemblies in which two strain gauges are mounted on a cantilever beam, one on top and one on bottom. These two gauges ( $R_c$ ) serve as two arms of the Wheatstone bridge. The bridge can be balanced to a null condition by a suitable adjustment of the deflecting screw which imparts bending strain to the cantilever beam, thus changing the resistance of the two gauges  $R_c$ . The balancing units were built at the University of Alberta.

Power to the Wheatstone bridge is wired into the 50 channel balancing units and to the junction boxes by interconnecting wires.

The wires from the balancing units are connected to a scanning unit by means of shielded cables. The scanning unit sequentially selects one channel at a time and feeds the corresponding signal through to the amplifier.

This system uses a single amplifier to service up to 100 channels. This puts very rigid requirements on the amplifier as regards to rise and settling times. In more elaborate systems, such as that at Boeing in Seattle, an individual amplifier is used for each channel. Such systems cost about \$141,000 for 100 channels exclusive of the measuring and output equipment.

When an amplifier is used after a mechanical switching device, certain noise problems arise. To eliminate these unwanted transients the signal is passed through a filter.

After the signal leaves the filter it is measured and converted to a digital reading in the ADVN. The digital signal was then fed to the appropriate output devices via the program unit. These units are discussed in more detail in Section 4.3.



### 4.3 DESCRIPTION OF SYSTEM

#### 4.3.1 Circuit Scanner

A circuit scanner sometimes called a "multiplexer" sequentially samples, or scans, automatically a group of input channels whose voltages are to be measured by some companion equipment. The scanner used in this system was a Type 42B circuit scanner made by Telecomputing Corporation which is capable of scanning up to one hundred two-wire inputs. Commutation from one channel to another is performed by two magnetically operated switches whose contacts are gold plated to reduce contact resistance and minimize thermal effects. The automatic operation of the scanner is controlled by the program unit. The channel being measured at any instant is indicated by a neon light on the front panel.

#### 4.3.2 Amplifier

The purpose of the amplifier in this system is to accurately extend the range of the ADVM from the millivolt to the microvolt region in order that strains may be read to the nearest microinch per inch or better. The amplifier chosen for this system is an Astrodata Model TDA-875 with fixed gain steps of 50, 100, 200, 500 and 1000, with two modes of operation, differential, and floating. This amplifier has been designed specifically for fast overload recovery, high common mode rejection, and low noise and drift. These are the important features to consider when an amplifier is switched from one channel to another.





Figure 4.7 shows, in a block diagram, the amplifier to be composed of three main items; a system of electrostatic shielding, a high gain amplifier, and a d-c isolator. The electrostatic shielding is composed of a guard shield and an output shield. The purpose of the guard shield is to eliminate any coupling between the input terminals and the ground, in order that an infinite common-mode rejection might be achieved. The output shield permits the floating output to be grounded at points other than at the amplifier without introducing common mode rejection problems. The high gain amplifier operates such that the input signal after passing through an overload protection circuit reaches the junction point 1. At this point the signal is divided; the high frequency a-c component feeds through a transformer into the d-c amplifier; the remaining part of the signal is modulated, passed through an a-c amplifier, demodulated, and then fed into the d-c amplifier. After amplification a large portion of the signal is fed back to the input of the amplifier.

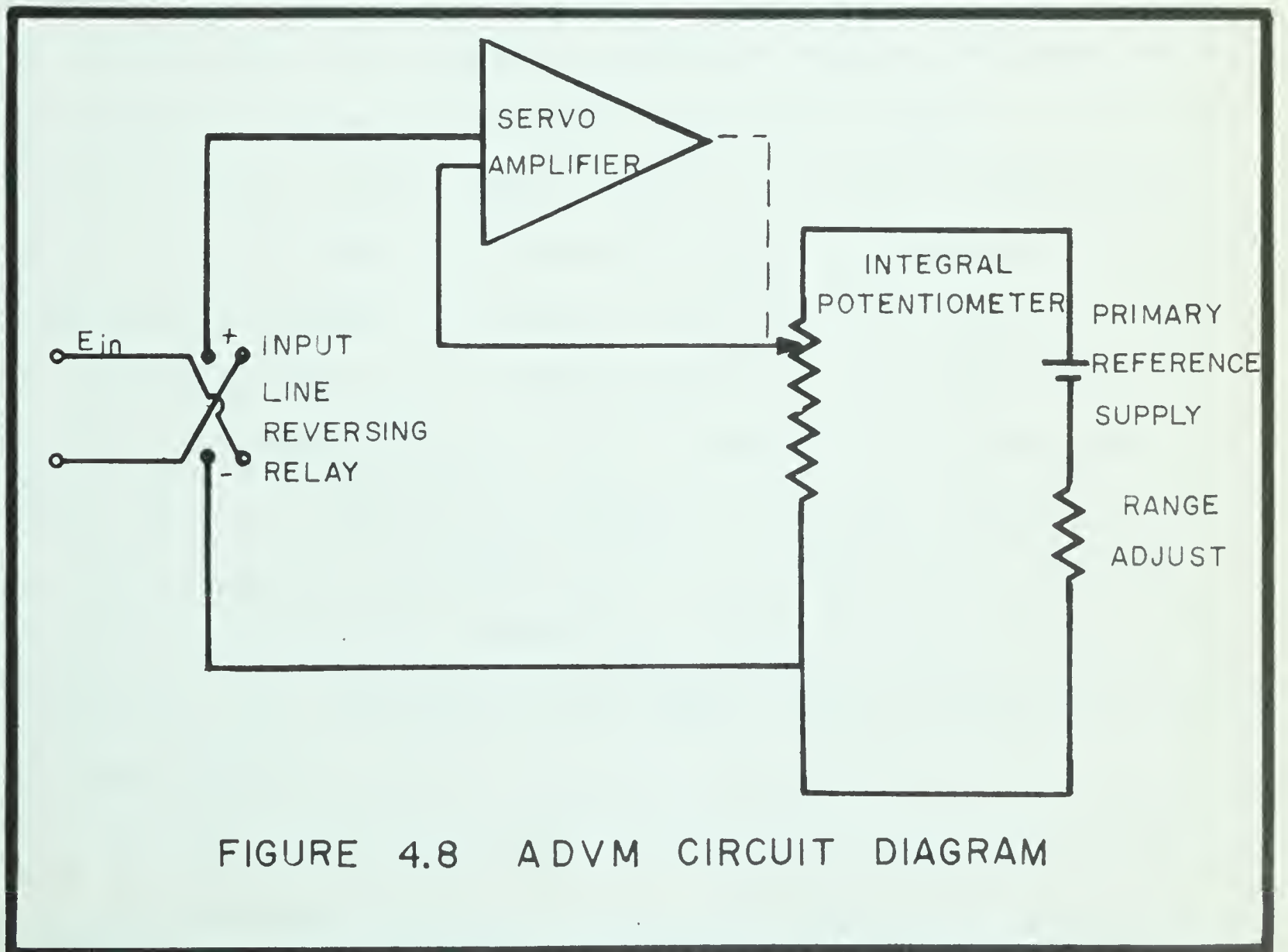
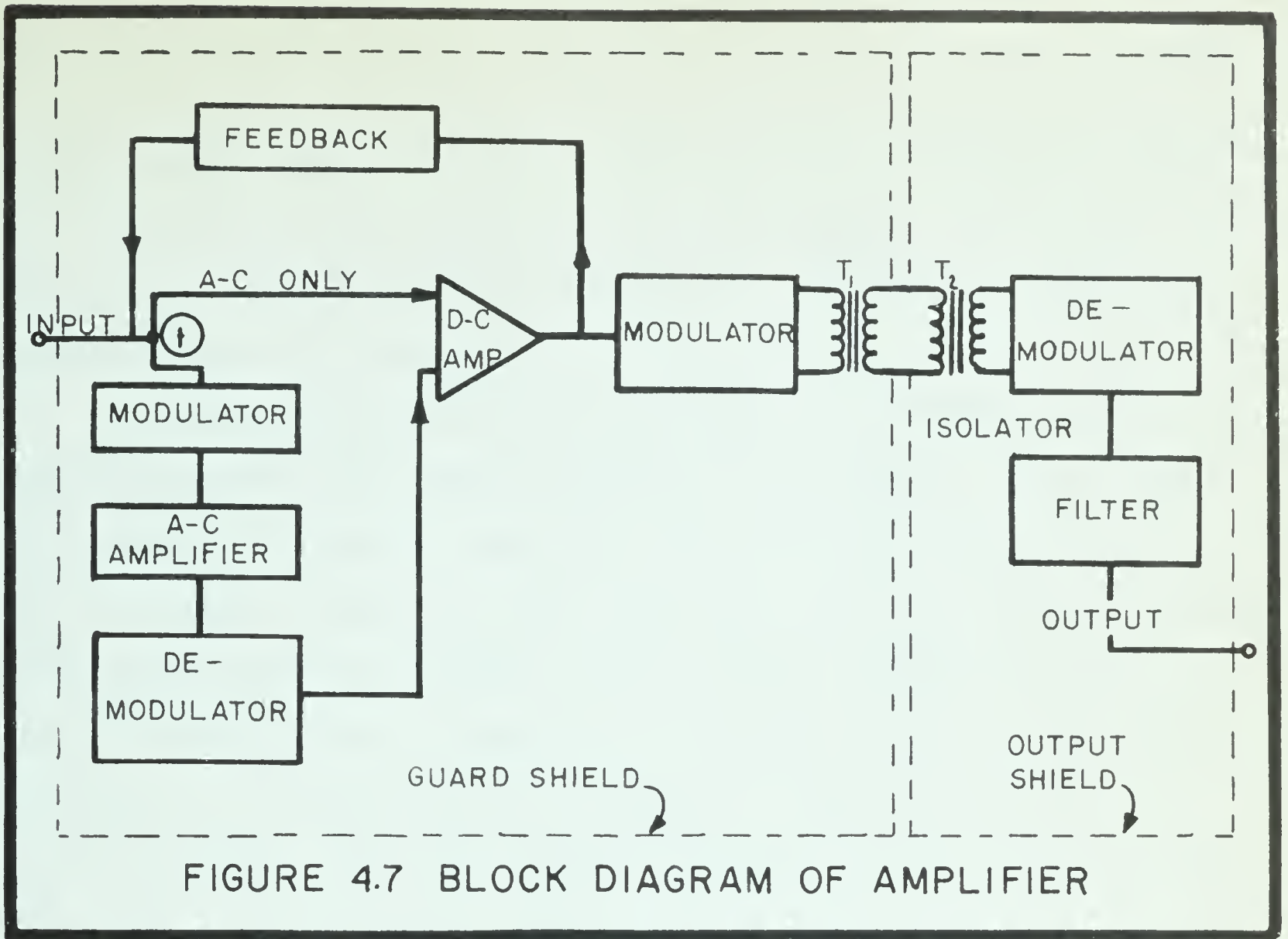
The output is isolated from the input by modulating the signal to a-c, passing it through an isolation transformer and then demodulating it. Switching transients of the isolator and the high frequency carrier wave are removed by passing the signal through a filter before reaching the output terminals.

#### 4.3.3 Analog Digital Voltmeter

The analog digital voltmeter chosen for this system is a Teleducer Type 24A made by Telecomputing Corporation. It is









a three digit ratio instrument which measures an unknown voltage by comparing it with a primary reference supply. The basic circuit of the ADVN is shown in Figure 4.8. The dotted line indicates a mechanical link.

When a channel is to be measured, the unknown signal is impressed across the input terminals of the ADVN. If the signal is negative, the input reversing relay automatically reverses; if the signal is positive the relay does nothing. The difference between the unknown voltage and the output voltage from the integral potentiometer is known as the error voltage. This error voltage is converted to an a-c signal by means of a high frequency chopper. The error signal is amplified and is then used to initiate drive control signals which advance three relay type stepping switches, to which are wired resistive elements between the gold-plated step contacts. In this way the reference voltage is varied in increments of units, tens, and hundreds. When the unknown voltage and the output voltage from the potentiometer circuit are the same, the unknown voltage is suppressed and a null condition is reached. A null is defined as the condition when the absolute value of the error voltage is less than that required to initiate changes in the stepping switch positions. After the null condition is reached an external circuit is closed allowing companion equipment such as a typewriter or tape perforator to permanently record the voltage reading. The voltage reading is also indicated on the front panel of the ADVN by means of neon lights.



#### 4.3.4 Program Unit

The program unit selected for this system is a Type 33G-2 produced by Telecomputing Corporation. It is a serial converter which changes digital signals from the ADVN and position signals from the scanner into high voltage signals arranged in a serial form (that is, arranges the information so that the outputs receive only one digit of information at a time). In addition to controlling the format and sequencing of events in the Scanner, ADVN and the outputs, the program unit also allows other pieces of data to be recorded such as time, date, test number, etc, by means of the program plug board.

The program unit consists of two cascaded stepping switches which scan the input circuits and, via the program plug board, connect them to the appropriate circuits in the outputs. All sequencing and automatic operations are controlled by an interlocking relay system contained in the program unit. In addition to controlling the typewriter and tape perforator the program unit is wired to operate an IBM card punch. This feature has not been used in this sytem.

#### 4.3.5 Paper Tape Punch

The motorized tape perforator selected for this system is a Type 236B made by Telecomputing Corporation. It has been designed to be compatible with the six-channel code used on the Royal McBee LGP-30 computer. This has the advantage that if the data requires subsequent numerical calculation, recordings taken from a test can be fed directly into the computer with no intermediate operator steps.







#### 4.3.6 Typewriter

As an additional output a standard IBM electric typewriter was modified by the Telecomputing Corporation to enable readings from the ADVDM to be printed in several vertical columns or horizontal rows. The typewriter can operate alone or simultaneously with the tape perforator.

#### 4.3.7 Combined Operation

To illustrate the combined operation of all units, consider the plug board of the program unit wired as in Figure 4.9. Let it be desired to read out the channel number, actuate two typewriter spaces, read out the sign, and the three digit number from the ADVDM. The sequence of events is such that after the start button is pressed the program stepping switch is advanced from its "off position" to the first hub of the program output while at the same time the ADVDM balances. This initiates the selector input to scan row II of the plug board. In so doing the scanner channel number is printed out, two spaces are actuated on the typewriter, and the selector stepping switch is homed to its starting position. Each typewriter operation is controlled by interlocking relays so that the selector stepping switch does not advance to the next command until the previous operation is complete. Homing the selector stepping switch also advances the program stepping switch to the second hub of the program output. Now the selector input scans row I of the plug board and the selector stepping switch reads out the sign followed by the three digit number previously balanced by the ADVDM.



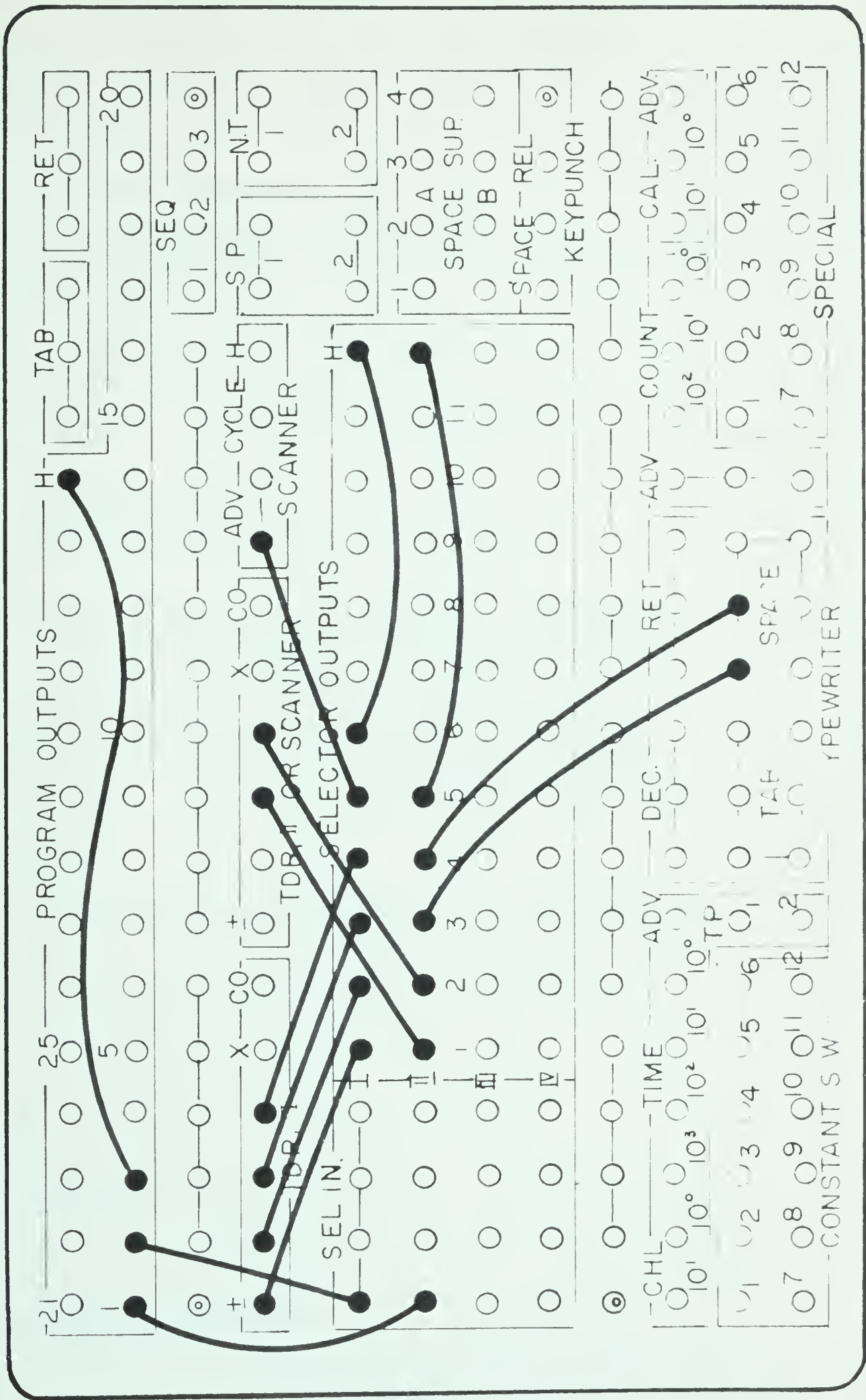


FIGURE 4.9 PROGRAM SEQUENCE SELECTOR BOARD



The fifth exit of row I advances the scanner to the next channel and resets the ADVN. The sixth exit homes the selector stepping switch and advances the program output to hub three which in turn is homed to hub one. The whole sequence of operations is repeated until all channels have been scanned and recorded. The stop signal comes from the scanner when the last channel has been recorded.

#### 4.4 SENSITIVITY

The sensitivity, sometimes referred to as "dead band", of any measuring instrument is defined as the total range through which the input voltage can be varied without changing the reading at the output. Another term commonly used for sensitivity is resolution.

The maximum sensitivity of the ADVN is 10  $\mu$ v per digit. This is also the maximum sensitivity of the entire system.

#### 4.5 NOISE

##### 4.5.1 General Remarks

Noise can be defined as any unwanted transient which is introduced into the signal coming from the transducer. To obtain







consistent readings, this noise must be reduced to a level less than the maximum sensitivity of the ADVM. Noise may be reduced by adequate shielding and proper grounding of all signal lines, utilizing the common mode rejection of the amplifier, and placing a filter at the input of the ADVM.

Generally, noise is of two types; spurious and inherent. Spurious noise is that which enters the signal lines from nearby fluorescent fixtures, high voltage cabinets, electromagnets and transformers. Inherent noise is introduced into the system by the components themselves.

#### 4.5.2 Inherent Noise

The TDA-815 amplifier, in the differential mode, has a noise level of  $5\text{ }\mu\text{v rms}$ \* referred to the input plus  $150\text{ }\mu\text{v rms}$  referred to the output taken over a bandwidth of 0.05 cps to 5 kc. The noise at the output, for a gain of 200, becomes  $1150\text{ }\mu\text{v rms}$  and attenuating 10:1 this becomes  $115\text{ }\mu\text{v rms}$  fed to the ADVM.

The power supply has a total hum and noise of  $50\text{ }\mu\text{v rms}$ . However, the amount of noise reaching the transducers is reduced to a negligible amount because of the "voltage divider" in the Wheatstone bridge.

Therefore, the noise of the amplifier is the greatest cause for concern and can be taken as the noise figure for the entire system.

---

\* For a sine curve, rms is 0.707 times the peak value.



### 4.5.3 Noise Filter

The purpose of this filter is to by-pass or suppress any a-c components in a signal, allowing only the d-c voltage to reach the ADVN. This can be accomplished with a  $\pi$ -section filter. By trial and error a combination of three  $\pi$ -sections was found to reduce the noise level to less than 10  $\mu$ v. The circuit for this filter is shown in Figure 4.10. The reason for the 1000 and 100 ohm resistors\* is that the amplifier works best with a load of 1000 ohms while the ADVN works best when connected to a low resistance of around 100 ohms. If these resistances are not in circuit, or of different values, the linearity of the amplifier is drastically changed.

The amplifier rise and overload recovery times are increased and the bandwidth is decreased with the addition of a filter to the circuit. The reduced bandwidth is of no concern in the strain gauge work of this thesis. However, the rise time and overload recovery times are increased from 1 millisecond to 15 milliseconds.

### 4.5.4 Common Mode Rejection

Common mode rejection (CMR) is the ability of an amplifier to distinguish between a differential signal and a common mode signal. A common mode signal is that voltage present in a signal line which does not contain any worthwhile information. For example, if the low side of the signal line is at a potential

---

\* These resistors attenuate the signal in the ratio 10:1.



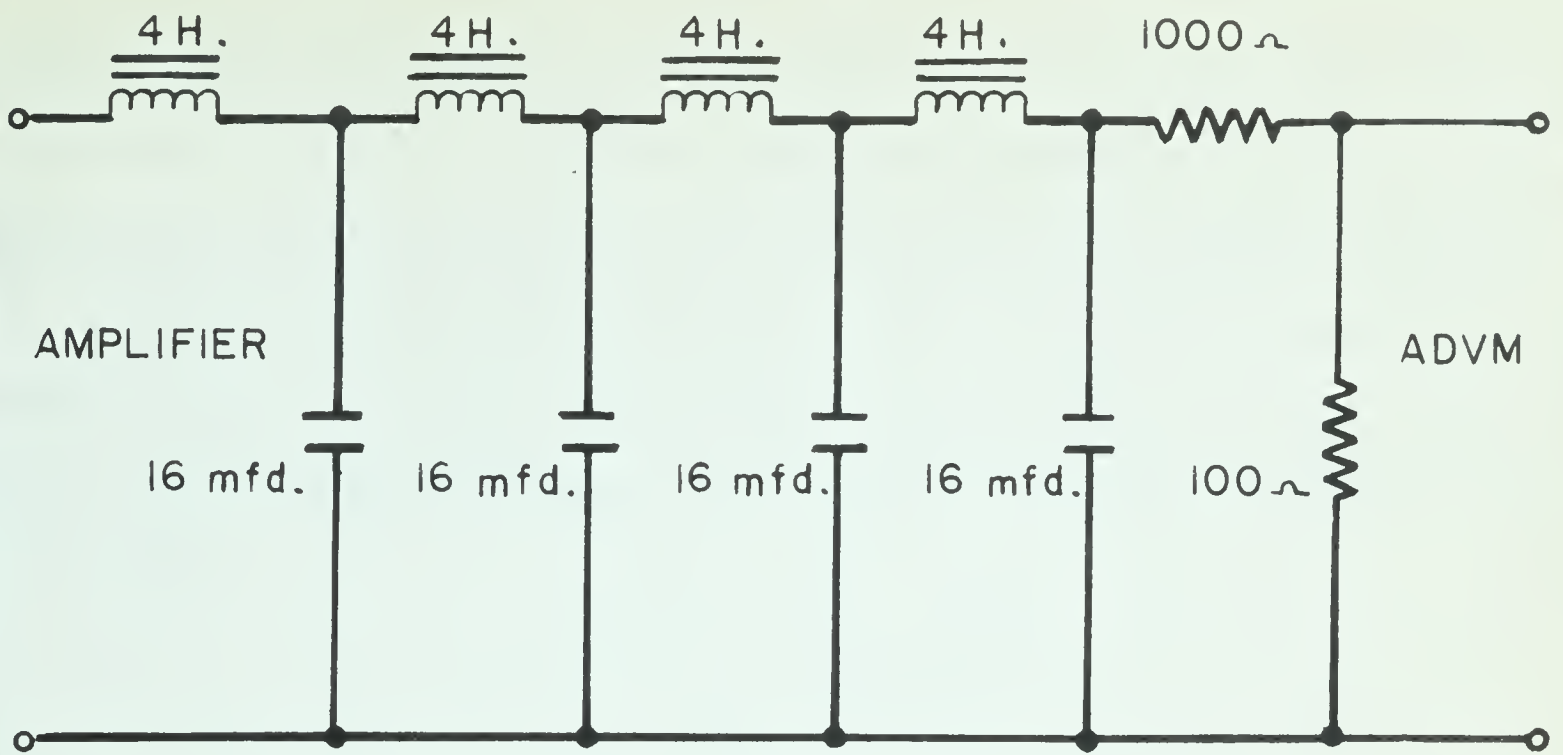


FIGURE 4.10 NOISE FILTER

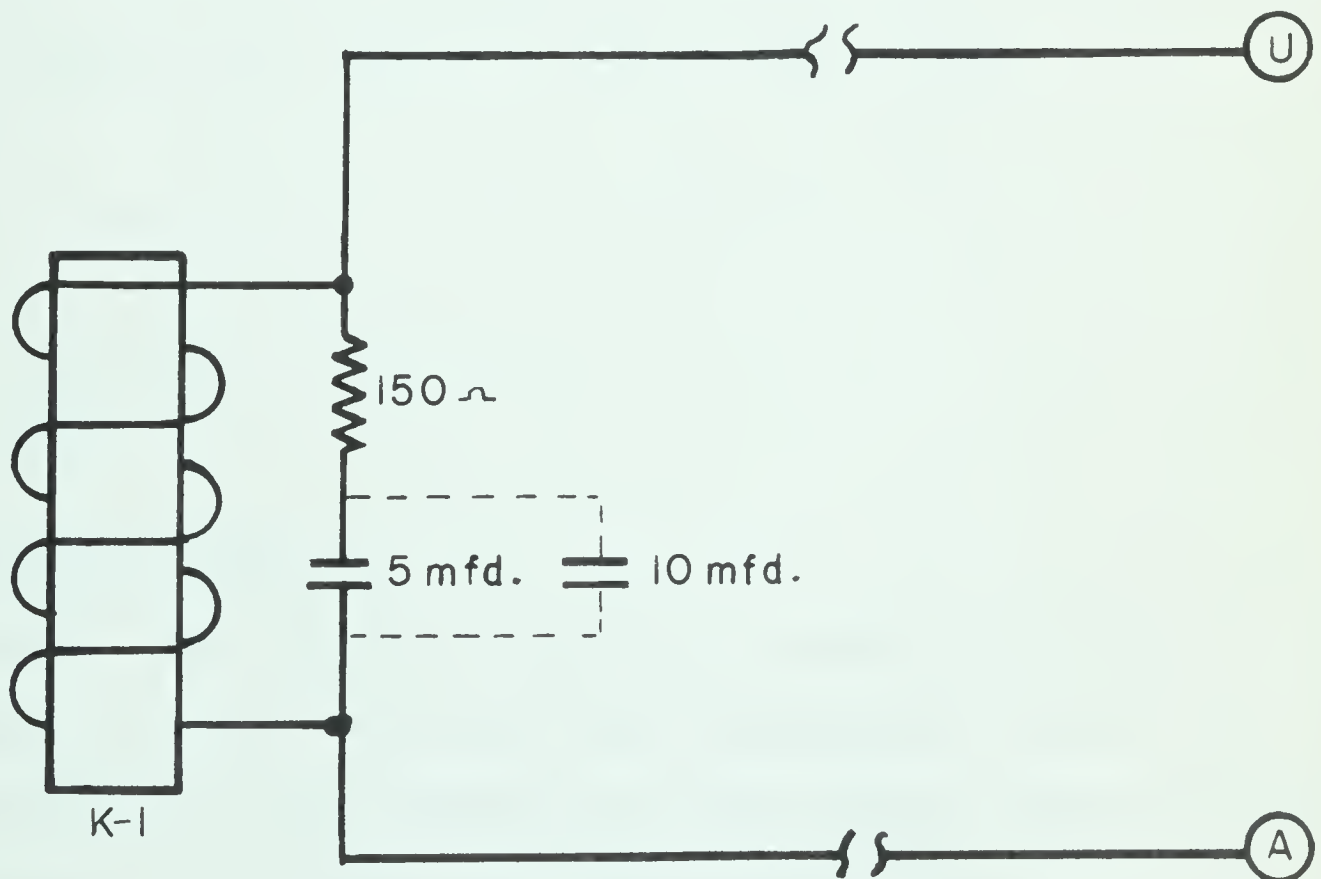


FIGURE 4.11 MODIFICATION TO SCANNER





10.0 v, the high side at 10.5 v, then the worthwhile part of this signal is 0.5 v, and the common mode signal is 10.0 v. An amplifier which has a high CMR can reject this unwanted signal.

The TDA-875 amplifier has a CMR of 140 db at d-c for a line unbalance of 1000 ohms. For line unbalances of less than 1000 ohms the CMR is better. It follows from the definition of noise that

$$\text{db} = 20 \log_{10} \frac{V_{\text{in}}}{V_{\text{o}}}$$

where,  $V_{\text{in}}$  = input voltage to the amplifier.  
 $V_{\text{o}}$  = output voltage from the amplifier.

Thus, for 140 db, the ratio becomes

$$\frac{V_{\text{o}}}{V_{\text{in}}} = 10^{-7},$$

which says that any noise impressed on the input signal lines will be reduced by a factor of  $10^7$  at the output.

## 4.6 DRIFT

### 4.6.1 General Remarks

Zero point drift is a problem usually encountered in the measurement of small voltages from transducers. Drift can occur in any component which "conditions" the signal, beginning with the transducer and ending with the readout device.



#### 4.6.2 Sources of Drift

The transducer, or strain gauge as used in this thesis, can be one of the largest contributors to drift. An improperly mounted and connected strain gauge can result in a low resistance between the strain gauge and the specimen ground. This results in zero point drift. The manufacturers of strain gauges recommend a minimum resistance of 100 megohms between the gauge and ground.

The power supply is a source of drift. The output voltage, of Model T3610-R used in this system, will remain constant over an eight hour period of continuous operation to within  $\pm 0.01$  percent or  $\pm 1$  mv, whichever is greater. This is based on a constant ambient temperature. If the ambient temperature changes 1.0 C then the output voltage will vary  $\pm 0.01$  percent or  $\pm 1$  mv, whichever is greater. For example, if the output voltage is 2 v and the ambient temperature changes 10.0 C then the total drift will be  $\pm 11$  mv. It was shown in Section 4.2.1 that the "voltage divider" of the Wheatstone bridge is in the ratio 2000:1 for a measured strain of 1000  $\mu$ in. per in. Therefore, if the power supply drifted  $\pm 11$  mv the output signal from the strain gauge would only drift by  $\pm 5$   $\mu$ v, which is less than the maximum sensitivity of the ADVM. Therefore drift of the power supply is negligible.

The ADVM measures the ratio of resistances and not their absolute values\*. Although it is a very stable instrument, it

---

\* The ratio of two resistances is more stable than their absolute values over long time intervals.



is subject to drift, because it uses a mercury battery as its primary reference supply. The voltage of this battery is 1.3 v and, according to the manufacturer, will not change more than 0.1 percent per week. The battery voltage also changes with changing ambient temperature but the effect of this is eliminated by placing a compensating resistor in series with the battery. The temperature - resistance characteristic of this resistor is such that a constant current drain is maintained on the battery for all ranges of the instrument. The effects of battery drain are eliminated by calibrating the instrument each day. Any change in the reference supply can be compensated by a suitable adjustment of the "Range Adjust" control on the ADVN. If, however, a test were run continuously for one week then the reference supply could drift by 0.1 percent. This would result in only one digit change in the output of the ADVN. Therefore, drift of the ADVN is negligible.

The TDA-875 amplifier is the greatest source of drift in the entire system. It has a maximum drift over a forty hour period of  $\pm 2 \mu\text{v}$  referred to the input plus  $\pm 0.01$  percent of full scale at 25 C. For example, if the gain is 200, full scale input is 50 mv, the drift will be  $\pm 1400 \mu\text{v}$  referred to the output. This drift is attenuated 10:1 in the filter. The resulting drift reaching the ADVN is  $\pm 140 \mu\text{v}$  over a forty hour period. A change in ambient temperature of 5 C can increase the limits of drift to  $\pm 160 \mu\text{v}$ . If the ADVN is set on its lowest range (that is, maximum sensitivity of 10  $\mu\text{v}$  per digit) the drift is  $\pm 16$  digits.







It is concluded from the foregoing that the forty hour drift of the digital processor excluding transducers, is within  $\pm 17$  digits when the ADVN is in its most sensitive range. Since the manufacturers prefer to quote drift limits over forty hours the apparatus was checked for drift by experiment over shorter periods of time as discussed below.

#### 4.6.3 Drift Measurements

In order to check the drift of the system a number of tests were conducted with the input terminals of the amplifier shorted. This checked the total drift of the amplifier, filter, and ADVN. It did not include the power supply or the effects of variation in contact resistance in the scanner. The results of these tests indicate that, after a two hour warmup recommended by the amplifier manufacturer, the maximum drift of the system is within  $\pm 20 \mu\text{v}$  or  $\pm 2$  digits over a six hour test period. Expressed in terms of full scale reading of 1000 digits this is a drift of 0.2 percent full scale.

### 4.7 ACCURACY

#### 4.7.1 General Remarks

The accuracy of an instrument is usually defined in terms of a percentage of full scale reading. This refers to the full scale range in use, meaning the error is a fixed value



over a particular range. An error of 0.1 percent of full scale in use is an error of 0.001 v for any reading on the 1.0 v range, 0.00001 v for any reading on the 0.01 v range. Expressed another way, if full scale is represented by 1000 digits and the accuracy is 0.1 percent full scale and a reading of 10 digits is recorded, then the error in this reading is 1 in 10 or 10 percent.

Sometimes accuracy is expressed as a percentage of reading indicating the magnitude of the error is governed by the value of the measurement. An error of 0.1 percent of reading indicates an error of 0.001 v in a 1.0 v measurement and 0.0001 v in a 0.1 v measurement.

#### 4.7.2 Accuracy of DIDAP

The accuracy of the system described herein is affected by the ADVM and the amplifier. The ADVM has an accuracy of 0.1 percent full scale. The accuracy of the amplifier is derived from four sources; gain accuracy, which is  $\pm 0.1$  percent full scale; linearity which is  $\pm 0.1$  percent full scale; gain stability which is  $\pm 0.1$  percent full scale; drift, which is  $\pm 0.2$  percent full scale. Gain accuracy is not important in this system because the system is calibrated at the ADVM, after the signal has passed through the amplifier. Gain stability is important. Adding the units together, the accuracy of DIDAP is  $\pm 0.6$  percent full scale, or  $\pm 6$  digits as read out from the ADVM on its most sensitive range.



## 4.8 CALIBRATION

### 4.8.1 General Remarks

To calibrate any d-c measuring instrument the most obvious method would be to use an accurate, variable voltage power supply, or use an accurate voltage source in conjunction with a precision voltage divider. In strain gauge work it is more convenient to check accuracy and linearity by shunting a suitable resistor across one arm of the Wheatstone bridge. This will not only check linearity and accuracy but will also serve to calibrate the ADVN to read strain directly in micro-inches per inch. Furthermore, if the shunt resistance is placed across an active gauge the equipment plus the lead-in wires can be calibrated together.

### 4.8.2 From Microvolts to Microinches per Inch

The relationship between the change in resistance and the change in gauge length has been shown to be

$$k = \frac{\delta R/R}{\delta L/L} ,$$

where  $k$  is the gauge factor of the strain gauge. Let the resistance of the unstrained gauge be  $R_g$  and let  $R_s$  be a suitable shunt resistance. When  $R_s$  is shunted across  $R_g$  the change in resistance is

$$\delta R = R_g - R$$

where

$$\frac{1}{R} = \frac{1}{R_g} + \frac{1}{R_s}$$







therefore,

$$\frac{\delta R}{R_g} = 1 - \frac{R_s}{R_g + R_s} \cdot$$

But

$$e = \frac{\delta L}{L} = \frac{\delta R}{k R_g}$$

and finally,

$$e = \frac{R_g}{k(R_g + R_s)}$$

Using this formula a table of apparent strains can be obtained for various values of shunt resistance. The procedure for calibration and checking linearity of the system is as follows;

1. Select an input channel and balance to a null position by adjusting the appropriate cantilever bridge.
2. Shunt across the active gauge of this balanced channel a resistance which will give an apparent strain of three digits using the above formula.
3. Adjust the amplifier gain so that sufficient signal reaches the ADVM to enable a three digit number to be read.
4. Adjust the "Range Selector" and the "Range Adjust" of the ADVM so that the three digit number which is displayed is the apparent strain value as calculated from the above formula.
5. Select another shunt resistance and without adjusting any of the controls press the "Readout" of the ADVM. This should give the value of the strain as calculated.

The entire range of strain values from 001 to 999  $\mu\text{in per in.}$  can be checked for linearity by varying the shunt resistance. It is very important that the Wheatstone bridge is balanced to zero before calibration and linearity checks are made.



## 4.9 SPEED OF OPERATION

### 4.9.1 General Remarks

In scanning, balancing, and recording data from a multi channel system it is important that the entire operation be completed as quickly as possible to minimize time temperature effects. Also, if many channels are to be analyzed many times in a single day then clearly there is a definite saving when fifteen tests can be run per day instead of say ten.

Although it is desirable to operate the system at its optimum rate there are a few factors which require careful consideration. Since DIDAP is an assembly of six different pieces of inter-connected electrical equipment, each having its own optimum operating speed, the maximum speed of the overall system can be no faster than that of the slowest component.

### 4.9.2 Output Speeds

Of the two outputs the tape perforator is faster than the typewriter. The maximum speed of the perforator can be as high as 30 characters per second. The speed can be varied by changing the diameter of the drive pulley. The drive pulley used in this system allows a maximum speed of 10 characters per second. The fastest speed of the typewriter as wired by Telecomputing is 5 characters per second. Therefore, the tape perforator has been slowed down to operate at the speed of the typewriter when both outputs are in operation simultaneously. When operating alone the speed of the tape perforator is 6.6 characters per second.





#### 4.9.3 Speed of ADV M

The speed of the ADV M is approximately 800 milliseconds from initiation of the reset condition to final readout. This speed will be less than this if the voltage to be measured only requires a few movements of the stepping switches. After reset the first relay to be energized is the one which senses whether the incoming signal is positive or negative, and if it is negative it fires the negative control thyatron of the balancing circuit. It takes just 10 milliseconds to decide if the signal is positive or negative and a further 10 milliseconds to fire the negative thyatron after which the unknown input signal is balanced. This balancing operation may require anywhere from 40 to 750 milliseconds.

#### 4.9.4 Amplifier Speed

Two characteristic speeds are important in the operation of an amplifier; overload recovery time and settling time. As stated in Section 4.5.3, the addition of a filter in the circuit increases the overload recovery and settling times to 15 milliseconds.

#### 4.9.5 Modifications and Operating Speed of System

From what has been said above it is clear that the ADV M begins to balance out before the amplifier has time to recover from overload or settle down. Either the ADV M had to be slowed down or the settling time of the amplifier interlocked with the operation of the ADV M. Of the two choices the first is the least expensive and was the course followed here.





It will be remembered from Section 4.9.3 that after a channel has been switched there is only a minimum 10 millisecond delay before balancing is initiated in the ADVN. It is required that this delay be increased to 15 milliseconds.

Figure 4.11 shows the relay K-1 of the scanner which is the start readout relay control of the ADVN. Assuming the delay circuit of K-1 causes a delay of 10 milliseconds then the equivalent resistance of K-1 is 2000 ohms. A 10  $\mu$ f capacitor was placed in parallel with the existing capacitor. This increased the delay of this network to approximately 30 milliseconds allowing sufficient time for settling of the amplifier.

On the ADVN there is a delay adjustment connected with the balancing stepping switches. This delay controls the rate at which each stepper switch advances to its next position. This delay control was set in its maximum position (fully clockwise).

The above modifications decrease the scanning speed of the overall system from an optimum of one hundred channels per minute to about 30 channels per minute.

## 4.10 DISCUSSION OF SYSTEM

### 4.10.1 General Remarks

The discussion of the overall apparatus will be limited to the advantages and disadvantages of this system versus similar



automatic systems; it being assumed that there is unanimous agreement on the superiority of an automatic digital system to that of a conventional manual recorder.

#### 4.10.2 Advantages

One of the greatest advantages in the system discussed in this chapter and shown in Figure 4.12 is the relatively low cost compared with comparable commercial systems. It has been mentioned that when an individual amplifier and individual power supply is used for each channel the cost is about \$141,000 per 100 channels. To this must be added the cost of the scanning, analog-digital converter, and recording equipment, which can be anywhere between \$10,000 and \$50,000. Other systems using a common bridge supply and amplifier system can be obtained for about \$25,000 to \$30,000 for 100 channels. These units employ a point plotter as the final output. If a printed or punch format is required then these figures will be increased. The basic costs of the system built in Mechanical Engineering is \$15,700. This includes a punch tape and typewriter output and 200 zero balance units. This figure does not include the cost of labour in assembling the zero balance unit. On the basis of the above, it is of considerable economical advantage to build up a system one piece at a time as was done here.

Another advantage of this system is that it is very versatile. The output can be either on a typewriter, perforated tape, or key punch. Also, through the program board, a variety of information can be recorded along with the reading from the ADVN.





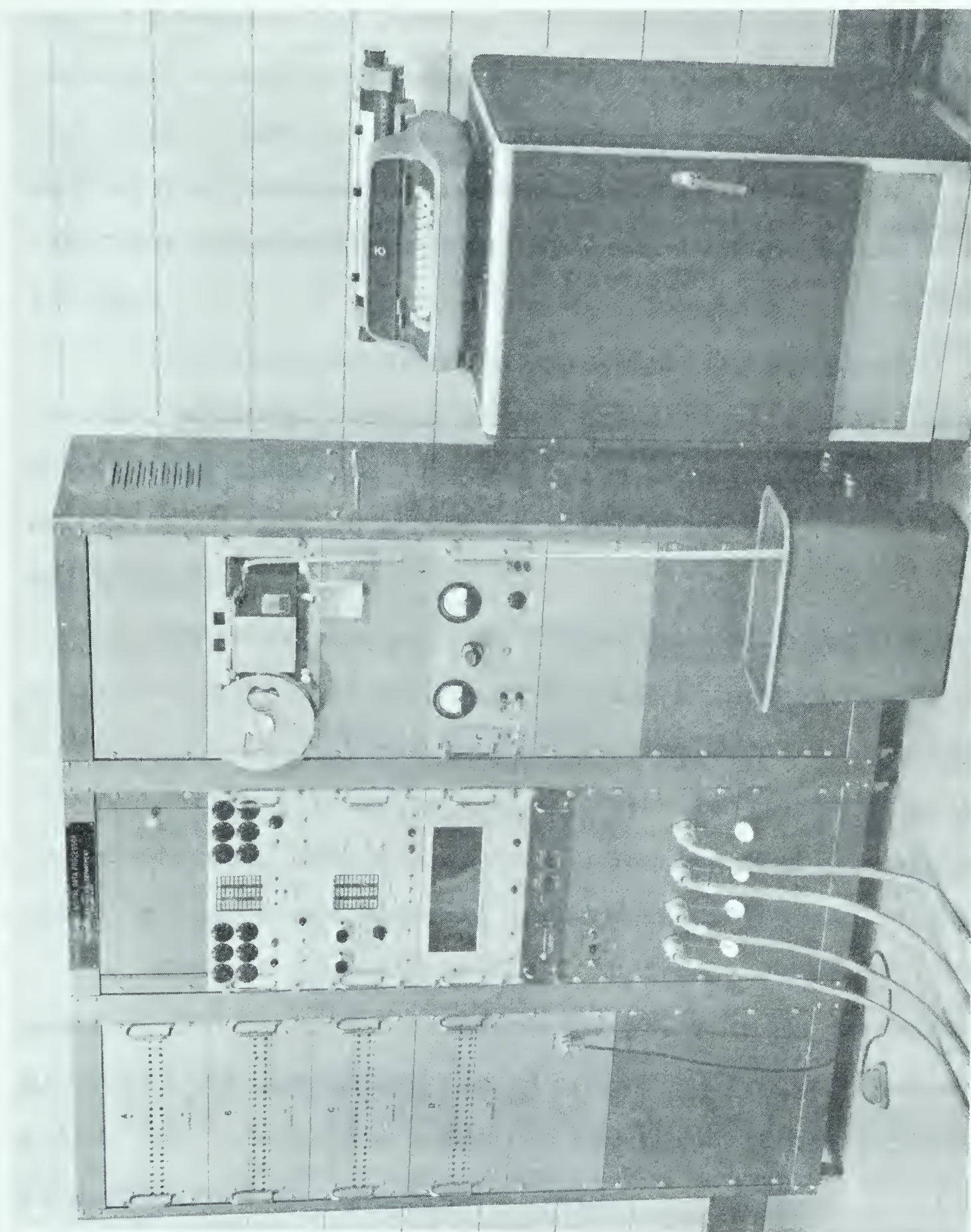


FIGURE 4.12 DIDAP





#### 4.10.3 Disadvantages

In Section 4.7.2 the accuracy of the system was found to be  $\pm 0.6$  percent full scale. For low level strain readings this accuracy is not good enough; a 0.01 percent accuracy being more desirable. However, this compares favorably with the 0.75 percent system produced by Baldwin-Lima-Hamilton and the 2.0 percent system produced by Budd Instruments; both of which are over \$25,000.

The scanning speed of approximately one channel per two seconds, although fast by manual standards, is slow compared to some of the commercial systems using complete solid state circuitry which scan at a rate of between 300 and 30,000 channels per second.

For measuring strains to the nearest microinch per inch it is very difficult to adjust the balancing bridges to achieve a complete null. It was found that a null could be obtained only to within  $\pm 2$  digits. Also, there is considerable interference between channels so that balancing must be repeated three or four times before a reasonable "zero" can be obtained.

Since the system is built up from a number of components manufactured by different companies there is no guarantee issued. Of course the guarantees issued on the individual components are valid; but it would be a decided advantage if one supplier could be responsible for the entire system.

The ADVN chosen for this system has a three digit read-out. If strains are to be measured up to 9999  $\mu\text{in. per in.}$  then they can be read only to the nearest 10  $\mu\text{in. per in.}$  And if



measurements up to 99,999  $\mu\text{in.}$  per in. are required then they may be read only to the nearest 100  $\mu\text{in.}$  per in. To remedy this a four or five digit ADVMM is required.

It should be pointed out that when this project was initiated in 1960 there were very few ADVMM's on the market and of these, although unknown to the author at that time, only a few had a four or five digit readout. Yet today, two and one half years later, there are many four, five and even six digit ADVMMs available and at prices comparable to the three digit ADVMM of a few years ago. Such is the speed of advancement of the electronic industry.

#### 4.10.4 Summary

Most of the criticism raised against this system can only be corrected by substituting higher priced components, thus eliminating one of its main advantages. Also the disadvantage of buying from several suppliers is overcome by the advantage of being able to build up the system a piece at a time. Therefore, it is believed, the advantages outweigh the disadvantages of the system as built by the Mechanical Engineering Department.

#### 4.10.5 Recommendations

The cantilever bridge assemblies as designed by the National Aeronautical Establishment are excellent if built for a null to within  $\pm 5 \mu\text{in.}$  per in. If a null to within  $\pm 0.5 \mu\text{in.}$  per in. is desired it is recommended that high resistance single turn potentiometers be shunted across the two gauges on the



cantilever thus giving an additional control for "fine" balance. This will of course increase the costs.

In order to prevent interference between channels, the cantilever supports should be constructed from heavier sections and not cascaded in groups of five (which was done at U. of A. to reduce costs) but built individually so that the mechanical action of one bridge does not affect the balance of the neighbouring channels.

It is interesting to note that the National Aeronautical Establishment were aware of the inadequacies of balance control and interference. For the former they recommended a finer screw adjustment on the cantilever. This was carried out by using 64 threads per inch on the screw adjustment. As for the problem of interference it must be admitted that not much thought was given to this, and indeed, was not experienced until it was desired to measure strains to the nearest  $1 \mu\text{in.}$  per in.







## CHAPTER V

### CONCLUDING REMARKS

This chapter summarizes the results of the thesis. Some recommendations are made for the improvement of the experimental method. The practical applications of the results are shown in an example problem and some additional problems are suggested as a possible extension of the work in this thesis.

#### 5.1 SUMMARY

In Chapter I the history of the problem of transverse deflections of plates is given. It is shown that Lamb's theoretical solution (1891) satisfies both beam and plate behaviour and probably is the exact solution to the problem. The experimental method of Chapter II and the results of Chapter III show that the theory of Lamb is valid for  $b^2/Rd$  ratios up to 55. It is reasonable to expect that the theory is valid for all  $b^2/Rd$  ratios up to infinity.

It is also shown by experiment that the transverse deflections are unaffected by the supports and loading conditions for an equivalent span to width ratio of  $1/3$ .

The experimental results discussed in the preceding chapters give a good illustration of what can be accomplished when a digital computer is linked with an automatic digital



recording system. Certainly, work of this kind was not possible ten years ago but is quite common in experimental analysis laboratories today. The problem also illustrates how numerical analysis and computer operation must be kept in mind at all times even when doing such practical tasks as locating strain gauges.

## 5.2 IMPROVEMENTS AND RECOMMENDATIONS

Any discrepancies between Lamb's theory and experiment are probably due to experimental error and initial imperfections in the plate. As noted in Chapter III disagreement between theory and experiment is more pronounced at low  $b^2/Rd$  values. It is suggested that greater accuracy at low  $b^2/Rd$  values could be obtained, using the present measuring equipment, if a narrower plate were chosen. In connection with some previous work<sup>29</sup>, good agreement between experiment and theory was obtained for a  $b^2/Rd$  value of 0.65 with a plate size of 0.125 x 10.0 x 72 in.

Larger  $b^2/Rd$  values are possible only if the test frame is modified. For the test which produced a  $b^2/Rd$  ratio of 55, the plate touched the floor at the ends as illustrated in Figure 4.12. Relative to the ends of the plate there was a center deflection of 32 in.

---

29 Bellow, D.G., and Kennedy, J.S., "Multi-Channel Strain Analysis," Trans., Engineering Institute of Canada, Aug. 1963 EIC-63 and A-12.





All numerical calculations were run on the LGP-30 computer which is a relatively slow speed machine. Faster computations are possible if an IBM-1620 or 7040 were used. This would necessitate replacing the tape perforator of DIDAP with an IBM key punch.

Improvements in the measuring equipment (DIDAP) are possible only at considerable expense and considerable modification. It would be desirable to improve the accuracy of DIDAP from  $\pm 6$  digits to  $\pm 1$  digit but the effect on the overall accuracy of the transverse deflections would be small.

### 5.3 PRACTICAL APPLICATIONS

Apart from the fact that Lamb's theory is valid and may be applied to any problem satisfying the same differential equation and boundary conditions, a possibly more significant feature of this work is that the dimensionless parameter  $b^2/Rd$  determines the mode of transverse curvature. A great number of plate problems involving two opposite edges supported, the others being free, and cantilever plates, can be analyzed simply as beams by using the effective elastic modulus  $E/(1-\nu^2)$  instead of  $E$ ; the former being known as plate  $E$  or modified  $E$ . Calculation of the  $b^2/Rd$  ratio will determine which  $E$  should be used for any given problem. If  $b^2/Rd$  is less than one, then  $E$  should be used as the elastic modulus, and if  $b^2/Rd$  is greater than 100 then plate  $E$





can be used. If the  $b^2/Rd$  ratio is somewhere between these values then a Timoshenko  $k$  or  $\phi$  value must be used.

As an example illustrating this approach, an experiment<sup>30</sup> was set up to determine the frequencies of vibration of a swept-back cantilever wing. A model of the wing was made from an aluminum plate 0.613 x 10.0 x 25.84 in., built in along one of the 10 in. sides with a maximum deflection of approximately 1/8 in. occurring at the free end. It was assumed because of the shape of the wing, that the plate E was valid for the analysis of the deflection. It was of some concern to the investigators that better agreement between experiment and theory could be obtained if E were used instead of  $E/(1-\nu^2)$ . This result is not surprising in the light of the work of this thesis. A calculation shows the  $b^2/Rd$  value for the cantilever plate was 0.5 which indicates the cantilever wing behaved like a beam.

Engineers too often regard a plate as one whose width is many times its depth and apply plate theory directly. The results of this thesis show that such a criterion is not valid and can lead to very inaccurate results. A better criterion is to calculate the  $b^2/Rd$  ratio and, from it, use the corresponding value of  $k$  or  $\phi$ .

---

30 Hall, A.H., Pinkney, H.F.L., and Tullock, Helen A., "On the Analytical Determination of the Normal Modes and Frequencies of Swept Cantilever Vibrations," NAE R.21, 1953, National Research Council.



#### 5.4 PROBLEMS FOR FURTHER STUDY

The problem of plates with initial transverse curvatures has been treated theoretically in the literature. It would be interesting to set up some experiments for plates with corrugated and channel cross sections. Also, concerning initially curved plates there exists a stability problem for certain loaded conditions. This can be illustrated by bending a steel pocket tape of the type which has an initial curvature to impart rigidity to the tape.

All of these problems could readily be adapted to the present experimental equipment. Of course, the automatic recording system (DIDAP) can be adapted to almost any problem which requires the measurement of large quantities of transducer data.



## REFERENCES

- Alcoa Aluminum Handbook, Aluminum Company of America, 1956.
- Ashwell, D.G., and Greenwood, E.D., "Measuring Small Changes in Curvature with an Angle Dekkor," Machinery, Dec. 1948.
- Ashwell, D.G., and Greenwood, E.D., "The Pure Bending of Rectangular Plates," Engineering, 21st and 28th July 1950.
- Ashwell, D.G., "The Anticlastic Curvature of Rectangular Beams and Plates," Royal Aeronautical Society Journal, Vol. 54, 1950.
- Ashwell, D.G., "The Equilibrium Equations of the Inextensional Theory for Thin Flat Plates," Quarterly Journal Mechanics and Applied Mathematics, Vol. X, Part 2, 1957.
- Baumberger, R., and Hines, F., "Practical Reduction Formulas for Use on Bonded Wire Strain Gauges in Two-Dimensional Stress Fields," Proceedings Society Experimental Stress Analysis, 1944.
- Bellow, D.G., Transverse Curvature of Plates under Large Deflections, Unpublished M.Sc. Thesis, University of Alberta, 1960.
- Bellow, D.G., and Kennedy, J.S., "Multi-Channel Strain Analysis," Transactions Engineering Institute of Canada, EIC-63-CE and A-12, Aug. 1963.
- Case, J., Strength of Materials, Arnold, 1938.
- Crandall, S.H., Engineering Analysis, McGraw-Hill, 1956.
- Digital Voltmeters, Non-Linear Systems Inc., March 1962.
- Flugge, W., Handbook of Engineering Mechanics, McGraw-Hill, 1962.
- Fung, Y.C., and Wittrick, W.H., "A Boundary Layer Phenomenon in the Large Deflections of Thin Plates," Quarterly Journal Mechanics and Applied Mathematics, Vol. VIII, Part 2, 1955.
- Gerard, G., "Note on Beams and Plates," Journal of the Aeronautical Sciences, March 1952.
- Green, A.E. and Zerna, W., Theoretical Elasticity, Oxford, 1954.







- Hall, A.H., Pinkney, H.F.L., and Tulloch, Helen A., "On the Analytical Determination of the Normal Modes and Frequencies of Swept Cantilever Vibrations," National Research Council, NAE R21, 1953.
- "Instruction Manual BG-3100," Budd Instruments Division, 1960.
- "Instruction Manual for Model TDA-875 Amplifier," Astrodata Incorporated, 1962.
- "Instruction Manual for Model UHR-T3610R Power Supply," Krohn-Hite Corporation, 1962.
- "Instruction Manuals for Teleducer Type 24A, Circuit Scanner Type 42B, Program Unit Type 33G-2, Tape Perforator Type 136B, and Typewriter Type 12E," Telecomputing Corporation, 1961.
- Kelvin, Lord, and Tait, P.G., Treatise on Natural Philosophy, Cambridge, Part II, 1879.
- Lamb, H., "On the Flexure of a Flat Elastic Spring," Philosophical Magazine, Series 5, Vol. 31, 1891.
- Love, A.E.H., Mathematical Theory of Elasticity, Dover, 1944.
- McCracken, D.D., A Guide to Fortran Programming, Wiley, 1961.
- Melsheimer, R.S., "D-C Instrumentation Amplifiers: Their Design and Use," Instrument Society of America, Feb. 1962.
- Navier, L.M.H., Résumé des Leçons Troisième édition avec des notes et des appendices par M. Barré de Saint-Venant, Paris, 1864.
- Pohl, P., "Common Mode Rejection," Technical Data Sheet V565, Endevco Corporation, April 1962.
- Searle, G.F.C., Experimental Elasticity, Cambridge, 1908.
- Strain Gauge Handbook, Baldwin-Lima-Hamilton Corporation, Bulletin 4311A.
- Timoshenko, S.P., "Determination of the Modulus of Elasticity," Mechanical Engineering, 45 (4), 1923.
- Timoshenko, S.P., Collected Papers, McGraw-Hill, 1953.
- Timoshenko, S.P., History of Strength of Materials, McGraw-Hill, 1953.
- Timoshenko, S.P., Strength of Materials, Van Nostrand, Vol. 2, 1956.



Timoshenko, S.P., and Woinowsky-Krieger, S., Theory of Plates and Shells, McGraw-Hill, 1959.

Todhunter, J., and Pearson, K., A History of the Theory of Elasticity, Cambridge, Vol. 1, Part 2, 1893.

Wu, C.T., "Transverse Sensitivity of Bonded Strain Gauges," Experimental Mechanics, Nov. 1962.



## APPENDIX I

FORTRAN PROGRAM FOR EVALUATION OF  
THEORETICAL TRANSVERSE DEFLECTIONS

In Section 1.1.4 it was shown that the transverse deflection could be expressed in the form

$$w = \bar{A} \cosh \alpha x \cos \alpha x + \bar{B} \sinh \alpha x \sin \alpha x \quad 1.36$$

where  $\bar{A}$  and  $\bar{B}$  are constants of integration derived from the boundary conditions and defined in equations 1.34 and 1.35.

Equation 1.36 was made dimensionless by dividing both sides by the thickness  $d$  and was written in Fortran for computation on the IBM-1620 computer.

Most of the terms used in the program are self-explanatory except, possibly, those listed below;

$D$  = thickness of plate

$B$  = width of plate

$ANU$  = Poisson's ratio

$R$  = longitudinal radius of curvature

$DELB$  = increment in  $B$

$DELR$  = increment in  $R$

$NB$  = number of times  $B$  is to be incremented

$NR$  = number of times  $R$  is to be incremented

The program, as written below, evaluated the transverse deflections from the centerline of the plate out to the edge at





0.5 in. intervals for varying plate widths and varying longitudinal curvatures. If it was not required to evaluate  $w/d$  for various plate widths, the IBM data cards were set with  $NB = 1$  and  $DELB = 0.0$ . This instructed the computer to evaluate only one plate width, given by whatever floating point number was inserted for  $B$ . Example data format for the tabulated results below are shown at the end of the Fortran program. Fixed point numbers are used for  $NB$  and  $NR$ , all other data are floating point numbers.



```

C MECHANICAL ENGINEERING PROJECT 923107 W/D VERSUS X
C THIS PROGRAM EVALUATES THE TRANSVERSE DEFLECTION
C OF A PLATE USING THE EQUATION AS DERIVED BY LAMB.
C OUTPUT PRINTS  $B^2/RD$ , W/D FOR VARIOUS PLATE WIDTHS
C AND VARIOUS LONGITUDINAL CURVATURES.
1000 READ 1,D,ANU,B,R,DELR,NR
1   FORMAT(1X5F10.0,1I10)
   ETOP=SQRTF(3.*(1.-ANU**2))
3   RR=R
   DO 60 N=1,NR
4   ALPH2=ETOP/(D*RR)
5   ALPH4=ALPH2**2
6   ALPH1=SQRTF(ALPH2)
7   BETA=ANU/(ALPH2*RR)
8   THET1=0.5*ALPH1*B
9   POWE1=EXPF(THET1)
10  REPO1=1./POWE1
11  SINH1=(POWE1-REPO1)*0.5
12  COSH1=(POWE1+REPO1)*0.5
13  THET2=2.*THET1
14  POWE2=EXPF(THET2)
15  REPO2=1./POWE2
16  SINH2=(POWE2-REPO2)*0.5
17  SHCO=SINH1*COSF(THET1)
18  CHSI=COSH1*SINF(THET1)
19  DENOM=SINF(THET2)+SINH2
20  RHOP=BETA/DENOM
   ABAR=-RHOP*(SHCO-CHSI)
   BBAR=-RHOP*(SHCO+CHSI)
23  X=0.0
24  ASHR=B**2/(RR*D)
   J=B+1.0
   PUNCH 52
52  FORMAT(13X1HD13X1HB13X1HR13X4HASHR)
   PUNCH 9999,D,B,RR,ASHR
9999 FORMAT(1X4F15.4)
   PUNCH 55
55  FORMAT(13X3HANU)
   PUNCH 54,ANU
54  FORMAT(1X1F15.4)
   PUNCH 53
   53 FORMAT(13X1HX13X5HWBARD)
26  DO 47 K=1,J
27  GAMMA=ALPH1*X
28  POWEG=EXPF(GAMMA)
29  REPEG=1./POWEG
30  SINHG=(POWEG-REPEG)*0.5
31  COSHG=(POWEG+REPEG)*0.5
32  WBARD=(ABAR*COSF(GAMMA)*COSHG+BBAR*SINH1*SINF(GAMMA))/D
   PUNCH 33,X,WBARD
33  FORMAT(1XF15.2,5XE15.8)
47  X=0.5+X
60  RR=RR+DELR
   GO TO 1000
END

```



C INPUT DATA USED FOR TABULATED  
C RESULTS ON NEXT SEVENTEEN PAGES

D	ANU	B	R	DELR	NR
.125	.333	20.0	10.0	10.0	10
.125	.333	20.0	125.0	25.0	4
.125	.333	20.0	200.0	5.0	20
.125	.333	20.0	250.0	50.0	4
.125	.333	20.0	500.0	100.0	6
.125	.333	20.0	2000.0	1000.0	9





D	R	R	ASHR
.1250	20.0000	10.0000	320.0000
ANU			
.3330			
X	WBARD		
0.00	-.29409485E-05		
.50	-.25378826E-05		
1.00	-.72941640E-06		
1.50	.40675212E-05		
2.00	.13534971E-04		
2.50	.27285907E-04		
3.00	.38848922E-04		
3.50	.30256391E-04		
4.00	-.31615553E-04		
4.50	-.18902225E-03		
5.00	-.46392494E-03		
5.50	-.78921205E-03		
6.00	-.89608112E-03		
6.50	-.19424704E-03		
7.00	.22317172E-02		
7.50	.72575832E-02		
8.00	.14621240E-01		
8.50	.20795158E-01		
9.00	.16092767E-01		
9.50	-.17279184E-01		
10.00	-.10194727E+00		

D	R	R	ASHR
.1250	20.0000	20.0000	160.0000
ANU			
.3330			
X	WBARD		
0.00	.75611095E-04		
.50	.67589901E-04		
1.00	.39634775E-04		
1.50	-.19003853E-04		
2.00	-.12275941E-03		
2.50	-.28323516E-03		
3.00	-.49792624E-03		
3.50	-.73314015E-03		
4.00	-.90168600E-03		
4.50	-.83932576E-03		
5.00	-.28970872E-03		
5.50	.10844149E-02		
6.00	.36365489E-02		
6.50	.75835352E-02		
7.00	.12729360E-01		
7.50	.18047458E-01		
8.00	.21149868E-01		
8.50	.17762189E-01		
9.00	.14685408E-02		
9.50	-.35812848E-01		
10.00	-.10194730E+00		



D	R	R	ASHR
.1250	20.0000	30.0000	106.6666
ANU			

X	WBARD
0.00	-.17747654E-03
.50	-.21523803E-03
1.00	-.32401594E-03
1.50	-.48853532E-03
2.00	-.67771510E-03
2.50	-.83711168E-03
3.00	-.88037840E-03
3.50	-.68238808E-03
4.00	-.78170720E-04
4.50	.11263939E-02
5.00	.31243876E-02
5.50	.60492073E-02
6.00	.98787568E-02
6.50	.14296924E-01
7.00	.18514473E-01
7.50	.21065752E-01
8.00	.19620288E-01
8.50	.10880193E-01
9.00	-.93252000E-02
9.50	-.45591917E-01
10.00	-.10194682E+00

D	B	R	ASHR
.1250	20.0000	40.0000	80.0000
ANU			

X	WBARD
0.00	-.92785984E-03
.50	-.94356720E-03
1.00	-.97824472E-03
1.50	-.99419408E-03
2.00	-.92770656E-03
2.50	-.68892001E-03
3.00	-.16399264E-03
3.50	.77802160E-03
4.00	.22705900E-02
4.50	.44239776E-02
5.00	.72849475E-02
5.50	.10779106E-01
6.00	.14634932E-01
6.50	.18291764E-01
7.00	.20799448E-01
7.50	.20725025E-01
8.00	.16092196E-01
8.50	-.43921088E-02
9.00	-.17281932E-01
9.50	-.51909434E-01
10.00	-.10195132E+00



D	R	R	ASHR
.1250	20.0000	50.0000	64.0000
ANU			
.3330			
X	WBARD		
0.00	-.16096008E-02		
.50	-.15657317E-02		
1.00	-.14205105E-02		
1.50	-.11338824E-02		
2.00	-.64194488E-03		
2.50	.13797784E-03		
3.00	.12987008E-02		
3.50	.29295997E-02		
4.00	.50965428E-02		
4.50	.78138600E-02		
5.00	.11007310E-01		
5.50	.14467907E-01		
6.00	.17797992E-01		
6.50	.20353296E-01		
7.00	.21187911E-01		
7.50	.19013373E-01		
8.00	.12188069E-01		
8.50	-.12409584E-02		
9.00	-.23415957E-01		
9.50	-.56433092E-01		
10.00	-.10195794E+00		

D	B	R	ASHR
.1250	20.0000	60.0000	53.3333
ANU			
.3330			
X	WBARD		
0.00	-.18278103E-02		
.50	-.17178220E-02		
1.00	-.13772404E-02		
1.50	-.77553960E-03		
2.00	.13361840E-03		
2.50	.14051576E-02		
3.00	.30917020E-02		
3.50	.52283972E-02		
4.00	.78128480E-02		
4.50	.10779791E-01		
5.00	.13970585E-01		
5.50	.17098356E-01		
6.00	.19710730E-01		
6.50	.21153646E-01		
7.00	.20541694E-01		
7.50	.16742735E-01		
8.00	.83874128E-02		
8.50	-.60831160E-02		
9.00	-.28315042E-01		
9.50	-.59867104E-01		
10.00	-.10194396E+00		





D	B	R	ASHR
.1250	20.0000	70.0000	45.7142
ANU			
.3330			
X	WBARD		
0.00	-.14696088E-02		
.50	-.13038719E-02		
1.00	-.80050264E-03		
1.50	.57525440E-04		
2.00	.12936950E-02		
2.50	.29304382E-02		
3.00	.49783411E-02		
3.50	.74218658E-02		
4.00	.10201540E-01		
4.50	.13192765E-01		
5.00	.16181780E-01		
5.50	.18839918E-01		
6.00	.20698056E-01		
6.50	.21124141E-01		
7.00	.19307924E-01		
7.50	.14258423E-01		
8.00	.48211832E-02		
8.50	-.10276062E-01		
9.00	-.32339376E-01		
9.50	-.62575184E-01		
10.00	-.10189639E+00		
D	B	R	ASHR
.1250	20.0000	80.0000	40.0000
ANU			
.3330			
X	WBARD		
0.00	-.57914968E-03		
.50	-.37354373E-03		
1.00	.24497664E-03		
1.50	.12801458E-02		
2.00	.27336021E-02		
2.50	.45979812E-02		
3.00	.68472340E-02		
3.50	.94242240E-02		
4.00	.12225788E-01		
4.50	.15085668E-01		
5.00	.17756024E-01		
5.50	.19888614E-01		
6.00	.21017401E-01		
6.50	.20544833E-01		
7.00	.17734992E-01		
7.50	.11717549E-01		
8.00	.15074771E-02		
8.50	-.13953725E-01		
9.00	-.35728764E-01		
9.50	-.64780319E-01		
10.00	-.10182469E+00		



D	B	R	ASHR
.1250	20.0000	90.0000	35.5555
ANU			
.3330			
X	WBARD		
0.00	.74051394E-03		
.50	.97028344E-03		
1.00	.16574396E-02		
1.50	.27943159E-02		
2.00	.43641183E-02		
2.50	.63349492E-02		
3.00	.86515640E-02		
3.50	.11225042E-01		
4.00	.13920646E-01		
4.50	.16544393E-01		
5.00	.18829016E-01		
5.50	.20420376E-01		
6.00	.20865735E-01		
6.50	.19605771E-01		
7.00	.15972720E-01		
7.50	.91976048E-02		
8.00	-.15699530E-02		
8.50	-.17225287E-01		
9.00	-.38651164E-01		
9.50	-.66634525E-01		
10.00	-.10175293E+00		
D	B	R	ASHR
.1250	20.0000	100.0000	32.0000
ANU			
.3330			
X	WBARD		
0.00	.23778552E-02		
.50	.26184316E-02		
1.00	.33349172E-02		
1.50	.45105525E-02		
2.00	.61140207E-02		
2.50	.80944488E-02		
3.00	.10374602E-01		
3.50	.12842494E-01		
4.00	.15341719E-01		
4.50	.17661045E-01		
5.00	.19523896E-01		
5.50	.20578640E-01		
6.00	.20390905E-01		
6.50	.18439373E-01		
7.00	.14116958E-01		
7.50	.67395640E-02		
8.00	-.44349776E-02		
8.50	-.20174887E-01		
9.00	-.41226234E-01		
9.50	-.68245195E-01		
10.00	-.10170775E+00		



D	R	R	ASHR
.1250	20.0000	125.0000	25.6000
ANU			

.3330	WBARD
X	
0.00	.72556984E-02
.50	.74828798E-02
1.00	.81544128E-02
1.50	.92396448E-02
2.00	.10685461E-01
2.50	.12413348E-01
3.00	.14315473E-01
3.50	.16250026E-01
4.00	.18036075E-01
4.50	.19448376E-01
5.00	.20212590E-01
5.50	.20001548E-01
6.00	.18433327E-01
6.50	.15071982E-01
7.00	.94320360E-02
7.50	.98789440E-03
8.00	-.10810540E-01
8.50	-.26514532E-01
9.00	-.46644020E-01
9.50	-.71644538E-01
10.00	-.10183198E+00

D	R	P	ASHR
.1250	20.0000	150.0000	21.3333
ANU			

.3330	WBARD
X	
0.00	.12483020E-01
.50	.12665664E-01
1.00	.13201706E-01
1.50	.14055110E-01
2.00	.15164704E-01
2.50	.16442574E-01
3.00	.17771990E-01
3.50	.19005017E-01
4.00	.19960042E-01
4.50	.20419488E-01
5.00	.20128081E-01
5.50	.18792048E-01
6.00	.16079771E-01
6.50	.11624420E-01
7.00	.50292192E-02
7.50	-.41239824E-02
8.00	-.16262060E-01
8.50	-.31803137E-01
9.00	-.51133397E-01
9.50	-.74577520E-01
10.00	-.10236188E+00





D	B	R	ASHR
.1250	20.0000	175.0000	18.2857
ANU			
.3330			
X	WBARD		
0.00	.17528212E-01		
.50	.17655260E-01		
1.00	.18024169E-01		
1.50	.18598032E-01		
2.00	.19314783E-01		
2.50	.20086407E-01		
3.00	.20797951E-01		
3.50	.21306494E-01		
4.00	.21440179E-01		
4.50	.20997538E-01		
5.00	.19747362E-01		
5.50	.17429370E-01		
6.00	.13756012E-01		
6.50	.84157568E-02		
7.00	.10782960E-02		
7.50	-.85979408E-02		
8.00	-.20955491E-01		
8.50	-.36324269E-01		
9.00	-.55004320E-01		
9.50	-.77244280E-01		
10.00	-.10321532E+00		

D	B	R	ASHR
.1250	20.0000	200.0000	16.0000
ANU			
.3330			
X	WBARD		
0.00	.22156752E-01		
.50	.22226924E-01		
1.00	.22425620E-01		
1.50	.22717266E-01		
2.00	.23042345E-01		
2.50	.23317108E-01		
3.00	.23433216E-01		
3.50	.23257488E-01		
4.00	.22631792E-01		
4.50	.21373264E-01		
5.00	.19275001E-01		
5.50	.16107449E-01		
6.00	.11620677E-01		
6.50	.55478072E-02		
7.00	-.23901608E-02		
7.50	-.12477812E-01		
8.00	-.24996796E-01		
8.50	-.40215027E-01		
9.00	-.58373252E-01		
9.50	-.79668808E-01		
10.00	-.10423617E+00		



D	B	R	ASHR
.1250	20.0000	250.0000	12.8000
ANU			

X	WBARD
0.00	.29878442E-01
.50	.29846169E-01
1.00	.29739153E-01
1.50	.29526828E-01
2.00	.29158330E-01
2.50	.28562648E-01
3.00	.27648888E-01
3.50	.26306693E-01
4.00	.24406872E-01
4.50	.21802335E-01
5.00	.18329397E-01
5.50	.13809605E-01
6.00	.80520848E-02
6.50	.85669664E-03
7.00	-.79820565E-02
7.50	-.18670045E-01
8.00	-.31407509E-01
8.50	-.46381665E-01
9.00	-.63758088E-01
9.50	-.83670328E-01
10.00	-.10620820E+00

D	B	R	ASHR
.1250	20.0000	300.0000	10.6666
ANU			

X	WBARD
0.00	.35581644E-01
.50	.35468532E-01
1.00	.35120772E-01
1.50	.34513142E-01
2.00	.33603768E-01
2.50	.32334460E-01
3.00	.30631101E-01
3.50	.28404285E-01
4.00	.25550119E-01
4.50	.21951296E-01
5.00	.17478445E-01
5.50	.11991856E-01
6.00	.53436144E-02
6.50	-.26197872E-02
7.00	-.12054286E-01
7.50	-.23114478E-01
8.00	-.35949092E-01
8.50	-.50695768E-01
9.00	-.67474941E-01
9.50	-.86382848E-01
10.00	-.10748357E+00



D	B	R	ASHR
.1250	20.0000	350.0000	9.1428
ANU			
.3330			
X	WBARD		
0.00	.39540936E-01		
.50	.39367645E-01		
1.00	.38840908E-01		
1.50	.37940143E-01		
2.00	.36631270E-01		
2.50	.34867018E-01		
3.00	.32587368E-01		
3.50	.29720195E-01		
4.00	.26182050E-01		
4.50	.21879169E-01		
5.00	.16708715E-01		
5.50	.10560276E-01		
6.00	.33176672E-02		
6.50	-.51388928E-02		
7.00	-.14930293E-01		
7.50	-.26175527E-01		
8.00	-.38988340E-01		
8.50	-.53473216E-01		
9.00	-.69721026E-01		
9.50	-.87803824E-01		
10.00	-.10776937E+00		
D	B	R	ASHR
.1250	20.0000	400.0000	8.0000
ANU			
.3330			
X	WBARD		
0.00	.42094282E-01		
.50	.41877892E-01		
1.00	.41223127E-01		
1.50	.40113229E-01		
2.00	.38520464E-01		
2.50	.36406427E-01		
3.00	.33722464E-01		
3.50	.30410216E-01		
4.00	.26402380E-01		
4.50	.21623560E-01		
5.00	.15991355E-01		
5.50	.94176352E-02		
6.00	.18100528E-02		
6.50	-.69262328E-02		
7.00	-.16886451E-01		
7.50	-.28163977E-01		
8.00	-.40847572E-01		
8.50	-.55018463E-01		
9.00	-.70746920E-01		
9.50	-.88088416E-01		
10.00	-.10707955E+00		





D	B	R	ASHR
.1250	20.0000	500.0000	6.4000
ANU			
.3330			
X	WBARD		
0.00	.44208992E-01		
.50	.43943296E-01		
1.00	.43142452E-01		
1.50	.41795204E-01		
2.00	.39882952E-01		
2.50	.37379970E-01		
3.00	.34253755E-01		
3.50	.30465429E-01		
4.00	.25970282E-01		
4.50	.20718438E-01		
5.00	.14655596E-01		
5.50	.77239480E-02		
6.00	-.13679360E-03		
6.50	-.89882024E-02		
7.00	-.18891824E-01		
7.50	-.29907596E-01		
8.00	-.42092250E-01		
8.50	-.55497347E-01		
9.00	-.70167208E-01		
9.50	-.86136720E-01		
10.00	-.10342866F+00		
D	B	R	ASHR
.1250	20.0000	600.0000	5.3333
ANU			
.3330			
X	WBARD		
0.00	.43886344E-01		
.50	.43602285E-01		
1.00	.42747515E-01		
1.50	.41314281E-01		
2.00	.39289773E-01		
2.50	.36656296E-01		
3.00	.33391508E-01		
3.50	.29468733E-01		
4.00	.24857351E-01		
4.50	.19523268E-01		
5.00	.13429443E-01		
5.50	.65365504E-02		
6.00	-.11963216E-02		
6.50	-.98108344E-02		
7.00	-.19348498E-01		
7.50	-.29849636E-01		
8.00	-.41352268E-01		
8.50	-.53890842E-01		
9.00	-.67494888E-01		
9.50	-.82187536E-01		
10.00	-.97983880E-01		



D	R	R	ASHR
.1250	20.0000	700.0000	4.5714
ANU			
.3330			
X	WBARD		
0.00	.42344660E-01		
.50	.42058900E-01		
1.00	.41199787E-01		
1.50	.39761828E-01		
2.00	.37735940E-01		
2.50	.35109603E-01		
3.00	.31867000E-01		
3.50	.27989284E-01		
4.00	.23454828E-01		
4.50	.18239584E-01		
5.00	.12317460E-01		
5.50	.56608064E-02		
6.00	-.17591088E-02		
6.50	-.99714928E-02		
7.00	-.19005382E-01		
7.50	-.28888936E-01		
8.00	-.39648664E-01		
8.50	-.51308504E-01		
9.00	-.63888984E-01		
9.50	-.77406080E-01		
10.00	-.91870280E-01		

D	R	R	ASHR
.1250	20.0000	800.0000	4.0000
ANU			
.3330			
X	WBARD		
0.00	.40271163E-01		
.50	.39992236E-01		
1.00	.39154128E-01		
1.50	.37752836E-01		
2.00	.35781755E-01		
2.50	.33231768E-01		
3.00	.30091377E-01		
3.50	.26346876E-01		
4.00	.21982566E-01		
4.50	.16980994E-01		
5.00	.11323236E-01		
5.50	.49892592E-02		
6.00	-.20417216E-02		
6.50	-.97908200E-02		
7.00	-.18279000E-01		
7.50	-.27526572E-01		
8.00	-.37552612E-01		
8.50	-.48374363E-01		
9.00	-.60006536E-01		
9.50	-.72460616E-01		
10.00	-.85744080E-01		



D	B	R	ASHR
.1250	20.0000	900.0000	3.5555
ANU			
.3330			
X	WBARD		
0.00	.38032190E-01		
.50	.37764161E-01		
1.00	.36959075E-01		
1.50	.35613948E-01		
2.00	.33723853E-01		
2.50	.31281994E-01		
3.00	.28279793E-01		
3.50	.24707041E-01		
4.00	.20552040E-01		
4.50	.15801792E-01		
5.00	.10442224E-01		
5.50	.44584384E-02		
6.00	-.21650200E-02		
6.50	-.94438112E-02		
7.00	-.17393504E-01		
7.50	-.26029132E-01		
8.00	-.35364844E-01		
8.50	-.45413376E-01		
9.00	-.56185616E-01		
9.50	-.67690048E-01		
10.00	-.79932192E-01		
D	B	R	ASHR
.1250	20.0000	1000.0000	3.2000
ANU			
.3330			
X	WBARD		
0.00	.35813937E-01		
.50	.35558442E-01		
1.00	.34791203E-01		
1.50	.33509937E-01		
2.00	.31710888E-01		
2.50	.29388877E-01		
3.00	.26537361E-01		
3.50	.23148570E-01		
4.00	.19213579E-01		
4.50	.14722494E-01		
5.00	.96646024E-02		
5.50	.40285720E-02		
6.00	-.21973480E-02		
6.50	-.90250664E-02		
7.00	-.16466401E-01		
7.50	-.24532779E-01		
8.00	-.33234912E-01		
8.50	-.42582475E-01		
9.00	-.52583696E-01		
9.50	-.63245032E-01		
10.00	-.74570624E-01		





D	B	R	ASHR
.1250	20.0000	2000.0000	1.6000
ANU			
.3330			
X	WBARD		
0.00	.20959532E-01		
.50	.20804244E-01		
1.00	.20338272E-01		
1.50	.19561285E-01		
2.00	.18472731E-01		
2.50	.17071854E-01		
3.00	.15357697E-01		
3.50	.13329125E-01		
4.00	.10984844E-01		
4.50	.83234064E-02		
5.00	.53432584E-02		
5.50	.20427536E-02		
6.00	-.15798064E-02		
6.50	-.55261472E-02		
7.00	-.97979776E-02		
7.50	-.14396942E-01		
8.00	-.19324584E-01		
8.50	-.24582280E-01		
9.00	-.30171219E-01		
9.50	-.36092317E-01		
10.00	-.42346168E-01		

D	B	R	ASHR
.1250	20.0000	3000.0000	1.0666
ANU			
.3330			
X	WBARD		
0.00	.14421539E-01		
.50	.14313960E-01		
1.00	.13991192E-01		
1.50	.13453132E-01		
2.00	.12699615E-01		
2.50	.11730404E-01		
3.00	.10545210E-01		
3.50	.91436880E-02		
4.00	.75254360E-02		
4.50	.56900184E-02		
5.00	.36369600E-02		
5.50	.13657544E-02		
6.00	-.11241168E-02		
6.50	-.38331792E-02		
7.00	-.67619504E-02		
7.50	-.99109328E-02		
8.00	-.13280602E-01		
8.50	-.16871375E-01		
9.00	-.20683612E-01		
9.50	-.24717594E-01		
10.00	-.28973501E-01		



D	B	R	ASHR
.1250	20.0000	4000.0000	.8000
ANU			

X	WBARD
0.00	.10938657E-01
.50	.10856865E-01
1.00	.10611478E-01
1.50	.10202450E-01
2.00	.96297120E-02
2.50	.88931624E-02
3.00	.79926776E-02
3.50	.69281112E-02
4.00	.56992896E-02
4.50	.43060312E-02
5.00	.27481280E-02
5.50	.10253696E-02
6.00	-.86247200E-03
6.50	-.29156096E-02
7.00	-.51342792E-02
7.50	-.75186832E-02
8.00	-.10069026E-01
8.50	-.12785485E-01
9.00	-.15668220E-01
9.50	-.18717344E-01
10.00	-.21932941E-01

D	B	R	ASHR
.1250	20.0000	5000.0000	.6400
ANU			

X	WBARD
0.00	.87969824E-02
.50	.87311328E-02
1.00	.85335768E-02
1.50	.82042920E-02
2.00	.77432440E-02
2.50	.71503776E-02
3.00	.64256328E-02
3.50	.55689312E-02
4.00	.45801856E-02
4.50	.34592992E-02
5.00	.22061688E-02
5.50	.82068480E-03
6.00	-.69727040E-03
6.50	-.23478080E-02
7.00	-.41310448E-02
7.50	-.60470880E-02
8.00	-.80960464E-02
8.50	-.10278004E-01
9.00	-.12593050E-01
9.50	-.15041234E-01
10.00	-.17622606E-01



D	B	R	ASHR
.1250	20.0000	6000.0000	.5333

ANU

.3330

X	WBARD
0.00	.73518252E-02
.50	.72967608E-02
1.00	.71315626E-02
1.50	.68562188E-02
2.00	.64707084E-02
2.50	.59750000E-02
3.00	.53690573E-02
3.50	.46528365E-02
4.00	.38262864E-02
4.50	.28893508E-02
5.00	.18419714E-02
5.50	.68408040E-03
6.00	-.58438488E-03
6.50	-.19634960E-02
7.00	-.34533104E-02
7.50	-.50539040E-02
8.00	-.67653264E-02
8.50	-.85876352E-02
9.00	-.10520876E-01
9.50	-.12565086E-01
10.00	-.14720286E-01

D	B	R	ASHR
.1250	20.0000	7000.0000	.4571

ANU

.3330

X	WBARD
0.00	.63124733E-02
.50	.62651766E-02
1.00	.61232834E-02
1.50	.58867866E-02
2.00	.55556720E-02
2.50	.51299216E-02
3.00	.46095101E-02
3.50	.39944110E-02
4.00	.32845927E-02
4.50	.24800202E-02
5.00	.15806524E-02
5.50	.58645304E-03
6.00	-.50262296E-03
6.50	-.16866160E-02
7.00	-.29655680E-02
7.50	-.43395192E-02
8.00	-.58085096E-02
8.50	-.73725672E-02
9.00	-.90317264E-02
9.50	-.10786012E-01
10.00	-.12635429E-01





D	R	R	ASHR
.1250	20.0000	8000.0000	.4000
ANU			
.3330			
X	WBARD		
0.00	.55296202E-02		
.50	.54881792E-02		
1.00	.53638555E-02		
1.50	.51566429E-02		
2.00	.48665317E-02		
2.50	.44935103E-02		
3.00	.40375629E-02		
3.50	.34986718E-02		
4.00	.28768128E-02		
4.50	.21719656E-02		
5.00	.13841021E-02		
5.50	.51319624E-03		
6.00	-.44078064E-03		
6.50	-.14778560E-02		
7.00	-.25980584E-02		
7.50	-.38014144E-02		
8.00	-.50879496E-02		
8.50	-.64576888E-02		
9.00	-.79106464E-02		
9.50	-.94468416E-02		
10.00	-.11066283E-01		

D	B	R	ASHR
.1250	20.0000	9000.0000	.3555
ANU			
.3330			
X	WBARD		
0.00	.49190181E-02		
.50	.48821472E-02		
1.00	.47715348E-02		
1.50	.45871757E-02		
2.00	.43290641E-02		
2.50	.39971916E-02		
3.00	.35915472E-02		
3.50	.31121169E-02		
4.00	.25588857E-02		
4.50	.19318378E-02		
5.00	.12309540E-02		
5.50	.45621640E-03		
6.00	-.39239576E-03		
6.50	-.13148994E-02		
7.00	-.23113186E-02		
7.50	-.33816704E-02		
8.00	-.45259704E-02		
8.50	-.57442384E-02		
9.00	-.70364872E-02		
9.50	-.84027240E-02		
10.00	-.98429576E-02		



D	B	R	ASHR
.1250	20.0000	10000.0000	.3200
ANU			
.3330			
X	WBARD		
0.00	.44295566E-02		
.50	.43963511E-02		
1.00	.42967333E-02		
1.50	.41307008E-02		
2.00	.38982491E-02		
2.50	.35993714E-02		
3.00	.32340596E-02		
3.50	.28023048E-02		
4.00	.23040944E-02		
4.50	.17394196E-02		
5.00	.11082629E-02		
5.50	.41061264E-03		
6.00	-.35354440E-03		
6.50	-.11842258E-02		
7.00	-.20814437E-02		
7.50	-.30452107E-02		
8.00	-.40755440E-02		
8.50	-.51724480E-02		
9.00	-.63359416E-02		
9.50	-.75660248E-02		
10.00	-.88627104E-02		



## APPENDIX II

FORTRAN PROGRAM FOR EVALUATION RELATIONSHIP  
BETWEEN BENDING MOMENT, CURVATURE AND STIFFNESS

Equation 1.80 was written in Fortran language for computation on the IBM-1620 computer. In addition,  $\phi$  from equation 1.69 and the percentage increase in  $\phi$  have also been evaluated and are tabulated below for Poisson's ratio equal to 0.300, 0.310, 0.320, and 0.333.

Those terms in the program which are not obvious are defined below;

TIMK =  $k$ , defined by Timoshenko

PHIC = percentage increase in  $\phi$

$C = b^2/Rd$  ratio

DELC = increment in  $C$

NC = number of times  $C$  is to be incremented

Example data format statements are listed at the end of the Fortran program below. Fixed point numbers are used for NC, all the other input values are floating point.





C MECHANICAL ENGINEERING PROJECT 923115. THIS  
 C PROGRAM CALCULATES THE THEORETICAL RELATIONSHIPS  
 C BETWEEN THE BENDING MOMENT, CURVATURE, AND STIFFNESS  
 C OF A PLATE AS DERIVED BY TIMOSHENKO. OUTPUT DATA  
 C PRINTS PHI, PERCENTAGE INCREASE IN PHI, AND K.

```

999 READ 1,C,DELC,ANU,NC
  1 FORMAT(1X3F10.6,1I10)
    ANU2=ANU**2
    ETOP=SQRTF(SQRTF(3.0*(1.-ANU2)))
    DO 50 I=1,NC
      ALPB=ETOP*SQRTF(C)
      THET=0.5*ALPB
      POWE=EXPF(THET)
      REPO=1./POWE
      8 SINH1=(POWE-REPO)*0.5
      COSH1=(POWE+REPO)*0.5
      POWE2=EXPF(ALPB)
      REPO2=1.0/POWE2
      SINH2=(POWE2-REPO2)*0.5
      COSH2=(POWE2+REPO2)*0.5
    14 SIN1=SINF(THET)
      COS1=COSF(THET)
      SIN2=SINF(ALPB)
      COS2=COSF(ALPB)
      DENO=SINH2+SIN2
      SHC1=SINH1*COS1
      CHS1=COSH1*SIN1
      SHC2=SINH2*COS2
      CHS2=COSH2*SIN2
      ACON=(SHC1-CHS1)/DENO
      BCON=(SHC1+CHS1)/DENO
      ACON2=ACON**2
      BCON2=BCON**2
      FALB=(ACON+BCON)*SHC1+(BCON-ACON)*CHS1
      FIRS=2.0*ALPB*(ACON2-BCON2)
      SECO=(ACON2-2.0*ACON*BCON-BCON2)*SHC2
      THIR=2.0*(ACON2+BCON2)*DENO
      FOUR=(ACON2+2.0*ACON*BCON-BCON2)*CHS2
      GALB=FIR+SECO+THIR+FOUR
      TIMK=(2.*FALB-0.5*GALB)/ALPB
      PHI=(1.0-TIMK*ANU2)/(1.0-ANU2)
      PHIC=(PHI-1.0)*100.0
      PUNCH 73,C,TIMK,PHI,PHIC
    50 C=C+DELC
  73 FORMAT(1X,F8.2,5X,F10.6,5X,F10.6,5X,F10.6)
    GO TO 999
  END

```



C DATA INPUT USED FOR TABULATED RESULTS  
C ON NEXT FOUR PAGES

C	DELC	ANU	NC
0.1	0.1	0.300	9
1.0	1.0	0.300	30
40.0	10.0	0.300	7
150.0	50.0	0.300	8
600.0	100.0	0.300	5
0.1	0.1	0.310	9
1.0	1.0	0.310	30
40.0	10.0	0.310	7
150.0	50.0	0.310	8
600.0	100.0	0.310	5
0.1	0.1	0.320	9
1.0	1.0	0.320	30
40.0	10.0	0.320	7
150.0	50.0	0.320	8
600.0	100.0	0.320	5
0.1	0.1	0.333	9
1.0	1.0	0.333	30
40.0	10.0	0.333	7
150.0	50.0	0.333	8
600.0	100.0	0.333	5



C	TIMK	PHI	PHIC
.10	.999697	1.000030	.003010
.20	.998788	1.000120	.011990
.30	.997278	1.000269	.026920
.40	.995172	1.000478	.047760
.50	.992478	1.000744	.074400
.60	.989206	1.001068	.106760
.70	.985370	1.001447	.144690
.80	.980983	1.001881	.188090
.90	.976062	1.002368	.236760
1.00	.970625	1.002905	.290530
2.00	.892786	1.010604	1.060360
3.00	.790100	1.020760	2.075950
4.00	.685625	1.031092	3.109210
5.00	.593522	1.040201	4.020110
6.00	.518833	1.047588	4.758790
7.00	.460984	1.053309	5.330930
8.00	.417090	1.057651	5.765050
9.00	.383887	1.060934	6.093430
10.00	.358543	1.063441	6.344090
11.00	.338858	1.065388	6.538770
12.00	.323218	1.066935	6.693450
13.00	.310468	1.068196	6.819550
14.00	.299798	1.069251	6.925090
15.00	.290638	1.070157	7.015680
16.00	.282592	1.070953	7.095250
17.00	.275382	1.071666	7.166560
18.00	.268813	1.072315	7.231530
19.00	.262747	1.072915	7.291520
20.00	.257087	1.073475	7.347490
21.00	.251763	1.074002	7.400150
22.00	.246724	1.074500	7.449990
23.00	.241934	1.074974	7.497360
24.00	.237366	1.075426	7.542550
25.00	.232999	1.075857	7.585740
26.00	.228818	1.076271	7.627090
27.00	.224809	1.076667	7.666730
28.00	.220964	1.077048	7.704760
29.00	.217273	1.077413	7.741260
30.00	.213728	1.077763	7.776320
40.00	.185002	1.080604	8.060430
50.00	.165128	1.082570	8.256980
60.00	.150624	1.084004	8.400430
70.00	.139442	1.085110	8.511010
80.00	.130452	1.085999	8.599930
90.00	.123003	1.086736	8.673600
100.00	.116695	1.087360	8.735990
150.00	.095281	1.089478	8.947780
200.00	.082515	1.090740	9.074030
250.00	.073804	1.091602	9.160190
300.00	.067374	1.092238	9.223780
350.00	.062376	1.092732	9.273210
400.00	.058347	1.093131	9.313050
450.00	.055010	1.093461	9.346050
500.00	.052187	1.093740	9.373980
600.00	.047640	1.094190	9.418950
700.00	.044106	1.094539	9.453900
800.00	.041258	1.094821	9.482070
900.00	.038898	1.095054	9.505410
1000.00	.036902	1.095252	9.525150





C	TIMK	PHI	PHIC
.10	.999699	1.000032	.003210
.20	.998796	1.000128	.012800
.30	.997296	1.000288	.028750
.40	.995204	1.000510	.051000
.50	.992528	1.000794	.079440
.60	.989278	1.001140	.113990
.70	.985467	1.001545	.154520
.80	.981108	1.002009	.200860
.90	.976218	1.002529	.252850
1.00	.970815	1.003103	.310290
2.00	.893421	1.011331	1.133120
3.00	.791175	1.022202	2.220170
4.00	.686967	1.033281	3.328080
5.00	.594920	1.043066	4.306600
6.00	.520164	1.051015	5.101480
7.00	.462171	1.057181	5.718060
8.00	.418115	1.061864	6.186440
9.00	.384762	1.065410	6.541030
10.00	.359291	1.068118	6.811840
11.00	.339505	1.070222	7.022190
12.00	.323786	1.071893	7.189320
13.00	.310976	1.073255	7.325500
14.00	.300262	1.074394	7.439420
15.00	.291070	1.075372	7.537150
16.00	.283001	1.076229	7.622930
17.00	.275775	1.076998	7.699760
18.00	.269195	1.077697	7.769720
19.00	.263121	1.078343	7.834280
20.00	.257456	1.078945	7.894510
21.00	.252128	1.079512	7.951160
22.00	.247087	1.080048	8.004760
23.00	.242295	1.080557	8.055700
24.00	.237726	1.081043	8.104280
25.00	.233358	1.081507	8.150720
26.00	.229175	1.081952	8.195190
27.00	.225166	1.082378	8.237810
28.00	.221319	1.082787	8.278710
29.00	.217626	1.083180	8.317980
30.00	.214079	1.083557	8.355690
40.00	.185319	1.086615	8.661460
50.00	.165410	1.088731	8.873120
60.00	.150878	1.090276	9.027620
70.00	.139677	1.091467	9.146710
80.00	.130671	1.092425	9.242460
90.00	.123209	1.093218	9.321780
100.00	.116892	1.093890	9.388960
150.00	.095441	1.096170	9.617020
200.00	.082654	1.097530	9.752960
250.00	.073929	1.098457	9.845720
300.00	.067487	1.099142	9.914210
350.00	.062481	1.099674	9.967430
400.00	.058445	1.100103	10.010330
450.00	.055103	1.100459	10.045880
500.00	.052275	1.100759	10.075940
600.00	.047721	1.101244	10.124360
700.00	.044181	1.101620	10.162000
800.00	.041327	1.101923	10.192330
900.00	.038964	1.102175	10.217460
1000.00	.036964	1.102387	10.238720



C	TIMK	PHI	PHIC
.10	.999701	1.000034	.003420
.20	.998805	1.000136	.013640
.30	.997315	1.000306	.030640
.40	.995237	1.000543	.054340
.50	.992580	1.000847	.084660
.60	.989352	1.001215	.121480
.70	.985566	1.001647	.164670
.80	.981237	1.002141	.214060
.90	.976380	1.002695	.269470
1.00	.971012	1.003307	.330700
2.00	.894077	1.012084	1.208390
3.00	.792290	1.023696	2.369600
4.00	.688359	1.035553	3.555260
5.00	.596392	1.046045	4.604460
6.00	.521551	1.054583	5.458260
7.00	.463408	1.061216	6.121550
8.00	.419186	1.066261	6.626050
9.00	.385677	1.070083	7.008320
10.00	.360074	1.073004	7.300410
11.00	.340181	1.075274	7.527350
12.00	.324379	1.077076	7.707620
13.00	.311507	1.078545	7.854470
14.00	.300746	1.079772	7.977240
15.00	.291520	1.080825	8.082490
16.00	.283427	1.081748	8.174810
17.00	.276184	1.082574	8.257440
18.00	.269592	1.083326	8.332640
19.00	.263510	1.084020	8.402030
20.00	.257840	1.084667	8.466720
21.00	.252508	1.085275	8.527540
22.00	.247465	1.085851	8.585070
23.00	.242672	1.086398	8.639760
24.00	.238101	1.086919	8.691900
25.00	.233732	1.087417	8.741740
26.00	.229548	1.087895	8.789480
27.00	.225537	1.088352	8.835240
28.00	.221688	1.088791	8.879140
29.00	.217993	1.089213	8.921300
30.00	.214443	1.089618	8.961790
40.00	.185650	1.092903	9.290270
50.00	.165704	1.095178	9.517830
60.00	.151143	1.096839	9.683930
70.00	.139921	1.098120	9.811950
80.00	.130899	1.099149	9.914880
90.00	.123425	1.100002	10.000160
100.00	.117096	1.100724	10.072350
150.00	.095608	1.103175	10.317490
200.00	.082799	1.104636	10.463610
250.00	.074058	1.105633	10.563340
300.00	.067605	1.106370	10.636950
350.00	.062590	1.106942	10.694160
400.00	.058548	1.107403	10.740290
450.00	.055199	1.107785	10.778480
500.00	.052367	1.108108	10.810800
600.00	.047804	1.108629	10.862850
700.00	.044258	1.109033	10.903300
800.00	.041400	1.109359	10.935910
900.00	.039032	1.109629	10.962920
1000.00	.037029	1.109858	10.985770





C	TIMK	PHI	PHIC
.10	.999704	1.000037	.003700
.20	.998816	1.000148	.014790
.30	.997341	1.000332	.033230
.40	.995283	1.000590	.058950
.50	.992651	1.000919	.091860
.60	.989454	1.001318	.131820
.70	.985704	1.001787	.178690
.80	.981416	1.002323	.232300
.90	.976603	1.002925	.292450
1.00	.971278	1.003582	.358220
2.00	.894964	1.013100	1.310010
3.00	.793798	1.025717	2.571740
4.00	.690248	1.038632	3.863210
5.00	.598380	1.050090	5.008970
6.00	.523438	1.059436	5.943630
7.00	.465096	1.066713	6.671270
8.00	.420648	1.072256	7.225620
9.00	.386927	1.076462	7.646190
10.00	.361143	1.079678	7.967760
11.00	.341105	1.082177	8.217670
12.00	.325190	1.084162	8.416170
13.00	.312232	1.085778	8.577770
14.00	.301407	1.087128	8.712780
15.00	.292135	1.088284	8.828430
16.00	.284008	1.089298	8.929780
17.00	.276741	1.090204	9.020410
18.00	.270133	1.091028	9.102830
19.00	.264040	1.091788	9.178820
20.00	.258362	1.092496	9.249640
21.00	.253026	1.093162	9.316190
22.00	.247979	1.093791	9.379130
23.00	.243183	1.094390	9.438950
24.00	.238610	1.094960	9.495980
25.00	.234239	1.095505	9.550490
26.00	.230054	1.096027	9.602690
27.00	.226041	1.096527	9.652740
28.00	.222190	1.097008	9.700770
29.00	.218492	1.097469	9.746890
30.00	.214940	1.097912	9.791200
40.00	.186100	1.101509	10.150880
50.00	.166104	1.104003	10.400280
60.00	.151504	1.105824	10.582360
70.00	.140253	1.107227	10.722680
80.00	.131210	1.108355	10.835460
90.00	.123718	1.109289	10.928910
100.00	.117374	1.110080	11.008020
150.00	.095836	1.112767	11.276650
200.00	.082996	1.114368	11.436780
250.00	.074234	1.115461	11.546060
300.00	.067766	1.116267	11.626740
350.00	.062739	1.116894	11.689430
400.00	.058687	1.117400	11.739960
450.00	.055331	1.117818	11.781820
500.00	.052491	1.118172	11.817230
600.00	.047918	1.118743	11.874280
700.00	.044363	1.119186	11.918610
800.00	.041498	1.119544	11.954350
900.00	.039125	1.119839	11.983940





## APPENDIX III

## COMPUTER PROGRAM FOR LGP-30

The program in machine language reproduced below subtracts the initial strains from the final strains, performs two numerical integrations to obtain the transverse deflection, finds the centroidal axis of this deflected form and recalculates the transverse deflection so that the x-axis is the centroidal axis of the deflected form.

The data output from the tape perforator of DIDAP is in the form xxx +'. Since this data format is not compatible with any of the standard input routines a special input routine was written.\*

OPERATING INSTRUCTIONS

From the LGP-30 coding sheets a hexadecimal tape was made incorporating all input and output routines. This was accomplished by first punching the program tapes in decimal, putting them into the computer and then using a decimal to

---

\* The author acknowledges the help of the University of Alberta Computing Center and gives special thanks to Mr. B.J. Mailloux for writing the input and output subroutines and assisting in the "debugging" processes.



hexadecimal conversion subroutine. Once the hex tape is made and the data tapes are ready for computation the following sequence of instructions is carried out;

A. Computer Start Up

1. Console. "Manual Input" should be down except "Operate" button which is always down. All other switches should be up. Depress "Power On".
2. Flexowriter. "Manual Input" switch down. Turn "Connect" switch on and press "Power" switch on.
3. Photoreader. Put "Output" selector switch in "Typewriter" position and "Input" selector switch in "Typewriter" position. Depress "Reader Power" and "Punch Power".  
Allow at least ten minutes for warm up.

B. Loading Hexademical Tape

1. Place hex tape in photoreader. Depress "Reader Stop".
2. Turn "Input" selector switch on photoreader to "Reader" position.
3. On console sequentially depress "One Operation", "Clear Counter", "Normal, Start" (OCNS).

This procedure loads the program and all its input and output subroutines into the computer.

C. Loading Data Tape for Conversion

When it is desired to subtract initial readings from final readings the procedure below is carried out.

1. Place data tape in photoreader. Set "Input" and "Output" selector switches to the "Typewriter" position. Depress "Reader Stop".



2. OCNS.
3. Type .0001600'.
4. Start twice.
5. Type the number of channels (76', 150', etc.).
6. Set "Input" selector switch to "Reader" and "Output" selector switch to "Punch".
7. Depress "Break Point 32".
8. Depress console "Start".

After step 8 has been executed the computer will take the initial set of data and subtract these values from the corresponding channels of all subsequent sets of data which are fed into the computer. The converted data is produced on a perforated tape. To obtain the deflections from this tape using the multiple integration method the computer is set up according to the instructions below.

D. Loading Conversion Tape and Obtaining Deflections

1. Place "convert" tape in photoreader. Set "Input" and "Output" selector switches both to "Typewriter". Press "Reader Stop".
2. OCNS.
3. Type .0003200'.
4. Start twice.
5. When light on the flexowriter glows, type in n, the number of stations. Note, there will be half as many stations as there are channels since two channels, one on top and one on bottom directly underneath, constitute one measuring station.





6. Start once.
7. When light on the flexowriter glows again, type in M, the thickness of the plate in sixteenths of an inch. Both n and M must be integers.
8. Start once.
9. Type in distance between stations h, when flexowriter light glows again; that is, if 1.0 in., type 1000000', if 0.5 in., type 500000' (h is at a q of 4).
10. Put "Input" selector switch to "Reader".
11. Start once.
12. Depress "Breakpoint 4". If this is not done the computer will stop after the first set of data has been analyzed. Depressing the start again will set it back to input a new set of data.

#### E. Computer Shut Down

1. Set both selector switches to "Typewriter".
2. Depress "Power" on reader and on punch.

#### Console

1. Depress "One Operation" and Manual.
2. Lift all "Breakpoints".

#### Typewriter

1. Turn "Connect" switch to off.
2. Turn "Power" off.

#### Console

1. Depress "Power Off".



The program for the LGP-30 computer is given below in machine language. On pages 215 to 216 a special input subroutine is written which binarizes a four digit number with the sign trailing. On pages 217 to 219 a special output subroutine is given. The program used to subtract initial readings from final readings is given on pages 220 to 221. The main program used for the calculations of the deflections ( $w/d$ ) is given on pages 222 to 228.



## LGP-30 CODING SHEET

NO. 1

PAGE 1 OF 2

NO. \_\_\_\_\_ PROG. NO. \_\_\_\_\_ PREP. BY B.J.M. CK'D. BY B.J.M. DATE June 19, 1961

BLEM BINARIZE 4 DIGIT INTEGER, SIGN TRAILING TRACK 00

PROGRAM INPUT CODES	STOP	LOCATION	INSTRUCTION OP. ADDRESS	Notes	CONTENTS OF ADDRESS	NOTES
		<input checked="" type="checkbox"/> X X X X X X X X X X				
		0,0,00	X P 0,0,5,0			
		0,1	C 0,0,4,4		0 → acc.	
		0,2	X I 0,0,5,2			
		0,3	H 0,0,5,3	<input checked="" type="checkbox"/> T.S.		
		0,4	M 0,0,5,4		1 @ 3	
		0,5	H 0,0,5,5		T.S. 1	
		0,6	E 0,0,4,9		01010100	
		0,7	M 0,0,5,7	<input checked="" type="checkbox"/> -6 @ 4		K0000000
		0,8	U 0,0,1,2			
0,0,0,0,0,0,3		0,9				
		1,0				
		1,1	Q	<input checked="" type="checkbox"/> mask		
		1,2	A 0,0,5,5		T.S.1	
		1,3	H 0,0,5,6		T.S.2	
		1,4	E 0,0,5,0		1Q00WQ00	
		1,5	M 0,0,5,1	<input checked="" type="checkbox"/> -156 @ 8		G2000000
		1,6	U 0,0,2,0			
		1,7				
		1,8				
		1,9		<input checked="" type="checkbox"/>		
		2,0	A 0,0,5,6		T.S.2	
		2,1	H 0,0,4,3		T.S.3	
		2,2	U 0,0,2,4			
		2,3		<input checked="" type="checkbox"/>		
		2,4	B 0,0,5,3		T.S.	
		2,5	E 0,0,1,1		Q	save sign only
		2,6	S 0,0,4,8		1 @ 30	
		2,7	T 0,0,3,5	<input checked="" type="checkbox"/> →		neg. no.
		2,8	B 0,0,4,3		T.S.3	answer
		2,9	U ( )		→	exit
		3,0				
		3,1		<input checked="" type="checkbox"/>		

CONDITIONAL STOP CODE



CARRIAGE RETURN





## LGP-30 CODING SHEET

NO 2

PAGE 2 OF 2

NO \_\_\_\_\_ PROG. NO. \_\_\_\_\_ PREP. BY \_\_\_\_\_ CK'D. BY \_\_\_\_\_ DATE \_\_\_\_\_

LEM \_\_\_\_\_ TRACK 00

PROGRAM INPUT CODES	STOP	LOCATION	INSTRUCTION OP. ADDRESS	STOP	CONTENTS OF ADDRESS	NOTES
		<input checked="" type="checkbox"/> XXXXXX	XXXXXXXXXXXXXXXXXXXX			
		0 0 32				
		33				
		34				
		35	B 0 0 4 3	<input checked="" type="checkbox"/>		
		36	M 0 0 5 8		-1 @ 0	
		37	U 0 0 2 9			
0 0 0 0 0 2 1		38				
		39		<input checked="" type="checkbox"/>		
		40				
		41				
		42				
		43	( )	<input checked="" type="checkbox"/>	T.S.3	
		44	( )		dump	
		45				
		46				
		47		<input checked="" type="checkbox"/>		
		48	2		1 @ 30	
		49	0 1 Q 1 Q 1 Q 0		mask	
		50	1 Q 0 0 W Q 0 0		mask	
		51	G 2 0 0 0 0 0 0	<input checked="" type="checkbox"/>	-156 @ 8	
		52				
		53	( )		T.S.	
		54	1 0 0 0 0 0 0 0		1 @ 3	
		55	( )	<input checked="" type="checkbox"/>	T.S.1	
		56	( )		T.S.2	
		57	K 0 0 0 0 0 0 0 0		-6 @ 4	
		58	8 0 0 0 0 0 0 0		-1 @ 0	
0 0 0 0 0 0 0 0		59		<input checked="" type="checkbox"/>		
		60				
		61				
		62				
		63		<input checked="" type="checkbox"/>		

CM183 MCBEE TORONTO, CANADA

CONDITIONAL STOP CODE



CARRIAGE RETURN

COMPUTING CENTRE

JAN. 87



LGP-30 CODING SHEET

NO. 1

PAGE 1 OF 3

JOB NO. \_\_\_\_\_ PROG. NO. \_\_\_\_\_ PREP. BY B.J.M. CK'D. BY B.J.M. DATE \_\_\_\_\_

PROBLEM OUTPUT 3 DIGITS @ 30, SIGN TRAILING TRACK 00

PROGRAM INPUT CODES	STOP	LOCATION	INSTRUCTION OP. ADDRESS	STOP	CONTENTS OF ADDRESS	NOTES
		<input checked="" type="checkbox"/> X X X X X X X X X X				
		0,0,00	H 0 0 2 2		N	
		01	T 0 0 2 3			→ N<0
		02	H 0 0 4 5		N  @ 30	
		03	D 0 0 4 6	<input checked="" type="checkbox"/>	100 @ 9	
		04	H 0 0 4 7		N /100 @ 21	
		05	E 0 0 4 8		17 to 21	
		06	A 0 0 4 9		XZ0215	
		07	Y 0 0 2 9	<input checked="" type="checkbox"/>		
		08	U 0 0 2 9			
, 0 0 0 0 0 0 1		09	3 J 0 0			
		10	X Z 0 2 6 2			
		11	X Z 3 2 6 1	<input checked="" type="checkbox"/>	delay	
		12	X P 0 0 0 0		print tens	
		13	U 0 0 1 5			
		14				
		15	B 0 0 5 8	<input checked="" type="checkbox"/>		
		16	E 0 0 5 9		22 to 30	
		17	D 0 0 5 3		1 @ 20	
		18	M 0 0 5 4		10 @ 20	
		19	A 0 0 5 5	<input checked="" type="checkbox"/>	17 to 21	
		20	U 0 1 0 5			
, 0 0 0 0 0 0 2		21	5 0 0 0		10 @ 20	
		22	( )		N	
		23	C 0 0 4 5	<input checked="" type="checkbox"/>	dump	
		24	U 0 0 5 0			
		25				
		26				
, 0 0 0 0 0 0 1		27	3 J 0 0	<input checked="" type="checkbox"/>	17 to 21	
		28				
		29	X P 0 0 0 0		print hundreds	
		30	U 0 0 3 2			
		31		<input checked="" type="checkbox"/>		

CM100 CODE PRACTICE, CANADA

CONDITIONAL STOP CODE

☒ CARRIAGE RETURN





NO. \_\_\_\_\_ PROG. NO. \_\_\_\_\_ PREP. BY \_\_\_\_\_ CK'D. BY \_\_\_\_\_ DATE \_\_\_\_\_

PROBLEM \_\_\_\_\_ TRACK 00

PROGRAM INPUT CODES	STOP	LOCATION	INSTRUCTION OP. ADDRESS	STOP	CONTENTS OF ADDRESS	NOTES
		<input checked="" type="checkbox"/> XXXXX	XXXXXXXXXXXXXXXXXX			
		0, 0, 32	B 0, 0, 4, 7		N  / 100 @ 21	
		33	E 0, 0, 6, 2		22 to 30	
		34	D 0, 0, 6, 3		1 @ 20	
		35	M 0, 0, 2, 1	<input checked="" type="checkbox"/>	10 @ 20	N  - H/10 @ 21
		36	H 0, 0, 5, 8			
		37	E 0, 0, 0, 9		17 to 21	
		38	A 0, 0, 1, 0		XZ0262	
		39	U 0, 0, 4, 0	<input checked="" type="checkbox"/>		
		40	Y 0, 0, 1, 2			
		41	U 0, 0, 1, 1			
, 0 0 0 0 0 0 7		42				
		43		<input checked="" type="checkbox"/>		
		44				
		45	( )		dump and  N  @ 30	
		46	1 9 0 0 0 0 0 0		100 @ 9	
		47	( )	<input checked="" type="checkbox"/>	N  / 100 @ 23	
		48	3 J 0, 0		17 to 21	
		49	X Z 0 2 1 5			
		50	S 0, 0, 2, 2		N	N
		51	U 0, 0, 0, 2	<input checked="" type="checkbox"/>		return
, 0 0 0 0 0 0 4		52				
		53	8 0 0		1 @ 20	
		54	5 0 0 0		10 @ 20	
		55	2 0 0	<input checked="" type="checkbox"/>	1/2 @ 21 = 1 @ 22	
		56	X Z 0 2 0 9			
, 0 0 0 0 0 1 2		57				
		58	( )		tens and ones @ 21	
		59	3 W Q	<input checked="" type="checkbox"/>	22 to 30	
		60	1 0 0 0 0 0 0		1 @ 7	
		61				
		62	3 W Q		24 to 30	
		63	8 0 0	<input checked="" type="checkbox"/>	1 @ 20	

CONDITIONAL STOP CODE



CARRIAGE RETURN

CM103 MCBEE TORONTO, CANADA





# LGP-30 CODING SHEET

NO. 1

PAGE 3 OF 3

OS NO. \_\_\_\_\_ PROG. NO. \_\_\_\_\_ PREP. BY \_\_\_\_\_ CK'D. BY \_\_\_\_\_ DATE \_\_\_\_\_

PROBLEM \_\_\_\_\_ TRACK 01

PROGRAM INPUT CODES	STOP	LOCATION	INSTRUCTION OP. ADDRESS	STOP	CONTENTS OF ADDRESS	NOTES
		<input checked="" type="checkbox"/> X X X X X X X X X X				
		0, 1, 00				
		0, 1				
		0, 2				
		0, 3		<input checked="" type="checkbox"/>		
		0, 4				
		0, 5	E 0 0 2 7		17 to 21	
		0, 6	A 0 0 5 6		Z0009	
		0, 7	U 0 1 0 8	<input checked="" type="checkbox"/>		
		0, 8	Y 0 1 2 3			
		0, 9	U 0 1 2 2			
		1, 0				
		1, 1		<input checked="" type="checkbox"/>		
		1, 2	X P 0 7 6 2		" - "	
		1, 3	U 0 1 2 8			
		1, 4				
		1, 5		<input checked="" type="checkbox"/>		
		1, 6				
		1, 7				
		1, 8				
		1, 9		<input checked="" type="checkbox"/>		
		2, 0				
		2, 1				
		2, 2	X Z 3 2 0 8		delay	
		2, 3	X P 0 0 0 0	<input checked="" type="checkbox"/>	print units	
		2, 4	B 0 0 2 2		N	
		2, 5	X Z 0 0 1 1		delay	
		2, 6	T 0 1 1 2			
		2, 7	X P 1 1 1 3	<input checked="" type="checkbox"/>	" + "	
		2, 8	X Z 0 0 1 4		delay	
		2, 9	X P 3 2 1 5		" 1 "	
		3, 0	X Z 0 0 1 6			
		3, 1	U ( )	<input checked="" type="checkbox"/>		exit

CM108 UNIV. MICROFILMS, CANADA

CONDITIONAL STOP CODE



CARRIAGE RETURN



## LGP-30 CODING SHEET

NO. 1

PAGE 1 OF 2

JOB NO. \_\_\_\_\_ PROG. NO. \_\_\_\_\_ PREP. BY D.G.B. CK'D. BY B.J.M. DATE \_\_\_\_\_

PROBLEM CONVERT TRACK 00

PROGRAM INPUT CODES	STOP	LOCATION	INSTRUCTION OP. ADDRESS	STOP	CONTENTS OF ADDRESS	NOTES
					special input 0300-0362	
					121001 0400-0531	
					special output 1000-1131	
		<input checked="" type="checkbox"/> X X X X X X X X X X				
		0,0,00	X P 1,6,0,0			
		0,1	X Z 0,0,0,0			
		0,2	X R 0,4,0,7		} input k @ 30	
		0,3	X U 0,4,0,0	<input checked="" type="checkbox"/>	k = no. of channels	
		0,4	H 0,0,3,6		k @ 30	
		0,5	N 0,0,3,4		1 @ 30	
		0,6	H 0,0,3,7		k @ 29	
		0,7	B 0,0,4,0	<input checked="" type="checkbox"/>	location e <sub>0</sub>	
		0,8	Y 0,0,1,3		C ( )	
		0,9	A 0,0,3,7		k @ 29'	
		1,0	Y 0,0,3,8		C ( )	flag 1
		1,1	X R 0,3,2,9	<input checked="" type="checkbox"/>	} input initial values	
		1,2	X U 0,3,0,0		} of e <sub>i</sub> @ 30	
		1,3	C ( )			
		1,4	B 0,0,1,3			
		1,5	A 0,0,3,5	<input checked="" type="checkbox"/>	1 @ 29	
		1,6	H 0,0,1,3			
		1,7	S 0,0,3,8		flag 1	
		1,8	T 0,0,1,1			
		1,9	B 0,0,4,0	<input checked="" type="checkbox"/>	location e <sub>0</sub>	
		2,0	Y 0,0,2,5		S ( )	
		2,1	A 0,0,3,7		k @ 29	
		2,2	Y 0,0,3,9		S ( )	flag 2
		2,3	X R 0,3,2,9	<input checked="" type="checkbox"/>	} input e	
		2,4	X U 0,3,0,0		} e <sub>i</sub>	
		2,5	S ( )			
		2,6	X R 1,1,3,1		} output	
		2,7	X U 1,0,0,0	<input checked="" type="checkbox"/>		
		2,8	B 0,0,2,5		S ( )	
		2,9	A 0,0,3,5		1 @ 29	
		3,0	H 0,0,2,5			
		3,1	S 0,0,3,9	<input checked="" type="checkbox"/>	flag 2	

CONDITIONAL STOP CODE



CARRIAGE RETURN





## LGP-30 CODING SHEET

NO 2

PAGE 2 OF 2

OBJ NO. \_\_\_\_\_ PROG. NO. \_\_\_\_\_ PREP. BY \_\_\_\_\_ CK'D. BY \_\_\_\_\_ DATE \_\_\_\_\_

PROBLEM \_\_\_\_\_ TRACK 00

PROGRAM INPUT CODES	STOP	LOCATION	INSTRUCTION OP. ADDRESS	STOP	CONTENTS OF ADDRESS	NOTES
		<input checked="" type="checkbox"/> XXXXX	XXXXXXXXXXXXXXXXXXXX			
		0 0 32	T 0 0 2 3			
		33	U 0 0 1 9			
, 0 0 0 0 0 0 2		34	2		1 @ 30	
		35	4	<input checked="" type="checkbox"/>	1 @ 29	
		36			k @ 30	
		37			k @ 29	
		38	C ( )		flag 1	
		39	S ( )	<input checked="" type="checkbox"/>	flag 2	
		40	Z 0 1 0 0		location e <sub>0</sub>	
. 0 0 0 0 0 0 0		41				
		42				
		43		<input checked="" type="checkbox"/>		
		44				
		45				
		46				
		47		<input checked="" type="checkbox"/>		
		48				
		49				
		50				
		51		<input checked="" type="checkbox"/>		
		52				
		53				
		54				
		55		<input checked="" type="checkbox"/>		
		56				
		57				
		58				
		59		<input checked="" type="checkbox"/>		
		60				
		61				
		62				
		63		<input checked="" type="checkbox"/>		

CM183 BCEE TORONTO, CANADA

CONDITIONAL STOP CODE



CARRIAGE RETURN





LGP-30 CODING SHEET  
NO. 1

PAGE 1 OF 7

JOB NO. \_\_\_\_\_ PROG. NO. \_\_\_\_\_ PREP. BY D.G.B. CK'D. BY B.J.M. DATE July, 1963

PROBLEM TRANSVERSE DEFLECTION w/d TRACK 00

PROGRAM INPUT CODES	STOP	LOCATION	INSTRUCTION OP. ADDRESS	STOP	CONTENTS OF ADDRESS	NOTES
		<input checked="" type="checkbox"/> X X X X X X X X X X				
		0,0,00	X P 1,6,0,0		carriage return	
		01	X Z 0,0,0,0			
		02	X R 0,4,0,7		} input	
		03	X U 0,4,0,0	<input checked="" type="checkbox"/>	n @ 30	
		04	H 0,3,1,8		n @ 30	
		05	N 0,2,6,3		1 @ 30	
		06	H 0,3,1,8		n @ 29	
		07	X R 0,4,0,7	<input checked="" type="checkbox"/>	} input	
		08	X U 0,4,0,0		} M @ 30	11.1
		09	D 0,3,0,7		1 @ 5'	
		10	H 0,3,1,9		M @ 25	
		11	B 0,3,0,2	<input checked="" type="checkbox"/>	16 @ 30	
		12	D 0,3,1,9			
		13	H 0,3,1,9		m @ 5	
		14	B 0,3,2,0		location h	
		15	A 0,3,0,5	<input checked="" type="checkbox"/>	1 @ 11	
		16	X R 0,5,2,1		} 11.1	
		17	X U 0,5,0,4			
		18	B 0,3,2,0		h @ 4	
		19	D 0,3,0,8	<input checked="" type="checkbox"/>	1 @ 3	
		20	H 0,3,2,0		h @ 1	
		21	B 0,3,1,5		location e <sub>t</sub>	
		22	Y 0,0,2,7			
		23	A 0,3,1,8	<input checked="" type="checkbox"/>	n @ 29	
		24	Y 0,3,1,1		C ( )	flag 1
		25	X R 0,3,2,9		} input	e <sub>t</sub> @ 30
		26	X U 0,3,0,0			
		27	C ( )	<input checked="" type="checkbox"/>		
		28	B 0,0,2,7			
		29	A 0,3,0,0		1 @ 29	
		30	H 0,0,2,7			
		31	S 0,3,1,1	<input checked="" type="checkbox"/>	flag 1	

CONDITIONAL STOP CODE

☒ CARRIAGE RETURN



## LGP-30 CODING SHEET

NO 2

PAGE 2 OF 7

JOB NO. \_\_\_\_\_ PROG. NO. \_\_\_\_\_ PREP. BY \_\_\_\_\_ CK'D. BY \_\_\_\_\_ DATE \_\_\_\_\_

PROBLEM \_\_\_\_\_ TRACK 00

PROGRAM INPUT CODES	STOP	LOCATION	INSTRUCTION OP. ADDRESS	STOP	CONTENTS OF ADDRESS	NOTES
		<input checked="" type="checkbox"/> XXXXXXXXXXXXXXXXXXXX				
		0, 0, 32	T 0 0 2 5			
		33	B 0 3 1 6		location eb	
		34	Y 0 0 3 9			
		35	A 0 3 1 8	<input checked="" type="checkbox"/>	n @ 29	
		36	Y 0 3 1 1		C ( )	flag 2
		37	X R 0 3 2 9		input eb	
		38	X U 0 3 0 0			
		39	C ( )	<input checked="" type="checkbox"/>		
		40	B 0 0 3 9			
		41	A 0 3 0 0		1 @ 29	
		42	H 0 0 3 9			
		43	S 0 3 1 1	<input checked="" type="checkbox"/>	flag 2	
		44	T 0 0 3 7			
		45	B 0 3 1 5		location et	
		46	Y 0 0 5 3			
		47	A 0 3 1 8	<input checked="" type="checkbox"/>	n @ 29	
		48	Y 0 3 1 2		B ( )	flag 3
		49	B 0 3 1 6		location eb	
		50	Y 0 0 5 4			
		51	B 0 3 1 7	<input checked="" type="checkbox"/>	location Δ	
		52	Y 0 0 5 7			
		53	B ( )		et @ 30	
		54	S ( )		eb @ 30	
		55	D 0 3 0 4	<input checked="" type="checkbox"/>	1 @ 13	
		56	M 0 3 1 9		m @ 5	
		57	C ( )		Δ <sub>i</sub> @ 22	
		58	B 0 0 5 3			
		59	A 0 3 0 0	<input checked="" type="checkbox"/>	1 @ 29	
		60	H 0 0 5 3			
		61	S 0 3 1 2		flag 3	
		62	T 0 1 0 0			
		63	U 0 1 0 6	<input checked="" type="checkbox"/>		

CM100 MODEL TORONTO, CANADA

CONDITIONAL STOP CODE



CARRIAGE RETURN





LGP-30 CODING SHEET  
NO. 1

PAGE 3 OF 7

JOB NO. \_\_\_\_\_ PROG. NO. \_\_\_\_\_ PREP. BY \_\_\_\_\_ CK'D. BY \_\_\_\_\_ DATE \_\_\_\_\_

PROBLEM \_\_\_\_\_ TRACK 01

PROGRAM INPUT CODES	STOP	LOCATION	INSTRUCTION OP. ADDRESS	STOP	CONTENTS OF ADDRESS	NOTES
		<input checked="" type="checkbox"/> X X X X X X X X X X				
		0, 1, 00	A 0, 3, 1, 2		flag 3	
		0, 1	A 0, 2, 6, 0		XZ0400	
		0, 2	Y 0, 0, 5, 4		S( )	
		0, 3	A 0, 2, 6, 0		<input checked="" type="checkbox"/> XZ0400	
		0, 4	Y 0, 0, 5, 7		C( )	
		0, 5	U 0, 0, 5, 3			
		0, 6	C 2, 1, 0, 0			
		0, 7	C 2, 1, 0, 0		<input checked="" type="checkbox"/>	
		0, 8	C 0, 3, 2, 1			
		0, 9	B 0, 3, 1, 7		location $\Delta$	
		1, 0	Y 0, 1, 1, 9			
		1, 1	A 0, 3, 0, 0		<input checked="" type="checkbox"/> 1 @ 29	
		1, 2	Y 0, 1, 2, 0			
		1, 3	A 0, 3, 1, 8		n @ 29	
		1, 4	S 0, 3, 0, 1		2 @ 29	
		1, 5	Y 0, 3, 1, 2		<input checked="" type="checkbox"/> flag 4	
		1, 6	B 0, 1, 0, 6		location $\int_0$	
		1, 7	A 0, 3, 0, 0		1 @ 29	
		1, 8	Y 0, 1, 2, 5		H( )	
		1, 9	B ( )		<input checked="" type="checkbox"/> $\Delta_i$ @ 22	
		2, 0	A ( )		$\Delta_{i+1}$ @ 22	
		2, 1	M 0, 3, 1, 0		1/2 @ 0 (2 @ 2)	
		2, 2	M 0, 3, 2, 0		h @ 1	
		2, 3	A 0, 3, 2, 1		<input checked="" type="checkbox"/> $\int$	
		2, 4	H 0, 3, 2, 1		$\int$	
		2, 5	H ( )		$\int_i$	
		2, 6	B 0, 1, 1, 9		B( )	
		2, 7	A 0, 3, 0, 0		<input checked="" type="checkbox"/> 1 @ 29	
		2, 8	H 0, 1, 1, 9			
		2, 9	S 0, 3, 1, 2		flag 4	
		3, 0	T 0, 1, 3, 2			
		3, 1	U 0, 1, 3, 8		<input checked="" type="checkbox"/>	

CH100 1201 100000 100000

CONDITIONAL STOP CODE



CARRIAGE RETURN





LGP-30 CODING SHEET

NO 2

PAGE 4 OF 7

225

B NO. \_\_\_\_\_ PROG. NO. \_\_\_\_\_ PREP. BY \_\_\_\_\_ CK'D. BY \_\_\_\_\_ DATE \_\_\_\_\_

OBLEM \_\_\_\_\_ TRACK 01

PROGRAM INPUT CODES	STOP	LOCATION	INSTRUCTION OP. ADDRESS	STOP	CONTENTS OF ADDRESS	NOTES
		<input checked="" type="checkbox"/> XXXXX	XXXXXXXXXXXXXXXXXX			
		0 1 32	A 0 3 1 2		flag 4	
		33	A 0 3 0 0		1 @ 29	
		34	Y 0 1 2 0		A( )	
		35	A 0 2 6 0	<input checked="" type="checkbox"/>	XZ0400	
		36	Y 0 1 2 5			
		37	U 0 1 1 9			
		38	C 2 5 0 0		location $\int\int$	
		39	C 2 5 0 0	<input checked="" type="checkbox"/>	$\int\int$	
		40	C 0 3 2 2			
		41	B 0 1 0 6		location $\int$	
		42	Y 0 1 5 1			
		43	A 0 3 0 0	<input checked="" type="checkbox"/>	1 @ 29	
		44	Y 0 1 5 2			
		45	A 0 3 1 8		n @ 29	
		46	S 0 3 0 1		2 @ 29	
		47	Y 0 3 1 2	<input checked="" type="checkbox"/>	flag 5	
		48	B 0 1 3 8		location $\int\int$	
		49	A 0 3 0 0		1 @ 29	
		50	Y 0 1 5 7			
		51	B ( )	<input checked="" type="checkbox"/>	$\int_i @ 23$	
		52	A ( )		$\int_{i+1} @ 23$	
		53	M 0 3 1 0		1/2 @ 0	
		54	M 0 3 2 0		h @ 1	$h/2 (\int_i + \int_{i+1})$
		55	A 0 3 2 2	<input checked="" type="checkbox"/>	$\int\int$	
		56	H 0 3 2 2		$\int\int$	
		57	H ( )		$\int\int_i$	
		58	B 0 1 5 1		B( )	
		59	A 0 3 0 0	<input checked="" type="checkbox"/>	1 @ 29	
		60	H 0 1 5 1			
		61	S 0 3 1 2		flag 5	
		62	T 0 2 0 0			
		63	U 0 2 0 6	<input checked="" type="checkbox"/>		

CONDITIONAL STOP CODE



CARRIAGE RETURN



LGP-30 CODING SHEET  
NO. 1

PAGE 5 OF 7

JOB NO. \_\_\_\_\_ PROG. NO. \_\_\_\_\_ PREP. BY \_\_\_\_\_ CK'D. BY \_\_\_\_\_ DATE \_\_\_\_\_

PROBLEM \_\_\_\_\_ TRACK 02

PROGRAM INPUT CODES	STO	LOCATION	INSTRUCTION OP. ADDRESS	STO	CONTENTS OF ADDRESS	NOTES
		<input checked="" type="checkbox"/> X X X X X X X X X X				
		0, 2, 00	A 0, 3, 1, 2		flag 5	
		01	A 0, 3, 0, 0		1 @ 29	
		02	Y 0, 1, 5, 2		A( )	
		03	A 0, 2, 6, 0	<input checked="" type="checkbox"/>	XZ0400	
		04	Y 0, 1, 5, 7		H( )	
		05	U 0, 1, 5, 1			
		06	X P 1, 6, 0, 0		carriage return	
		07	X Z 0, 0, 0, 0	<input checked="" type="checkbox"/>		
		08	B 0, 3, 1, 8		n @ 29	
		09	C 0, 3, 1, 4		counter	
		10	B 0, 1, 3, 8		location	
		11	Y 0, 2, 1, 8	<input checked="" type="checkbox"/>	B( )	
		12	C 0, 3, 2, 3		$\sum$	
		13	C 0, 3, 2, 3			
		14	B 0, 3, 1, 4		counter	
		15	S 0, 3, 0, 0	<input checked="" type="checkbox"/>	1 @ 29	
		16	H 0, 3, 1, 4		counter	
		17	T 0, 2, 2, 5			
		18	B ( )			
		19	A 0, 3, 2, 3	<input checked="" type="checkbox"/>	partial sum @ 24	$\sum$
		20	C 0, 3, 2, 3			
		21	B 0, 2, 1, 8			
		22	A 0, 3, 0, 0		1 @ 29	
		23	Y 0, 2, 1, 8	<input checked="" type="checkbox"/>		
		24	U 0, 2, 1, 4			
		25	B 0, 2, 1, 4			
		26	S 0, 3, 0, 0		1 @ 29	
		27	Y 0, 2, 3, 1	<input checked="" type="checkbox"/>	S( )	
		28	B 0, 3, 2, 3		$\sum$ @ 24	
		29	D 0, 3, 1, 0		$1/2 @ 0 = 2 \sum$ @ 24	
		30	S 2, 5, 0, 0		$\sum$	
		31	S ( )	<input checked="" type="checkbox"/>	$1/2(w_0 + 2 \sum w_n)$	

CONDITIONAL STOP CODE

☒ CARRIAGE RETURN





## LGP-30 CODING SHEET

PAGE 6 OF 7

NO 2

NO. \_\_\_\_\_ PROG. NO. \_\_\_\_\_ PREP. BY \_\_\_\_\_ CK'D. BY \_\_\_\_\_ DATE \_\_\_\_\_

BLEM

TRACK 02

PROGRAM INPUT CODES	STOP	LOCATION	INSTRUCTION OP. ADDRESS	STOP	CONTENTS OF ADDRESS	NOTES
		<input checked="" type="checkbox"/> XXXXX	XXXXXXXXXXXXXXXXXX			
		0, 2, 32	H 0, 3, 2, 4			
		33	B 0, 3, 1, 8		n @ 29	
		34	S 0, 3, 0, 0		1 @ 29	
		35	D 0, 3, 0, 3	<input checked="" type="checkbox"/>	1 @ 23	(n - 1) @ 6
		36	H 0, 3, 2, 5			
		37	B 0, 3, 2, 4		$1/2(w_0 + 2 \sum_{j=1}^n w_j)$	
		38	D 0, 3, 2, 5		(n - 1)	
		39	M 0, 3, 0, 6	<input checked="" type="checkbox"/>	1 @ 7	
		40	H 0, 3, 2, 6		$\bar{w} = \frac{1}{2(n-1)} (w_0 + 2 \sum_{j=1}^n w_j)$	
		41	B 0, 3, 1, 8		n @ 29	
		42	C 0, 3, 1, 4		counter	
		43	B 0, 1, 3, 8	<input checked="" type="checkbox"/>	location $\int_0$	
		44	Y 0, 2, 4, 9		B( )	
		45	B 0, 3, 1, 4		counter	
		46	S 0, 3, 0, 0		1 @ 29	
		47	H 0, 3, 1, 4	<input checked="" type="checkbox"/>	counter	
		48	T 0, 2, 6, 1			
		49	B ( )			
		50	S 0, 3, 2, 6		$\bar{w}$ @ 24	
		51	M 0, 3, 2, 7	<input checked="" type="checkbox"/>	$m(\int - \bar{w})$ @ 29	
		52	H 0, 3, 2, 7			
		53	X R 0, 6, 0, 3		} output	12.4
		54	X U 0, 6, 0, 0		}	
		55	Z 0, 3, 2, 7	<input checked="" type="checkbox"/>		
		56	X Z 0, 1, 2, 9		1 no. @ q of 29	
		57	B 0, 2, 4, 9		B( )	
		58	A 0, 3, 0, 0		1 @ 29	
		59	Y 0, 2, 4, 9	<input checked="" type="checkbox"/>		
		60	U 0, 2, 4, 5		Breakpoint #4	
		61	X Z 0, 4, 0, 0			
		62	U 0, 0, 2, 1			
, 0 0 0 0 0 1 2		63	2	<input checked="" type="checkbox"/>	1 @ 30	

CONDITIONAL STOP CODE



CARRIAGE RETURN





LGP-30 CODING SHEET  
NO. 1

PAGE 7 OF 7

OB NO \_\_\_\_\_ PROG. NO. \_\_\_\_\_ PREP. BY \_\_\_\_\_ CK'D. BY \_\_\_\_\_ DATE \_\_\_\_\_

PROBLEM \_\_\_\_\_ TRACK 03

PROGRAM INPUT CODES	STOP	LOCATION	INSTRUCTION OP. ADDRESS	STOP	CONTENTS OF ADDRESS	NOTES
		<input checked="" type="checkbox"/> X X X X X X X X X X				
		0, 3, 00	4		1 @ 29	
		01	8		2 @ 29	
		02	2, 0		16 @ 30	
		03	1, 0, 0		<input checked="" type="checkbox"/> 1 @ 23	
		04	4, 0, 0, 0, 0		1 @ 13	
		05	1, 0, 0, 0, 0, 0		1 @ 11	
		06	1, 0, 0, 0, 0, 0, 0		1 @ 7	
		07	4, 0, 0, 0, 0, 0, 0		<input checked="" type="checkbox"/> 1 @ 5	
		08	1, 0, 0, 0, 0, 0, 0, 0		1 @ 3	
		09	2, 0, 0, 0, 0, 0, 0, 0		1 @ 2	
		10	4, 0, 0, 0, 0, 0, 0, 0		2 @ 2	1/2 @ 0
		11	C ( )		<input checked="" type="checkbox"/> flag 1, 2	
		12	B ( )		flag 3, 4, 5, 7	
		13	Z ( )		flag 6	
		14	Z, 0, 0, 0, 0		counter	
		15	Z, 0, 9, 0, 0		<input checked="" type="checkbox"/> location	$e_t$
		16	Z, 1, 3, 0, 0		location	$e_b$
		17	Z, 1, 7, 0, 0		location	$o$
		18	( )		n @ 29	
		19	( )		<input checked="" type="checkbox"/> m @ 5	
		20	( )		h @ 1	
		21	( )		$\int$	
		22	( )		$\int \int$	
		23	( )		<input checked="" type="checkbox"/> $\sum \int \int$	
		24	( )		$1/2 (w_o + 2 \sum \int \int + w_n)$	@ 25
		25	( )		(n - 1) @	24
		26	( )		$\bar{w}$ @ 24	
		27	( )		<input checked="" type="checkbox"/> $m (\int \int - \bar{w}) = (\int \int - \bar{w})/d$	
		28				
		29				
		30				
		31			<input checked="" type="checkbox"/>	

CONDITIONAL STOP CODE

☒ CARRIAGE RETURN











**B29813**